Constitutive activity of the human histamine H_4 receptor: Molecular modelling, binding and functional studies on wild-type and mutant H_4R orthologs

Dissertation

zur Erlangung des Doktorgrades der Naturwissenschaften (Dr. rer. nat.)

an der Fakultät für Chemie und Pharmazie

der Universität Regensburg

vorgelegt von

David Wifling

aus Bad Griesbach

2015

Die vorliegende Arbeit entstand in der Zeit von Mai 2011 bis Dezember 2014 unter der Anleitung von Herrn Prof. Dr. A. Buschauer und Herrn Prof. Dr. S. Dove am Institut für Pharmazie der Fakultät für Chemie und Pharmazie der Universität Regensburg.

Das Promotionsgesuch wurde eingereicht im Februar 2015

Tag der mündlichen Prüfung: 13. März 2015

Prüfungsausschuss:

Prof. Dr. A. Slenczka   (Vorsitzender)

Prof. Dr. A. Buschauer   (Erstgutachter)

Prof. Dr. S. Dove   (Zweitgutachter)

Prof. Dr. S. Elz   (Drittprüfer)

Für meine liebste Maria

„Phantasie ist wichtiger als Wissen, denn Wissen ist begrenzt.“

Albert Einstein, 1879-1955

Danksagungen

Contents

Abbreviations

[A]	ligand concentration
[R]	receptor concentration
3D	three-dimensional
$5\text{-}HT_{1B}R$; $5\text{-}HT_{2B}R$; $5\text{-}HT_4R$	serotonin receptor subtypes
Å	Ångström
$A_{2A}R$	adenosine receptor subtype
AC	adenylyl cyclase
ATP	adenosine 5'-triphosphate
B_{max}	maximal specific binding of a radioligand determined in saturation binding assays, reflecting the number of receptors
bp	base pairs
BSA	bovine serum albumin
c	canine
cAMP	3',5'-cyclic adenosine monophosphate
cDNA	complementary DNA copied from a messenger RNA
CNS	central nervous system
CRE	cAMP response element
CREB	cAMP response element binding protein
CYP450	Cytochrome P450
D_2R; D_3R	dopamine receptor subtypes
DAG	1,2-diacylglycerol
DAO	diamine oxidase
DMSO	dimethyl sulfoxide
DNA	deoxyribonucleic acid
E. coli	*Escherichia coli*
EC_{50}	molar concentration of an agonist producing 50 % of the maximum response for that agonist
ECL1, ECL2, ECL3	first, second and third extracellular loop of a GPCR
EDTA	ethylenediaminetetraacetic acid
E_{max}	maximal possible response in a given system
ERK	extracellular signal regulated kinase
FLAG	FLAG-tag, octapeptide epitope (mostly DYKDDDDK) for labelling of proteins
GDP	guanosine 5'-diphosphate
gp	guinea pig
GPCR	G-protein coupled receptor

G-protein	guanine nucleotide binding protein
GPS	GPCR proteolytic site
GRK	G-protein coupled receptor kinase
GTP	guanosine 5'-triphosphate
GTPase	guanosine 5'-triphosphate hydrolase
GTPγS	guanosine 5'-O-[gamma-thio]triphosphate
$G\alpha_{i/o}$	α subunit of G-proteins that inhibits the adenylyl cyclase
$G\alpha_{q/11}$	α subunit of G-proteins that stimulates phospholipase C-β
$G\alpha_s$	α subunit of G-proteins that stimulates the adenylyl cyclase
Gβγ	βγ-subunits of a heterotrimeric G-protein
h	human or hour(s)
H_1R; H_2R; H_3R; H_4R	histamine H_1, H_2, H_3 and H_4 receptor subtypes
H8	helix 8
H-bond	hydrogen bond
HDC	histidine decarboxylase
His_6	hexahistidine tag, epitope for labelling of proteins
HNMT	histamine-N-methyltransferase
IC	ion channel
ICL1, ICL2, ICL3	first, second and third intracellular loop of a GPCR
IP_3	inositol-1,4,5-trisphosphate
IP_3R	inositol-1,4,5-trisphosphate receptor
IUPHAR	International Union of Pharmacology
K_a	equilibrium association constant for the binding of a ligand to an inactive receptor
K_A	equilibrium dissociation constant for the binding of a ligand to an inactive receptor
K_b	equilibrium dissociation constant of an antagonist-receptor complex in a functional assay; molar concentration occupying 50 % of the receptors at equilibrium
K_d	equilibrium dissociation constant for a radioligand-receptor complex
kDa	kilodalton
K_g	equilibrium association constant of the receptor/G-protein complex
K_G	equilibrium dissociation constant of the receptor/G-protein complex
K_i	analogue to K_b, but determined in radioligand competition binding assays; molar concentration of the competing ligand occupying 50 % of the receptors
L	allosteric constant for the activation of the receptor
LGIC	ligand-gated ion channel
m	mouse

M_1R; M_2R; M_3R; M_4R; M_5R	muscarinic receptor subtypes
MAO B	monoamine oxidase B
MAPK	mitogen-activated protein kinase
min	minute(s)
mk	monkey
n.a.	not applicable
n.d.	not determined
NHR	nuclear hormone receptor
NMS	N-methylscopolamine
OCT	organic cation transporter
ORF	open reading frame
p	pig
$P2Y_1R$	P2 purinoceptor subtype
PAGE	polyacrylamide gel electrophoresis
PAM250	Point Accepted Mutation matrix
PCR	polymerase chain reaction
PDB	Protein Data Bank
pEC_{50}	negative decadic logarithm of the EC_{50} value
P_i	inorganic phosphate
PI3K	phosphatidylinositol-3-kinase
PIP_2	phosphatidylinositol-4,5-bisphosphate
PKA	protein kinase A
pK_b	negative decadic logarithm of the K_b value
PKC	protein kinase C
pK_i	negative decadic logarithm of the K_i value
PLA_2	phospholipase A_2
PLC	phospholipase C
PLC-β	phospholipase C-β
QNB	3-quinuclidinyl benzilate
r	rat
R_a	active state of the receptor
RGS	regulators of G-protein signalling
R_i	inactive state of the receptor
rpm	revolutions per minute
R_t	total number of receptor sites
s	second(s)
SDS	sodiumdodecylsulfate

SEM	standard error of the mean
SF	signal peptide and FLAG N-terminal tag
*Sf*9	*Spodoptera frugiperda* insect cell line
t	turkey
TM1-TM7	transmembrane domains 1-7 of GPCRs
Tris	tris(hydroxymethyl)aminomethane
TSHR	thyroid stimulating hormone receptor
VFTM	Venus flytrap mechanism
VGIC	voltage-gated ion channel
X-ray	roentgen radiation (wavelength in the range of 0.01 to 10 nanometres)
α	intrinsic activity or constant describing the affinity of the ligand for R_a over R_i (effect of receptor activation on ligand binding)
$\alpha_{1B}AR$	adrenergic receptor subtype
β	effect of receptor activation on the coupling of G-protein to the receptor (effect of G-protein coupling on receptor activation)
β_1AR; β_2AR	adrenergic receptor subtypes
γ	effect of ligand binding on the coupling of G-protein to the receptor (effect of G-protein coupling on the binding of ligand)
δ	constant describing the synergism between receptor activation, G-protein coupling or the binding of a ligand
τ	power of the agonist to produce response

Colour codes and symbols

Wild-type or mutant H$_4$ receptors

- ⊖ hH$_4$R-R341E
- ● hH$_4$R
- ◆ hH$_4$R-S179M
- ◆ hH$_4$R-S179A
- ▽ hH$_4$R-S330R
- ⊖ hH$_4$R-R341S
- ⬓ hH$_4$R-F169V
- ◈ hH$_4$R-F169V+S179M
- ◈ hH$_4$R-F169V+S179A
- ◇ mH$_4$R-V171F+M181S
- △ hH$_4$R-F168A
- ☐ mH$_4$R-V171F
- ■ mH$_4$R
- ◆ rH$_4$R

Ligands

- ● histamine
- ○ UR-PI294
- ▲ thioperamide
- △ JNJ7777120
- ◆ VUF8430
- ◇ immepip
- ■ clozapine
- ☐ isoloxapine
- ▼ UR-PI376
- ▽ clobenpropit

Chapter 1

Introduction

1.1 G-protein coupled receptors

There are approximately 20,000–25,000 protein encoding genes in the human genome (Pennisi, 2012). The number of both, disease modifying and "druggable" genes (Rask-Andersen et al., 2014), was estimated to be in the range of 3000 for each group (Hopkins and Groom, 2002), with an overlap, representing potential drug targets (Rask-Andersen et al., 2011), of about 600 to 1500 genes (Hopkins and Groom, 2002). G-protein coupled receptors (GPCRs) represent the most important class of biological targets (Figure 1.1) of the currently approved drugs (~30 %) and are considered as promising targets for the discovery and development of future drugs as well (Jacoby et al., 2006). About 800 GPCRs are encoded in the human genome. As a kind of molecular switches, GPCRs play a major role in signal transduction from the outside into the cell. Signals may be external sensory stimuli or molecules emitted from other cells (cellular communication, e. g., neurotransmission). Various signals such as photons, ions, biogenic amines, purines, lipids, nucleic acid derivatives, peptides and proteins (Jacoby et al., 2006) are recognized by GPCRs which include 388 olfactory receptors and roughly 400 receptors recognizing hormones, neurotransmitters and other endogenous ligands (Pawson et al., 2014).

- Enzymes: 1138
- Catalytic receptors: 240
- Transporter: 508
- GPCRs: 394
- VGICs: 141
- LGICs: 84
- Other ICs: 47
- NHRs: 48
- Other proteins: 108
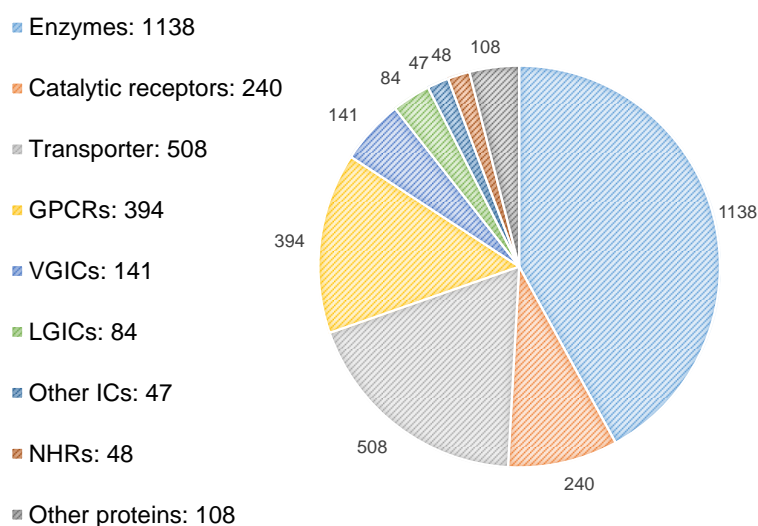
Figure 1.1: Number of human targets, measured by the number of distinct human UniProt entries: enzymes, catalytic receptors (enzyme-linked receptors); transporter, GPCRs (without olfactory receptors), VGICs (voltage-gated ion channels); LGICs (ligand-gated ion channels); other ICs (other ion channels), NHRs (nuclear hormone receptors) and other proteins. Adapted from the IUPHAR DB (Pawson et al., 2014) on 05.11.2014

1.1.1 GPCR classes

GPCRs (Davenport et al., 2013; Foord et al., 2005) are subdivided into families (classes A-F). All proteins that were proven to bind G-proteins were included and the remaining 7TM receptors were assigned to the O (Other) family (Kolakowski, 1994). The well-known system of the International Union of Pharmacology (IUPHAR) is similar with the exception that the Frizzled class is referred to as a separate family instead of being included in family O (Foord et al., 2005; Kolakowski, 1994), dividing GPCRs into classes A-C, Frizzled GPCRs, Other 7TM proteins and Adhesion GPCRs (Figure 1.2; Fredriksson et al., 2003; Pawson et al., 2014).

- Class A: 282 (89)
- Class B: 15 (0)
- Class C: 22 (7)
- Frizzled: 11 (0)
- Other 7TM proteins: 6 (6)
- Adhesion: 33 (33)
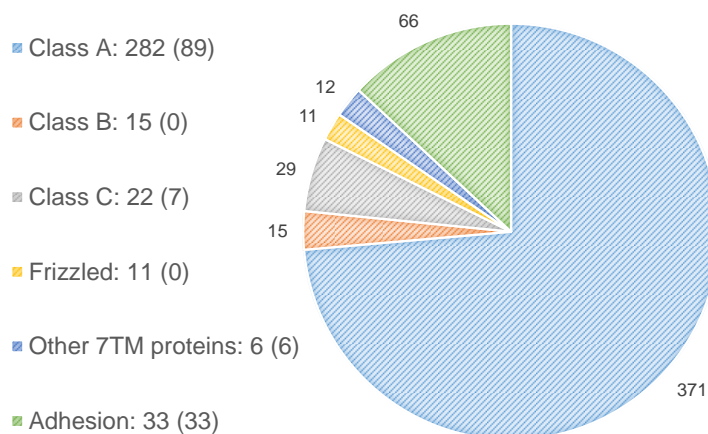
Figure 1.2: Members of different GPCR classes (A (without olfactory receptors), B, C, Frizzled, Other and Adhesion). Numbers in parentheses indicate orphan GPCRs included in the figure. Adapted from the IUPHAR DB (Pawson et al., 2014) on 05.11.2014.

Class A, also called the Rhodopsin-like family, represents the largest class, comprising more than 75 % of all GPCRs (Figure 1.2). It is a very heterogeneous group of GPCRs with a highly conserved short N-terminus and differently conserved motifs within the TMs, for example the DRY motif in TM3, the FxxCWxP motif in the middle of TM6, the NPxxY motif at the bottom of TM7 and the disulphide bond forming cysteines in TM3 and ECL2. All in all the conservation in TM regions is very low (Lagerström and Schiöth, 2008). Class A of GPCRs is subdivided into four groups (α, β, γ and δ). Receptors of biogenic amines such as adrenaline, dopamine, serotonin or histamine, belong to group α.

Characteristic of the small Secretin family (class B) is an extracellular hormone-binding domain, a disulphide bond between two cysteine residues in ECL1 and ECL2 as well as a relatively long N-terminus with three cysteines (Lagerström and Schiöth, 2008).

The Glutamate family is assigned to class C of GPCRs. Typical for this class is a long N-terminus, which is the region where the endogenous ligand is bound according to the so-called Venus flytrap mechanism (VFTM). Like in most GPCRs the disulphide bond between ECL1 and ECL2 is present (Lagerström and Schiöth, 2008).

Long highly glycosylated and diverse N-termini, a GPCR proteolytic site (GPS) as well as conserved cysteines in ECL1 and ECL2 are characteristic of the Adhesion family (Lagerström and Schiöth, 2008).

The less characterized Frizzled GPCR class consists of the frizzled and smoothened receptors (Lagerström and Schiöth, 2008).

1.1.2 Structure of G-protein coupled receptors

The first high resolution crystal structure of a GPCR, the bovine rhodopsin, was published in 2000 (Palczewski et al., 2000). Bovine rhodopsin was used as a template for homology modelling until the first structure of a biogenic amine GPCR, the $β_2$ adrenoceptor ($β_2$AR) in the inactive state, was published in 2007 (Cherezov et al., 2007; Rasmussen et al., 2007). As the stabilization of the active state proved to be particularly challenging, the resolution of the structure of the $β_2$AR active state in 2011 (Rasmussen et al., 2011a) may be considered as the beginning of a new era of GPCR research.

A GPCR consists of an extracellularilly located N-terminus, seven transmembrane domains, connected by three extracellular (ECL1-3) and three intracellular loops (ICL1-3), and an intracellular C-terminus, including a membrane-associated helical domain (helix 8, H8) (Figure 1.3; Alexander et al., 2013).
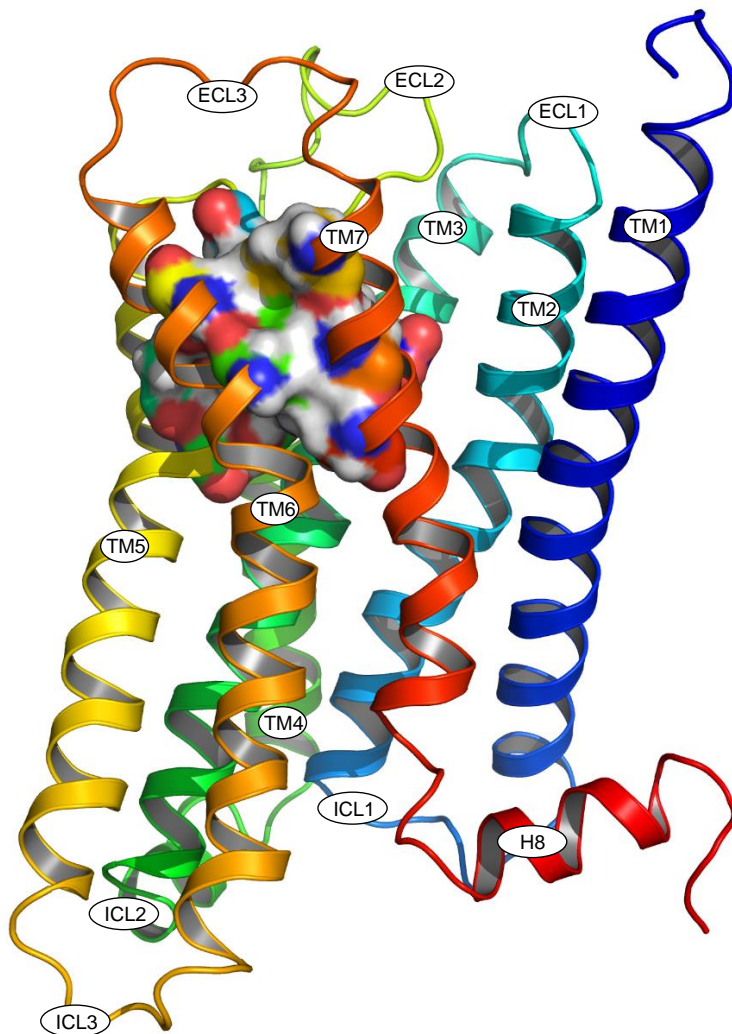
Figure 1.3: Structure of the human histamine H_4R in the active state. Homology model was generated based on the nanobody stabilized active state of the $β_2$AR (PDB (Protein Data Bank) ID: 3P0G) as template (Rasmussen et al., 2011a). The surface illustrates the binding pocket region.

GPCRs are embedded in the membrane lipids and the binding pocket (orthosteric site, in Figure 1.3 illustrated as surface) is formed by extracellular parts of the TMs as well as by ECL2 on top of the binding pocket (Granier and Kobilka, 2012). GPCR function can be modulated by ligand binding to allosteric sites, which are less conserved than orthosteric sites as demonstrated by X-ray structures of muscarinic acetylcholine receptor subtypes (Christopoulos, 2014; Granier and Kobilka, 2012; Haga et al., 2012; Kruse et al., 2012; Kruse et al., 2014; Kruse et al., 2013).

1.1.3 Function of G-protein coupled receptors

A GPCR toggles between both the inactive and active state (Figure 1.4). An agonist elicits a biological response by stabilizing the receptor in the active state R_a (Figure 1.4 and Figure 1.5). The intrinsic activity of partial agonists ranges from 0 to 100 %. Partial agonists are ligands not capable of producing the maximal response. This is in agreement with the idea that partial agonists stabilize the active state less effective than full agonists (Kenakin, 2001).

A neutral antagonist (intrinsic activity = 0 %) neither activates nor inhibits the receptor, i. e., the basal equilibrium between both active R_a and inactive R_i states remains unaltered. A neutral antagonist is capable of competing with both agonists and inverse agonists for orthosteric binding.

Considering constitutive activity as a prerequisite, an inverse agonist decreases the elevated level of basally activated receptors by stabilizing the inactive state (Kenakin, 2004). Differentiation between full and partial inverse agonists is possible, enabling full inverse agonists to stabilize the inactive state R_i more effectively ($\alpha \leq -100$ %) than partial inverse agonists ($0 > \alpha > -100$ %). In terms of intrinsic activity, the responses to GPCR ligands are referenced to the maximal effect produced by the endogenous ligand as the standard agonist (e. g. histamine in case of the H_4R, i. a. = 100 %). Therefore, depending on the basal activity of the GPCR of interest in the respective assay, the intrinsic activity of a full inverse agonist can by definition be lower than -100 %. (Seifert and Wieland, 2005).
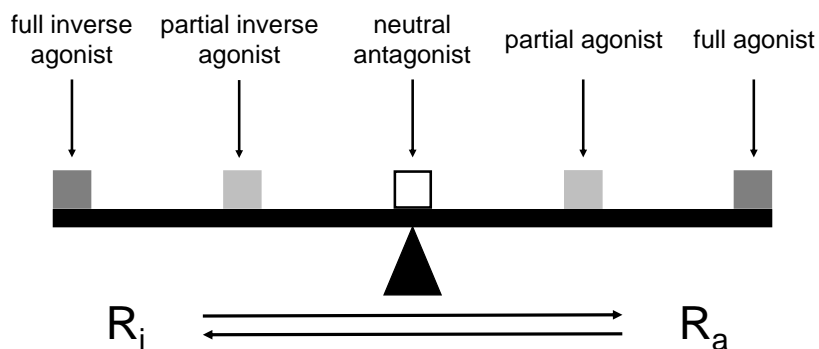
Figure 1.4: Two state model of a GPCR. The receptor toggles between the inactive state R_i and the active state R_a. Adapted from Seifert and Wenzel-Seifert (2002).
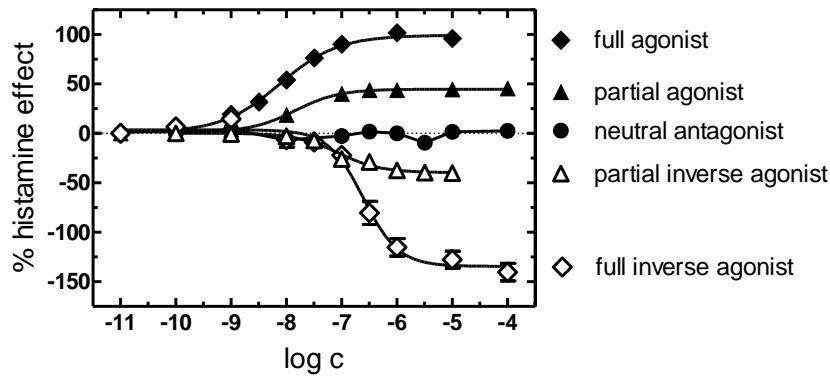
Figure 1.5: Effects of ligands with different intrinsic activities shown as concentration-response curves. [35S]GTPγS assays were performed with different H_4 receptor species orthologs. Modified from Seifert and Wieland (2005).

1.1.4 Models of ligand binding and G-protein coupling

1.1.4.1 Classical model

Binding of ligand A to a receptor R is described by the Langmuir adsorption isotherm according to Clark (1933) and Clark (1937) (Equation 1.1):

$$\rho = \frac{[AR]}{[R_t]} = \frac{[A]}{[A] + K_A} \tag{1.1}$$

Herein, AR is referred to as the ligand bound receptor, R_t corresponds to the total number of receptor sites and K_A to the equilibrium dissociation constant (K_a to the equilibrium association constant) of the agonist receptor complex. ρ describes the fraction of ligand bound and total receptor concentration (Kenakin, 2009).

Different modifications, introduced by Ariens (1954), Stephenson (1956) and Furchgott (1966) led to the assumption (Equation 1.2):

$$A + R \underset{K_A}{\overset{K_a}{\rightleftharpoons}} AR \longrightarrow Stimulus \longrightarrow Response \tag{1.2}$$
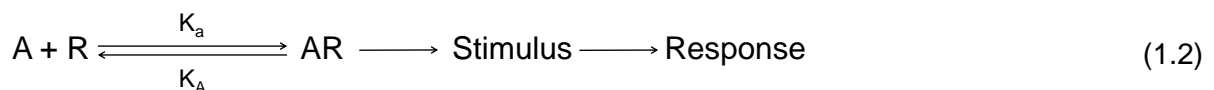
The term ε, referring to the agonist-specific term intrinsic efficacy, and the total concentration of receptors $[R_t]$ were introduced in the binding function (Equation 1.3):

$$Response = f\left(\frac{[A]}{[A] + K_A} \times \varepsilon \times [R_t]\right) \tag{1.3}$$

1.1.4.2 Operational model

The "operational" model, developed by Black and Leff (1983), improved the model describing the relationship between agonist concentration and response (Kenakin, 2009). The assumption of one ligand binding to one receptor is valid.

The response is dependent on the agonist concentration [A], K_A, τ (power of the agonist to produce response) and E_{max} (maximal response of the system). Both E_{max} and τ are receptor and system dependent (Equation 1.4):

$$\text{response} = \frac{[A] \times \tau \times E_{max}}{[A] \times (\tau + 1) + K_A} \tag{1.4}$$

High levels of τ (e. g. 100-1000) imply a relatively high percentage of activated receptor species over a broad range of τ. But if τ → 0, the maximal response → 0. Moreover, the smaller K_A (higher affinity), the less agonist is required to attain the same response.

1.1.4.3 Ternary complex models

The ternary complex model – firstly described by De Lean et al. (1980) – takes into account the binding of the activated receptor to membrane proteins such as G-proteins (Equation 1.5; Kenakin, 2009):

$$A + R \underset{K_A}{\overset{K_a}{\rightleftharpoons}} AR + G \underset{K_G}{\overset{K_g}{\rightleftharpoons}} ARG \tag{1.5}$$
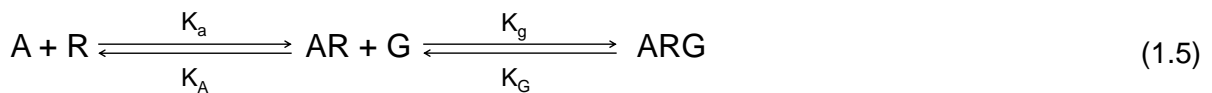
The extended ternary complex model additionally implies the equilibrium between the inactive R_i and the active R_a receptor states (Figure 1.6; Kenakin, 2009; Samama et al., 1993).
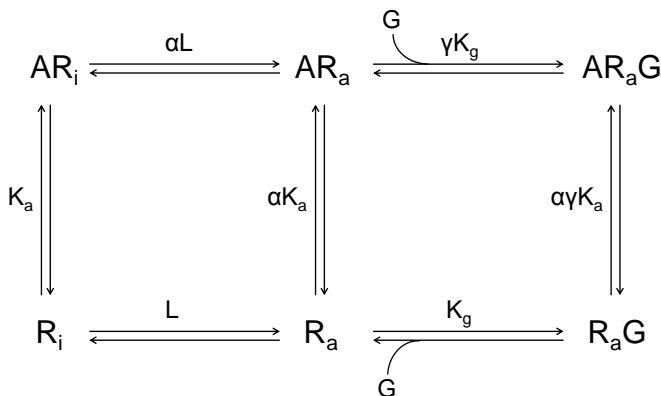
Figure 1.6: Illustration of the extended ternary complex model. According to Kenakin (2009). K_G: equilibrium dissociation constant of the receptor/G-protein complex and K_g: respective equilibrium association constant.

The conversion of R_i to R_a is considered in the allosteric constant L (Equation 1.6):

$$L = \frac{[R_a]}{[R_i]} \tag{1.6}$$

Furthermore, the terms α, referring to differences in affinity of the ligand to R_a compared to R_i, and γ, referring to differences in affinity of the ligand bound receptor to the G-proteins compared to the ligand-unbound receptor, were introduced (Kenakin, 2009). For example, an α or a γ value of 10 means, that the ligand has a tenfold higher affinity to R_a compared to R_i or

a tenfold higher affinity of the ligand-receptor complex to G-proteins compared to the ligand-free receptor.

The fraction ρ (Equation 1.7) of the two G-protein activated receptor species [R_aG] and [AR_aG] and the total receptor population is given as:

$$\rho = \frac{\frac{L \times [G]}{K_G}\left(1 + \frac{\alpha \times \gamma \times [A]}{K_A}\right)}{\frac{[A]}{K_A}\left(1 + \alpha \times L\left(1 + \frac{\gamma \times [G]}{K_G}\right)\right) + L\left(1 + \frac{[G]}{K_G}\right) + 1} \tag{1.7}$$

The terms α and γ define the intrinsic activity (Kenakin, 2004). If a ligand binds with high affinity to the active state of the receptor (α > 1) and this ligand-bound receptor binds to G-proteins with high affinity (γ > 1), the ligand will be an agonist with positive intrinsic activity. By contrast, α and γ < 1 means that the ligand preferentially stabilizes the inactive state of the receptor with high affinity and the affinity of the ligand-bound receptor to G-proteins decreases. The corresponding quality of action becomes obvious in a functional system with constitutive activity, and the respective ligand is referred to as an inverse agonist.

Further refinements were made with the cubic ternary complex model (Figure 1.7), taking into account the interaction of inactive receptor states (R_i and AR_i) with G-proteins (Kenakin, 2009; Weiss et al., 1996a; Weiss et al., 1996b; c).
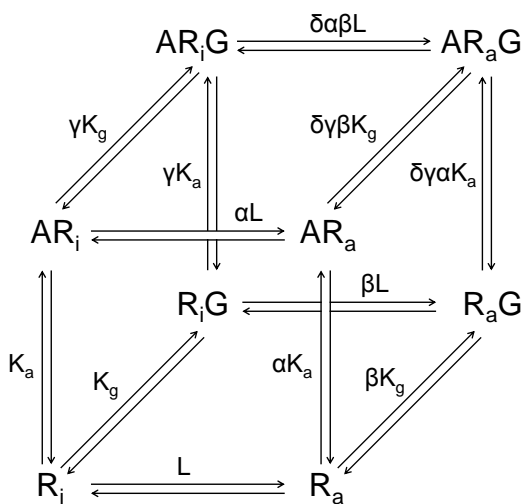
Figure 1.7: Cubic ternary complex model, according to Kenakin (2009). β: effect of receptor activation on the coupling of G-protein to the receptor (effect of G-protein coupling on receptor activation); δ: constant describing the synergism between receptor activation, G-protein coupling or the binding of a ligand.

1.1.5 Constitutive activity of GPCRs

Constitutive activity describes the ability of a GPCR to spontaneously produce a cellular response in the absence of a ligand (Lefkowitz et al., 1993). So far, constitutive activity has been observed for more than 60 wild-type GPCRs and several disease-causing mutants (Seifert and Wenzel-Seifert, 2002).

The higher the constitutive activity of a GPCR, the more the basal equilibrium between inactive and active state is shifted towards the active state. Therefore, the amplitude of the response elicited by a full agonist is lower at a constitutively active receptor compared to a GPCR devoid of constitutive activity (Kenakin, 2004). Inversely, the maximum effect of an inverse agonist increases with the level of constitutive activity of the receptor of interest. The hallmarks of a constitutively active receptor are a high basal activity, a high intrinsic activity and potency of partial agonists and a high inverse agonistic effect of inverse agonists (Seifert et al., 1998).

The phenomenon of constitutive activity can be derived from the extended ternary complex model (Equation 1.8; Kenakin, 2004; 2009):

$$R_i \xrightleftharpoons[\quad]{L} R_a \xrightleftharpoons[K_G]{} R_aG \qquad\qquad (1.8)$$

$$G$$
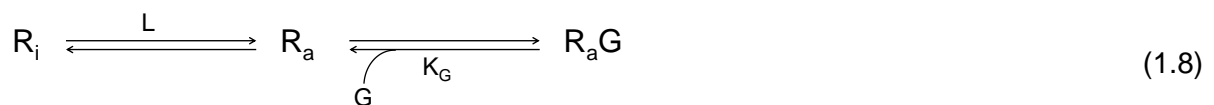
1.1.6 Signal transduction

GPCRs may be considered as molecular switches transferring extracellular signals to intracellular responses. Conformational changes from inactive to active state(s) allow for activation of signal transducers, i. e., effectors such as G-proteins (Chapter 1.1.6.2) or β-arrestins (Chapter 1.1.6.3) (Granier and Kobilka, 2012).

1.1.6.1 Structure of G-proteins and G-protein cycle

Currently, 16 different Gα G-protein subunits as well as 5 Gβ and 12 Gγ subunits are known (Cabrera-Vera et al., 2003; Downes and Gautam, 1999). In G-proteins not activated by a GPCR, the GDP-bound Gα subunit is combined with the Gβγ-dimer to form a heterotrimeric complex (Figure 1.8 and Figure 1.9; Hurowitz et al., 2000). Both the Gα as well as the Gβγ subunit are attached to the membrane via lipid anchors (Chen and Manning, 2001; Dupre et al., 2009). Binding of a ligand to a GPCR gives a ternary complex consisting of the agonist-bound active receptor and the nucleotide free Gα and Gβγ subunit (Bünemann et al., 2003; De Lean et al., 1980; Kling et al., 2013; Ratnala and Kobilka, 2009). Upon Gα activation by a GPCR, GDP is released and replaced by GTP, and Gα (Figure 1.10) dissociates from Gβγ (Rasmussen et al., 2011b). Gα and Gβγ have their own effectors and influence the levels of second messengers (Tuteja, 2009). The active state of the Gα subunit is switched off by the intrinsic GTPase activity to give inactive GDP-bound Gα, which re-associates with Gβγ. Regulators of G-protein signalling (RGS proteins; GTPase activating proteins, GAPs) can enhance the activity of the GTPase (Neitzel and Hepler, 2006; Wieland et al., 2007; Willars, 2006).
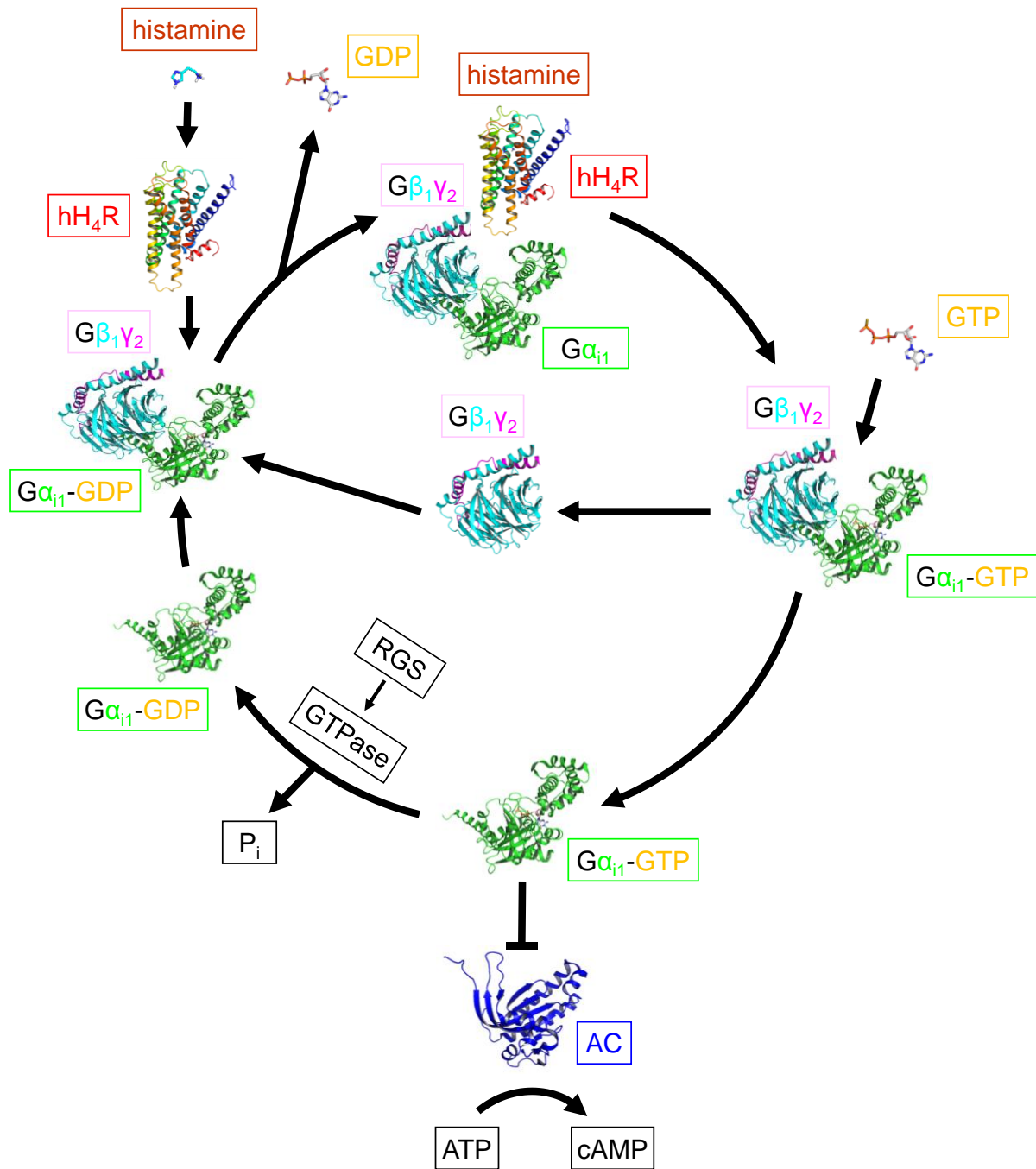
Figure 1.8: G-protein cycle, turned on by histamine H$_4$ receptor stimulation as an example. Gα_{i1} is coloured in green, the Gβ_1 subunit in turquoise, the Gγ_2 subunit in pink and the adenylyl cyclase (AC) in blue. The following crystal structures were used: inactive heterotrimeric complex of Gα_{i1} and G$\beta_1\gamma_2$ (PDB ID: 1GG2 (Wall et al., 1995)), active Gα_{i1} (PDB ID: 1GIA (Coleman et al., 1994)), adenylyl cyclase (1CUL (Tesmer et al., 2000)); hH$_4$R was generated as a homology model with the active state of the β_2AR (PDB ID: 3P0G (Rasmussen et al., 2011a)) as template. Modified from Gilman (1987) and Rasmussen et al. (2011b).
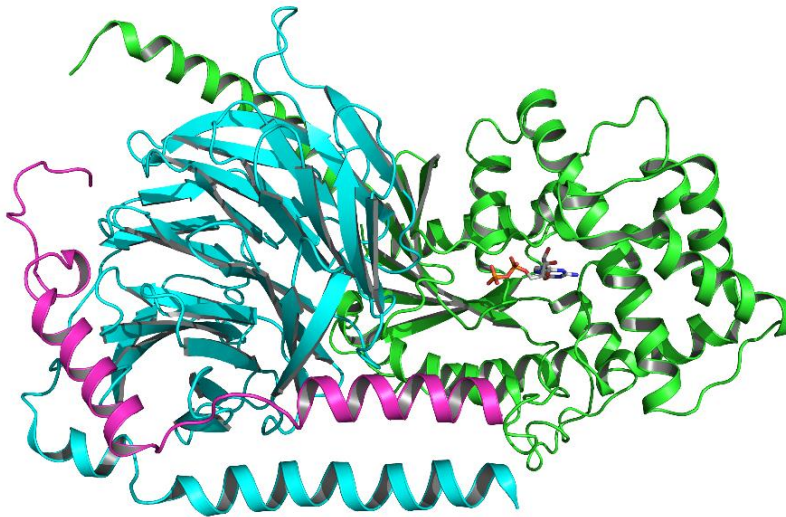
Figure 1.9: Crystal structure of heterotrimeric G-proteins Gα$_{i1}$ and Gβ$_1$γ$_2$. PDB ID: 1GG2 (Wall et al., 1995). Gα$_{i1}$ is coloured in green, Gβ$_1$ in turquoise and Gγ$_2$ in pink. The bound GDP is illustrated as sticks.
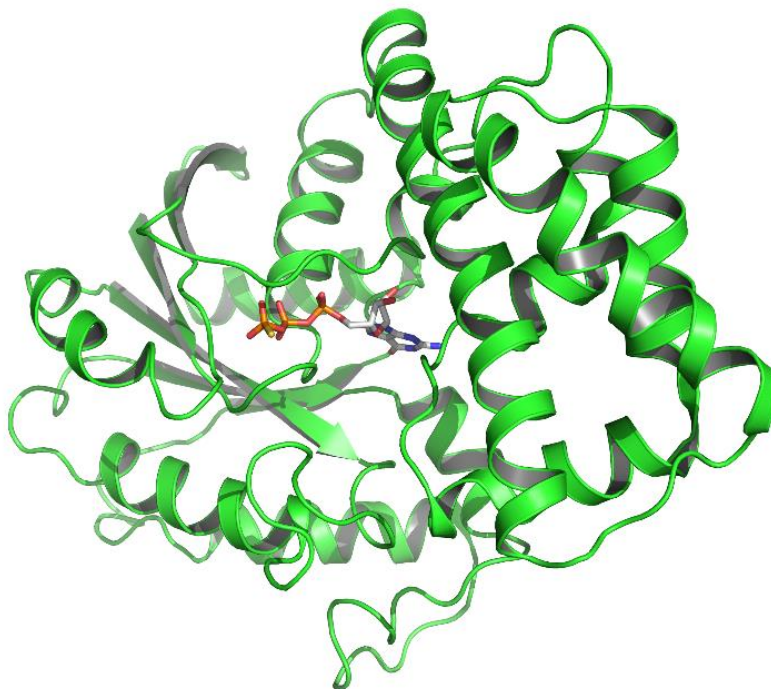
Figure 1.10: Crystal structure of Gα$_{i1}$ in the active state. The non-hydrolysable GTP analogue GTPγS is bound to the Gα$_{i1}$ subunit. PDB ID: 1GIA (Coleman et al., 1994).

1.1.6.2 Functions of different G-protein subtypes

According to the α subunits, G-proteins are usually divided into four families: G$_s$, G$_{i/o}$, G$_{q/11}$ and G$_{12}$ (Downes and Gautam, 1999). Activation of Gα$_s$, for instance mediated by the histamine H$_2$R, leads to an increase in the production of 3',5'-cyclic adenosine monophosphate (cAMP) by the adenylyl cyclase (AC) (Figure 1.11; Liu et al., 2003; Neves et al., 2002). By contrast, the stimulation of Gα$_{i/o}$-coupled receptors such as the H$_3$R and H$_4$R results in an inhibition of the AC activity and a decreasing cAMP level (Figure 1.11; Neves et al., 2002). cAMP stimulates many kinases, most prominently the protein kinase A (PKA), which is capable of phosphorylating numerous substrates, including the cAMP response element binding protein (CREB) (Birnbaumer, 2007; Hur and Kim, 2002).

Although the term inhibitory G protein (G_i) was initially derived from the inhibitory effect on the AC, members of the $G\alpha_i$ family reveal also signal transmission via the $G\beta\gamma$-subunit (Khan et al., 2013), e. g., by activation of phospholipase C-β (PLC-β; Harden et al., 1987)) (Figure 1.11). Moreover, K^+ channels are activated and inactive Ca^{2+} channels are stabilized resulting in hyperpolarization and inhibition of excitation. Kinase (Akt) pathways are activated via the stimulation of PI3K (phosphatidylinositol-3-kinase) and formation of the second messenger PIP_3 (phosphatidylinositol-3,4,5-trisphosphate) (Hur and Kim, 2002). Activation of PLC-$\beta 2$ and 3 induces synthesis of the second messengers IP_3 (inositol-1,4,5-trisphosphate) and DAG (1,2-diacylglycerol) (Hokin and Hokin, 1955; Hokin and Hokin, 1953). Whereas DAG activates the PKC directly, IP_3 increases the intracellular calcium level (Berridge et al., 1983) and therefore indirectly activates the PKC (Birnbaumer, 2007).

$G\alpha_{q/11}$-coupled receptors such as the H_1R activate PLC-$\beta 1$ and 4 (Wu et al., 1992) cleaving PIP_2 (phosphatidylinositol-4,5-bisphosphate) to give IP_3 and DAG (Birnbaumer, 2007; Neves et al., 2002) (Figure 1.11).
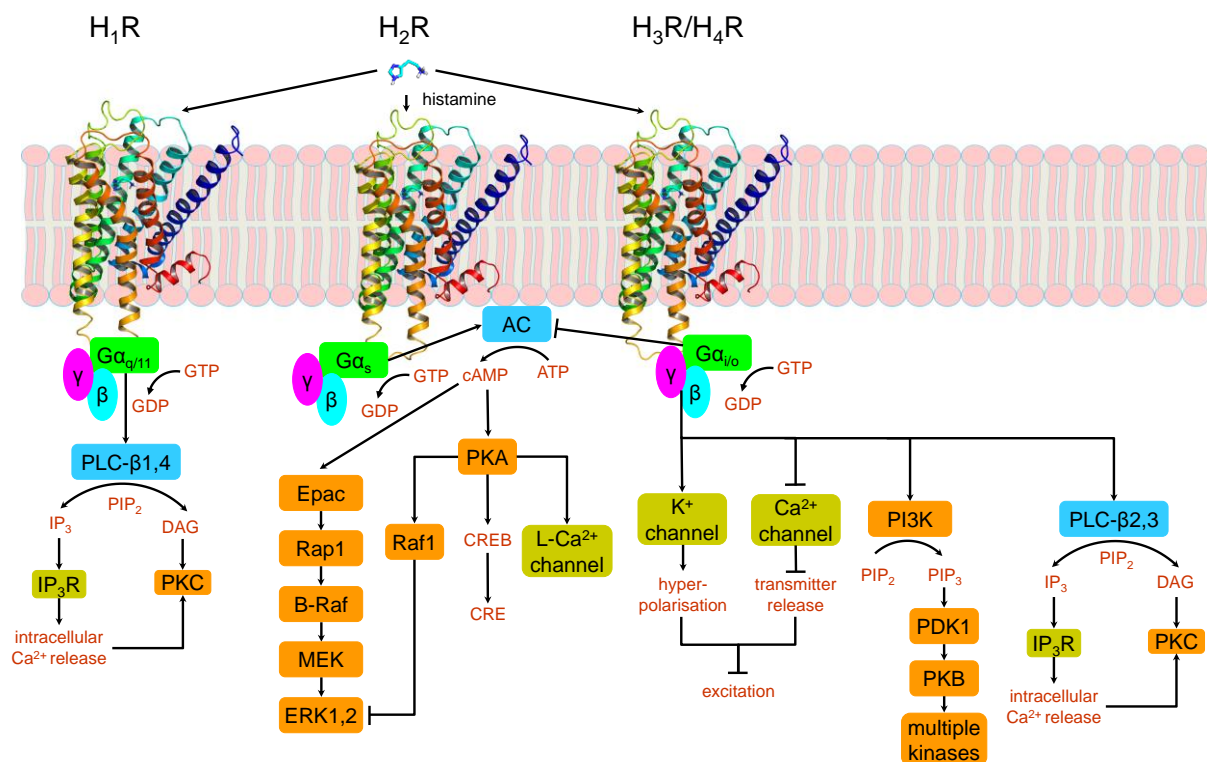
Figure 1.11: Signalling pathways of GPCRs, exemplified by the histamine receptor subtypes H_1R-H_4R. Gα proteins are marked in green, the Gβ-subunit in turquoise and the Gγ-subunit in pink; enzymes are highlighted in blue, except for kinases (orange), and ion channels are marked in yellow ochre. Modified from Steinhilber et al. (2005) and Aktories et al. (2006).

1.1.6.3 β-arrestin-mediated GPCR internalization and signalling

Out of four different known isoforms of arrestins, two arrestins are expressed in the retina ("visual arrestins") and two "non-visual" arrestins were identified, namely β-arrestin1 and 2

(Luttrell and Gesty-Palmer, 2010). β-arrestins are capable of both directly influencing diverse signalling pathways (e. g. protein kinases) as well as of modifying the number of active receptors by the internalization and downregulation machinery (Luttrell and Lefkowitz, 2002; Shenoy and Lefkowitz, 2011). In particular, continuous stimulation of a GPCR by an agonist implies a β-arrestin mediated desensitization (Hanyaloglu and von Zastrow, 2008). In the first step of this process the receptor is phosphorylated by GRKs (G-protein coupled receptor kinases) (Figure 1.12), a class of enzymes comprising seven different subtypes (Luttrell and Lefkowitz, 2002; Ribas et al., 2007; Watari et al., 2014). In detail, GPCRs are preferentially phosphorylated at serine and threonine residues in ICL3 and the C-terminus. Phosphorylation increases the affinity of β-arrestins to the receptor; β-arrestin binding precludes further coupling of G-proteins to the receptor. Unlike the visual arrestins, β-arrestins additionally contain clathrin and β2-adaptin (AP2 complex) binding motifs and are therefore involved in the processes of endocytosis, resensitization and downregulation (Goodman et al., 1996). Inhibiting the function of the GTPase dynamin (Zhang et al., 1996), being responsible for the endocytosis via clathrin-coated pits, prevents the internalization of GPCRs. After endocytosis, the receptor is either recycled or degraded in lysosomes, depending on the duration of β-arrestin binding to the receptor. If β-arrestins dissociate from the receptor upon endocytosis (e. g. β_2AR), the receptor is preferentially recycled to the plasma membrane (class A β-arrestin recruitment). However, in case that the receptor (e. g. V_2R) remains bound to β-arrestin, the receptor is most probably degraded (class B β-arrestin recruitment) (DeWire et al., 2007; Gurevich and Gurevich, 2006; Luttrell, 2008).

Apart from the internalization process, β-arrestins can directly modulate several effector proteins such as ERK (extracellular signal-regulated kinase), a MAPK (mitogen-activated protein kinase), and can activate PI3K or inhibit the transcription factor NFκB by activation of IκB (Figure 1.12; Reiter et al., 2012; Shenoy and Lefkowitz, 2011).

According to the concept of "functional selectivity" or "biased signalling", depending on the bound ligand, the receptor should be capable to activate, either G-proteins (G-protein biased ligand) or β-arrestins (β-arrestin biased ligand). Ligands causing the GPCR-mediated activation of both, G-proteins and β-arrestins, are referred to as balanced ligands (Reiter et al., 2012).
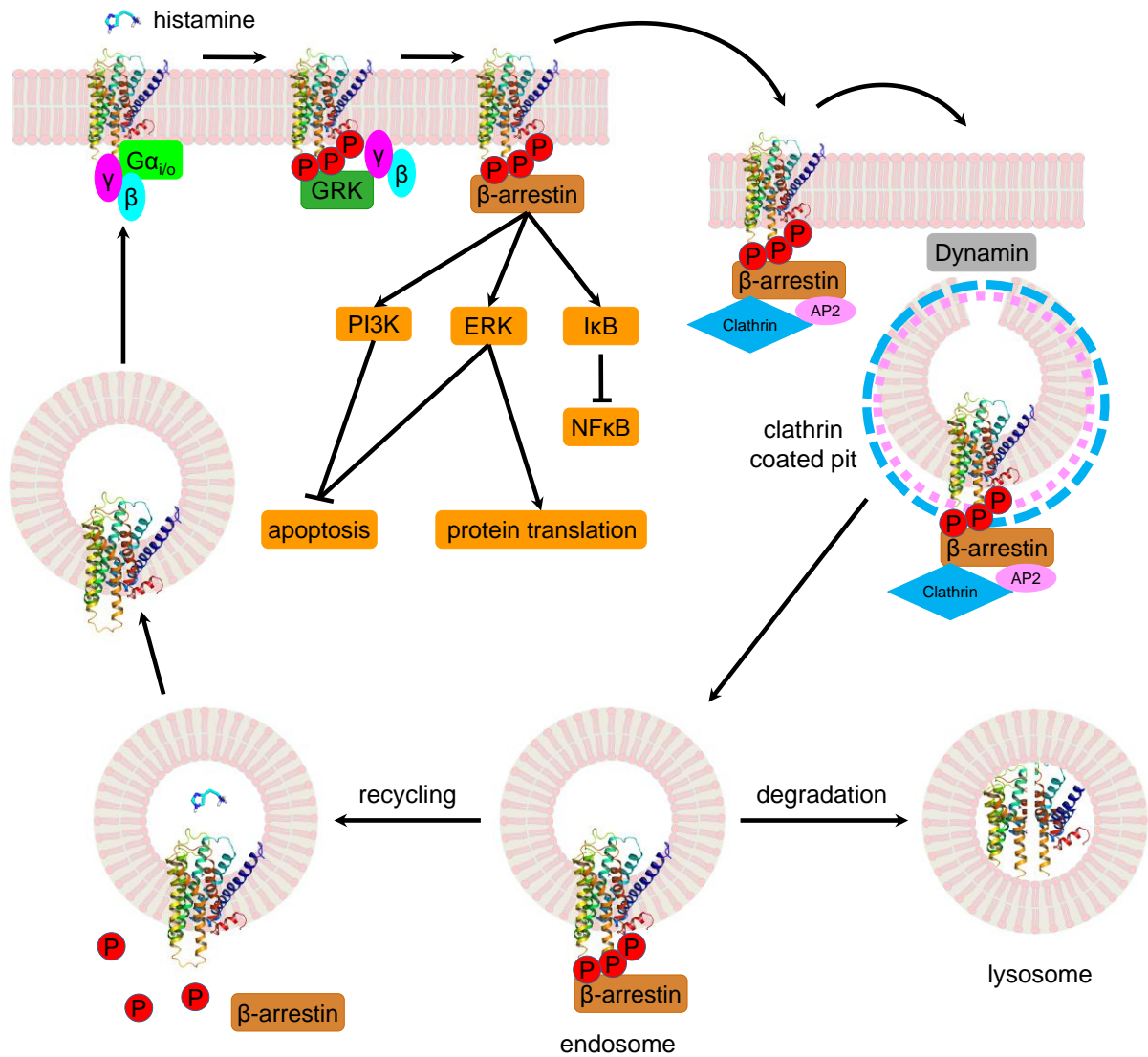
Figure 1.12: β-arrestin-mediated desensitization and signalling of GPCRs. On the one hand, agonist binding to a GPCR, e. g., histamine to the hH$_4$R, initiates G-protein dependent signalling. On the other hand, activated receptors are specifically phosphorylated (red) by GRKs (dark green). This phosphorylation increases β-arrestin recruitment (brown) to the receptor and precludes further G-protein activation. β-arrestin links the receptor to the internalization machinery of clathrin (blue) and clathrin adaptor (AP2, pink) leading to a dynamin-dependent (grey) receptor internalization via "clathrin coated pits". In the endosomes, the receptor is either degraded in lysosomes or agonist dissociation is facilitated by the low pH in the endosome leading to the dissociation of β-arrestin. The receptor is dephosphorylated and recycled to the plasma membrane. Besides, β-arrestins influence many signalling pathways such as ERK, PI3K or NFκB. Downregulation modified from Gurevich and Gurevich (2006) and β-arrestin signalling from Reiter et al. (2012).

1.2 Histamine and histamine receptors

1.2.1 Historical perspective of histamine

Histamine was firstly synthesized by Windaus and Vogt from histidine (Windaus and Vogt, 1907). Three years later, Sir Henry Dale and his colleagues isolated histamine from the mould ergot in the Wellcome Laboratories (Dale and Laidlaw, 1910). Subsequently, Dale and Laidlaw performed studies on the physiological effects of histamine. When injected into animals,

histamine caused contractions of smooth muscles in the gut and the respiratory tract, vasodepression, increase in cardiac contractility and a shock-like syndrome (Dale and Laidlaw, 1910; 1911; 1919; Parsons and Ganellin, 2006). In 1927, histamine was identified as an endogenous substance in the lung and liver (Best et al., 1927).

The finding that histamine induced anaphylaxis and was involved in allergies inspired the search for compounds antagonizing the pathological effects of histamine. The first antihistamines blocking the action of histamine in an anaphylactic reaction were identified in the 1930s (Bovet and Staub, 1937; Fourneau and Bovet, 1933).

1.2.2 Histamine: occurrence and metabolism

Stored in vesicles (granules), histamine predominates in mast cells (Riley and West, 1952), basophils (Falcone et al., 2006) and thrombocytes. Herein, histamine forms an ionic interaction with the acidic mucopolysaccharid heparin. Besides, histamine is stored in enterochromaffin-like cells in the gastric mucosa (Prinz et al., 2003) and acts as a neurotransmitter of histaminergic neurons (Dy and Schneider, 2004).

Histamine features two basic groups with the amine moiety in the side chain being more basic ($pKa_2 = 9.4$) than the nitrogen in the imidazole ring ($pKa_1 = 5.8$). Under physiological conditions (pH = 7.4), the monocationic form (amine in the side chain protonated) predominates (Figure 1.13). However, the monocation is not a single molecular entity, since the imidazole ring can undergo 1,3-tautomerism. In aqueous solution the N^τ-H-tautomer is preferred compared to the N^π-H-nitrogen tautomer (Figure 1.13; Ganellin, 1973).
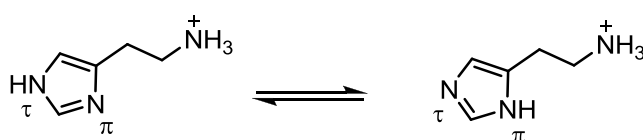
Figure 1.13: 1,3-Tautomerism of imidazole ring in the histamine monocation.

Histamine is a biogenic amine, synthesized from the amino acid L-histidine by the L-histidine-decarboxylase (HDC) (Figure 1.14; Beall and Vanarsdel, 1961). Whereas special transporters are known for catecholamines or serotonin, histamine re-uptake was reported to be mediated by organic cation transporters (OCTs; Gründemann et al., 1999; Schneider et al., 2011; Schneider et al., 2005). The main route of biotransformation and the only one in brain is the N^τ-methylation by histamine-N-methyltransferase (HNMT; Weinshilboum et al., 1999) prior to oxidation by aldehyde dehydrogenase and xanthine oxidase. The second route of inactivation leads to 1-ribosyl-imidazole-4-acetic acid by oxidation and ribosylation (Beall and Vanarsdel, 1961).
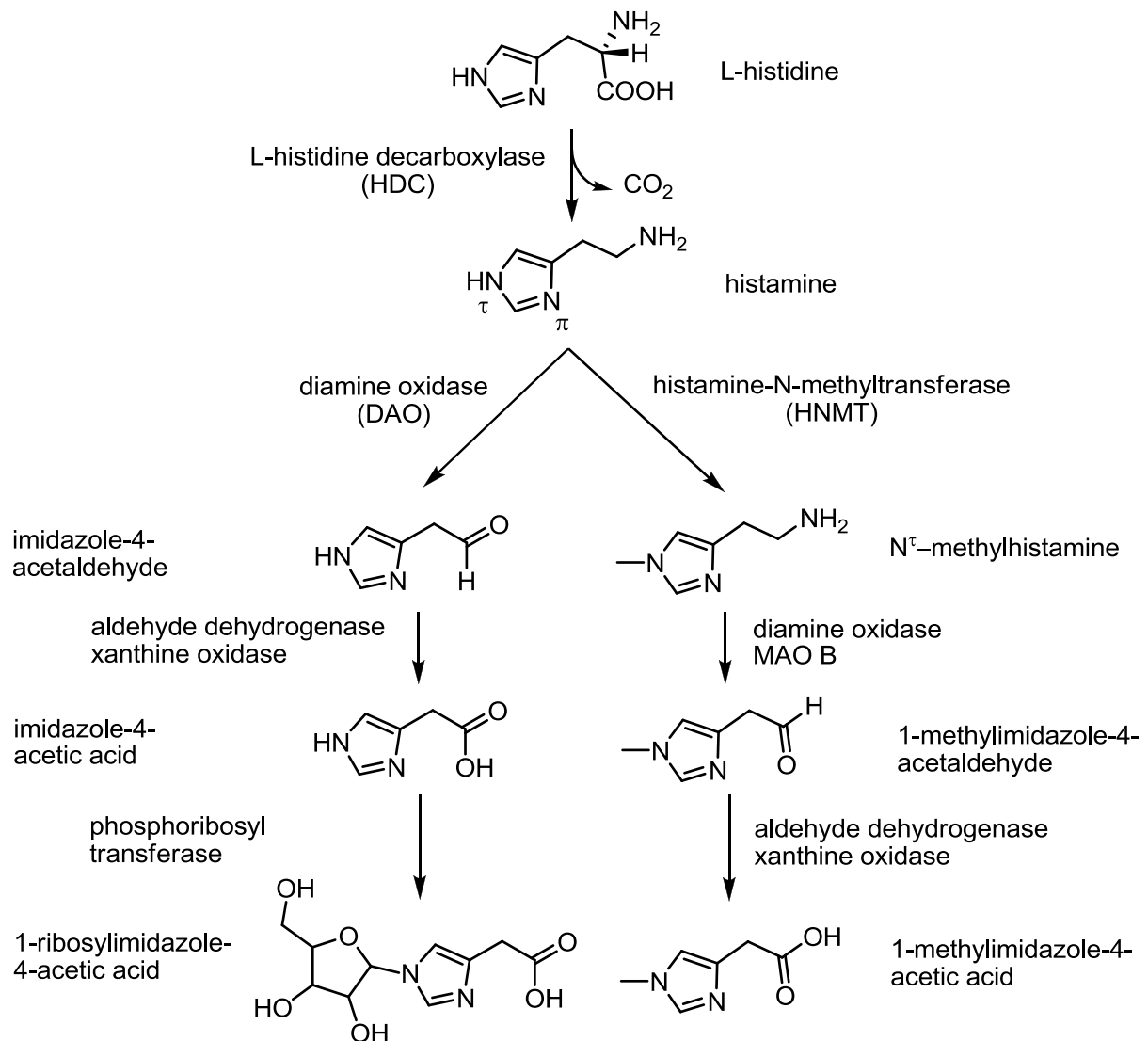
Figure 1.14: Histamine synthesis and metabolism. Modified from Aktories et al. (2006).

1.2.3 Histamine receptor subtypes and ligands

1.2.3.1 Homologies between the four histamine receptor subtypes

Whereas the hH_3R is highly related to the hH_4R (41 % sequence identity; Table 1.1; Hough, 2001; Leurs et al., 2009), the first two histamine receptor subtypes share a relatively low sequence homology to the hH_3R and hH_4R (18-22 % sequence identity; Table 1.1; Leurs et al., 2009; Lovenberg et al., 1999). For example, the hH_1R is more similar to the muscarinic receptors (De Backer et al., 1993), and the hH_2R shares a higher level of sequence identity with the $5\text{-}HT_4R$ or the D_2R-like family than with hH_3R and hH_4R (Vassilatis et al., 2003).

Table 1.1: Homologies (%) between the four human histamine receptor subtypes hH$_1$R, hH$_2$R, hH$_3$R and hH$_4$R.

Receptor	hH$_1$R	hH$_2$R	hH$_3$R	hH$_4$R
hH$_1$R	100			
hH$_2$R	25	100		
hH$_3$R	21	21	100	
hH$_4$R	22	18	41	100

Sequence alignment was performed with Clustal-X 2.1 together with about 80 class A GPCRs. Identities between histamine receptor subtypes hH$_1$R-hH$_4$R were calculated and the number of identical amino acids were divided by the number of amino acids of the respective shorter sequence.

1.2.3.2 Key amino acids of the four histamine receptor subtypes

All histamine receptor subtypes feature the highly conserved residues among class A GPCRs (grey; Mirzadegan et al., 2003), the conserved disulphide bond forming cysteine residues in TM3 and ECL2 (yellow; Strader et al., 1994) as well as the DRY motif (DRF motif in H$_3$R), the FxxCWxP and the NPxxY motif (green; Figure 1.15). The presence of an acidic residue at the bottom of TM6 (D/E$^{6.30}$) enables the H$_1$R, H$_2$R and the H$_3$R, unlike the H$_4$R (A298$^{6.30}$), to form an ionic lock. Besides, the acidic D$^{3.32}$, a very important residue for ligand binding (Gantz et al., 1992; Ohta et al., 1994; Shin et al., 2002), and Y$^{6.51}$ are highly conserved. The in ECL2 located FF motif is highly conserved in case of the H$_3$R and H$_4$R, but replaced by FY in the H$_1$R and VQ in the H$_2$R. S$^{5.43}$, present in case of the H$_3$R and H$_4$R, is replaced by A at the H$_1$R and G at the H$_2$R. Position 5.46 (E in H$_3$R and H$_4$R, N in H$_1$R and T in H$_2$R) has been proven to be very important for ligand binding, in particular in case of agonists (Gantz et al., 1992; Ohta et al., 1994; Shin et al., 2002; Uveges et al., 2002). In TM7, residues, which are probably also involved in ligand binding and activation, are only poorly conserved: This is, e. g., the case for the basic R341$^{7.36}$ at the hH$_4$R, which is replaced by an acidic E at the hH$_3$R and neutral residues (M and A) at the hH$_1$R and hH$_2$R, respectively.

```
              N-term                              TM1              ICL1              TM2
hH₁R   ------MSLPNSSCLLEDKMCEGNKTTMASP--QLMPLVVVLSTICLVTVGLNLLVLYAVRS--ERKLHTVGNLYIVSLSVADLIVGAVVMPMNILYLLM
hH₂R   ......-------MAPNGTASSFCLDST---.ACKITIT...AVLI.I..AG.VV.CL..GLN.-.R.RNLT.CF....AIT..LL.LL.L.FSAI.Q.S
hH₃R   MERAPPDGPL.A.GA.AGEAAAAGGARGF.-AAWTAV.AALMALLIVA..LG.A..ML.FVA.DSSLRT-QN.FFLLN.AIS.FL...FCI.LYVP.V.T
hH₄R   ......-------------.PDT.S.INL.-LSTRVT.AFFM.LVAFAIMLG.A..IL.FVV.DKNLR.-RSSYFFLN.AIS.FF..VISI.LY.PHT.F
       1       10        20        30        40        50        60        70        80        90       100
conserv. 00000000000000011112223111321120010232732226625132361192592392120013113013515355976693359231693131 3291

              ECL1             TM3                  ICL2              TM4                  ECL2
hH₁R   SKWSLGRPLCLFWLSMDYVASTASIFSVFILCIDRYRSVQQPLRYL-KYRTKTRASATILGAWFLSFLWVIPILGWNHFMQQTSVR---REDKCETDFYD
hH₂R   C...F.KVF.NIYT.L.VMLC....LNL.MISL..CA.MD....P.VLV.PV.VAISLVLI.VI.ITLSFLSIHLGWNSRNETSK..GNHTTSKCKVQV
hH₃R   GR.TF..G..KL..VV..LLC.S.A.NIVLISY..FL..TRAVS.RAQQGDTR..VRKM.LV.V.A..LYG.AILSWEYLSGG---SSIP.GH.YAE.FY
hH₄R   -E.DF.KEI.V...TT..LLC...VYNIVLISY..L..SNAVS.RTQHTGVLKIVTLMVAV.V.A..VNG.MILVSESWKDE---GSE----.PG.FS
       110       120       130       140       150       160       170       180       190       200
conserv. 0594496139123333392522979335626722995179233539102112217222265139376331102271111111432000000011112113 311

                         TM5                         ICL3
hH₁R   VTWFKVMTAIINFYLPTLLMLWFYAKIYKAVRQHCQHRELIN-------RSLPSFSEIKLRPENPKGDAKKPGKESPWEVLKRKPKDAGGGSVLKSPSQT
hH₂R   NEVYGLVDGLVT...L.I.CIT.YR.F.VA.D---------.....------------Q..RINHI.-----------------------
hH₃R   NWY.LITASTLE.FT.F.SVTF.NLS..LNIQRRTRL.LDGAREAAGPEPPPEAQPSPPPP.GCWGCWQ.GH.EAM.LHRYGVGEAAV.AEAGEATLGGG
hH₄R   EWYILAI.SFLE.VI.VI.VAY.NMN..WSLWKRDHL-----.......--SRCQ.HPG---------------LTAVSSNICGHSFR.RL.SRR.L.--
       210       220       230       240       250       260       270       280       290       300
conserv. 20121333325492291725111114951231410110000000000000011011110000000001210111310110001110121011111111 00

                                              ICL3
hH₁R   PKEMKSPVVFSQEDDREVDKLYCFPLDIVHMQAAAEGSSRDYVAVNRSHGQLKTDEQGLNTHGASEISEDQMLGDSQSFSRTDSDTTTETAPGKGKLRSG
hH₂R   ----------------------------------------------------------------------------------------------------
hH₃R   -------------------------GGGGSV.SPT.SSGSSSRGTERPRSLKRGSKPSASSA--------------------------------.L
hH₄R   -----------------------ASTEVPA.FHSERQR---RKSSLMFSSRTKMNSN-------------------------------------TI
       310       320       330       340       350       360       370       380       390       400
conserv. 00000000000000000000000000000001111111201011110001111110111111111100000000000000000000000000000000 10

              ICL3                        TM6              ECL3          TM7              H8
hH₁R   SNTGLDYIKFTWKRLRSHSRQYVSGLHMNRERKAAKQLGFIMAAFILCWIPYFIFFMVIAFCKNCCN---EHLHMFTILWGYINSTLNPLIYPLCNENFK
hH₂R   ----------------.WKAATIR------H..TVT.AAV.G...I..F..TA.VYRGLRGDDAIN...V.EAIVL....A..A...IL.AAL.RD.R
hH₃R   EKRMKMVSQS------FTQ.FRL.R-----D..V..S.AV.VSI.G...A..TLLMIIR.A.HGH.V.P.DYWYETSF..LWA..AV..VL....HHS.R
hH₄R   ASKMGSFSQSDSVA.HQREHVELLR-----A.RL..S.AILLGV.AV..A..SL.TI.LS.YSSATG.PKSVWYRIAF..QWF..FV...L...HKR.Q
       410       420       430       440       450       460       470       480       490       500
conserv. 11100111100000001143115210000044726259326522915991991211521311231110004111113299121991599579422333 95

              H8                                            C-term
hH₁R   KTFKRILHIRS------------------------------------------------------
hH₂R   TGYQQLFCC.LANRNS.........HKTSLRSNASQLSRTQSREPRQQEEKPLKLQVWSGTEVTAPQGATDR
hH₃R   RA.TKL.CPQKLKIQPHSSLEHCWK.................................................
hH₄R   .A.LK.FC.KKQPLPSQHSRSVSS.................................................
       510       520       530       540       550       560       570
conserv. 43526663215211111000000000000000000000000000000000000000000000000000000000
```

Figure 1.15: Multiple sequence alignment of the human histamine receptor subtypes hH₁R, hH₂R, hH₃R and hH₄R. Most conserved amino acids among class A GPCRs are coloured in grey, amino acids involved in ligand binding and receptor activation in blue, the two cysteines forming a disulphide bond in yellow and the DRY motif, the FxxCWxP and NPxxY motifs as well as the amino acid 6.30 are coloured in green. Dots in the sequence indicate identity with the hH₁R. Sequence alignment and conservations were computed with Clustal-X 2.1 together with about 80 class A GPCRs. The conservation score ranges from 0 (0 % homology) to 9 (100 % homology). TMs were calculated with DSSP implemented in SYBYL-X 1.3 (Chapter 3.3.2.2).

1.2.3.3 Selectivity profile of histamine receptor ligands

The endogenous ligand histamine binds with high affinity and potency to the hH₃R and hH₄R, with lower affinity to the hH₁R and lowest affinity to the hH₂R (Table 1.2; Seifert et al., 2013). The selectivities of other histamine receptor ligands are described in the following sections.

Table 1.2: Selectivity profiles of various histamine receptor ligands.

Ligand	hH$_1$R	hH$_2$R	hH$_3$R	hH$_4$R
histamine	6.7–6.9 [5.6–5.7][1,2]	5.9–6.0[1,2] [4.3][2,4]	7.6–7.9 [8.2][1,2]	7.6–7.9 [7.9][1,2]
2-methylhistamine	6.1[1,3]			5.4 [6.1][1,3]
histaprodifen	7.0 [6.5][1,2]			4.4 [4.6][1,2]
mepyramine	(8.3) [8.4][1,2]			5.2 [< 4][1,2]
diphenhydramine	[7.9][2,4]	[< 5][2,4]	[< 5][2,4]	n.a.[1,5], [< 5][2,4]
chlorpheniramine				4.6 [4.6][1,5]
cetirizine	[8.0][6]			n.a. [< 4][1,5], [< 5][6]
loratadine	[6.8][6]			n.a. [4.7][1,5], [< 5][6]
terfenadine				n.a. [4.8][1,5]
dimaprit	n.a.[1,2]	5.7–6.0[1,2]		5.8 [6.5][3,7]
amthamine	n.a.[1,2]	6.4–6.7[1,2]		5.3[3,7]
arpromidine	(6.5) [6.5][1,2]	6.7–7.1[1,2]		
cimetidine	[< 5][2,4]	[6.2][2,4]	[< 5][2,4]	[< 5][2,4]
ranitidine	[< 4][2,4]	[7.1][2,4]	[< 5][2,4]	[< 5][2,4]
famotidine		7.3–7.5[1,2]		
N$^\alpha$-methylhistamine			[8.9][1,2], 9.5 [8.2][3,7]	6.6[1,2], 6.2 [6.6][3,7]
immepip			10.4 [9.3][3,7]	7.8 [7.7][3,7]
imetit			[9.2][1,2], 9.9 [8.8][3,7]	8.2[1,2], 7.9 [8.2][3,7]
proxyfan			[7.9][1,2], 8.5 [7.9][3,7]	7.2 [7.3][3,7]
thioperamide	[< 5][2,4]	[< 4][2,4]	7.0 [7.3][1,2]	6.9–7.0 [6.9][1,2]
clobenpropit			9.4 [8.6][3,7]	7.7 [8.1][3,7]
4(5)-methylhistamine	4.8[1,2]	5.5[1,2]	n.a.[1,2]	7.1–7.5 [7.6][1,2]
UR-PI294	5.5[1,2]	6.4[1,2]	8.8[1,2]	8.5[1,2]
VUF8430	n.d.[3,7], [< 4][2,4]	n.d.[3,7], [< 4][2,4]	6.5 [6.0][3,7]	7.3 [7.5][3,7]
UR-PI376	< 5 [4.6][1,2]	< 5 [5.4][1,2]	6.0 [6.3][1,2]	7.5 [7.2][1,2]
OUP-16			5.5 [5.7][3,7]	7.1 [6.9][3,7]
JNJ28610244	[< 5][3,8]	[< 6][3,8]	[< 5][3,8]	7.0 [7.3][3,8]
2-arylbenzimidazole[9]				9.3 [9.7][3,7]
clozapine	(8.4) [8.6][1,2]	(6.3)[1,2]	< 4 [< 4][1,2]	5.8 [5.9][1,2], 6.8 [6.7][3,10]
isoloxapine				7.6 [7.4][10]
JNJ7777120	[4.33][1,2], [< 5][6]	[> 4.5][6]	[5.3][6]	7.4–8.3 [7.5][1,2], [8.4][6]

Intrinsic activity is highlighted in colours: dark green (agonism, 0.75 < α), light green (partial agonism, 0.25 < α ≤ 0.75), orange (neutral antagonism, -0.25 ≤ α ≤ 0.25), light red (partial inverse agonism, -0.25 > α ≥ -0.75) and red (inverse agonism, -0.75 > α). Intrinsic activities from GTPase or [^{35}S]GTPγS assays on Sf9 cells, unless otherwise indicated. Potencies of agonists and inverse agonists are given as pEC$_{50}$ values (without parentheses or brackets), affinities or antagonist activities are given as [pK$_i$] or (pK$_b$), respectively.

1.2.3.4 H$_1$ receptor

In 1966, Ash and Schild introduced the term H$_1$ receptor (H$_1$R) as histamine was obviously exerting its biological effects via two different receptor subtypes (Ash and Schild, 1966). The gene encoding the H$_1$R (487 amino acids) is located on chromosome 3 (genlocus 3q25) and

---

[1]pEC$_{50}$/pK$_b$ determined in GTPase assay, pK$_i$ in competition binding assay on Sf9 insect cells
[2]Seifert et al. (2013)
[3]Igel et al. (2010)
[4]pK$_i$ determined on mammalian cells
[5]Deml et al. (2009)
[6]Thurmond et al. (2008)
[7]pK$_i$ determined in competition binding assay, pEC$_{50}$/α in CRE-β-galactosidase reporter gene assay on SK-N-MC cells
[8]pK$_i$ determined on SK-N-MC cells, pEC$_{50}$/α with SRE-luciferase reporter gene assay
[9]2-arylbenzimidazole as shown in Figure 1.23 (Lee-Dutra et al., 2006)
[10]pK$_i$ determined by displacement with [^{3}H]mepyramine, pEC$_{50}$/α by NFκB-luciferase reporter assay on COS-7 cells

was firstly cloned in 1993 (De Backer et al., 1993). Stimulating $G\alpha_{q/11}$ proteins, the H_1R increases the intracellular calcium level (Chapter 1.1.6.2).

The H_1R is expressed on smooth muscle cells, endothelial cells, in the hearth and in the central nervous system. Mediated by the H_1R, histamine contracts smooth muscle cells, stimulates the production of nitric oxide (NO) and increases the vascular permeability (Hill et al., 1997). Moreover, in allergic reactions arachidonic acid metabolism and prostaglandin synthesis have been shown to play a major role (Carter et al., 1988; Leurs et al., 1994; Murayama et al., 1990; Resink et al., 1987). Furthermore, histamine provokes a negative inotropic effect via the H_1R (Genovese et al., 1988; Guo et al., 1984; Zavecz and Levi, 1978).

Generally, H_1R agonists are interesting pharmacological tools without therapeutic value. However, there is one exception: Betahistine (Aequamen®; Figure 1.16) is approved for the treatment of Menière's disease (Barak, 2008). Starting from histamine as a model compound, H_1R selectivity was achieved by 2-substitution as in 2-methylhistamine or 2-phenylhistamines (Figure 1.16; Leschke et al., 1995). Furthermore, Elz et al. developed a new series of highly selective and potent H_1R-agonists, namely histaprodifen and derivatives (Figure 1.16; Elz et al., 2000a; Elz et al., 2000b). The potency of histaprodifen was further increased by structural modification resulting in suprahistaprodifen (Figure 1.16; Menghin et al., 2003).

betahistine   2-methylhistamine   2-(3-bromophenyl)histamine

histaprodifen   suprahistaprodifen
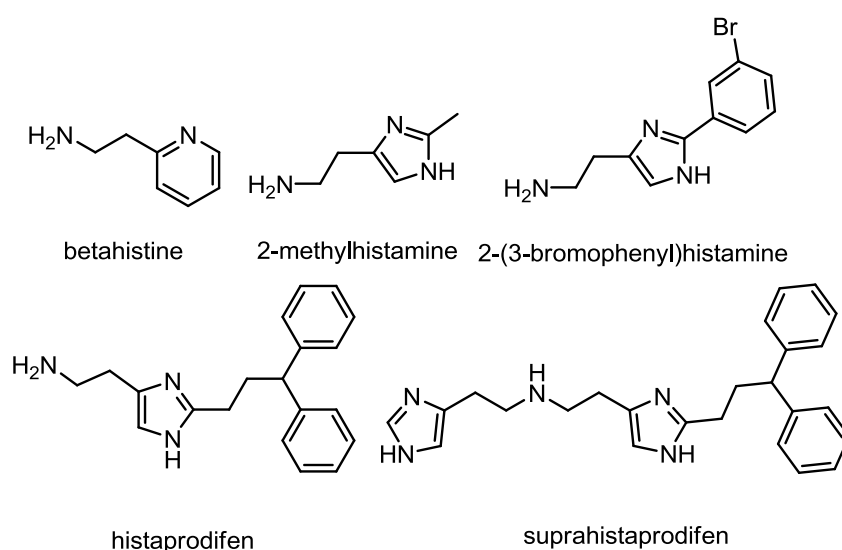
Figure 1.16: Structures of selected H_1R agonists.

H_1R antagonists are well-established drugs for the treatment of allergy symptoms, e. g., in allergic rhinitis, urticaria and pruritus. Systemically available, H_1R antagonists prevent the symptoms of nausea as the H_1R is expressed both in the vestibular apparatus and in the *Nucleus tractus solitarius* (Jensen et al., 2008; Krakauer et al., 2005).

Revealing high selectivity compared to non-H_1 histamine receptor subtypes ($\geq$ 100-fold; Table 1.2; Deml et al., 2009), the H_1R antagonists ("antihistamines") are classified into centrally active compounds of the first generation (mepyramine (Pyrilamine®),

diphenhydramine (Dolestan®) and chlorpheniramine) and compounds without (or with reduced) central availability of the second generation (cetirizine (Zyrtec®), loratadine (Claritine®) and terfenadine (Teldane®)) (Figure 1.17). Second generation H_1R antagonists are (at least theoretically) non-sedating and therefore of advantage in the treatment of allergy symptoms such as allergic rhinitis. Centrally active H_1R antagonists inhibit histamine-induced arousal and can be used as sedatives or hypnotics (Doxylamine, Hydroxyzine (Atarax®)) (Hill et al., 1997).

mepyramine   diphenhydramine   chlorpheniramine

cetirizine   loratadine   terfenadine
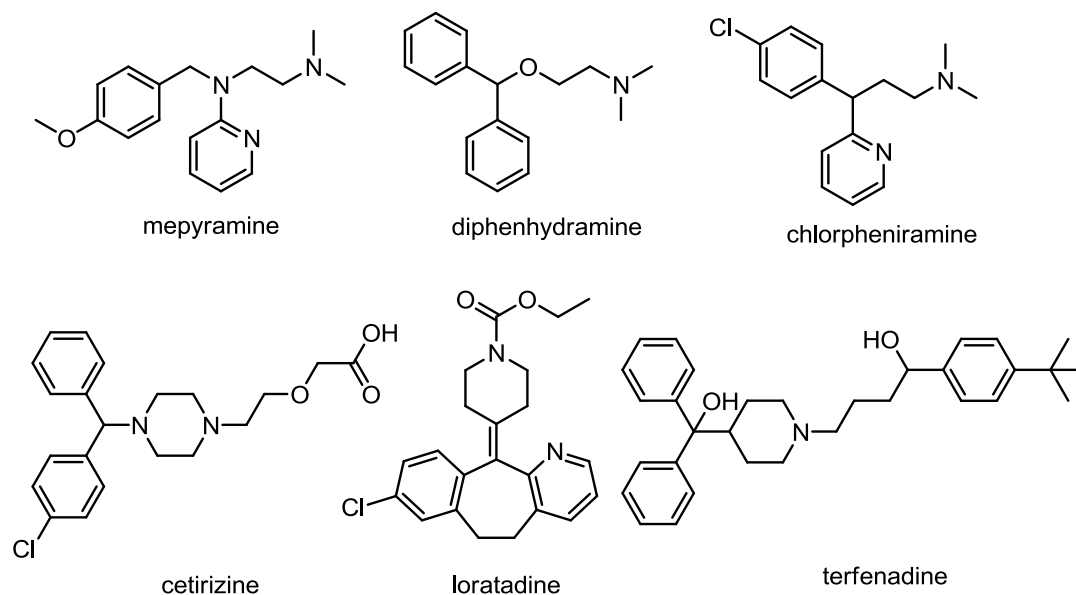
Figure 1.17: Structures of selected H_1R antagonists.

1.2.3.5 H_2 receptor

The existence of the H_2R was confirmed by pharmacological experiments using the first antagonist, burimamide, capable of inhibiting the histamine-stimulated gastric acid secretion and the positive chronotropic response at the heart (Black et al., 1972). The cDNA of the H_2R was cloned by Gantz et al. (1991a; 1991b). The human H_2R gene is located on chromosome 5 (genlocus 5q35). The receptor consists of 359 amino acids and couples to the $G\alpha_s$ protein (Chapter 1.1.6.2).

The H_2R is expressed on the parietal cell of the stomach, on smooth muscle cells, suppressor-T-cells, neutrophils, in the CNS and in the hearth (Hill et al., 1997). Via H_2R-mediated stimulation of the proton pump (H^+/K^+-ATPase) histamine increases gastric acid secretion. H_2R activation results in relaxation of smooth muscles and results in a positive inotropic and chronotropic response in the heart (Hill et al., 1997).

Dimaprit was one of the first H_2R selective agonists (Durant et al., 1977), followed by highly potent and selective guanidine-type ligands (Lim et al., 2005; Seifert et al., 2013) such as impromidine (Durant et al., 1978; Durant et al., 1985), arpromidine (Buschauer, 1989) and

amthamine (Eriks et al., 1992) (Figure 1.18 and Table 1.2). Bivalent agonists revealed dramatically enhanced potency and selectivity (Birnkammer et al., 2012). Interestingly, 30 years ago impromidine, which is not approved as a drug, was very successfully used as an ultima ratio to treat patients suffering from severe catecholamine-insensitive congestive heart failure (Baumann et al., 1984). However, H_2R agonists have not been routinely used in the clinic, but represent valuable pharmacological tools.

dimaprit   amthamine   arpromidine
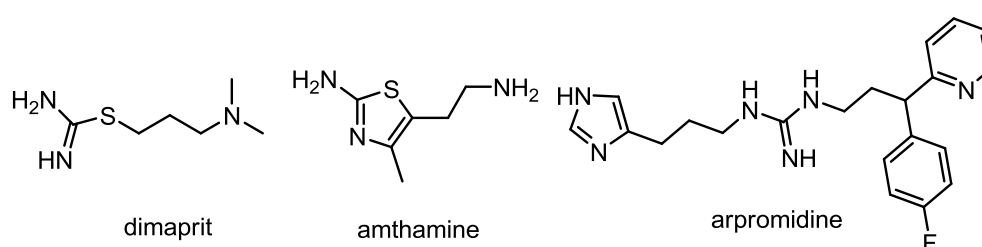
Figure 1.18: Structures of selected H_2R agonists.

Cimetidine (Tagamet®) was the first clinically available H_2R antagonist (Parsons and Ganellin, 2006), followed by non-imidazoles such as ranitidine and famotidine (Figure 1.19 and Table 1.2), which have improved properties, for example, less or no pharmacokinetic interactions due to inhibition of CYP450 enzymes (Parsons and Ganellin, 2006). The H_2R antagonists (Thurmond et al., 2008) had been very important antiulcer drugs over decades, but were replaced by the more effective proton pump inhibitors.

cimetidine   ranitidine   famotidine
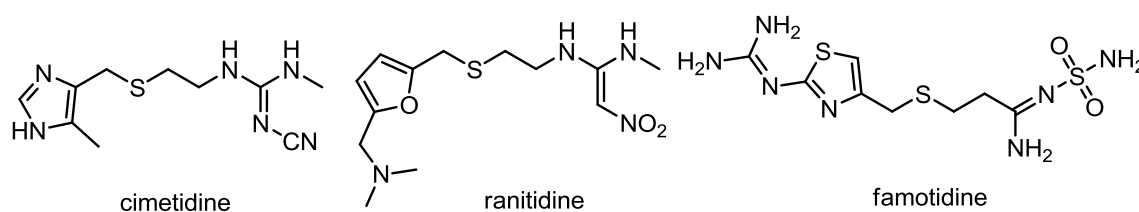
Figure 1.19: Structures of selected H_2R antagonists.

1.2.3.6 H_3 receptor

Arrang et al. (1983) discovered the inhibitory effect of histamine on its own neuronal synthesis and release by a negative feedback mechanism mediated stimulation of presynaptic H_3 autoreceptors. In a further study, the agonist (R)-α-methylhistamine and the inverse agonist thioperamide were used to pharmacologically define the third histamine receptor subtype (Arrang et al., 1987). In 1999, the cloning of the H_3R cDNA was reported (Lovenberg et al., 1999). The gene locus is 20q13.33. Both the H_3R (445 amino acids) and the H_4R are $G\alpha_{i/o}$ coupled GPCRs inhibiting the AC (Clark and Hill, 1996; Seifert et al., 2013).

The H_3R is mainly expressed in the central nervous system with highest densities in the basal ganglia, cortical areas and hippocampus (Martinez-Mir et al., 1990). Apart from its function as a presynaptic autoreceptor, the H_3R is acting as a presynaptic heteroreceptor, modulating the

release of other neurotransmitters such as serotonin, norepinephrine, dopamine and acetylcholine (Gemkow et al., 2009). As a consequence, H_3R stimulation or inhibition can influence the regulation of a broad variety of physiological functions. For example, the H_3R is associated with regulation of food intake, sleep-wake cycle, body temperature and blood pressure. It might furthermore contribute to the pathogenesis of schizophrenia, Parkinson's disease, obesity and attention deficit hyperactivity disorder (ADHD) (Berlin et al., 2011). Recently, the first H_3R ligand, the inverse agonist pitolisant was introduced into the clinic (Figure 1.20; Schwartz, 2011). Pitolisant is applied against excessive diurnal sleepiness of patients with narcolepsy and considered of potential value in the treatment of Parkinson's disease or obstructive sleep apnoea (Schwartz, 2011).

Thioperamide (Arrang et al., 1987) and clobenpropit (van der Goot et al., 1992) were among the first H_3R antagonists described in literature (Figure 1.20). As the H_3R is constitutively active, these ligands act as inverse H_3R agonists, decreasing the elevated level of basal receptor activation (Arrang et al., 2007; Morisset et al., 2000).
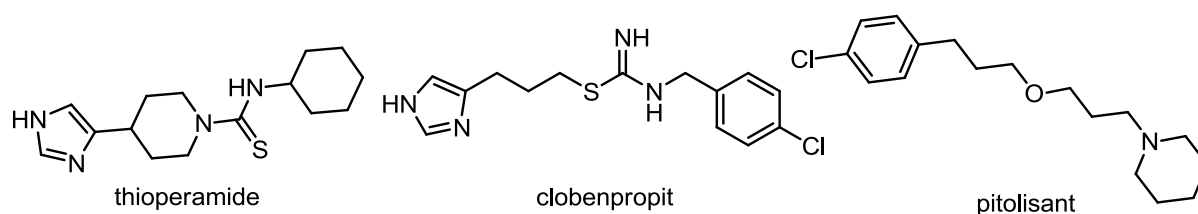
Figure 1.20: Structures of three H_3R inverse agonists.

Numerous H_3R ligands, e. g., (R)-α-methylhistamine, immepip, proxyfan and imetit, were chemically derived from histamine and related compounds (Figure 1.21). It should be stressed that the selectivity for the H_3R compared to the H_4R and vice versa is a major problem, in particular regarding imidazole-type ligands (Chapter 1.2.3.3).
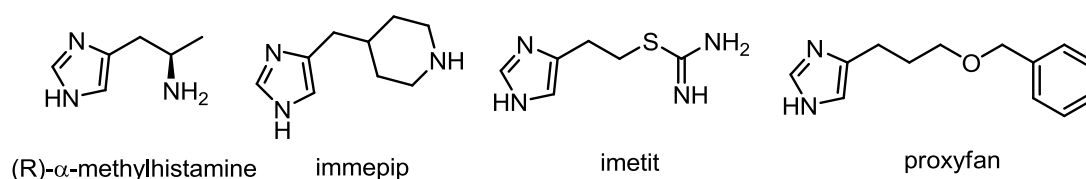
Figure 1.21: Structures of selected H_3R agonists.

1.2.3.7 H_4 receptor

In 1975, Clark et al. reported on a chemotactic effect of histamine on eosinophils. This effect could not be antagonized by H_1R- or H_2R-blockers (Clark et al., 1975). Moreover, the histamine-induced H_3R-mediated increase in cytosolic calcium in human eosinophils (Chapter 1.1.6.2) was not affected by H_1R- and H_2R-antagonists, but could be inhibited by the H_3R-antagonist thioperamide. Ultimately, discrepancies between the potencies of the H_3R

agonists (R)-α-methylhistamine and N^α-methylhistamine on the one hand and histamine on the other hand gave reason to postulate a fourth "eosinophil" histamine receptor (Raible et al., 1994). The 390 amino acid spanning hH4R shares a high sequence homology (41 %) with the hH3R (Chapter 1.2.3.1) and was independently discovered by six research groups at the beginning of the new century (Liu et al., 2001a; Morse et al., 2001; Nakamura et al., 2000; Nguyen et al., 2001; Oda et al., 2000; Zhu et al., 2001). Located on chromosome 18 (genlocus 18q11.2), the H4R contains three exons and two introns (Leurs et al., 2009).

Like the H3R, the H4R inhibits the $G\alpha_{i/o}$ protein, leading to inhibition of the AC and decreasing cAMP levels as well as to activation of phospholipase C-β (PLC-β) via Gβγ complexes (Leurs et al., 2009; Seifert et al., 2013; Thurmond et al., 2008). The hH4R was proven to exhibit higher constitutive activity than the hH3R (Schneider et al., 2009).

In the extracellular space, sodium is the prevailing cation at a concentration of about 140 mM (Katritch et al., 2014). Activation or constitutive activity of several GPCRs, for instance the hH3R or the D2R, were proven to be highly dependent on the sodium chloride concentration (Katritch et al., 2014; Neve et al., 1991; Selent et al., 2010). The conserved amino acid $D^{2.50}$ was found to be strongly involved in sodium-dependent regulation of GPCRs (Fenalti et al., 2014; Katritch et al., 2014; Liu et al., 2012). Sodium ions act as allosteric modulators of GPCRs, stabilizing the inactive state (Katritch et al., 2014). In contrast to other GPCRs, the constitutive activity of the hH4R, mH4R and rH4R is more or less insensitive against sodium chloride (Schneider et al., 2009; Schnell et al., 2011; Wittmann et al., 2014).

The H4R is reported to be mainly expressed on mast cells, basophils, eosinophils, dendritic and T cells (Zampeli and Tiligada, 2009) and to play an essential role in processes such as the migration of immune cells, cytokine release and chemotaxis. H4R antagonists harbour a potential as drugs for the treatment of allergic reactions including bronchial asthma, allergic rhinitis, atopic dermatitis, itch and pruritus as well as of autoimmune diseases such as arthritis (Cowden et al., 2014; de Esch et al., 2005; Dunford and Holgate, 2011; Dunford et al., 2006; Marson, 2011; Pini et al., 2014; Thurmond et al., 2014b; Wifling et al., 2015b; Zampeli and Tiligada, 2009).

In a clinical study in healthy volunteers JNJ39758979 (Figure 1.22; Thurmond et al., 2014a) was demonstrated to inhibit histamine induced pruritus (Kollmeier et al., 2014). The results were interpreted as a proof of concept (Seifert, 2014; Thurmond et al., 2014a). Unfortunately, a phase II clinical trial, evaluating the adverse effects of JNJ39758979, had to be prematurely terminated due to two cases of drug-induced agranulocytosis (Murata et al., 2015).

Due to the high sequence identity, many H3R agonists, for example, N^α-methylhistamine, (R)-α-methylhistamine and immepip, were found to possess agonistic activity at the H4R, too (Figure 1.23; Lim et al., 2005). Imetit as well as proxyfan show lower potency, affinity and

intrinsic activity at the hH$_4$R compared to the hH$_3$R (Figure 1.21 and Table 1.2; Lim et al., 2005). The hH$_3$R inverse agonist clobenpropit turns to partial agonism at the hH$_4$R, albeit with lower potency and affinity compared to the hH$_3$R (Figure 1.23 and Table 1.2; Lim et al., 2009; Lim et al., 2005). 4(5)-Methylhistamine, initially used as a rather weak "selective" agonist for the definition of the H$_2$R by Black et al. (1972), proved to be a highly potent and selective H$_4$R agonist (Figure 1.23 and Table 1.2; Lim et al., 2005). Moreover, the H$_2$R agonist dimaprit and its analogue, the H$_3$R agonist VUF8430, initially described as a weak H$_2$R agonist as well (Sterk et al., 1986), are both H$_4$R agonists (Figure 1.23; Lim et al., 2006; Lim et al., 2005). Revealing good selectivity against the H$_1$R and H$_2$R, the imidazole-containing compound UR-PI294 is equipotent at both the H$_3$R and H$_4$R (Figure 1.23; Igel et al., 2009b). To increase the selectivity for the H$_4$R over the H$_3$R, cyanoguanidines derived from OUP-16 (Hashimoto et al., 2003) were synthesized, for example UR-PI376 (Igel et al., 2009a) and trans-(+)-(1S,3S)-UR-RG98 (Geyer, 2011) (Figure 1.23). These H$_4$R agonists revealed up to 100-fold selectivity over the H$_3$R with even higher selectivity over the H$_1$R and H$_2$R. Derived from the H$_4$R antagonist JNJ7777120, oxime-type ligands such as JNJ28610244 with agonistic activity at the hH$_4$R were developed (Figure 1.23 and Table 1.2). In contrast to other H$_4$R agonists, these oximes were almost equipotent at all investigated H$_4$R species orthologs (human, mouse, rat, guinea pig, monkey and dog H$_4$R; Yu et al., 2010). 2-Arylbenzimidazole-type compounds were developed as new ligand class (Figure 1.23; Lee-Dutra et al., 2006) . Clozapine, known to address numerous GPCRs, binds to all histamine receptor subtypes and acts as a neutral antagonist at the hH$_1$R (highest potency and affinity) and hH$_2$R, a partial inverse agonist at the hH$_3$R (lowest potency and affinity) and partial agonist at the hH$_4$R (Figure 1.23 and Table 1.2; Appl et al., 2011). The clozapine analogue isoloxapine revealed even higher potency and affinity than the parent compound (Figure 1.23; Smits et al., 2006).

thioperamide   JNJ7777120   JNJ39758979
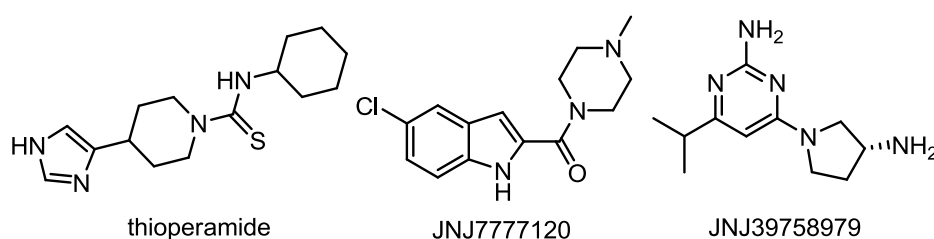
Figure 1.22: Structures of representative H$_4$R antagonists/inverse agonists.

The full inverse agonist thioperamide was shown to be equipotent at the hH$_4$R and the hH$_3$R. The higher maximum of the inverse agonistic effect at the hH$_4$R most probably reflects the higher constitutive activity of the hH$_4$R (Figure 1.22 and Table 1.2; Lim et al., 2005; Seifert et al., 2013). A high-throughput-screening campaign at Johnson & Johnson led to the discovery of the H$_4$R partial inverse agonist JNJ7777120 (Jablonowski et al., 2003), which was reported to possess the same affinity to the hH$_4$R and the rodent H$_4$Rs (Thurmond et al., 2004). Therefore, JNJ7777120 has been widely used as a standard antagonist in animal models

(Beermann et al., 2012; Cowden et al., 2010; Deml et al., 2009; Dunford et al., 2006; Morgan et al., 2007; Rossbach et al., 2009a; Rossbach et al., 2009b; Zampeli et al., 2009). However, the quality of action of JNJ7777120 is species- and assay-dependent. For instance, the compound acts as a partial agonist at the mH_4R, rH_4R and the cH_4R, when investigated in the GTPase assay (Brunskole et al., 2011; Schnell et al., 2011). Therefore, results from animal models should be interpreted with caution. The aforementioned discrepancies might partly be explained with the high constitutive activity of the human H_4R; most other species orthologs, e. g., the rodent H_4Rs, are devoid of constitutive activity (Schnell et al., 2011). Furthermore, JNJ7777120 activates β-arrestins in a $G\alpha_i$ protein independent manner, supporting the idea of functional selectivity or biased signalling (Seifert et al., 2011).
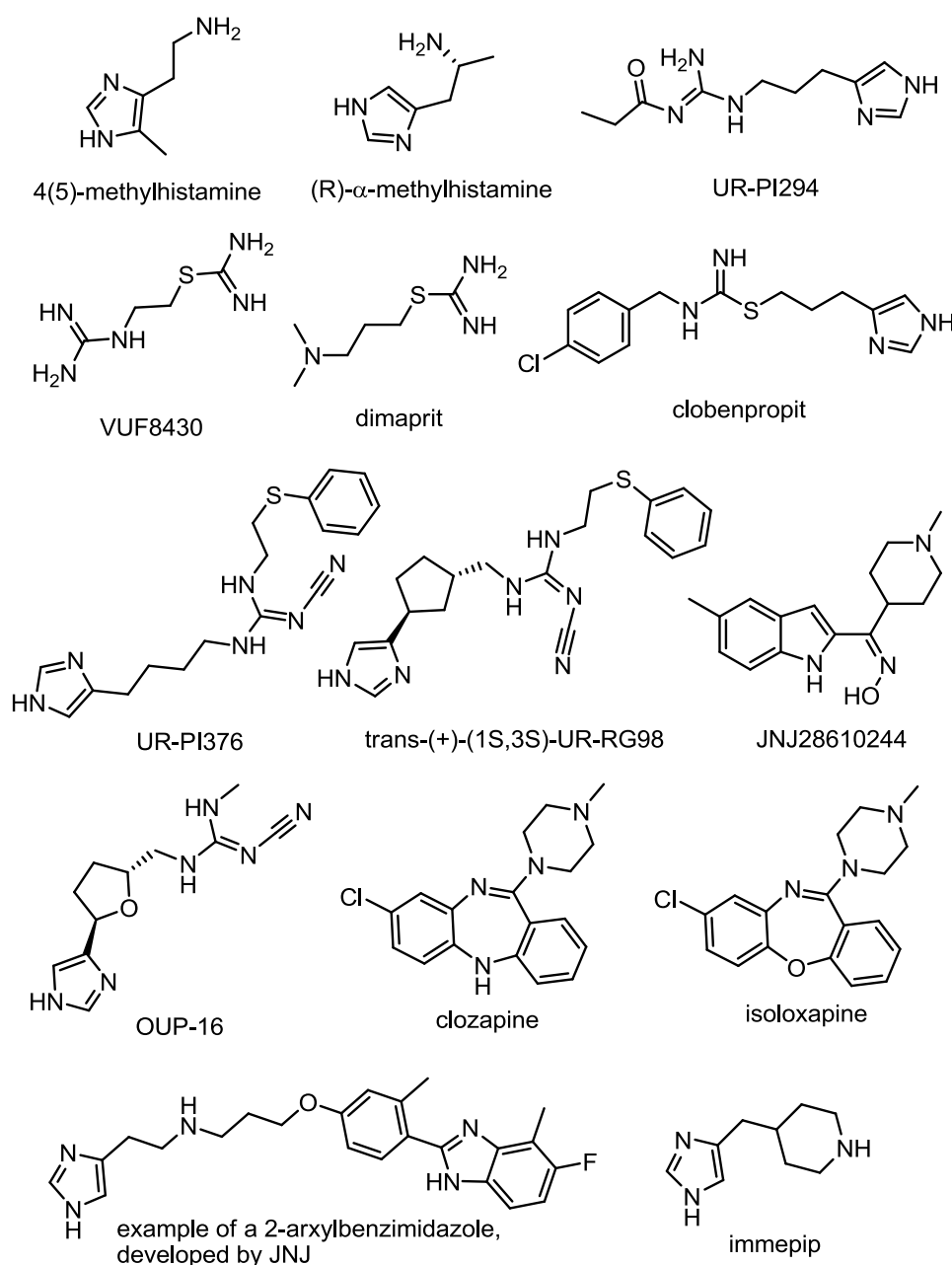
Figure 1.23: Structures of selected H$_4$R agonists.

High affinity H_4R antagonists were identified in different chemical classes of compounds, for example quinazolines (Smits et al., 2008) and 2-aminopyrimidines (Cowart et al., 2008; Mowbray et al., 2011; Savall et al., 2015) (for review on H_4R ligands, see, e. g. Schreeb et al. (2013) and Igel et al. (2010)).

1.3 Species differences

Several H_4R species orthologs, namely rH_4R (rat, *Rattus norvegicus*), mH_4R (murine, *Mus musculus*), gpH_4R (guinea pig, *Cavia porcellus*), pH_4R (porcine, *Sus scrofa*), mkH_4R (monkey, *Macaca fascicularis*) and cH_4R (canine, *Canis lupus familiaris*), were cloned and pharmacologically characterized soon after the exploration of the human H_4R (Jiang et al., 2008; Liu et al., 2001b; Oda et al., 2002; Oda et al., 2005).

1.3.1 Homologies between H_4R species variants

As illustrated in Table 1.3 the sequence homologies between the H_4R orthologs are rather low. Whereas the mkH_4R shares a high homology of 94 % with the hH_4R (Lim et al., 2010), the homology is only 65-69 % between the hH_4R and the rodent receptors, mH_4R, rH_4R and gpH_4R, respectively. The homology between the hH_4R and the cH_4R as well as the pH_4R is equal to 72 %. In conclusion, the hH_4R is most similar to the mkH_4R, the pH_4R to cH_4R and mH_4R to rH_4R, respectively. These different degrees of homology may be reflected by different pharmacological behaviour in a ligand-dependent manner, compromising the value of translational animal models.

Table 1.3: Sequence homologies (%) between different H_4R species variants: hH_4R (human), mkH_4R (monkey), cH_4R (canine), pH_4R (pig), gpH_4R (guinea pig), mH_4R (mouse) and rH_4R (rat).

Receptor	hH_4R	mkH_4R	cH_4R	pH_4R	gpH_4R	mH_4R	rH_4R
hH_4R	100						
mkH_4R	94	100					
cH_4R	72	73	100				
pH_4R	72	73	73	100			
gpH_4R	65	65	63	63	100		
mH_4R	68	68	66	67	63	100	
rH_4R	69	69	65	67	62	85	100

Identities between H_4R species variants were calculated and the number of identical amino acids were divided by the number of amino acids of the respective shorter sequence.

1.3.2 Key amino acids of the H_4R species orthologs

Among the amino acids in the binding pocket, $D94^{3.32}$ (Figure 1.24) plays a key role, as mutation to A, E or N resulted in a complete loss of specific [³H]histamine binding (Shin et al., 2002). Another anchoring point for ligands is $E182^{5.46}$; mutation to A or Q prevented

[³H]histamine binding, and mutation to D decreased affinity about 15-fold (Shin et al., 2002). T178$^{5.42}$, S179$^{5.43}$, N147$^{4.57}$ and S320$^{6.52}$ were found to be of minor relevance for [³H]histamine binding (Shin et al., 2002). Interestingly, the amino acid corresponding to Y95$^{3.33}$ in the hH₄R was shown to fulfil a key role in ligand binding at the M₃R (Han et al., 2005), and the same holds for the M₁R in case of the amino acid corresponding to Y319$^{6.51}$ in the hH₄R (Ward et al., 1999).
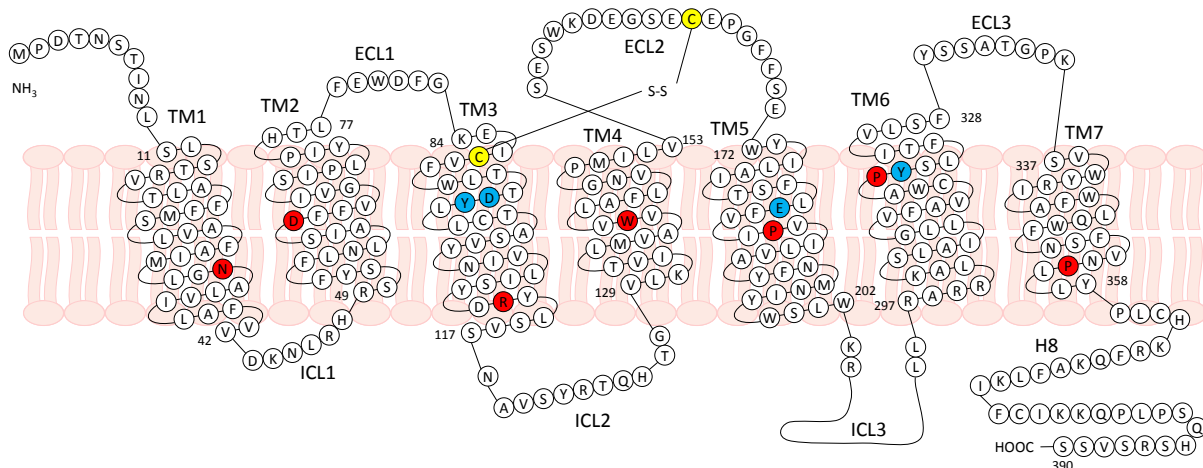
Figure 1.24: Snake plot representation of the hH₄R. Amino acids with highest conservation among class A GPCRs are highlighted in red, amino acids important for ligand binding and activation in blue (D94$^{3.32}$, Y95$^{3.33}$, E182$^{5.46}$ and Y319$^{6.51}$). Cysteines forming a disulphide bridge are marked in yellow. TMs were calculated with DSSP implemented in SYBYL-X 1.3 (Chapter 3.3.2.2).

As illustrated in Figure 1.25, all seven H₄R orthologs share the most conserved amino acids among class A GPCRs (grey; Mirzadegan et al., 2003). Furthermore, most important amino acids involved in the binding and activation process are conserved: D94$^{3.32}$, Y95$^{3.33}$, E182$^{5.46}$ and Y319$^{6.51}$, whereas F169^{ECL2}, S179$^{5.43}$ and R341$^{7.36}$ are poorly conserved among H₄R species orthologs. The FxxCWxP and the NPxxY motifs (green) as well as the two conserved disulphide bond forming cysteines in TM3 and ECL2 (yellow; Strader et al., 1994) are present within all orthologs.

In many GPCRs, e. g., the β₂AR, the DRY motif – positioned at the intracellular part of the receptor – forms the "ionic lock" with an acidic amino acid in TM6 (D/E$^{6.30}$). This ionic lock is not present in the H₄R species orthologs (A/G$^{6.30}$) and was supposed to be the reason for the high constitutive activity of the hH₄R. However, the hH₄R-A6.30E mutant showed only slightly reduced constitutive activity compared to the wild-type (Schneider et al., 2010). The DRY motif was proven to play a key role in the activation of the hH₄R. In particular, the hH₄R-R3.50A mutant did not stimulate G-proteins at all, i. e., agonistic activity was completely lost, suggesting stabilization of the hH₄R inactive state. This is supported by binding data of antagonists and agonists: thioperamide affinity increased by 300-400 %, whereas histamine affinity decreased by ~50 %.

```
              N-term              TM1              ICL1              TM2        ECL1    TM3
hH4R    MPDTNS--TINLSLSTRVTLAFFMSLVAFAIMLGNALVILAFVVDKNLRHRSSYFFLNLAISDFFVGVISIPLYIPHTLFEWDFGKEICVFWLTTDYLLC
mkH4R   ..................I.....L......V.....................M....................
cH4R    .SA..G...T.P...I...L..L....V.......K.....N.....A....M.......D..NKL.A...IA..
pH4R    .SAI.DTN.NT.P.N..IA...L..L.LV....V..............N..L..................K.KLEDN.A...II..
rH4R    .SES.G...DV.P.TAQ.P...L...L....TI...V.....A.R.......N................N.N..SG..M...I..
mH4R    .SES.....GI.PPAAQ.P...L..SF.....V...V......R.....N.........L..L.......V..N.N..SG..M...I..
gpH4R   .LAN......A.T-.IKIS.T.L..L.I....VV.....I..R.....N.......A....A.A.......SS.TY.TS..QA..I..
         1        10        20        30        40        50        60        70        80        90       100
conserv. 9233930091293153456397939934935946995699997596669999959955999996995994979999995393293253243939992499999

              TM3            ICL2            TM4                    ECL2              TM5
hH4R    TASVYNIVLISYDRYLSVSNAVSYRTQHTGVLKIVTLMVAVWVLAFLVNGPMILVSESWKDE------GSECEPGFFSEWYILAITSFLEFVIPVILVAY
mkH4R   ....................I............................T.............V.......
cH4R    .T..........Q........A....I...S.........H..I.....NSSFGVVEEKD......TR..V...S..F..LV..FS..
pH4R    ...........F..Q.......I..A...G....H..V....A..QG....KQD......LK..V....L.F..LA..L...
rH4R    .....S..........Q......R..A...I....AQ......I........A.D...NSTN....TE......VT......A..LL..S..V.
mH4R    ............Q........A....IM..A....I........A.D...NSTN....TKD......VT....T..ML..LL..S..
gpH4R   ...........Q.......W..A...S.TW..A.Q....IFS.MT.....I.D..QNS......TT......LKK..FALP..L..IL..
         110       120       130       140       150       160       170       180       190       200
conserv. 9799969999969992999999299699794399561995996579754996993966975300000024699992459943437233996397222959

              TM5                              ICL3
hH4R    FNMNIYWSLWKRDHLSRCQSHPGLTAVSSNI-CGHSFRGRLSSRRSLSASTEVPASFHSERQRRKSSLMFSSRTKMNSNTIASKMGSFSQSDSVALHQRE
mkH4R   ..................P......S...Q...CG....G........M.V.L.........Y.L......R.............G.....
cH4R    ...Y........GN...W..Q.T..S...SN...SLL..G.F..T...EQK.TAP.VPLK.HE...N.LL.L.AQ...SI.T...A.LTH...LC.....
pH4R    ..LY........GS.......C...P...GS.W.....CG.F..T...DPK.AA..L....P....T.W..L..R.-.SLT..NK.FL.H...L...K.
rH4R    .SVQ........GS...P..A.FI.T...RG.T...R.TG.AC.T..PGLK.PA..L...SP.G....LV.L..H.SGSI...F.V...CR.E.PV.....
mH4R    ..VQ.......RA...P..A.FSTT..SA.S..LH.AGVAC.T.NPGLK.SA..R.....SP....ILV.L..H...SIT.F.V...WR.E.A..R...
gpH4R   .SAH........EK....L...V.PSD..SSDH...C.QDPD..AT.P.RK.TT..LG.DKS......L..I.AYK...V......FL.H...L..Q...
         210       220       230       240       250       260       270       280       290       300
conserv. 9531999999992299992296222342993201942191331293733215923492236426499673293962435522716351313969229497

              ICL3         TM6            ECL3        TM7            H8            C-term
hH4R    HVELLRARRLAKSLAILLGVFAVCWAPYSLFTIVLSFYSSATGPKSVWYRIAFWLQWFNSFVNPLLYPLCHKRFQKAFLKIFCIKKQPLPSQHSRSVSS
mkH4R   .A................E..S...................................................P......
cH4R    .I.....K................IR.I.PLEQR..QI.G.E.T.....L.....F......H..........HM..PSI..-QN.....
pH4R    .L.....K..R...........I....L..TR.V.PTNPF.STAV.KF.....C...F...............L...STL.-.N..T..
rH4R    ......G.K..R...V..SA...I.....C.......T.RRGER...I..S.......LI...F....R......W..L.VT...A..-QTQ....
mH4R    YA....G.K..R...SA..I......C...T.PRTER.............R......R......W..L.VT...AL.-QNQ....
gpH4R   .I..F..K.........AA..I....Y...T.VIY..FPERNLT..T..HT...........F...........LPVRR.ST.P-.N..I.T
         310       320       330       340       350       360       370       380       390
conserv. 4399593969969997993339969999929297419163223135331933379999959927993999999965999919931547532150446959
```

Figure 1.25: Sequence alignment of the histamine H4 receptor orthologs hH4R (human), mkH4R (monkey), cH4R (canine), pH4R (pig), rH4R (rat), mH4R (mouse) and gpH4R (guinea pig). Amino acids with highest conservation among class A GPCRs are coloured in grey. Amino acids involved in the ligand binding and activation process are highlighted in blue, the two cysteine residues forming a disulphide bond in yellow, and the DRY motif, the FxxCWxP motif, the NPxxY motif, as well as the position equivalent to A298[6.30] in the hH4R are coloured in green. Dots in the sequence indicate identity with the hH4R. Sequence alignment and conservations were computed with Clustal-X 2.1: The score ranges from 0 (0 %) to 9 (100 %). TMs were calculated with DSSP implemented in SYBYL-X 1.3 (Chapter 3.3.2.2).

1.3.3 Pharmacological characteristics of H4R species orthologs

Pharmacological differences between the human and monkey H4R became obvious in particular for the ligands clozapine, JNJ7777120 and its analogue VUF6002 (Table 1.4; Lim et al., 2010). Clozapine bound to the monkey H4R with approximately 10 times higher affinity than to the human H4R (pK_i 7.3 vs. 6.4), whereas the antagonists JNJ7777120 and VUF6002 revealed an about 10-fold decrease in affinity from the human to the monkey H4R (pK_i 8.3 vs. 7.5 and 7.5 vs. 6.7) (Lim et al., 2010). However, similar binding and/or functional profiles of histamine, clobenpropit, imetit, (R)-α-methylhistamine, 4(5)-methylhistamine, VUF8430 and thioperamide at both the human and monkey H4R were determined by Lim et al. (2010) and Oda et al. (2005). The mutant hH4R-L175V, bearing the same amino acid as the mkH4R in position 5.39, and the mkH4R showed a similar binding profile for clozapine and JNJ7777120 (Lim et al., 2010), indicating an important contribution of L175[5.39] to different ligand binding profiles at the mkH4R and the hH4R, respectively.

Table 1.4: Effects of H₄R ligands on different H₄R species orthologs.

Ligand	Para-meter	hH$_4$R	mkH$_4$R	cH$_4$R	pH$_4$R	rH$_4$R	mH$_4$R	gpH$_4$R
[³H]histamine	K_d [nM]	9[11], 5[12], 10[13,14], 3[15]	15[11], 3[16]	75[11], 16[13,14], 18[16]	11[11], 4[15]	134[11], 136[12], n.a.[14]	78[11], 42[12], n.a.[14]	11[11], 6[12]
histamine	α	1.0[12,13,14,16,18]	1.0[17]	1.0[13,14,16]	1.0[15,17]	1.0[12,14,18]	1.0[12,14,18]	1.0[12]
	pEC$_{50}$	8.1[12], 7.6[13,15], 7.9[14], 7.3[16,17], 7.8[18]	7.4[17]	6.8[13], 7.1[14], 6.1[16]	6.7[15], 5.9[17]	7.1[12], 5.2[14], 6.5[18]	7.5[12], 5.8[14], 5.9[17], 7.1[18]	8.1[12]
	pK$_i$	7.9[11], 8.2[12], 7.9[13], 8.4[15]	7.8[11]	7.2[11], 7.6[13], 7.5[16]	7.9[11], 7.7[15]	7.0[11], 7.2[12]	7.1[11], 7.4[12]	8.0[11], 7.9[12]
4(5)-methyl-histamine	α	1.0[13,16,18], 0.9[14]		0.9[13,14], 0.8[16]		1.1[14], 1.0[18]	1.0[14,18]	
	pEC$_{50}$	7.1[13], 7.2[14], 7.3[18], 6.9[16]		6.1[13], 6.2[14], 5.2[16]		5.1[14], 6.0[18]	6.0[14], 6.9[18]	
	pK$_i$	7.3[11], 7.6[13], 7.7[14]	7.0[11]	6.3[11], 7.0[16], 6.9[13,14]	7.7[11]	6.4[11]	6.8[11]	7.3[11]
VUF8430	α	1.0[18]				1.0[18]	1.0[18]	
	pEC$_{50}$	7.0[18]				6.1[18]	6.8[18]	
	pK$_i$	7.5[11]	7.3[11]	5.9[11]	6.5[11]	6.8[11]	6.7[11]	6.3[11]
clozapine	α	0.7[13], 1.3[18]		0[13]		1.1[18]	1.0[18]	
	pEC$_{50}$	6.0[13], < 4[15], 7.0[18]		n.a.[13]	< 4[15]	5.7[18]	5.4[18]	
	pK$_i$	6.4[11], 6.2[12], 6.3[13], 6.1[15]	7.3[11]	4.5[11], 3.8[13]	5.2[11], 4.7[15]	5.6[11], 5.7[12]	5.5[11], 5.5[12]	7.3[11], 7.1[12]
immepip	α	1.0[18]				0.9[18]	1.0[18]	
	pEC$_{50}$	7.6[18]				7.2[18]	6.9[18]	
UR-PI294	α	0.9[14], 1.0[18]		0.8[14]		1.6[14], 1.0[18]	1.0[14,18]	
	pEC$_{50}$	8.5[14], 8.7[18]		7.2[14]		4.6[14], 8.2[18]	6.5[14], 8.3[18]	
	pK$_i$	7.8[14]		7.0[14]				
UR-PI376	α	0.9[14], 1.0[18]		0.3[14]		0.4[14], 0.1[18]	0.2[14], 0.5[18]	
	pEC$_{50}$	7.5[14], 7.7[18]		4.8[14]		4.5[14], (5.2)[18]	6.9[14], 6.6[18]	
	pK$_i$	7.1[14]		< 5[14]				
clobenpropit	α	1.0[18]				0.4[18]	0.6[18]	
	pEC$_{50}$	7.0[15], 7.6[17], 7.9[18]	7.2[17]		< 4[15], 5.7[17]	6.8[18]	6.8[17], 6.7[18]	
	pK$_i$	7.5[11], 8.3[12], 8.0[15]	7.5[11]	6.5[11]	6.6[11], 6.4[15]	7.3[11], 7.2[12]	7.3[11], 7.8[12]	8.2[11], 8.8[12]
JNJ7777120	α	-0.2[13], -0.4[14], 0[16], -0.3[18]		0.7[13,14], 0[16]		0.5[14,18]	0.6[14], -0.2[18]	
	pEC$_{50}$	8.3[13], 7.5[14], < 4[16], (7.8)[18]		6.2[13], 6.8[14], < 4[16]		6.5[14], 8.2[18]	6.7[14], (7.6)[18]	
	pK$_i$	8.3[11], 7.5[13,14]	7.5[11]	7.1[11], 6.8[13], 7.0[14], 7.3[16]	6.3[11]	8.4[11]	8.4[11]	6.0[11]
JNJ28610244	α	0.7[19]	0.8[19]			0.9[19]	1.2[19]	
	pEC$_{50}$	7.0[19]	5.9[19]			6.3[19]	6.7[19]	
	pK$_i$	7.3[19]	6.7[19]	5.0[19]		6.7[19]	7.7[19]	6.5[19]
VUF6002	pK$_i$	7.5[11]	6.7[11]	6.2[11]	5.1[11]	7.3[11]	6.9[11]	5.8[11]
thioperamide	α	-0.9[13], -1.0[14], -0.3[18], 0[15]		0.3[13,14]	0[15]	0[14], -0.2[18]	-0.1[14], -0.4[18]	
	pEC$_{50}$	6.9[13,18], 7.0[14]		6.4[13], 6.9[14]		n.a.[14], (6.9)[18]	n.a.[14], 6.5[18]	
	pK$_i$	7.1[11], 7.3[12], 6.9[13,15], 6.3[14]	7.1[11]	6.4[11], 6.7[13], 6.3[14], 7.1[16]	7.0[11], 6.4[15]	7.5[11], 7.6[12]	7.6[11], 7.6[12]	7.1[11], 7.5[12]
(R)-α-methyl-histamine	α	0.8[12], 1.1[16], 1.0[18]		0.6[16]		0.4[12], 1.0[18]	0.8[12], 1.0[18]	0.4[12]
	pEC$_{50}$	7.0[12], 5.8[16], 6.0[15,17], 6.5[18]	6.1[17]	5.5[16]	5.2[15], 5.1[17]	6.0[12], 5.6[18]	6.6[12], 4.9[17], 6.2[18]	6.5[12]
	pK$_i$	6.8[12,15]		7.0[16]	6.6[15]	6.2[12]	6.4[12]	6.7[12]
imetit	α	0.3[12], 0.8[16], 0.9[18]		0.7[16]		0.3[12], 1.0[18]	0.8[12], 1.0[18]	0[12]
	pEC$_{50}$	8.5[12], 7.4[16], 7.5[15], 7.8[17], 7.5[18]	7.3[17]	5.9[16]	6.2[15], 5.9[17]	8.1[12], 7.2[18]	8.1[12], 6.8[17], 7.4[18]	n.a.[12]
	pK$_i$	8.9[12], 8.5[15]		7.3[16]	7.1[15]	8.2[12]	8.2[12]	7.9[12]

Intrinsic activities/potencies/affinities of agonists and inverse agonists are given as α/pEC$_{50}$/pK$_i$ values (without parentheses), and antagonist activities as (pK$_b$); n.a., not applicable.

[11]Lim et al. (2010); transiently transfected HEK 293T cells

[12]Liu et al. (2001b); binding: stably transfected SK-N-MC cells; Ca^{2+} assays: cotransfection of 293-EBNA cells with Gq$_{i5}$ + xH$_4$R

[13]Brunskole et al. (2011); binding and GTPase assays: xH$_4$R co-expressed with Gα$_{i2}$, Gβ$_1$γ$_2$ and GAIP (Sf9 cells)

[14]Schnell et al. (2011); binding and GTPase assays: xH$_4$R co-expressed with Gα$_{i2}$, Gβ$_1$γ$_2$ and GAIP (Sf9 cells)

[15]Oda et al. (2002); binding and cAMP assays: CHO cells transfected with xH$_4$R;

[16]Jiang et al. (2008); binding: transfected COS-7 cells (cH$_4$R), transfected SK-N-MC cells (mkH$_4$R); SRE-luciferase reporter gene assay: HEK 293 cells transfected with SRE-luciferase reporter gene construct, xH$_4$R and Gq$_{i5}$.

[17]Oda et al. (2005); SRE-luciferase reporter gene assay: HEK 293 cells transfected with SRE-luciferase reporter gene construct, xH$_4$R and Gq$_{i5}$

[18]Nordemann et al. (2013); luciferase reporter gene assay: transfected HEK 293T-CRE-Luc cells, co-expressing the CRE-controlled luciferase and xH$_4$R.

[19]Yu et al. (2010); binding: stably transfected SK-N-MC cells; SRE-luciferase reporter gene assay: HEK 293 cells transfected with SRE-luciferase reporter gene construct, xH$_4$R and Gq$_{i5}$.

Differences between human, porcine and canine H_4Rs are reflected by distinct ligand binding and functional data (Table 1.4). VUF8430, clozapine, clobenpropit, JNJ7777120 and VUF6002 revealed a significant decrease in affinity and/or potency at both the cH_4R and pH_4R compared to the hH_4R. By contrast, affinity and/or potency of histamine, 4(5)-methylhistamine and thioperamide were reduced only in case of the cH_4R, but remained nearly constant at the pH_4R (Brunskole et al., 2011; Jiang et al., 2008; Lim et al., 2010; Oda et al., 2002; Oda et al., 2005; Schnell et al., 2011). Both potency and affinity of UR-PI294 and UR-PI376 decreased at the cH_4R compared to the hH_4R (Schnell et al., 2011). Intrinsic activity decreased only in case of UR-PI376. The fact that both JNJ7777120 and thioperamide behaved as partial agonists at the cH_4R implies the absence of constitutive activity at this H_4R species ortholog (Brunskole et al., 2011; Schnell et al., 2011). A site-directed mutagenesis study was performed to identify amino acids determining the pharmacological differences between human and porcine H_4R. $N147^{4.57}$ in the hH_4R was mutated to H, the corresponding residue in the pH_4R and cH_4R, and the double mutant hH_4R-N147H+S179L, corresponding to the amino acids of the pH_4R in positions $147^{4.57}$ and $179^{5.43}$, was generated. These mutants partly mimicked the cH_4R and the pH_4R, but could not fully explain the different ligand binding data at human, porcine and canine H_4Rs (Lim et al., 2010). A chimeric approach revealed the region between the DRY motif and $E182^{5.46}$ to be responsible for different ligand affinities at human and porcine H_4R (Lim et al., 2010). Additionally, a recent chimeric approach identified both ECL2 and ECL3 to contribute to distinct ligand binding and functional properties as well as to different constitutive activities of human and canine H_4R (Brunskole et al., 2011). The respective hH_4R chimera containing either ECL2 or ECL3 of the cH_4R exhibited a binding and functional profile comparable to that of the cH_4R.

Likewise, species-dependent differences in binding and functional data of H_4R ligands became obvious comparing the human and the rodent H_4R orthologs, i. e., the gpH_4R, mH_4R and rH_4R (Table 1.4). Compared to the hH_4R, affinities of VUF8430, JNJ7777120 and VUF6002 significantly decreased at the gpH_4R, whereas the affinities of histamine, 4(5)-methylhistamine and thioperamide remained constant and the affinities of clozapine and clobenpropit even increased (Lim et al., 2010; Liu et al., 2001b). Measured on HEK 293T cells expressing the receptor of interest, the affinities of most investigated ligands decreased at the mouse and rat H_4R orthologs compared to the human H_4R. This in particular holds for the ligands histamine (pK_i: hH_4R, 7.9; mH_4R, 7.1; rH_4R, 7.0), 4(5)-methylhistamine (pK_i: hH_4R, 7.3; mH_4R, 6.8; rH_4R, 6.4), VUF8430 (pK_i: hH_4R, 7.5; mH_4R, 6.7; rH_4R, 6.8) and clozapine (pK_i: hH_4R, 6.4; mH_4R, 5.5; rH_4R, 5.6) (Lim et al., 2010). However, clobenpropit, JNJ7777120 and thioperamide revealed a comparable or even higher affinity at the mouse and rat H_4R orthologs than at the hH_4R (Lim et al., 2010). For these compounds, Nordemann et al. (2013) reported comparable functional data determined in the luciferase gene reporter assay on H_4R orthologs expressed

in HEK 293T cells. By contrast, on membranes of H_4R-expressing Sf9 insect cells, Schnell et al. (2011) determined a very low potency of histamine at the mH_4R (pEC_{50} = 5.8) and rH_4R (pEC_{50} = 5.2) compared to the potency at the hH_4R (pEC_{50} = 7.9). A similar ortholog-dependent selectivity profile was determined for the H_4R agonist UR-PI294. The pharmacological behaviour of many other H_4R ligands changed as well: The human H_4R inverse agonist thioperamide turned to neutral antagonism at the mH_4R and rH_4R. Characteristic of a protean agonist, the intrinsic activity of JNJ7777120 increased from the human H_4R to the mouse and rat H_4R orthologs, turning from partial inverse agonism to partial agonism. Furthermore, the intrinsic activity of UR-PI376 decreased from the hH_4R to the mouse and rat H_4R orthologs. Unfortunately, mutagenesis studies are not available in case of the gpH_4R, but Lim et al. (2008) determined the region between $V141^{4.51}$ and $E182^{5.46}$ to be responsible for differences in agonist affinity between the hH_4R and the mH_4R. In particular, F169 was suggested as "the key amino acid" accounting for differences in the ligand binding profile between hH_4R and mH_4R.

1.4 References

Aktories, K.; Förstermann, U.; Hofmann, F. B.; Starke, K. (2006). *Allgemeine und Spezielle Pharmakologie und Toxikologie*. 9 ed.; Elsevier: München, p 1190.

Alexander, S. P.; Benson, H. E.; Faccenda, E.; Pawson, A. J.; Sharman, J. L.; Spedding, M.; Peters, J. A.; Harmar, A. J. (2013). The Concise Guide to PHARMACOLOGY 2013/14: G protein-coupled receptors. *Br. J. Pharmacol.* 170(8): 1459-1581.

Appl, H.; Holzammer, T.; Dove, S.; Haen, E.; Strasser, A.; Seifert, R. (2011). Interactions of recombinant human histamine H(1)R, H(2)R, H(3)R, and H(4)R receptors with 34 antidepressants and antipsychotics. *Naunyn Schmiedebergs Arch. Pharmacol.* 385(2): 145-170.

Ariens, E. J. (1954). Affinity and intrinsic activity in the theory of competitive inhibition. I. Problems and theory. *Arch. Int. Pharmacodyn. Ther.* 99(1): 32-49.

Arrang, J. M.; Garbarg, M.; Lancelot, J. C.; Lecomte, J. M.; Pollard, H.; Robba, M.; Schunack, W.; Schwartz, J. C. (1987). Highly potent and selective ligands for histamine H3-receptors. *Nature* 327(6118): 117-123.

Arrang, J. M.; Garbarg, M.; Schwartz, J. C. (1983). Auto-inhibition of brain histamine release mediated by a novel class (H3) of histamine receptor. *Nature* 302(5911): 832-837.

Arrang, J. M.; Morisset, S.; Gbahou, F. (2007). Constitutive activity of the histamine H3 receptor. *Trends Pharmacol. Sci.* 28(7): 350-357.

Ash, A. S.; Schild, H. O. (1966). Receptors mediating some actions of histamine. *Br. J. Pharmacol. Chemother.* 27(2): 427-439.

Barak, N. (2008). Betahistine: what's new on the agenda? *Expert Opin. Investig. Drugs* 17(5): 795-804.

Baumann, G.; Permanetter, B.; Wirtzfeld, A. (1984). Possible value of H2-receptor agonists for treatment of catecholamine-insensitive congestive heart failure. *Pharmacol. Ther.* 24(2): 165-177.

Beall, G. N.; Vanarsdel, P. P., Jr. (1961). Histamine metabolism. *Calif. Med.* 95(4): 237-238.

Beermann, S.; Glage, S.; Jonigk, D.; Seifert, R.; Neumann, D. (2012). Opposite effects of mepyramine on JNJ 7777120-induced amelioration of experimentally induced asthma in mice in sensitization and provocation. *PLoS One* 7(1): e30285.

Berlin, M.; Boyce, C. W.; Ruiz Mde, L. (2011). Histamine H3 receptor as a drug discovery target. *J. Med. Chem.* 54(1): 26-53.

Berridge, M. J.; Dawson, R. M.; Downes, C. P.; Heslop, J. P.; Irvine, R. F. (1983). Changes in the levels of inositol phosphates after agonist-dependent hydrolysis of membrane phosphoinositides. *Biochem. J.* 212(2): 473-482.

Best, C. H.; Dale, H. H.; Dudley, H. W.; Thorpe, W. V. (1927). The nature of the vaso-dilator constituents of certain tissue extracts. *J. Physiol.* 62(4): 397-417.

Birnbaumer, L. (2007). Expansion of signal transduction by G proteins. The second 15 years or so: from 3 to 16 alpha subunits plus betagamma dimers. *Biochim. Biophys. Acta* 1768(4): 772-793.

Birnkammer, T.; Spickenreither, A.; Brunskole, I.; Lopuch, M.; Kagermeier, N.; Bernhardt, G.; Dove, S.; Seifert, R.; Elz, S.; Buschauer, A. (2012). The bivalent ligand approach leads to highly potent and selective acylguanidine-type histamine H(2) receptor agonists. *J. Med. Chem.* 55(3): 1147-1160.

Black, J. W.; Duncan, W. A.; Durant, C. J.; Ganellin, C. R.; Parsons, E. M. (1972). Definition and antagonism of histamine H 2 -receptors. *Nature* 236(5347): 385-390.

Black, J. W.; Leff, P. (1983). Operational models of pharmacological agonism. *Proc. R. Soc. Lond. B. Biol. Sci.* 220(1219): 141-162.

Bovet, D.; Staub, A. M. (1937). Action protectrice des éthers phénolique au cours de l'intoxication histaminique. *C. R. Soc. Biol.* 124: 547-549.

Brunskole, I.; Strasser, A.; Seifert, R.; Buschauer, A. (2011). Role of the second and third extracellular loops of the histamine H(4) receptor in receptor activation. *Naunyn Schmiedebergs Arch. Pharmacol.* 384(3): 301-317.

Bünemann, M.; Frank, M.; Lohse, M. J. (2003). Gi protein activation in intact cells involves subunit rearrangement rather than dissociation. *Proc. Natl. Acad. Sci. U. S. A.* 100(26): 16077-16082.

Buschauer, A. (1989). Synthesis and in Vitro Pharmacology of Arpromidine and Related Phenyl(pyridylalkyl)guanidines, a Potential New Class of Positive Inotropic Drugs. *J. Med. Chem.* 32(8): 1963-1970.

Cabrera-Vera, T. M.; Vanhauwe, J.; Thomas, T. O.; Medkova, M.; Preininger, A.; Mazzoni, M. R.; Hamm, H. E. (2003). Insights into G protein structure, function, and regulation. *Endocr. Rev.* 24(6): 765-781.

Carter, T. D.; Hallam, T. J.; Cusack, N. J.; Pearson, J. D. (1988). Regulation of P2y-purinoceptor-mediated prostacyclin release from human endothelial cells by cytoplasmic calcium concentration. *Br. J. Pharmacol.* 95(4): 1181-1190.

Chen, C. A.; Manning, D. R. (2001). Regulation of G proteins by covalent modification. *Oncogene* 20(13): 1643-1652.

Cherezov, V.; Rosenbaum, D. M.; Hanson, M. A.; Rasmussen, S. G.; Thian, F. S.; Kobilka, T. S.; Choi, H. J.; Kuhn, P.; Weis, W. I.; Kobilka, B. K.; Stevens, R. C. (2007). High-resolution crystal structure of an engineered human beta2-adrenergic G protein-coupled receptor. *Science* 318(5854): 1258-1265.

Christopoulos, A. (2014). Advances in G protein-coupled receptor allostery: from function to structure. *Mol. Pharmacol.* 86(5): 463-478.

Clark, A. J. (1933). *The mode of action of drugs on cells*. Edward Arnold: London.

Clark, A. J. (1937). General pharmacology. In *Handbuch der experimentellen Pharmakologie, Ergänzungswerk Band 4*, Heffter, A., Ed. Springer: Berlin, pp 165-176.

Clark, E. A.; Hill, S. J. (1996). Sensitivity of histamine H_3 receptor agonist-stimulated [^{35}S]GTP γ[S] binding to pertussis toxin. *Eur. J. Pharmacol.* 296(2): 223-225.

Clark, R. A.; Gallin, J. I.; Kaplan, A. P. (1975). The selective eosinophil chemotactic activity of histamine. *J. Exp. Med.* 142(6): 1462-1476.

Coleman, D. E.; Berghuis, A. M.; Lee, E.; Linder, M. E.; Gilman, A. G.; Sprang, S. R. (1994). Structures of active conformations of Gi alpha 1 and the mechanism of GTP hydrolysis. *Science* 265(5177): 1405-1412.

Cowart, M. D.; Altenbach, R. J.; Liu, H.; Hsieh, G. C.; Drizin, I.; Milicic, I.; Miller, T. R.; Witte, D. G.; Wishart, N.; Fix-Stenzel, S. R.; McPherson, M. J.; Adair, R. M.; Wetter, J. M.; Bettencourt, B. M.; Marsh, K. C.; Sullivan, J. P.; Honore, P.; Esbenshade, T. A.; Brioni, J. D. (2008). Rotationally constrained 2,4-diamino-5,6-disubstituted pyrimidines: a new class of histamine H4 receptor antagonists with improved druglikeness and in vivo efficacy in pain and inflammation models. *J. Med. Chem.* 51(20): 6547-6557.

Cowden, J. M.; Riley, J. P.; Ma, J. Y.; Thurmond, R. L.; Dunford, P. J. (2010). Histamine H4 receptor antagonism diminishes existing airway inflammation and dysfunction via modulation of Th2 cytokines. *Respir. Res.* 11: 86.

Cowden, J. M.; Yu, F.; Banie, H.; Farahani, M.; Ling, P.; Nguyen, S.; Riley, J. P.; Zhang, M.; Zhu, J.; Dunford, P. J.; Thurmond, R. L. (2014). The histamine H4 receptor mediates inflammation and Th17 responses in preclinical models of arthritis. *Ann. Rheum. Dis.* 73(3): 600-608.

Dale, H. H.; Laidlaw, P. P. (1910). The physiological action of beta-iminazolylethylamine. *J. Physiol.* 41(5): 318-344.

Dale, H. H.; Laidlaw, P. P. (1911). Further observations on the action of beta-iminazolylethylamine. *J. Physiol.* 43(2): 182-195.

Dale, H. H.; Laidlaw, P. P. (1919). Histamine shock. *J. Physiol.* 52(5): 355-390.

Davenport, A. P.; Alexander, S. P.; Sharman, J. L.; Pawson, A. J.; Benson, H. E.; Monaghan, A. E.; Liew, W. C.; Mpamhanga, C. P.; Bonner, T. I.; Neubig, R. R.; Pin, J. P.; Spedding, M.; Harmar, A. J. (2013). International Union of Basic and Clinical Pharmacology. LXXXVIII. G protein-coupled receptor list: recommendations for new pairings with cognate ligands. *Pharmacol. Rev.* 65(3): 967-986.

De Backer, M. D.; Gommeren, W.; Moereels, H.; Nobels, G.; Van Gompel, P.; Leysen, J. E.; Luyten, W. H. (1993). Genomic cloning, heterologous expression and pharmacological characterization of a human histamine H1 receptor. *Biochem. Biophys. Res. Commun.* 197(3): 1601-1608.

de Esch, I. J.; Thurmond, R. L.; Jongejan, A.; Leurs, R. (2005). The histamine H4 receptor as a new therapeutic target for inflammation. *Trends Pharmacol. Sci.* 26(9): 462-469.

De Lean, A.; Stadel, J. M.; Lefkowitz, R. J. (1980). A ternary complex model explains the agonist-specific binding properties of the adenylate cyclase-coupled beta-adrenergic receptor. *J. Biol. Chem.* 255(15): 7108-7117.

Deml, K. F.; Beermann, S.; Neumann, D.; Strasser, A.; Seifert, R. (2009). Interactions of histamine H1-receptor agonists and antagonists with the human histamine H4-receptor. *Mol. Pharmacol.* 76(5): 1019-1030.

DeWire, S. M.; Ahn, S.; Lefkowitz, R. J.; Shenoy, S. K. (2007). Beta-arrestins and cell signaling. *Annu. Rev. Physiol.* 69: 483-510.

Downes, G. B.; Gautam, N. (1999). The G protein subunit gene families. *Genomics* 62(3): 544-552.

Dunford, P. J.; Holgate, S. T. (2011). The role of histamine in asthma. *Adv. Exp. Med. Biol.* 709: 53-66.

Dunford, P. J.; O'Donnell, N.; Riley, J. P.; Williams, K. N.; Karlsson, L.; Thurmond, R. L. (2006). The histamine H4 receptor mediates allergic airway inflammation by regulating the activation of CD4+ T cells. *J. Immunol.* 176(11): 7062-7070.

Dupre, D. J.; Robitaille, M.; Rebois, R. V.; Hebert, T. E. (2009). The role of Gbetagamma subunits in the organization, assembly, and function of GPCR signaling complexes. *Annu. Rev. Pharmacol. Toxicol.* 49: 31-56.

Durant, G. J.; Duncan, W. A.; Ganellin, C. R.; Parsons, M. E.; Blakemore, R. C.; Rasmussen, A. C. (1978). Impromidine (SK&F 92676) is a very potent and specific agonist for histamine H2 receptors. *Nature* 276(5686): 403-405.

Durant, G. J.; Ganellin, C. R.; Hills, D. W.; Miles, P. D.; Parsons, M. E.; Pepper, E. S.; White, G. R. (1985). The histamine H2 receptor agonist impromidine: synthesis and structure-activity considerations. *J. Med. Chem.* 28(10): 1414-1422.

Durant, G. J.; Ganellin, C. R.; Parsons, M. E. (1977). Dimaprit, (S-[3-(N,N-dimethylamino)propyl]isothiourea). A highly specific histamine H2-receptor agonist. Part 2. Structure-activity considerations. *Agents Actions* 7(1): 39-43.

Dy, M.; Schneider, E. (2004). Histamine-cytokine connection in immunity and hematopoiesis. *Cytokine Growth Factor Rev.* 15(5): 393-410.

Elz, S.; Kramer, K.; Leschke, C.; Schunack, W. (2000a). Ring-substituted histaprodifen analogues as partial agonists for histamine H(1) receptors: synthesis and structure-activity relationships. *Eur. J. Med. Chem.* 35(1): 41-52.

Elz, S.; Kramer, K.; Pertz, H. H.; Detert, H.; ter Laak, A. M.; Kuhne, R.; Schunack, W. (2000b). Histaprodifens: synthesis, pharmacological in vitro evaluation, and molecular modeling of a new class of highly active and selective histamine H(1)-receptor agonists. *J. Med. Chem.* 43(6): 1071-1084.

Eriks, J. C.; van der Goot, H.; Sterk, G. J.; Timmerman, H. (1992). Histamine H2-receptor agonists. Synthesis, in vitro pharmacology, and qualitative structure-activity relationships of substituted 4- and 5-(2-aminoethyl)thiazoles. *J. Med. Chem.* 35(17): 3239-3246.

Falcone, F. H.; Zillikens, D.; Gibbs, B. F. (2006). The 21st century renaissance of the basophil? Current insights into its role in allergic responses and innate immunity. *Exp. Dermatol.* 15(11): 855-864.

Fenalti, G.; Giguere, P. M.; Katritch, V.; Huang, X.-P.; Thompson, A. A.; Cherezov, V.; Roth, B. L.; Stevens, R. C. (2014). Molecular control of [dgr]-opioid receptor signalling. *Nature* 506(7487): 191-196.

Foord, S. M.; Bonner, T. I.; Neubig, R. R.; Rosser, E. M.; Pin, J. P.; Davenport, A. P.; Spedding, M.; Harmar, A. J. (2005). International Union of Pharmacology. XLVI. G protein-coupled receptor list. *Pharmacol. Rev.* 57(2): 279-288.

Fourneau, E.; Bovet, D. (1933). Recherches sur l'action sympathicolytique d'un nouveau dérivé du dioxane. *Arch. Int. Pharmacodyn. Ther.* 46: 178-191.

Fredriksson, R.; Lagerström, M. C.; Lundin, L. G.; Schiöth, H. B. (2003). The G-protein-coupled receptors in the human genome form five main families. Phylogenetic analysis, paralogon groups, and fingerprints. *Mol. Pharmacol.* 63(6): 1256-1272.

Furchgott, R. F. (1966). The use of β-haloalkylamines in the differentiation of receptors and in the determination of dissociation constants of receptor-agonist eomplexes. *Adv. Drug Res.* 3: 21-55.

Ganellin, C. R. (1973). The tautomer ratio of histamine. *J. Pharm. Pharmacol.* 25(10): 787-792.

Gantz, I.; DelValle, J.; Wang, L. D.; Tashiro, T.; Munzert, G.; Guo, Y. J.; Konda, Y.; Yamada, T. (1992). Molecular basis for the interaction of histamine with the histamine H2 receptor. *J. Biol. Chem.* 267(29): 20840-20843.

Gantz, I.; Munzert, G.; Tashiro, T.; Schaffer, M.; Wang, L.; DelValle, J.; Yamada, T. (1991a). Molecular cloning of the human histamine H2 receptor. *Biochem. Biophys. Res. Commun.* 178(3): 1386-1392.

Gantz, I.; Schaffer, M.; DelValle, J.; Logsdon, C.; Campbell, V.; Uhler, M.; Yamada, T. (1991b). Molecular cloning of a gene encoding the histamine H2 receptor. *Proc. Natl. Acad. Sci. U. S. A.* 88(13): 5937.

Gemkow, M. J.; Davenport, A. J.; Harich, S.; Ellenbroek, B. A.; Cesura, A.; Hallett, D. (2009). The histamine H3 receptor as a therapeutic drug target for CNS disorders. *Drug Discov. Today* 14(9-10): 509-515.

Genovese, A.; Gross, S. S.; Sakuma, I.; Levi, R. (1988). Adenosine promotes histamine H1-mediated negative chronotropic and inotropic effects on human atrial myocardium. *J. Pharmacol. Exp. Ther.* 247(3): 844-849.

Geyer, R. (2011). Hetarylalkyl(aryl)cyanoguanidines as histamine H4 receptor ligands: Synthesis, chiral separation, pharmacological characterization, structure-activity and -selectivity relationships. PhD thesis, University of Regensburg, Regensburg.

Gilman, A. G. (1987). G proteins: transducers of receptor-generated signals. *Annu. Rev. Biochem.* 56: 615-649.

Goodman, O. B., Jr.; Krupnick, J. G.; Santini, F.; Gurevich, V. V.; Penn, R. B.; Gagnon, A. W.; Keen, J. H.; Benovic, J. L. (1996). Beta-arrestin acts as a clathrin adaptor in endocytosis of the beta2-adrenergic receptor. *Nature* 383(6599): 447-450.

Granier, S.; Kobilka, B. (2012). A new era of GPCR structural and chemical biology. *Nat. Chem. Biol.* 8(8): 670-673.

Gründemann, D.; Liebich, G.; Kiefer, N.; Köster, S.; Schömig, E. (1999). Selective substrates for non-neuronal monoamine transporters. *Mol. Pharmacol.* 56(1): 1-10.

Guo, Z. G.; Levi, R.; Graver, L. M.; Robertson, D. A.; Gay, W. A., Jr. (1984). Inotropic effects of histamine in human myocardium: differentiation between positive and negative components. *J. Cardiovasc. Pharmacol.* 6(6): 1210-1215.

Gurevich, V. V.; Gurevich, E. V. (2006). The structural basis of arrestin-mediated regulation of G-protein-coupled receptors. *Pharmacol. Ther.* 110(3): 465-502.

Haga, K.; Kruse, A. C.; Asada, H.; Yurugi-Kobayashi, T.; Shiroishi, M.; Zhang, C.; Weis, W. I.; Okada, T.; Kobilka, B. K.; Haga, T.; Kobayashi, T. (2012). Structure of the human M2 muscarinic acetylcholine receptor bound to an antagonist. *Nature* 482(7386): 547-551.

Han, S. J.; Hamdan, F. F.; Kim, S. K.; Jacobson, K. A.; Bloodworth, L. M.; Li, B.; Wess, J. (2005). Identification of an agonist-induced conformational change occurring adjacent to the ligand-binding pocket of the M(3) muscarinic acetylcholine receptor. *J. Biol. Chem.* 280(41): 34849-34858.

Hanyaloglu, A. C.; von Zastrow, M. (2008). Regulation of GPCRs by endocytic membrane trafficking and its potential implications. *Annu. Rev. Pharmacol. Toxicol.* 48: 537-568.

Harden, T. K.; Stephens, L.; Hawkins, P. T.; Downes, C. P. (1987). Turkey erythrocyte membranes as a model for regulation of phospholipase C by guanine nucleotides. *J. Biol. Chem.* 262(19): 9057-9061.

Hashimoto, T.; Harusawa, S.; Araki, L.; Zuiderveld, O. P.; Smit, M. J.; Imazu, T.; Takashima, S.; Yamamoto, Y.; Sakamoto, Y.; Kurihara, T.; Leurs, R.; Bakker, R. A.; Yamatodani, A. (2003). A selective human H(4)-receptor agonist: (-)-2-cyano-1-methyl-3-[(2R,5R)-5-[1H-imidazol-4(5)-yl]tetrahydrofuran-2-y] methylguanidine. *J. Med. Chem.* 46(14): 3162-3165.

Hill, S. J.; Ganellin, C. R.; Timmerman, H.; Schwartz, J. C.; Shankley, N. P.; Young, J. M.; Schunack, W.; Levi, R.; Haas, H. L. (1997). International Union of Pharmacology. XIII. Classification of histamine receptors. *Pharmacol. Rev.* 49(3): 253-278.

Hokin, L. E.; Hokin, M. R. (1955). Effects of acetylcholine on the turnover of phosphoryl units in individual phospholipids of pancreas slices and brain cortex slices. *Biochim. Biophys. Acta* 18(1): 102-110.

Hokin, M. R.; Hokin, L. E. (1953). Enzyme secretion and the incorporation of P32 into phospholipides of pancreas slices. *J. Biol. Chem.* 203(2): 967-977.

Hopkins, A. L.; Groom, C. R. (2002). The druggable genome. *Nat. Rev. Drug Discov.* 1(9): 727-730.

Hough, L. B. (2001). Genomics meets histamine receptors: new subtypes, new receptors. *Mol. Pharmacol.* 59(3): 415-419.

Hur, E. M.; Kim, K. T. (2002). G protein-coupled receptor signalling and cross-talk: achieving rapidity and specificity. *Cell. Signal.* 14(5): 397-405.

Hurowitz, E. H.; Melnyk, J. M.; Chen, Y. J.; Kouros-Mehr, H.; Simon, M. I.; Shizuya, H. (2000). Genomic characterization of the human heterotrimeric G protein alpha, beta, and gamma subunit genes. *DNA Res.* 7(2): 111-120.

Igel, P.; Dove, S.; Buschauer, A. (2010). Histamine H4 receptor agonists. *Bioorg. Med. Chem. Lett.* 20(24): 7191-7199.

Igel, P.; Geyer, R.; Strasser, A.; Dove, S.; Seifert, R.; Buschauer, A. (2009a). Synthesis and structure-activity relationships of cyanoguanidine-type and structurally related histamine H4 receptor agonists. *J. Med. Chem.* 52(20): 6297-6313.

Igel, P.; Schneider, E.; Schnell, D.; Elz, S.; Seifert, R.; Buschauer, A. (2009b). N(G)-acylated imidazolylpropylguanidines as potent histamine H4 receptor agonists: selectivity by variation of the N(G)-substituent. *J. Med. Chem.* 52(8): 2623-2627.

Jablonowski, J. A.; Grice, C. A.; Chai, W.; Dvorak, C. A.; Venable, J. D.; Kwok, A. K.; Ly, K. S.; Wei, J.; Baker, S. M.; Desai, P. J.; Jiang, W.; Wilson, S. J.; Thurmond, R. L.; Karlsson, L.; Edwards, J. P.; Lovenberg, T. W.; Carruthers, N. I. (2003). The first potent and selective non-imidazole human histamine H4 receptor antagonists. *J. Med. Chem.* 46(19): 3957-3960.

Jacoby, E.; Bouhelal, R.; Gerspacher, M.; Seuwen, K. (2006). The 7 TM G-protein-coupled receptor target family. *ChemMedChem* 1(8): 761-782.

Jensen, A. A.; Davies, P. A.; Brauner-Osborne, H.; Krzywkowski, K. (2008). 3B but which 3B and that's just one of the questions: the heterogeneity of human 5-HT3 receptors. *Trends Pharmacol. Sci.* 29(9): 437-444.

Jiang, W.; Lim, H. D.; Zhang, M.; Desai, P.; Dai, H.; Colling, P. M.; Leurs, R.; Thurmond, R. L. (2008). Cloning and pharmacological characterization of the dog histamine H4 receptor. *Eur. J. Pharmacol.* 592(1-3): 26-32.

Katritch, V.; Fenalti, G.; Abola, E. E.; Roth, B. L.; Cherezov, V.; Stevens, R. C. (2014). Allosteric sodium in class A GPCR signaling. *Trends Biochem. Sci.* 39(5): 233-244.

Kenakin, T. (2001). Inverse, protean, and ligand-selective agonism: matters of receptor conformation. *FASEB J.* 15(3): 598-611.

Kenakin, T. (2004). Efficacy as a vector: the relative prevalence and paucity of inverse agonism. *Mol. Pharmacol.* 65(1): 2-11.

Kenakin, T. (2009). *A pharmacology primer: theory, applications, and methods.* 3 ed.; Academic Press/Elsevier: Amsterdam; Boston, p 416.

Khan, S. M.; Sleno, R.; Gora, S.; Zylbergold, P.; Laverdure, J. P.; Labbe, J. C.; Miller, G. J.; Hebert, T. E. (2013). The expanding roles of Gbetagamma subunits in G protein-coupled receptor signaling and drug action. *Pharmacol. Rev.* 65(2): 545-577.

Kling, R. C.; Lanig, H.; Clark, T.; Gmeiner, P. (2013). Active-state models of ternary GPCR complexes: determinants of selective receptor-G-protein coupling. *PLoS One* 8(6): e67244.

Kolakowski, L. F., Jr. (1994). GCRDb: a G-protein-coupled receptor database. *Receptors Channels* 2(1): 1-7.

Kollmeier, A.; Francke, K.; Chen, B.; Dunford, P. J.; Greenspan, A. J.; Xia, Y.; Xu, X. L.; Zhou, B.; Thurmond, R. L. (2014). The histamine H(4) receptor antagonist, JNJ 39758979, is effective in reducing histamine-induced pruritus in a randomized clinical study in healthy subjects. *J. Pharmacol. Exp. Ther.* 350(1): 181-187.

Krakauer, E. L.; Zhu, A. X.; Bounds, B. C.; Sahani, D.; McDonald, K. R.; Brachtel, E. F. (2005). Case records of the Massachusetts General Hospital. Weekly clinicopathological exercises. Case 6-2005. A 58-year-old man with esophageal cancer and nausea, vomiting, and intractable hiccups. *N. Engl. J. Med.* 352(8): 817-825.

Kruse, A. C.; Hu, J.; Pan, A. C.; Arlow, D. H.; Rosenbaum, D. M.; Rosemond, E.; Green, H. F.; Liu, T.; Chae, P. S.; Dror, R. O.; Shaw, D. E.; Weis, W. I.; Wess, J.; Kobilka, B. K. (2012). Structure and dynamics of the M3 muscarinic acetylcholine receptor. *Nature* 482(7386): 552-556.

Kruse, A. C.; Kobilka, B. K.; Gautam, D.; Sexton, P. M.; Christopoulos, A.; Wess, J. (2014). Muscarinic acetylcholine receptors: novel opportunities for drug development. *Nat. Rev. Drug Discov.* 13(7): 549-560.

Kruse, A. C.; Ring, A. M.; Manglik, A.; Hu, J.; Hu, K.; Eitel, K.; Hubner, H.; Pardon, E.; Valant, C.; Sexton, P. M.; Christopoulos, A.; Felder, C. C.; Gmeiner, P.; Steyaert, J.; Weis, W. I.; Garcia, K. C.; Wess, J.; Kobilka, B. K. (2013). Activation and allosteric modulation of a muscarinic acetylcholine receptor. *Nature* 504(7478): 101-106.

Lagerström, M. C.; Schiöth, H. B. (2008). Structural diversity of G protein-coupled receptors and significance for drug discovery. *Nat. Rev. Drug Discov.* 7(4): 339-357.

Lee-Dutra, A.; Arienti, K. L.; Buzard, D. J.; Hack, M. D.; Khatuya, H.; Desai, P. J.; Nguyen, S.; Thurmond, R. L.; Karlsson, L.; Edwards, J. P.; Breitenbucher, J. G. (2006). Identification of 2-arylbenzimidazoles as potent human histamine H4 receptor ligands. *Bioorg. Med. Chem. Lett.* 16(23): 6043-6048.

Lefkowitz, R. J.; Cotecchia, S.; Samama, P.; Costa, T. (1993). Constitutive activity of receptors coupled to guanine nucleotide regulatory proteins. *Trends Pharmacol. Sci.* 14(8): 303-307.

Leschke, C.; Elz, S.; Garbarg, M.; Schunack, W. (1995). Synthesis and histamine H1 receptor agonist activity of a series of 2-phenylhistamines, 2-heteroarylhistamines, and analogues. *J. Med. Chem.* 38(8): 1287-1294.

Leurs, R.; Chazot, P. L.; Shenton, F. C.; Lim, H. D.; de Esch, I. J. (2009). Molecular and biochemical pharmacology of the histamine H4 receptor. *Br. J. Pharmacol.* 157(1): 14-23.

Leurs, R.; Traiffort, E.; Arrang, J. M.; Tardivel-Lacombe, J.; Ruat, M.; Schwartz, J. C. (1994). Guinea pig histamine H1 receptor. II. Stable expression in Chinese hamster ovary cells reveals the interaction with three major signal transduction pathways. *J. Neurochem.* 62(2): 519-527.

Lim, H. D.; de Graaf, C.; Jiang, W.; Sadek, P.; McGovern, P. M.; Istyastono, E. P.; Bakker, R. A.; de Esch, I. J.; Thurmond, R. L.; Leurs, R. (2010). Molecular determinants of ligand binding to H4R species variants. *Mol. Pharmacol.* 77(5): 734-743.

Lim, H. D.; Istyastono, E. P.; van de Stolpe, A.; Romeo, G.; Gobbi, S.; Schepers, M.; Lahaye, R.; Menge, W. M.; Zuiderveld, O. P.; Jongejan, A.; Smits, R. A.; Bakker, R. A.; Haaksma, E. E.; Leurs, R.; de Esch, I. J. (2009). Clobenpropit analogs as dual activity ligands for

the histamine H3 and H4 receptors: synthesis, pharmacological evaluation, and cross-target QSAR studies. *Bioorg. Med. Chem.* 17(11): 3987-3994.

Lim, H. D.; Jongejan, A.; Bakker, R. A.; Haaksma, E.; de Esch, I. J.; Leurs, R. (2008). Phenylalanine 169 in the second extracellular loop of the human histamine H4 receptor is responsible for the difference in agonist binding between human and mouse H4 receptors. *J. Pharmacol. Exp. Ther.* 327(1): 88-96.

Lim, H. D.; Smits, R. A.; Bakker, R. A.; van Dam, C. M.; de Esch, I. J.; Leurs, R. (2006). Discovery of S-(2-guanidylethyl)-isothiourea (VUF 8430) as a potent nonimidazole histamine H4 receptor agonist. *J. Med. Chem.* 49(23): 6650-6651.

Lim, H. D.; van Rijn, R. M.; Ling, P.; Bakker, R. A.; Thurmond, R. L.; Leurs, R. (2005). Evaluation of histamine H1-, H2-, and H3-receptor ligands at the human histamine H4 receptor: identification of 4-methylhistamine as the first potent and selective H4 receptor agonist. *J. Pharmacol. Exp. Ther.* 314(3): 1310-1321.

Liu, C.; Ma, X.; Jiang, X.; Wilson, S. J.; Hofstra, C. L.; Blevitt, J.; Pyati, J.; Li, X.; Chai, W.; Carruthers, N.; Lovenberg, T. W. (2001a). Cloning and pharmacological characterization of a fourth histamine receptor (H(4)) expressed in bone marrow. *Mol. Pharmacol.* 59(3): 420-426.

Liu, C.; Wilson, S. J.; Kuei, C.; Lovenberg, T. W. (2001b). Comparison of human, mouse, rat, and guinea pig histamine H4 receptors reveals substantial pharmacological species variation. *J. Pharmacol. Exp. Ther.* 299(1): 121-130.

Liu, J.; Erlichman, B.; Weinstein, L. S. (2003). The stimulatory G protein alpha-subunit Gs alpha is imprinted in human thyroid glands: implications for thyroid function in pseudohypoparathyroidism types 1A and 1B. *J. Clin. Endocrinol. Metab.* 88(9): 4336-4341.

Liu, W.; Chun, E.; Thompson, A. A.; Chubukov, P.; Xu, F.; Katritch, V.; Han, G. W.; Roth, C. B.; Heitman, L. H.; AP, I. J.; Cherezov, V.; Stevens, R. C. (2012). Structural basis for allosteric regulation of GPCRs by sodium ions. *Science* 337(6091): 232-236.

Lovenberg, T. W.; Roland, B. L.; Wilson, S. J.; Jiang, X.; Pyati, J.; Huvar, A.; Jackson, M. R.; Erlander, M. G. (1999). Cloning and functional expression of the human histamine H3 receptor. *Mol. Pharmacol.* 55(6): 1101-1107.

Luttrell, L. M. (2008). Reviews in molecular biology and biotechnology: transmembrane signaling by G protein-coupled receptors. *Mol. Biotechnol.* 39(3): 239-264.

Luttrell, L. M.; Gesty-Palmer, D. (2010). Beyond desensitization: physiological relevance of arrestin-dependent signaling. *Pharmacol. Rev.* 62(2): 305-330.

Luttrell, L. M.; Lefkowitz, R. J. (2002). The role of beta-arrestins in the termination and transduction of G-protein-coupled receptor signals. *J. Cell Sci.* 115(Pt 3): 455-465.

Marson, C. M. (2011). Targeting the histamine H4 receptor. *Chem. Rev.* 111(11): 7121-7156.

Martinez-Mir, M. I.; Pollard, H.; Moreau, J.; Arrang, J. M.; Ruat, M.; Traiffort, E.; Schwartz, J. C.; Palacios, J. M. (1990). Three histamine receptors (H1, H2 and H3) visualized in the brain of human and non-human primates. *Brain Res.* 526(2): 322-327.

Menghin, S.; Pertz, H. H.; Kramer, K.; Seifert, R.; Schunack, W.; Elz, S. (2003). N(alpha)-imidazolylalkyl and pyridylalkyl derivatives of histaprodifen: synthesis and in vitro

evaluation of highly potent histamine H(1)-receptor agonists. *J. Med. Chem.* 46(25): 5458-5470.

Mirzadegan, T.; Benko, G.; Filipek, S.; Palczewski, K. (2003). Sequence analyses of G-protein-coupled receptors: similarities to rhodopsin. *Biochemistry* 42(10): 2759-2767.

Morgan, R. K.; McAllister, B.; Cross, L.; Green, D. S.; Kornfeld, H.; Center, D. M.; Cruikshank, W. W. (2007). Histamine 4 receptor activation induces recruitment of FoxP3+ T cells and inhibits allergic asthma in a murine model. *J. Immunol.* 178(12): 8081-8089.

Morisset, S.; Rouleau, A.; Ligneau, X.; Gbahou, F.; Tardivel-Lacombe, J.; Stark, H.; Schunack, W.; Ganellin, C. R.; Schwartz, J. C.; Arrang, J. M. (2000). High constitutive activity of native H3 receptors regulates histamine neurons in brain. *Nature* 408(6814): 860-864.

Morse, K. L.; Behan, J.; Laz, T. M.; West, R. E., Jr.; Greenfeder, S. A.; Anthes, J. C.; Umland, S.; Wan, Y.; Hipkin, R. W.; Gonsiorek, W.; Shin, N.; Gustafson, E. L.; Qiao, X.; Wang, S.; Hedrick, J. A.; Greene, J.; Bayne, M.; Monsma, F. J., Jr. (2001). Cloning and Characterization of a Novel Human Histamine Receptor. *J. Pharmacol. Exp. Ther.* 296(3): 1058-1066.

Mowbray, C. E.; Bell, A. S.; Clarke, N. P.; Collins, M.; Jones, R. M.; Lane, C. A.; Liu, W. L.; Newman, S. D.; Paradowski, M.; Schenck, E. J.; Selby, M. D.; Swain, N. A.; Williams, D. H. (2011). Challenges of drug discovery in novel target space. The discovery and evaluation of PF-3893787: a novel histamine H4 receptor antagonist. *Bioorg. Med. Chem. Lett.* 21(21): 6596-6602.

Murata, Y.; Song, M.; Kikuchi, H.; Hisamichi, K.; Xu, X. L.; Greenspan, A.; Kato, M.; Chiou, C. F.; Kato, T.; Guzzo, C.; Thurmond, R. L.; Ohtsuki, M.; Furue, M. (2015). Phase 2a, randomized, double-blind, placebo-controlled, multicenter, parallel-group study of a H4 R-antagonist (JNJ-39758979) in Japanese adults with moderate atopic dermatitis. *J. Dermatol.* 42(2): 129-139.

Murayama, T.; Kajiyama, Y.; Nomura, Y. (1990). Histamine-stimulated and GTP-binding proteins-mediated phospholipase A2 activation in rabbit platelets. *J. Biol. Chem.* 265(8): 4290-4295.

Nakamura, T.; Itadani, H.; Hidaka, Y.; Ohta, M.; Tanaka, K. (2000). Molecular cloning and characterization of a new human histamine receptor, HH4R. *Biochem. Biophys. Res. Commun.* 279(2): 615-620.

Neitzel, K. L.; Hepler, J. R. (2006). Cellular mechanisms that determine selective RGS protein regulation of G protein-coupled receptor signaling. *Semin. Cell Dev. Biol.* 17(3): 383-389.

Neve, K. A.; Cox, B. A.; Henningsen, R. A.; Spanoyannis, A.; Neve, R. L. (1991). Pivotal role for aspartate-80 in the regulation of dopamine D2 receptor affinity for drugs and inhibition of adenylyl cyclase. *Mol. Pharmacol.* 39(6): 733-739.

Neves, S. R.; Ram, P. T.; Iyengar, R. (2002). G protein pathways. *Science* 296(5573): 1636-1639.

Nguyen, T.; Shapiro, D. A.; George, S. R.; Setola, V.; Lee, D. K.; Cheng, R.; Rauser, L.; Lee, S. P.; Lynch, K. R.; Roth, B. L.; O'Dowd, B. F. (2001). Discovery of a novel member of the histamine receptor family. *Mol. Pharmacol.* 59(3): 427-433.

Nordemann, U.; Wifling, D.; Schnell, D.; Bernhardt, G.; Stark, H.; Seifert, R.; Buschauer, A. (2013). Luciferase reporter gene assay on human, murine and rat histamine H4 receptor

orthologs: correlations and discrepancies between distal and proximal readouts. *PLoS One* 8(9): e73961.

Oda, T.; Matsumoto, S.; Masuho, Y.; Takasaki, J.; Matsumoto, M.; Kamohara, M.; Saito, T.; Ohishi, T.; Soga, T.; Hiyama, H.; Matsushime, H.; Furuichi, K. (2002). cDNA cloning and characterization of porcine histamine H4 receptor. *Biochim. Biophys. Acta* 1575(1-3): 135-138.

Oda, T.; Matsumoto, S.; Matsumoto, M.; Takasaki, J.; Kamohara, M.; Soga, T.; Hiyama, H.; Kobori, M.; Katoh, M. (2005). Molecular cloning of monkey histamine H4 receptor. *J. Pharmacol. Sci.* 98(3): 319-322.

Oda, T.; Morikawa, N.; Saito, Y.; Masuho, Y.; Matsumoto, S. (2000). Molecular cloning and characterization of a novel type of histamine receptor preferentially expressed in leukocytes. *J. Biol. Chem.* 275(47): 36781-36786.

Ohta, K.; Hayashi, H.; Mizuguchi, H.; Kagamiyama, H.; Fujimoto, K.; Fukui, H. (1994). Site-directed mutagenesis of the histamine H1 receptor: roles of aspartic acid107, asparagine198 and threonine194. *Biochem. Biophys. Res. Commun.* 203(2): 1096-1101.

Palczewski, K.; Kumasaka, T.; Hori, T.; Behnke, C. A.; Motoshima, H.; Fox, B. A.; Le Trong, I.; Teller, D. C.; Okada, T.; Stenkamp, R. E.; Yamamoto, M.; Miyano, M. (2000). Crystal structure of rhodopsin: A G protein-coupled receptor. *Science* 289(5480): 739-745.

Parsons, M. E.; Ganellin, C. R. (2006). Histamine and its receptors. *Br. J. Pharmacol.* 147 Suppl 1: S127-135.

Pawson, A. J.; Sharman, J. L.; Benson, H. E.; Faccenda, E.; Alexander, S. P.; Buneman, O. P.; Davenport, A. P.; McGrath, J. C.; Peters, J. A.; Southan, C.; Spedding, M.; Yu, W.; Harmar, A. J.; Nc, I. (2014). The IUPHAR/BPS Guide to PHARMACOLOGY: an expert-driven knowledgebase of drug targets and their ligands. *Nucleic Acids Res.* 42(Database issue): D1098-1106.

Pennisi, E. (2012). Genomics. ENCODE project writes eulogy for junk DNA. *Science* 337(6099): 1159, 1161.

Pini, A.; Somma, T.; Formicola, G.; Lucarini, L.; Bani, D.; Thurmond, R.; Masini, E. (2014). Effects of a selective histamine H(4)R antagonist on inflammation in a model of carrageenan-induced pleurisy in the rat. *Curr. Pharm. Des.* 20(9): 1338-1344.

Prinz, C.; Zanner, R.; Gratzl, M. (2003). Physiology of gastric enterochromaffin-like cells. *Annu. Rev. Physiol.* 65: 371-382.

Raible, D. G.; Lenahan, T.; Fayvilevich, Y.; Kosinski, R.; Schulman, E. S. (1994). Pharmacologic characterization of a novel histamine receptor on human eosinophils. *Am. J. Respir. Crit. Care Med.* 149(6): 1506-1511.

Rask-Andersen, M.; Almen, M. S.; Schioth, H. B. (2011). Trends in the exploitation of novel drug targets. *Nat. Rev. Drug Discov.* 10(8): 579-590.

Rask-Andersen, M.; Masuram, S.; Schioth, H. B. (2014). The druggable genome: Evaluation of drug targets in clinical trials suggests major shifts in molecular class and indication. *Annu. Rev. Pharmacol. Toxicol.* 54: 9-26.

Rasmussen, S. G.; Choi, H. J.; Fung, J. J.; Pardon, E.; Casarosa, P.; Chae, P. S.; Devree, B. T.; Rosenbaum, D. M.; Thian, F. S.; Kobilka, T. S.; Schnapp, A.; Konetzki, I.; Sunahara,

R. K.; Gellman, S. H.; Pautsch, A.; Steyaert, J.; Weis, W. I.; Kobilka, B. K. (2011a). Structure of a nanobody-stabilized active state of the beta(2) adrenoceptor. *Nature* 469(7329): 175-180.

Rasmussen, S. G.; Choi, H. J.; Rosenbaum, D. M.; Kobilka, T. S.; Thian, F. S.; Edwards, P. C.; Burghammer, M.; Ratnala, V. R.; Sanishvili, R.; Fischetti, R. F.; Schertler, G. F.; Weis, W. I.; Kobilka, B. K. (2007). Crystal structure of the human beta2 adrenergic G-protein-coupled receptor. *Nature* 450(7168): 383-387.

Rasmussen, S. G.; DeVree, B. T.; Zou, Y.; Kruse, A. C.; Chung, K. Y.; Kobilka, T. S.; Thian, F. S.; Chae, P. S.; Pardon, E.; Calinski, D.; Mathiesen, J. M.; Shah, S. T.; Lyons, J. A.; Caffrey, M.; Gellman, S. H.; Steyaert, J.; Skiniotis, G.; Weis, W. I.; Sunahara, R. K.; Kobilka, B. K. (2011b). Crystal structure of the beta2 adrenergic receptor-Gs protein complex. *Nature* 477(7366): 549-555.

Ratnala, V. R.; Kobilka, B. (2009). Understanding the ligand-receptor-G protein ternary complex for GPCR drug discovery. *Methods Mol. Biol.* 552: 67-77.

Reiter, E.; Ahn, S.; Shukla, A. K.; Lefkowitz, R. J. (2012). Molecular mechanism of beta-arrestin-biased agonism at seven-transmembrane receptors. *Annu. Rev. Pharmacol. Toxicol.* 52: 179-197.

Resink, T. J.; Grigorian, G.; Moldabaeva, A. K.; Danilov, S. M.; Buhler, F. R. (1987). Histamine-induced phosphoinositide metabolism in cultured human umbilical vein endothelial cells. Association with thromboxane and prostacyclin release. *Biochem. Biophys. Res. Commun.* 144(1): 438-446.

Ribas, C.; Penela, P.; Murga, C.; Salcedo, A.; Garcia-Hoz, C.; Jurado-Pueyo, M.; Aymerich, I.; Mayor, F., Jr. (2007). The G protein-coupled receptor kinase (GRK) interactome: role of GRKs in GPCR regulation and signaling. *Biochim. Biophys. Acta* 1768(4): 913-922.

Riley, J. F.; West, G. B. (1952). Histamine in tissue mast cells. *J. Physiol.* 117(4): 72P-73P.

Rossbach, K.; Stark, H.; Sander, K.; Leurs, R.; Kietzmann, M.; Baumer, W. (2009a). The histamine H receptor as a new target for treatment of canine inflammatory skin diseases. *Vet. Dermatol.* 20(5-6): 555-561.

Rossbach, K.; Wendorff, S.; Sander, K.; Stark, H.; Gutzmer, R.; Werfel, T.; Kietzmann, M.; Baumer, W. (2009b). Histamine H4 receptor antagonism reduces hapten-induced scratching behaviour but not inflammation. *Exp. Dermatol.* 18(1): 57-63.

Samama, P.; Cotecchia, S.; Costa, T.; Lefkowitz, R. J. (1993). A mutation-induced activated state of the beta 2-adrenergic receptor. Extending the ternary complex model. *J. Biol. Chem.* 268(7): 4625-4636.

Savall, B. M.; Meduna, S. P.; Tays, K.; Cai, H.; Thurmond, R. L.; McGovern, P.; Gaul, M.; Zhao, B. P.; Edwards, J. P. (2015). Diaminopyrimidines, diaminopyridines and diaminopyridazines as histamine H4 receptor modulators. *Bioorg. Med. Chem. Lett.* 25(4): 956-959.

Schneider, E.; Leite-de-Moraes, M.; Dy, M. (2011). Histamine, immune cells and autoimmunity. *Adv. Exp. Med. Biol.* 709: 81-94.

Schneider, E.; Machavoine, F.; Pleau, J. M.; Bertron, A. F.; Thurmond, R. L.; Ohtsu, H.; Watanabe, T.; Schinkel, A. H.; Dy, M. (2005). Organic cation transporter 3 modulates murine basophil functions by controlling intracellular histamine levels. *J. Exp. Med.* 202(3): 387-393.

Schneider, E. H.; Schnell, D.; Papa, D.; Seifert, R. (2009). High constitutive activity and a G-protein-independent high-affinity state of the human histamine H(4)-receptor. *Biochemistry* 48(6): 1424-1438.

Schneider, E. H.; Schnell, D.; Strasser, A.; Dove, S.; Seifert, R. (2010). Impact of the DRY motif and the missing "ionic lock" on constitutive activity and G-protein coupling of the human histamine H4 receptor. *J. Pharmacol. Exp. Ther.* 333(2): 382-392.

Schnell, D.; Brunskole, I.; Ladova, K.; Schneider, E. H.; Igel, P.; Dove, S.; Buschauer, A.; Seifert, R. (2011). Expression and functional properties of canine, rat, and murine histamine H(4) receptors in Sf9 insect cells. *Naunyn Schmiedebergs Arch. Pharmacol.* 383(5): 457-470.

Schreeb, A.; Łażewska, D.; Dove, S.; Buschauer, A.; Kieć-Kononiwcz, K.; Stark, H. (2013). Histamine H4 Receptor Ligands. In *Histamine H4 Receptor: A Novel Drug Target in Immunoregulation and Inflammation*, Stark, H., Ed. Versita: London, pp 21-62.

Schwartz, J. C. (2011). The histamine H3 receptor: from discovery to clinical trials with pitolisant. *Br. J. Pharmacol.* 163(4): 713-721.

Seifert, R. (2014). Therapeutic efficacy of a H(4) receptor antagonist in humans: a milestone in histamine research. *J. Pharmacol. Exp. Ther.* 350(1): 2-4.

Seifert, R.; Schneider, E. H.; Dove, S.; Brunskole, I.; Neumann, D.; Strasser, A.; Buschauer, A. (2011). Paradoxical stimulatory effects of the "standard" histamine H4-receptor antagonist JNJ7777120: the H4 receptor joins the club of 7 transmembrane domain receptors exhibiting functional selectivity. *Mol. Pharmacol.* 79(4): 631-638.

Seifert, R.; Strasser, A.; Schneider, E. H.; Neumann, D.; Dove, S.; Buschauer, A. (2013). Molecular and cellular analysis of human histamine receptor subtypes. *Trends Pharmacol. Sci.* 34(1): 33-58.

Seifert, R.; Wenzel-Seifert, K. (2002). Constitutive activity of G-protein-coupled receptors: cause of disease and common property of wild-type receptors. *Naunyn Schmiedebergs Arch. Pharmacol.* 366(5): 381-416.

Seifert, R.; Wenzel-Seifert, K.; Lee, T. W.; Gether, U.; Sanders-Bush, E.; Kobilka, B. K. (1998). Different effects of Gsalpha splice variants on beta2-adrenoreceptor-mediated signaling. The Beta2-adrenoreceptor coupled to the long splice variant of Gsalpha has properties of a constitutively active receptor. *J. Biol. Chem.* 273(18): 5109-5116.

Seifert, R.; Wieland, T. (2005). *G protein-coupled receptors as drug targets: analysis of activation and constitutive activity*. Wiley-VCH: Weinheim, p 304.

Selent, J.; Sanz, F.; Pastor, M.; De Fabritiis, G. (2010). Induced effects of sodium ions on dopaminergic G-protein coupled receptors. *PLoS Comput. Biol.* 6(8).

Shenoy, S. K.; Lefkowitz, R. J. (2011). beta-Arrestin-mediated receptor trafficking and signal transduction. *Trends Pharmacol. Sci.* 32(9): 521-533.

Shin, N.; Coates, E.; Murgolo, N. J.; Morse, K. L.; Bayne, M.; Strader, C. D.; Monsma, F. J., Jr. (2002). Molecular modeling and site-specific mutagenesis of the histamine-binding site of the histamine H4 receptor. *Mol. Pharmacol.* 62(1): 38-47.

Smits, R. A.; de Esch, I. J.; Zuiderveld, O. P.; Broeker, J.; Sansuk, K.; Guaita, E.; Coruzzi, G.; Adami, M.; Haaksma, E.; Leurs, R. (2008). Discovery of quinazolines as histamine H4

receptor inverse agonists using a scaffold hopping approach. *J. Med. Chem.* 51(24): 7855-7865.

Smits, R. A.; Lim, H. D.; Steglink, B.; Bakker, R. A.; de Esch, I. J.; Leurs, R. (2006). Characterization of the histamine H4 receptor binding site. Part 1. Synthesis and pharmacological evaluation of dibenzodiazepine derivatives. *J. Med. Chem.* 49(15): 4512-4516.

Steinhilber, D.; Schubert-Zsilavecz, M.; Roth, H. J. (2005). *Medizinische Chemie: Targets und Arzneistoffe*. 1 ed.; Dt. Apotheker-Verl.: Stuttgart, p 660.

Stephenson, R. P. (1956). A modification of receptor theory. *Br. J. Pharmacol. Chemother.* 11(4): 379-393.

Sterk, G. J.; van der Goot, H.; Timmerman, H. (1986). The influence of guanidino and isothiourea groups in histaminergic compounds on H2-activity. *Agents Actions* 18(1-2): 137-140.

Strader, C. D.; Fong, T. M.; Tota, M. R.; Underwood, D.; Dixon, R. A. (1994). Structure and function of G protein-coupled receptors. *Annu. Rev. Biochem.* 63: 101-132.

Tesmer, J. J.; Dessauer, C. W.; Sunahara, R. K.; Murray, L. D.; Johnson, R. A.; Gilman, A. G.; Sprang, S. R. (2000). Molecular basis for P-site inhibition of adenylyl cyclase. *Biochemistry* 39(47): 14464-14471.

Thurmond, R. L.; Chen, B.; Dunford, P. J.; Greenspan, A. J.; Karlsson, L.; La, D.; Ward, P.; Xu, X. L. (2014a). Clinical and preclinical characterization of the histamine H(4) receptor antagonist JNJ-39758979. *J. Pharmacol. Exp. Ther.* 349(2): 176-184.

Thurmond, R. L.; Desai, P. J.; Dunford, P. J.; Fung-Leung, W. P.; Hofstra, C. L.; Jiang, W.; Nguyen, S.; Riley, J. P.; Sun, S.; Williams, K. N.; Edwards, J. P.; Karlsson, L. (2004). A potent and selective histamine H_4 receptor antagonist with anti-inflammatory properties. *J. Pharmacol. Exp. Ther.* 309(1): 404-413.

Thurmond, R. L.; Gelfand, E. W.; Dunford, P. J. (2008). The role of histamine H1 and H4 receptors in allergic inflammation: the search for new antihistamines. *Nat. Rev. Drug Discov.* 7(1): 41-53.

Thurmond, R. L.; Kazerouni, K.; Chaplan, S. R.; Greenspan, A. J. (2014b). Peripheral Neuronal Mechanism of Itch: Histamine and Itch. In *Itch: Mechanisms and Treatment*, Carstens, E.; Akiyama, T., Eds. CRC Press: Boca Raton (FL).

Tuteja, N. (2009). Signaling through G protein coupled receptors. *Plant Signal. Behav.* 4(10): 942-947.

Uveges, A. J.; Kowal, D.; Zhang, Y.; Spangler, T. B.; Dunlop, J.; Semus, S.; Jones, P. G. (2002). The role of transmembrane helix 5 in agonist binding to the human H3 receptor. *J. Pharmacol. Exp. Ther.* 301(2): 451-458.

van der Goot, H.; Schepers, M. J. P.; Sterk, G. J.; Timmerman, H. (1992). Isothiourea analogues of histamine as potent agonists or antagonists of the histamine H3-receptor. *Eur. J. Med. Chem.* 27(5): 511-517.

Vassilatis, D. K.; Hohmann, J. G.; Zeng, H.; Li, F.; Ranchalis, J. E.; Mortrud, M. T.; Brown, A.; Rodriguez, S. S.; Weller, J. R.; Wright, A. C.; Bergmann, J. E.; Gaitanaris, G. A. (2003). The G protein-coupled receptor repertoires of human and mouse. *Proc. Natl. Acad. Sci. U. S. A.* 100(8): 4903-4908.

Wall, M. A.; Coleman, D. E.; Lee, E.; Iniguez-Lluhi, J. A.; Posner, B. A.; Gilman, A. G.; Sprang, S. R. (1995). The structure of the G protein heterotrimer Gi alpha 1 beta 1 gamma 2. *Cell* 83(6): 1047-1058.

Ward, S. D.; Curtis, C. A.; Hulme, E. C. (1999). Alanine-scanning mutagenesis of transmembrane domain 6 of the M(1) muscarinic acetylcholine receptor suggests that Tyr381 plays key roles in receptor function. *Mol. Pharmacol.* 56(5): 1031-1041.

Watari, K.; Nakaya, M.; Kurose, H. (2014). Multiple functions of G protein-coupled receptor kinases. *J. Mol. Signal.* 9(1): 1.

Weinshilboum, R. M.; Otterness, D. M.; Szumlanski, C. L. (1999). Methylation pharmacogenetics: catechol O-methyltransferase, thiopurine methyltransferase, and histamine N-methyltransferase. *Annu. Rev. Pharmacol. Toxicol.* 39: 19-52.

Weiss, J. M.; Morgan, P. H.; Lutz, M. W.; Kenakin, T. P. (1996a). The cubic ternary complex receptor-occupancy model. III. resurrecting efficacy. *J. Theor. Biol.* 181(4): 381-397.

Weiss, J. M.; Morgan, P. H.; Lutz, M. W.; Kenakin, T. P. (1996b). The Cubic Ternary Complex Receptor–Occupancy Model I. Model Description. *J. Theor. Biol.* 178(2): 151-167.

Weiss, J. M.; Morgan, P. H.; Lutz, M. W.; Kenakin, T. P. (1996c). The Cubic Ternary Complex Receptor–Occupancy Model II. Understanding Apparent Affinity. *J. Theor. Biol.* 178(2): 169-182.

Wieland, T.; Lutz, S.; Chidiac, P. (2007). Regulators of G protein signalling: a spotlight on emerging functions in the cardiovascular system. *Curr. Opin. Pharmacol.* 7(2): 201-207.

Wifling, D.; Löffel, K.; Nordemann, U.; Strasser, A.; Bernhardt, G.; Dove, S.; Seifert, R.; Buschauer, A. (2015b). Molecular determinants for the high constitutive activity of the human histamine H4 receptor: functional studies on orthologues and mutants. *Br. J. Pharmacol.* 172(3): 785-798.

Willars, G. B. (2006). Mammalian RGS proteins: multifunctional regulators of cellular signalling. *Semin. Cell Dev. Biol.* 17(3): 363-376.

Windaus, A.; Vogt, W. (1907). Synthese des Imidazolyl-äthylamins. *Ber. Dtsch. Chem. Ges.* 40(3): 3691-3695.

Wittmann, H. J.; Seifert, R.; Strasser, A. (2014). Mathematical analysis of the sodium sensitivity of the human histamine H3 receptor. *In Silico Pharmacol.* 2(1): 1-14.

Wu, D. Q.; Lee, C. H.; Rhee, S. G.; Simon, M. I. (1992). Activation of phospholipase C by the alpha subunits of the Gq and G11 proteins in transfected Cos-7 cells. *J. Biol. Chem.* 267(3): 1811-1817.

Yu, F.; Wolin, R. L.; Wei, J.; Desai, P. J.; McGovern, P. M.; Dunford, P. J.; Karlsson, L.; Thurmond, R. L. (2010). Pharmacological characterization of oxime agonists of the histamine H4 receptor. *J. Receptor Ligand Channel Res.* 3: 37-49.

Zampeli, E.; Thurmond, R. L.; Tiligada, E. (2009). The histamine H4 receptor antagonist JNJ7777120 induces increases in the histamine content of the rat conjunctiva. *Inflamm. Res.* 58(6): 285-291.

Zampeli, E.; Tiligada, E. (2009). The role of histamine H4 receptor in immune and inflammatory disorders. *Br. J. Pharmacol.* 157(1): 24-33.

Zavecz, J. H.; Levi, R. (1978). Histamine-induced negative inotropism: mediation by H1-receptors. *J. Pharmacol. Exp. Ther.* 206(2): 274-280.

Zhang, J.; Ferguson, S. S.; Barak, L. S.; Menard, L.; Caron, M. G. (1996). Dynamin and beta-arrestin reveal distinct mechanisms for G protein-coupled receptor internalization. *J. Biol. Chem.* 271(31): 18302-18305.

Zhu, Y.; Michalovich, D.; Wu, H.; Tan, K. B.; Dytko, G. M.; Mannan, I. J.; Boyce, R.; Alston, J.; Tierney, L. A.; Li, X.; Herrity, N. C.; Vawter, L.; Sarau, H. M.; Ames, R. S.; Davenport, C. M.; Hieble, J. P.; Wilson, S.; Bergsma, D. J.; Fitzgerald, L. R. (2001). Cloning, expression, and pharmacological characterization of a novel human histamine receptor. *Mol. Pharmacol.* 59(3): 434-441.

Chapter 2

Scope and Objectives

There are substantial pharmacological differences between various H_4R species orthologs (Brunskole et al., 2011; Lim et al., 2008; Schneider et al., 2009; Schnell et al., 2011), in particular, with respect to the potency and quality of action of H_4R-agonists as well as inverse agonists. For example, histamine and a number of other agonists have considerably higher potency at the human H_4R than at the mouse and rat H_4R (Schnell et al., 2011). Several ligands even show different qualities of action (agonism, inverse agonism) when investigated on different species. Whereas the hH_4R is highly constitutively active, the mH_4R and rH_4R are devoid of constitutive activity (Schnell et al., 2011). Such species-dependent differences represent a major problem regarding the validation of the H_4R as a drug target and the evaluation of ligands as potential drugs in translational animal models.

The aim of this project was to analyse molecular determinants of pharmacological differences between human, mouse and rat H_4Rs. Two complementary approaches were applied, namely molecular modelling and molecular pharmacological investigations. Based on previous data, homology models of inactive and active states and sequence comparisons, H_4R species variants were to be analysed with respect to amino acid exchanges, in particular close to the ligand binding pocket. Figure 2.1 presents an overview of all positions envisaged for analysis. Potential key amino acids and their role in receptor binding and function had to be verified by studies on H_4R mutants, co-expressed together with G-protein subunits $G\alpha_{i2}$ and $G\beta_1\gamma_2$ in Sf9 insect cells. The affinities, potencies and intrinsic activities of agonists, antagonists and inverse agonists were determined in [^{3}H]histamine saturation binding, [^{3}H]histamine competition binding and functional [^{35}S]GTPγS assays. Via receptor models and docking of investigated ligands, results from these experiments were to be analysed with the intention to elucidate the influence of mutated amino acids on constitutive activity and ligand binding and to suggest molecular determinants of receptor activation.

Lim et al. (2008) identified F169 as a key amino acid responsible for the large differences in ligand binding data between hH_4R and mH_4R. The question arose whether F169 may also contribute to the high constitutive activity of the hH_4R. Therefore, the hH_4R-F169V as well as

the reciprocal mH$_4$R-V171F mutant were generated. Indicated by hH$_4$R homology models, the role of S179[5.43], which is among those amino acids forming the orthosteric ligand binding site, on its own and in concert with F169 was to be investigated as well. The two single mutants hH$_4$R-S179M and hH$_4$R-S179A were envisaged as well as the two double mutants hH$_4$R-F169V+S179M and hH$_4$R-F169V+S179A, representing the amino acids of the mH$_4$R or rH$_4$R only in one or two positions, respectively, as well as the reciprocal double mutant mH$_4$R-V171F+M181S.

The second extracellular loop, ECL2, is important for ligand binding as well as for GPCR activation (Wheatley et al., 2012). Crystal structures of various GPCRs indicated that amino acids corresponding to the FF motif in the hH$_4$R are located close to the ligand binding pocket. Therefore, not only F169, but also F168 had to be considered by expression and characterization of a hH$_4$R-F168A mutant in Sf9 cells.

Brunskole et al. (2011) demonstrated by means of chimeras of the hH$_4$R containing ECL2 or ECL3 of the cH$_4$R that both, ECL2 and ECL3, contribute to ligand binding, receptor activation and constitutive activity. Sequence alignments and homology models revealed that the hH$_4$R has numerous acidic amino acids in ECL2, but only one basic residue in ECL3, whereas the mH$_4$R and the rH$_4$R comprise three or four basic amino acids in ECL3. In view of these differences regarding basic residues in ECL3 the single mutant hH$_4$R-S330R was generated, corresponding to an arginine in this position of the rat H$_4$R.

Based on previous investigations in our laboratory (Schnell et al., 2011) on the impact of hH$_4$R-R341S (as in mH$_4$R/rH$_4$R) and R341E (cH$_4$R) mutants on ligand potencies, it was envisaged to analyse the role of R341 with respect to constitutive activity, too. This implied the expression of both mutants in Sf9 cells and the characterization of ligands in binding and functional assays.
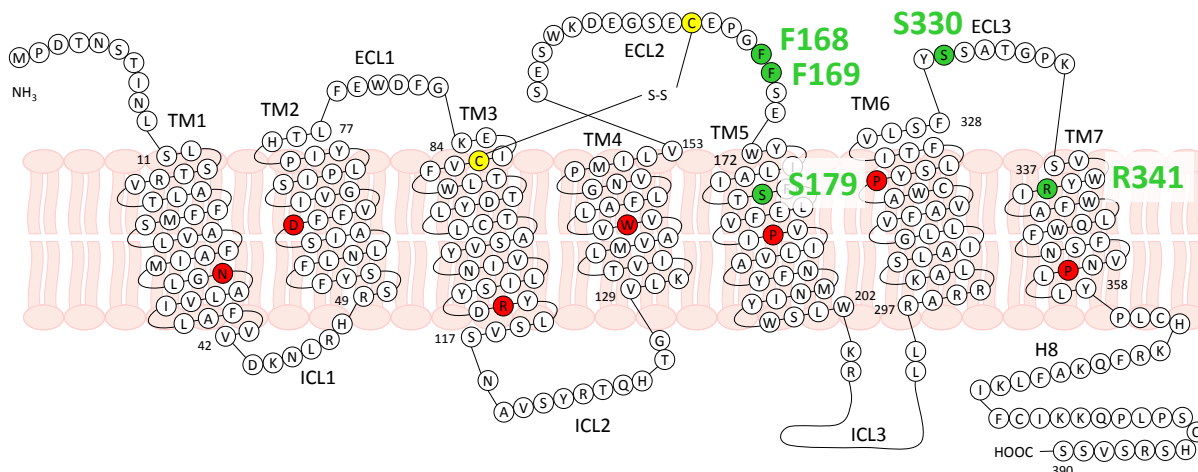
Figure 2.1: Snake plot of the hH₄R indicating all residues to be investigated by in-vitro mutagenesis (F168^{ECL2}, F169^{ECL2}, S179$^{5.43}$, S330^{ECL3} and R341$^{7.36}$; green colour). The two cysteines forming a disulphide bond are marked in yellow and the most conserved residue in each TM of class A GPCRs in red. TMs were calculated with DSSP implemented in SYBYL-X 1.3 (Chapter 3.3.2.2).

2.1 References

Brunskole, I.; Strasser, A.; Seifert, R.; Buschauer, A. (2011). Role of the second and third extracellular loops of the histamine H(4) receptor in receptor activation. *Naunyn Schmiedebergs Arch. Pharmacol.* 384(3): 301-317.

Lim, H. D.; Jongejan, A.; Bakker, R. A.; Haaksma, E.; de Esch, I. J.; Leurs, R. (2008). Phenylalanine 169 in the second extracellular loop of the human histamine H4 receptor is responsible for the difference in agonist binding between human and mouse H4 receptors. *J. Pharmacol. Exp. Ther.* 327(1): 88-96.

Schneider, E. H.; Schnell, D.; Papa, D.; Seifert, R. (2009). High constitutive activity and a G-protein-independent high-affinity state of the human histamine H(4)-receptor. *Biochemistry* 48(6): 1424-1438.

Schnell, D.; Brunskole, I.; Ladova, K.; Schneider, E. H.; Igel, P.; Dove, S.; Buschauer, A.; Seifert, R. (2011). Expression and functional properties of canine, rat, and murine histamine H(4) receptors in Sf9 insect cells. *Naunyn Schmiedebergs Arch. Pharmacol.* 383(5): 457-470.

Wheatley, M.; Wootten, D.; Conner, M. T.; Simms, J.; Kendrick, R.; Logan, R. T.; Poyner, D. R.; Barwell, J. (2012). Lifting the lid on GPCRs: the role of extracellular loops. *Br. J. Pharmacol.* 165(6): 1688-1703.

Chapter 3

Computational Chemistry

Homology modelling, analysis of inactive and active human H$_4$ receptor states and ligand docking

Note: Parts of this chapter were already published prior to submission of this thesis in *PLoS One* and *Br. J. Pharmacol.* (Wifling et al., 2015a; Wifling et al., 2015b). John Wiley & Sons granted me the permission to use the material incorporated in Wifling et al. (2015b) for this thesis. For detailed information on the contributions by co-authors, cf. "Danksagungen".

3.1 Summary

Background and purpose: Whereas the human H$_4$R shows a high degree of constitutive activity, the rodent orthologs mH$_4$R and rH$_4$R are devoid of basal activity. Aiming at the identification of the molecular determinants of species-dependent differences in terms of ligand binding and constitutive activity, molecular modelling studies were performed to suggest potential key amino acids, which were to be replaced by site-directed mutagenesis and verified by pharmacological in vitro studies.

Experimental approach: Homology models of the hH$_4$R inactive form based on the crystal structure of the hH$_1$R and of active conformations of H$_4$R orthologs based on the β$_2$AR were generated with SYBYL 7.3 and SYBYL-X 1.3. The binding pockets were investigated with respect to differences in the amino acid sequence, comparing the H$_4$R species orthologs. Important molecular switches were analysed and the investigated ligands were manually docked in the model of the hH$_4$R in its inactive state.

Results: Based on the homology models of the H$_4$R species orthologs, the amino acids F168^{ECL2}, F169^{ECL2}, S179$^{5.43}$, S330^{ECL3} and R341$^{7.36}$ were suggested for in-vitro mutagenesis studies. Among the conformational changes essential for GPCR activation, the tyrosine toggle

switch and the transmission switch were feasible in our homology models. By contrast, the ionic lock and the controversial rotamer toggle switch of $W316^{6.48}$ were not detectable. $F168^{ECL2}$ and $F169^{ECL2}$ were suggested to interact with surrounding hydrophobic and aromatic amino acids by hydrophobic and π-π interactions. These contacts were assumed to be crucial for the contraction of the binding pocket and, thus, for constitutive activity. $S179^{5.43}$ can form an H-bond with $T323^{6.55}$, which is impossible in case of mutation to M and A. Whereas this interaction alone was insufficient to explain the high constitutive activity of the hH_4R, $S179^{5.43}$ in concert with $F169^{ECL2}$ stabilized the H_4R active state. This supported the hypothesis that the contraction of the binding pocket and, in particular, the concomitant movement of both TM5 and TM6 is unlikely in case of the respective double mutants. Considering docking poses, key interactions of most ligands with $D94^{3.32}$, $E182^{5.46}$ and $Q347^{7.42}$ were detected.

Conclusions: Molecular modelling investigations were used to suggest amino acids to be mutated and were helpful to explain the data from experimental studies, which confirmed F168 and F169 alone and F169 in concert with S179 as key residues for the extraordinarily high constitutive activity of the hH_4R. The F/F/S motif is also present in other highly constitutively active GPCRs such as the hH_3R or the $β_2AR$. Therefore, the results may be interpreted as a hint to a general mechanism of GPCR activation.

3.2 Introduction

Since the first structure of a GPCR, the bovine rhodopsin, was disclosed in 2000 at a resolution of 2.8 Å (Palczewski et al., 2000), numerous crystal structures were reported for approximately 25 GPCRs from all classes. The files of the crystal structures can be downloaded from the Brookhaven Protein Data Bank (PDB; Bernstein et al., 1977). Meanwhile not only structures of agonist, antagonist or inverse agonist bound inactive states, but also of active states (agonist bound) and even complexes with allosteric modulators were resolved (for review, see, e. g. Granier and Kobilka (2012), Kruse et al. (2014) and Venkatakrishnan et al. (2013)). Furthermore, structures differ with respect to the stabilizing methods: insertion of lysozyme T4L at various sites, antibody, thermostabilization, mutations or coupling to G-proteins.

Inactive and active states are both available in case of the $β_2AR$ (Rasmussen et al., 2011a; Rasmussen et al., 2007; Rasmussen et al., 2011b). Intriguingly, not only agonist binding, but also coupling of a nanobody or the native G-protein $Gα_s$ and $Gβ_1γ_2$ at the cytoplasmic domain is necessary to stabilize the active $β_2AR$ state (Rasmussen et al., 2011a; Rasmussen et al., 2011b; Ring et al., 2013; Weichert et al., 2014).

Crystal structures of H_4R species orthologs and of the hH_3R are not available. Therefore, homology models based on crystal structures of other GPCRs must be generated. For this purpose, all known structures of biogenic amine GPCRs are generally eligible as templates

(see Table 3.1) due to the high conservation of TM domains, fulfilling the minimum requirement for homology modelling of 30 % sequence identity. In contrast, the intra- and extracellular regions are less similar. Such homology models enable deeper insights into key ligand-receptor interactions as well as into the molecular determinants of discrepancies observed among H_4R orthologs. In particular, homology models may be useful to search for amino acids accounting for the high constitutive activity of the human H_4R, i. e., for candidates to be investigated by the site-directed mutagenesis approach.

Homology models also serve for the simulation of ligand binding modes in docking experiments. All ligands were docked that were also studied in pharmacological assays, and pharmacological data as well as published material were utilized in order to find reasonable docking poses. Moreover, comparing the inactive state homology model of the hH_4R based on the hH_1R (Shimamura et al., 2011) with the active state homology model of the hH_4R based on the $β_2AR$ (Rasmussen et al., 2011a) enabled deeper insights into movements upon receptor activation and into molecular switches.

3.3 Methods

3.3.1 Available GPCR crystal structures

Table 3.1: Biogenic amine GPCR crystal structures.

Target	Ligand	G-protein substitution	PDB ID	Å	Reference
t$β_1$AR	cyanopindolol (antagonist)	stabilizing mutations	2VT4	2.70	Warne et al. (2008)
	dobutamine (partial agonist); dobutamine (partial agonist); carmoterol (agonist); isoprenaline (agonist); salbutamole (agonist)		2Y00; 2Y01; 2Y02; 2Y03; 2Y04	2.50; 2.60; 2.60; 2.85; 3.05	Warne et al. (2011)
	carazolol (inverse agonist); cyanopindolol (antagonist); iodocyanopindolol (antagonist); cyanopindolol (antagonist)		2YCW; 2YCX; 2YCZ; 2YCY	3.00; 3.25; 3.65; 3.15	Moukhametzianov et al. (2011)
	bucindolol (antagonist); carvediolol (inverse agonist)		4AMI; 4AMJ	3.20; 2.30	Warne et al. (2012)
	ligand-free		4GPO	3.50	Huang et al. (2013)
	compound 20; compound 19 (antagonists)		3ZPQ; 3ZPR	2.70; 2.80	Christopher et al. (2013)
	cyanopindolol (antagonist)		4BVN	2.10	Miller-Gallacher et al. (2014)

Table 3.1 (continued)

Target	Ligand	G-protein substitution	PDB ID	Å	Reference
hβ₂AR	carazolol (inverse agonist)	T4L chimera	2RH1	2.40	Cherezov et al. (2007)
	carazolol (inverse agonist); carazolol	Fab5 complex	2R4R; 2R4S	3.40; 3.40	Rasmussen et al. (2007)
	timolol (inverse agonist)	T4L chimera	3D4S	2.80	Hanson et al. (2008)
	ligand-free	Fab complex	3KJ6	3.40	Bokoch et al. (2010)
	ICI118551 (inverse agonist); compound 2 (inverse agonist); alprenolol (antagonist)	T4L chimera	3NY8; 3NY9; 3NYA	2.84; 2.84; 3.16	Wacker et al. (2010)
	FAUC50 (irreversible agonist)	T4L chimera	3PDS	3.50	Rosenbaum et al. (2011)
	BI-167107 (agonist)	Nb80 (nanobody)	3P0G	3.50	Rasmussen et al. (2011a)
	BI-167107 (agonist)	Gα$_s$β$_1$γ$_2$ heterotrimer	3SN6	3.20	Rasmussen et al. (2011b)
	carazolol (inverse agonist)	T4L chimera	4GBR	3.99	Zou et al. (2012)
	BI-167107; hydroxybenzyl isoproterenol; adrenaline (agonists)	Nb6B9	4LDE; 4LDL; 4LDO	2.79; 3.10; 3.20	Ring et al. (2013)
	compound 2 (covalent agonist)	Nb6B9	4QKX	3.30	Weichert et al. (2014)
hD₃R	eticlopride (antagonist)	T4L chimera	3PBL	2.89	Chien et al. (2010)
hH₁R	doxepin (antagonist)	T4L chimera	3RZE	3.10	Shimamura et al. (2011)
hM₂R	QNB (antagonist)	T4L chimera	3UON	3.00	Haga et al. (2012)
	iperoxo (agonist); iperoxo (agonist) + LY2119620 (allosteric modulator)	Nb9-8	4MQS; 4MQT	3.50; 3.70	Kruse et al. (2013)
rM₃R	tiotropium (inverse agonist)	T4L chimera	4DAJ	3.40	Kruse et al. (2012)
	tiotropium (inverse agonist); tiotropium (inverse agonist); NMS (antagonist)		4U14; 4U15; 4U16	3.57; 2.80; 3.70	Thorsen et al. (2014)
h5-HT₁ʙR	dihydroergotamine; ergotamine (agonists)	chimera with *E. coli* soluble cytochrome b562	4IAQ; 4IAR	2.80; 2.70	Wang et al. (2013)
h5-HT₂ʙR	ergotamine (agonist)	chimera with *E. coli* soluble cytochrome b562	4IB4	2.70	Wacker et al. (2013)
	ergotamine (agonist)		4NC3	2.80	Liu et al. (2013)

3.3.2 H₃R/H₄R homology models based on the active state of the β₂AR

3.3.2.1 Sequence alignment

Sequences of the β₂AR and of the target receptors were retrieved from the UniProt Knowledgebase (UniProt, 2013) and imported into Clustal-X 2.1 (Larkin et al., 2007) for multiple sequence alignment. Clustal-X 2.1 determines the phylogenetic relatedness of the respective amino acids and introduces gaps along the variable loop regions if necessary. The

alignment was performed with the Gonnet PAM250 matrix (Gonnet et al., 1992) and based on about 80 similar class A GPCR sequences as input. The resulting alignment of the template and target receptors is shown in Figure 3.1.

```
              N-term                                      TM1            ICL1        TM2
β₂AR    MGQPGNGSAFLLAPNGSHA----PDHDV--------TQERDEVWVVGMGIVMSLIVLAIVFGNVLVITAIAKFERLQTVTNYFITSLACADLVMGLAVVP
hH₄R    ------------------.MPDTNS---........INLSLSTR.TLAFF...VAF..ML..A...L.FVVDKN.RHRSS..FLN..IS.FFV.VISI.
mKH₄R   ------------------.MPDTNS---........INLSLSTRITLAFF...LAF..ML..AV..L.FVVDKN.RHRSS..FLN..IS.FFV.VISI.
cH₄R    ------------------.MSATNG---........ITLPLSTRITLAFL...LAF..ML..AV..L.FVVDKK.RHRS...FLN..I..FFV.MISI.
pH₄R    ------------------.MSAINDTN-........NTLPLNTRIALAFL...LA.V.ML..AV..L.FVVDKN.RHRS...FLN..IS.FFV.VISI.
rH₄R    ------------------.MSESNG---........DVLPLTAQ.PLAFL..LAF..TI..AV..L.FVADRN.RHRS...FLN..IS.FFV.VISI.
mH₄R    ------------------.MSESNS---........GILPPAAQ.PLAFL..SFAF..MV..AV..L.FVVDRN.RHRS...FLN..IS.FLV..ISI.
gpH₄R   ------------------.MLANNS---........-IALTSIKISLTFL...LAI..ML..V...L.FIVDRN.RHRS...FLN..I..FFV.AIAI.
hH₃R    ----------MERAPPDGPLNASGALAGEAAAAGGARGFSAA.TAVLAAL.A.LIV.T.L..A..ML.FVADSS.R.QN.F.LLN..IS.FLV.AFCI.
           1        10        20        30        40        50        60        70        80        90        100

             TM2    ECL1                  TM3               ICL2           TM4              ECL2
β₂AR    FGAAHILMKMWTFGNFWCEFWTSIDVLCVTASIETLCVIAVDRYFAITSPFKYQSLLT-KNKARVIILMVWIVSGLTSFLPIQMHWYRATHQ----EAIN
hH₄R    LYIP.T.F-E.D..KEI.V..LTT.Y.LC...VYNIVL.SY...LSVSNAVS.RTQH.GVL.IVTLMVA..VLAF.VNGPM.LVSESWKDE-....-GSE
mKH₄R   LYIP.M.F-E.D..KEI.V..LTT.Y.LC...VYNIVL.SY...LSVSNAVS.RTQH.GIL.IVTLMVA..VLAF.VNGPM.LVSETWKDE-....-GSE
cH₄R    LYIP.T.F-D.D..KL.A..LIA.Y.LC.T.VYNIVL.SY...QSVSNAVS.RAQH.GIL.IVSLMVA..VLAF.VHGPI.LVSESWKNSSFGVV.EKD
pH₄R    LYIP.T.F-K.KLEDNI.A..LI..Y.LC...VYNIVL.SF...QSVSNAVS.RTQH.GIL.IVALMVG..VLAF.VHGPV.LVSEAWKQG-....-KQD
rH₄R    LYIP.T.F-N.N..SGI.M..LIT.Y.LC...VYSIVL.SY...QSVSNAVR.RAQH.GIL.IVAQMVA...LAF.VNGPM.LASDSWKNSTN...-TEE
mH₄R    LYIP.V.F-N.N..SGI.M..LIT.Y.LC...VYNIVL.SY...QSVSNAVS.RAQH.GIM.IVAQMVA...LAF.VNGPM.LASDSWKNSTN...-TKD
gpH₄R   LYIPSS.T-Y..S.KQA.V..LIT.Y.LC...VYNIVL.SY...QSVSNAVW.RAQHSGTW.IATQMVA...F.FM.NGPM.LISDSWQNS-....-TTE
hH₃R    LYVPYV.TGR....RGL.KL.LVV.Y.LC.S.AFNIVL.SY...FLSV.RAVS.RAQQGDTRR.VRKM.L..VLAF.LYGPA.LSWE.LSGGSS..IPEGH
              110       120       130       140       150       160       170       180       190       200

            ECL2                     TM5                           ICL3
β₂AR    CYANETCCDFFTNQAYAIASSIVSFYVPLVIMVFVYSRVFQEAKR---------------------------------------------------------
hH₄R    .EPG-----..SEWYILAIT.FLE.VI.VILVAYFNMNIYWSLWAAAAAAAKRDHL....SRCQSHPGLTAVSSNI....................
mKH₄R   .EPG-----..SEWYIVAIT.FLE.LI.VILVAYFNMNIYWSLWAAAAAAAKRDHL....SRCQSHPGPTAVSSNS....................
cH₄R    .EPG-----...RWYVLAI..FFE.L..VFSVAYFNMYIYWSLWAAAAAAAKRGNL....SRWQSQPTLTSVSSSN....................
pH₄R    .EPG-----.LKEWYVLAITLFFE.LA.VLLVAYFNLYIYWSLWAAAAAAAKRGHL....SRCQSHCGLTPVSSGS....................
rH₄R    .EPG-----..V.EWYILAITAFLE.LI.VSLV.YFSVQIYWSLWAAAAAAAKRGSL....SRCPSHAGFIATSSRG....................
mH₄R    .EPG-----..V.EWYILTITMLLE.LL.VISVAYFNVQIYWSLWAAAAAAAKRRAL....SRCPSHAGFSTTSSSA....................
gpH₄R   .EPG-----.LKKWYF.LPT.LLE.LI.ILLVAYFSAHIYWSLWAAAAAAAKREKL....SRCLSHPVLPSDSSSSD....................
hH₃R    ...E-----...Y.WYFL.TA.TLE.FT.FLSVT.FNLSIYLNIQAAAAAAA.RTRLRLDGAREAAGPEPPPEAQPSPPPPPGCWGCWQKGHGEAMPLHRY
              210       220       230       240       250       260       270       280       290       300

                              ICL3                                                            TM6
β₂AR    ---QLQKIDKSEGRFH-------VQNLSQVEQ--------------------------DGRTGHGLRRSSKFCLKEHKALKTLGIIMGTFTLCWLP
hH₄R    .CGHSFRGRL.SR.SLSAS....TEVPASFHSERQRRKSSLMFSSRTKMNSNTIASKMGSFSQSDSVALHQ.EHVEL.RARRLA.S.A.LL.V.AV..A.
mKH₄R   .CG.SFRCGL.SRGSLSAS....TEMPVSLHSERQRRKSSLMYSLRTKMNSNRIASKMGSFSQSDSVGLHQ.EHAEL.RARRLA.S.A.LL.V.AV..A.
cH₄R    .CGS.LRGGLFSRTSLSEQ....KETAPS.PLKRHERKSNLLLSLRAQMNSSIITSKMASLTHSDSLCLHQ.EHIEL.RAR.LA.S.A.LL.V.AI..A.
pH₄R    .WGHSFRCGLFSRTSLSDP....KEAAASLHSERPRRKSTLWFSLRTRM.SSLTASNKGFLSHSDSLALHQKEHLEL.RAR.LARS.A.LL.V.AI..A.
rH₄R    .TGHSRRTGLACRTSLPGL....KEPAASLHSESPRGKSSLLVSLRTHMSGSIIAFKVGSFCRSESPVLHQ.EHVEL.RGR.LARS.AVLLSA.AI..A.
mH₄R    .SGH.HRAGVACRTSNPGL....KESAASRHSESPRRKSSLVSLRTHMSGSIIAFKVGSFWRSESAALRQ.HEAEL.RGR.LARS.A.LLSA.AI..A.
gpH₄R   .HGHSCRQ.PDSRATLPAR....KETTASLGGSDKSRRKSSLLFSIRAYKNSNVIASKMGFLSHSDSLALQQ.EHIELFRAR.LA.S.A.LLAA.AI..A.
hH₃R    GVGEAAVGAEAGEATLGGGGGGGVASPTSSSGSSSRGTERPRSLKRGSKPSASSASLEKRMKMVSQSFTQ.--FRLSRDR.VA.S.AV.VSI.G...A.
              310       320       330       340       350       360       370       380       390       400

            TM6    ECL3        TM7              H8
β₂AR    FFIVNIVHVIQD--NLIRKEVYILLNWIGYVNSGFNPLIYCRS-PDFRIAFQELLCLRRSSLK----AYGNGYSSNGNTGEQSGYHVEQEKENKLLCEDL
hH₄R    YSLFT..LSFYSSATGPKSVW.RIAF.LQWF..FV...L.PLCHKR.QK..LKIF.IKKQP.PSQHSRSVSS---------------------------
mKH₄R   YSLFT..LSFYSSETGSKSVW.RIAF.LQWF..FV...L.PLCHKR.QK..LKIF.IKKQP.PSPHSRSVSS---------------------------
cH₄R    YSLFT.IRS.YPLEQRPQIVG.EITF.LQWL..FV...FL.PLCHKR.QK..LKIFHMKKP.IPS.QNRSVSS---------------------------
pH₄R    YSLLT.TRSVYPTNPFPSTA..KFAF.LQWF..CV...FL.PLCHKR.QK..LKIF..KKQ.TLS.HNRSTSS---------------------------
rH₄R    YCLFT..LSTYRRGERPKSIW.SIAF.LQWF..LI...FL.PLCHKR.QK..WKI..VTKQPAPS.QTQSVSS---------------------------
mH₄R    YCLFT..LSTYPRTERPKSVW.SIAF.LQWF..FV...FL.PLCHKR.QK..WKI..VTKQPALS.QNQSVSS---------------------------
gpH₄R   YSLTTVIYSFFPER..TKSTW.HTAF.LQWF..FV...FL.PLCHKR.QK..LKI.PV..Q.TPP.HNRSIST---------------------------
hH₃R    YTLLM.IRAACHGHCVP-DYW.ETSF.LLWA..AV...VL.PLCHHS..R...TK...PQKLKIQPHSSLEHCWK---------------------------
              410       420       430       440       450       460       470       480       490       500

                       C-term
β₂AR    PGTEDFVGHQGTVPSDNIDSQGRNCSTNDSLL
hH₄R    ----------------------------
mKH₄R   ----------------------------
cH₄R    ----------------------------
pH₄R    ----------------------------
rH₄R    ----------------------------
mH₄R    ----------------------------
gpH₄R   ----------------------------
hH₃R    ----------------------------
              510       520       530
```

Figure 3.1: Multiple sequence alignment of the β₂AR (template) with the target receptors hH₄R, mkH₄R, cH₄R, pH₄R, rH₄R, mH₄R, gpH₄R and hH₃R. The most conserved amino acid in each TM of class A GPCRs is labelled in grey and the two cysteines forming a disulphide bond are coloured in yellow. Dots in the sequences indicate identity with the template structure. The cancelled amino acids were not resolved in the β₂AR crystal structure (PDB ID: 3P0G). ICL3 loops of the targets were replaced by seven A.

In case of no correspondence of all highly conserved amino acids in the TM domains (Mirzadegan et al., 2003) or of the conserved cysteine in TM3 (Strader et al., 1994) or if gaps occurred in the TM regions, a new alignment with more similar sequences was performed using the option "Reset all gaps before alignment". In the crystal structure of the β_2AR, ICL3 as well as parts of the N- and C-terminus are missing and were therefore removed in the alignment (Figure 3.1).

3.3.2.2 3D structure generation

After importing the PDB file of the active state β_2AR structure (Protein Data Bank ID: 3P0G) into SYBYL-X 1.3 (Tripos, St. Louis, MO USA), the amino acids of the template (β_2AR) were consecutively mutated into the corresponding residues of the target receptors along parts of the N-terminus, TM regions 1-7, ICL1, ECL1 (hH$_3$R), α-helical domain of ICL2, helix 8 and parts of the C-terminus. In case of the missing ICL3 loops, seven alanine residues were introduced. The positions of the conserved cysteine in ECL2 were preserved in order to retain the disulphide bridge with $C^{3.25}$. For the remaining extra- and intracellular regions (ECL1 in case of H$_4$R orthologs, non-helical part of ICL2, ECL2, ECL3 and loop connecting TM7 and helix 8), loop searches were performed with the Loop Search Tool implemented in SYBYL-X 1.3. This tool scans the PRODAT database (part of the Protein Data Bank (Bernstein et al., 1977)) for fragments with proper residue lengths and well-fitting anchor residues (Rossi et al., 2007). In case of ECL2, two loop searches were performed up- and downstream the conserved cysteine residue. The α-helical region in ECL2, being present in the crystal structure of the β_2AR, could not be reproduced in the homology models.

The side chains of the amino acids were added and their conformations were adjusted. If possible, side chain torsion angles of the template receptor were retained. In case of side chain clashes, most appropriate conformations were selected from the Lovell library (Lovell et al., 2000). Using the structure preparation tool of SYBYL-X 1.3, the protonation states of acidic (D, E) and basic (K, R) amino acids were manually adjusted, termini were fixed, hydrogens were added and all atoms were assigned with Amber7 FF99 atom types and charges. Afterwards, the target sequences were renumbered according to the primary structure retrieved from UniProt (UniProt, 2013).

Finally, for each target model a short minimization run (100 cycles, Powell method (Powell, 1964)) with the Amber7 FF99 force field (Cornell et al., 1995) and a dielectric constant of 4 was performed in order to eliminate strain.

TM definitions of the hH$_4$R model were assigned according to the DSSP (Define Secondary Structures of Proteins) algorithm (Kabsch and Sander, 1983) implemented in SYBYL-X 1.3 (second column in Table 3.2). In case of different results (especially in case of TM4, TM6, TM7 and helix 8), TM definitions of the β_2AR (Protein Data Bank ID: 3P0G) were assigned according

to the DSSP algorithm of SYBYL-X 1.3 (third column in Table 3.2) and the homologous regions in the hH$_4$R were determined by alignment with Clustal-X 2.1.

Table 3.2: TM/helix definitions of the hH$_4$R model based on the active β$_2$AR.

Helices	Protable definition of hH$_4$R	Protable definition of β$_2$AR
TM1	**S11**-**V42**	**S11**-**V42**
TM2	**R49**-**L77**	**R49**-**L77**
TM3	**K84**-**S117**	G83-**S117**
ICL2 (loop)	**A119**-Q125	**A119**-**H126**
TM4	I132-**V153**	**V129**-L152
TM5	**W172**-**W202**	**W172**-L201
TM6	**R297**-V325	**R297**-**F328**
TM7	**S337**-L357	K336-**Y358**
H8	F365-K371	**K363**-**I372**

Definitions were assigned according to DSSP of the hH$_4$R model (second column) or DSSP of the aligned β$_2$AR (PDB ID: 3P0G; third column). Implemented definitions in the PDB file are marked in bold.

3.3.3 hH$_4$R homology model based on the inactive state of the hH$_1$R

To suggest promising mutants and hH$_4$R-specific intramolecular interactions close to the ligand binding site, a homology model of the hH$_4$R was generated with the modelling suite SYBYL 7.3 (Tripos, St. Louis, MO USA) using the crystal structure of the hH$_1$R (Protein Data Bank ID: 3RZE) as template (Shimamura et al., 2011). For this purpose, the inactive state of the template is not inconsistent with the constitutively active state of the hH$_4$R since the binding pocket regions and extracellular domains of both states are probably as similar as in case of the β$_2$AR (Rasmussen et al., 2011a). The resulting model contains all extracellular (ECL) and intracellular (ICL) loops except ICL3 (G215-H292). To close the gap between the intracellular parts of TM5 and TM6, eight alanines were inserted in place of ICL3 (and the lysozyme domain of the template structure, respectively). 15 missing amino acids of the N-terminus were added by a recently established protocol (Strasser and Wittmann, 2013). The E2-loop is not completely resolved in the hH$_1$R structure. After removing the hH$_1$R residues W165, N166 and H167, the missing amino acids V153-K158 were included into the hH$_4$R model using the Loop-Search module within SYBYL. The inserted regions of the N-terminus and ECL2 were separately refined by energy minimization and a short gas phase MD simulation (500 ps). Histamine was manually docked considering interactions with the hH$_4$R suggested from results of in-vitro mutagenesis (Shin et al., 2002). Finally, the model was provided with Amber7 FF99 (histamine: Gasteiger-Hueckel) charges and energy minimized with the Amber7 FF99 force field (Cornell et al., 1995) and a dielectric constant of 4 up to a gradient of 0.01 kcal Mol^{-1} Å^{-1}. TM definitions were assigned according to the PDB file of the template (Table 3.3).

Table 3.3: TM/helix definitions of the hH$_4$R model based on the inactive hH$_1$R crystal structure (Shimamura et al., 2011).

Helices	TM definition
TM1	V16-V42
TM2	R49-F78
TM3	K84-S117
ICL2 (loop)	A119-H126
TM4	V129-V153
TM5	Y173-R204
TM6	R297-F328
TM7	S337-L360
H8	K363-I372

3.3.4 Illustration in PyMOL

The generated coordinate files (PDB) were imported into PyMOL Molecular Graphics System, Version 1.6 (Schrödinger LLC, Portland, OR USA) and illustrations were prepared with this software package.

3.3.5 Docking experiments

Ligands were manually docked into the binding pocket considering main interactions with the receptor (D94$^{3.32}$, E182$^{5.46}$ and Q347$^{7.42}$), currently available published literature and site-directed mutagenesis results. Ligands were provided with correct SYBYL and Amber7 FF99 atom types as well as with Gasteiger-Hueckel charges and the receptor with Amber7 FF99 charges. The ligand alone was firstly minimized with the Tripos force field and the Powell minimization method (Powell, 1964). Subsequently, the ligand was minimized together with the closest amino acids to the ligand-binding site with the Tripos force field as well as adjustment of constraints and afterwards the whole receptor was fully minimized with the Amber7 FF99 force field (Cornell et al., 1995). Minimization was essentially performed as described in Chapter 3.3.3.

3.4 Results and Discussion

3.4.1 Homology Modelling

3.4.1.1 Template selection

Depending on the intrinsic activities of investigated ligands (inverse agonist, neutral antagonist or agonist) or on the extraordinarily high constitutive activity of the hH$_4$R, inactive and active state crystal structures, respectively, are preferable as template. At the time of model preparation, only the active state of the hβ$_2$AR (PDB ID: 3P0G) was available (Rasmussen et al., 2011a).

In principle, models of inactive H_4R states may be based on all released structures of biogenic amine GPCRs (Table 3.1). To select an appropriate template, different criteria are useful: identity or conservation of amino acids with regard to the whole sequence, the TM regions or the ligand binding site as well as even ligand similarity (Lin et al., 2013). Table 3.4 presents the sequence identities (overall and TMs) of all targets with biogenic amine GPCRs from which structures were available. Obviously, the overall identities are only low, ranging from 13 % to 26 %. However, if one considers the TM regions, the minimal requirement for homology modelling, namely identities of 30 % and greater, is fulfilled in many cases. Among the possible templates, the hM_2R, rM_3R, hD_3R, $h5-HT_{1B}R$, $h5-HT_{2B}R$ or the hH_1R, the inactive crystal structure of the hH_1R (Shimamura et al., 2011) was selected for generation of an inactive state model of the hH_4R although the sequence similarity and phylogenetic relatedness with the rM_3R is somewhat greater. The main reason was that the FF motif in ECL2, one of the main determinants of constitutive activity of the hH_4R (see Chapter 5), is conserved (FY) in the hH_1R.

Table 3.4: Identical amino acids (overall and TM % identity) between biogenic amine GPCRs with available crystal structures (rows) and possible homology models (columns).

| Receptor	hH_4R		mkH_4R		cH_4R		pH_4R		rH_4R		mH_4R		gpH_4R		hH_3R	
	o/a	TM	o/a	TM	o/a	TM	o/a	TM	o/a	TM	o/a	TM	o/a	TM	o/a	TM
tβ_1AR	15	20	15	19	16	20	15	20	16	20	16	20	17	23	19	25
hβ_2AR	15	23	14	22	16	25	13	22	16	23	16	23	17	25	14	22
hD$_3$R	21	28	21	29	22	30	21	27	22	29	22	29	23	29	25	33
hH$_1$R	21	29	21	29	21	29	23	30	22	31	21	30	23	31	23	32
hM$_2$R	21	30	21	29	20	30	22	33	23	32	23	31	23	31	22	32
rM$_3$R	26	33	26	33	24	32	26	36	25	34	26	34	26	35	25	34
h5-HT$_{1B}$R	22	29	21	28	22	30	23	30	23	29	22	27	22	29	25	29
h5-HT$_{2B}$R	18	26	18	25	17	26	18	25	16	23	18	26	18	27	16	29

For calculation of the % identities, the number of identical amino acids was divided by the construct with less amino acids. For calculation of TM % identities, TM definitions shown in Table 3.2 were considered. o/a, overall % identity; TM, TM1-7 % identity.

3.4.1.2 3D structure validation

The stereochemical properties were checked with PROCHECK (Laskowski et al., 1993), available as online tool PDBsum. Ramachandran plots for all generated homology models were retrieved from the PDBsum server (Figure 3.2). About 90 % of all residues are positioned in the most favoured regions (A, B, L) and about 10 % in additional allowed regions (a, b, l, p) (Table 3.5). Disallowed regions are occupied by one amino acid in four homology models (hH_4R, mkH_4R, pH_4R and gpH_4R) and by six amino acids in case of the hH_4R model based on the inactive state structure of the hH_1R (Shimamura et al., 2011).

Furthermore, the side chain torsion angles (χ_1 up to χ_5), the RMSD distance from planarity (for planar groups such as aromatic rings) as well as bond lengths and G-factors were calculated

with PROCHECK. G-factors quantify deviations of given stereochemical properties from normality. Values below -0.5 are unusual and values below -1.0 highly unusual. The overall G-factors of the respective homology models were in the normal range (Table 3.5).
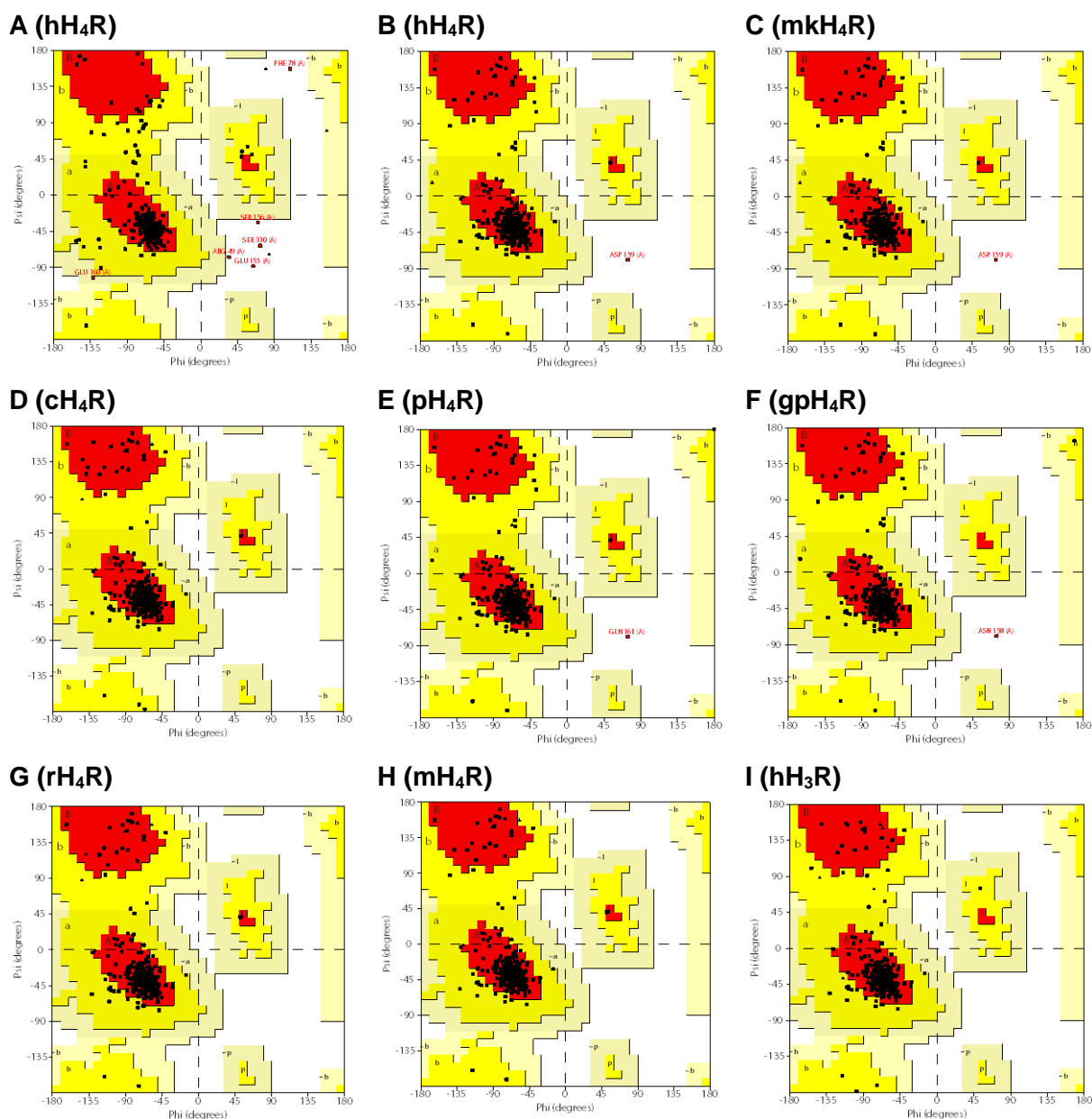
Figure 3.2: Ramachandran plots of the generated homology models illustrating the phi (φ) and psi (ψ) torsion angles. (A) The inactive state crystal structure of the hH$_1$R (PDB ID: 3RZE) was used as template; for all other homology models **(B-I)**, the active state of the β$_2$AR (PDB ID: 3P0G) was used as template. Glycines are shown as triangles and all other residues except prolines as squares. Red fields, most favoured regions; dark yellow fields, additional allowed regions; light yellow fields, generously allowed regions; white fields, disallowed regions. A and a, α-helix; B and b, β-strand; L and l, left-handed α-helix; p, allowed ε (Morris et al., 1992).

Table 3.5: Ramachandran plot statistics showing the %age of residues in each segment and the G-factors.

Residues in	hH$_4$R*	hH$_4$R	mkH$_4$R	cH$_4$R	pH$_4$R	gpH$_4$R	rH$_4$R	mH$_4$R	hH$_3$R
most favoured regions (A, B, L)	85.2	88.7	88.8	91.1	88.3	88.0	90.9	90.9	89.8
additional allowed regions (a, b, l, p)	12.7	10.9	10.9	8.9	11.4	11.6	9.1	9.1	10.2
generously allowed regions (~a, ~b, ~l, ~p)	0.4	0.0	0.0	0.0	0.0	0.0	0.0	0.0	0.0
disallowed regions	1.8	0.4	0.4	0.0	0.4	0.4	0.0	0.0	0.0
Overall G-factor	-0.19	-0.17	-0.17	-0.17	-0.20	-0.20	-0.16	-0.17	-0.23

*The inactive state crystal structure of the hH$_1$R (PDB ID: 3RZE) was used as template; for all other homology models, the active state of the β$_2$AR (PDB ID: 3P0G) was used as template.

3.4.2 Species differences between H$_4$R orthologs

Comparing the sequence alignments and homology models, a number of amino acids of the hH$_4$R were identified, which are mutated in at least one H$_4$R species ortholog. Most interesting are mutations in the ligand binding pocket, in TMs 3, 5, 6 and 7 which presumably move during receptor activation (Hulme, 2013; Rasmussen et al., 2011a) as well as within ECL2 and ECL3 also playing a role in recognition and binding of ligands and in receptor function (Brunskole et al., 2011; Peeters et al., 2011; Wheatley et al., 2012) (Figure 3.3 and Table 3.6).
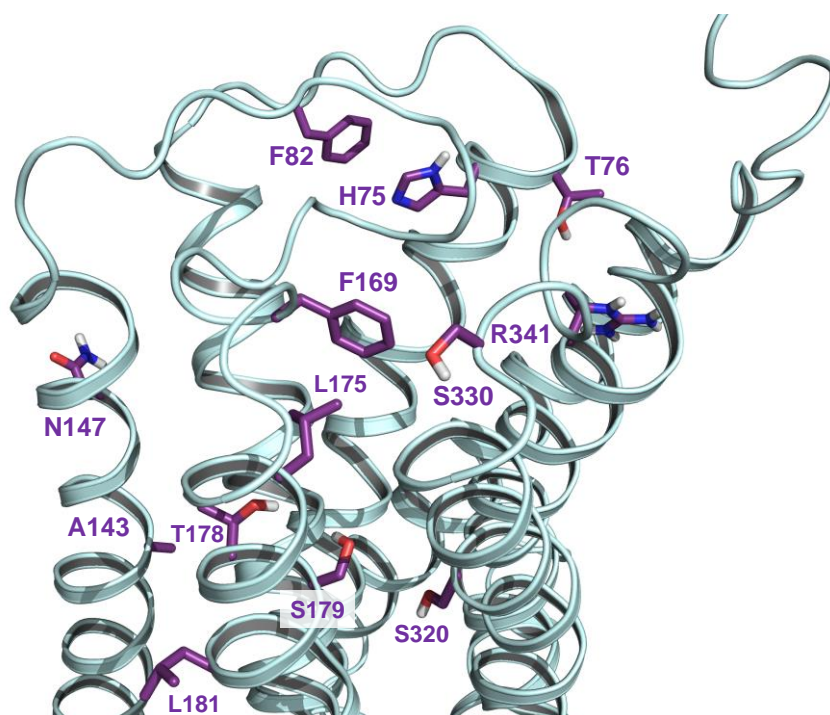
Figure 3.3: Amino acids close to the binding pocket of the hH$_4$R mutated in at least one H$_4$R species ortholog. Shown is the hH$_4$R homology model based on the inactive state of the hH$_1$R (PDB ID: 3RZE).

Mainly focusing on species differences between hH$_4$R, mH$_4$R and rH$_4$R, the following mutations are most striking: F169^{ECL2} in the hH$_4$R is exchanged by V in the mH$_4$R and rH$_4$R, S179$^{5.43}$ is replaced by M in the mH$_4$R and A in the rH$_4$R as well as R341$^{7.36}$ by S in both the mH$_4$R and rH$_4$R (Table 3.6). Moreover, S320$^{6.52}$ is exchanged by C in the mH$_4$R and rH$_4$R and

S330^{ECL3} by P in the mH$_4$R and R in the rH$_4$R. For further investigation by in-vitro mutagenesis, F169, S179, S330 and R341 were selected as potential key amino acids with respect to species differences of ligand binding and constitutive activity. With the promising results for the hH$_4$R-F169V mutant in hand, the role of F168 was additionally investigated.

Table 3.6: Positions close to the binding pocket with amino acids differing between the hH$_4$R and species variants.

Ballesteros	hH$_4$R	mkH$_4$R	cH$_4$R	pH$_4$R	rH$_4$R	mH$_4$R	gpH$_4$R
2.64	H75	H	H	H	H	H	S
2.65	T76	M	T	T	T	V	S
ECL1	F82	F	F	L	F	F	S
4.53	A143	A	A	A	A	A	S
4.57	N147	N	H	H	N	N	N
ECL2	F169	F	F	L	V	V	L
5.39	L175	V	L	L	L	L	A
5.42	T178	T	S	T	T	T	T
5.43	S179	S	S	L	A	M	S
5.45	L181	L	F	F	L	L	L
6.52	S320	S	S	S	C	C	S
ECL3	S330	S	P	P	R	P	P
7.36	R341	R	E	K	S	S	H

3.4.3 Comparison of inactive and active state hH$_4$R models

A ligand stabilizing the active receptor conformation (agonist) or the ability of a receptor to spontaneously form the active state (constitutively active receptor) are two independent and different prerequisites for receptor activation (Trzaskowski et al., 2012). Ligand binding to the receptor induces conformational changes (molecular switches) leading to a specific equilibrium of inactive and active states quantified by intrinsic activity (Figure 3.4). In case of an active receptor state, G-proteins are enabled to couple at the intracellular side where TM movements (Figure 3.4C) unclose a binding pocket for the C-terminus of the G$_\alpha$ subunit. Most prominent changes occur within TM6. At the β$_2$AR (Rasmussen et al., 2011a), a 11.4 Å outward movement of E$^{6.30}$ due to a clockwise rotation of this TM near the conserved P$^{6.50}$ (Trzaskowski et al., 2012) was demonstrated. Comparing inactive and active hH$_4$R models, a 9.8 Å outward movement of TM6 at the amino acid A298$^{6.30}$ was determined (Figure 3.4B, C) as well as a slight outward movement of TM5 (Figure 3.4C, D) and a slight inward movement of TM3 at the intracellular side (Figure 3.4C, D). Additionally, the binding pocket is contracted (Figure 3.4A) due to slight inward movements of TM3 (straight) and TMs 4 to 7 (clockwise).
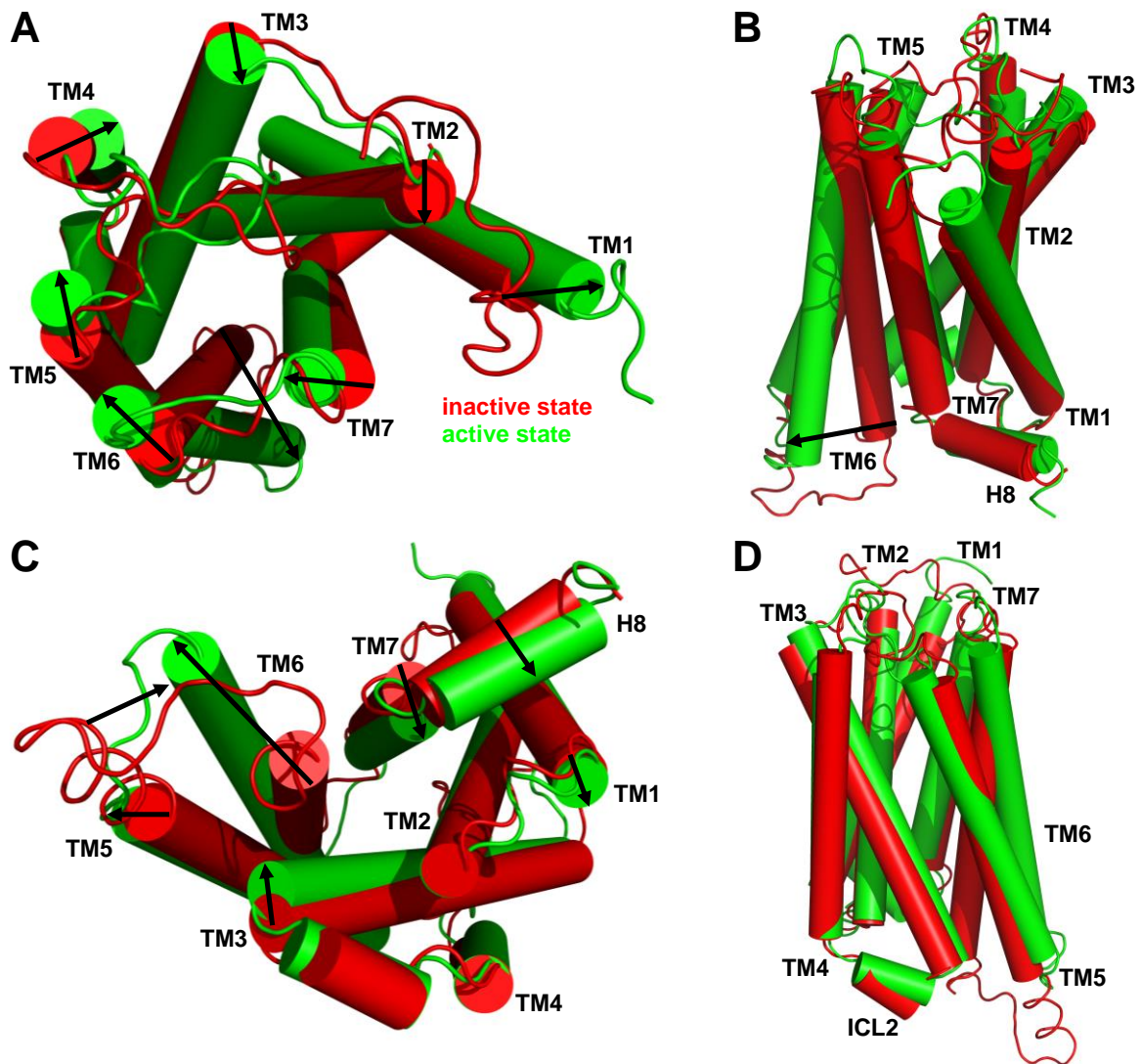
Figure 3.4: Comparison of an inactive hH4R model based on the hH1R (PDB ID: 3RZE; red) with an active state hH4R model based on the β2AR (PDB ID: 3P0G; green). Arrows indicate the movements upon activation. **(A)** Top view from the extracellular side, **(B)** side view illustrating the outward movement of TM6 at the intracellular face, **(C)** intracellular view also indicating the outward movement of TM6 and **(D)** side view at the opposite side compared to **(B)**.

The so-called ionic lock – a salt bridge between $R^{3.50}$ and $E^{6.30}$ – was first evident in the case of bovine rhodopsin (Palczewski et al., 2000) and supposed to restrain GPCRs in the inactive conformation (Angelova et al., 2002; Ballesteros et al., 2001; Greasley et al., 2002; Shapiro et al., 2002). However, the ionic lock is missing in H4R species orthologs due to substitution of glutamate by alanine (Figure 3.5) and even in inactive state structures of some biogenic amine GPCRs (see, e. g. β1AR (Moukhametzianov et al., 2011; Warne et al., 2008), β2AR (Cherezov et al., 2007; Hanson et al., 2008; Rasmussen et al., 2007), H1R (Shimamura et al., 2011) and M2R (Haga et al., 2012)) containing the $R^{3.50}$-$E^{6.30}$ couple. Other crystal structures of, e. g., the D3R (Chien et al., 2010) or the A2AR (Dore et al., 2011) feature the ionic lock. Nevertheless, $R^{3.50}$ belongs to the D/ERY motif which plays a key role in GPCR activation and interaction with G-proteins as approved by mutagenesis studies with the H2R (Alewijnse et al., 2000) and the H4R (Schneider et al., 2010). $D^{3.49}$ forms a salt bridge with the neighbouring $R^{3.50}$

constraining the receptor in the inactive conformation (hH$_4$R: D111$^{3.49}$ with R112$^{3.50}$; Figure 3.5; Ballesteros et al., 1998; Scheer et al., 1996; 1997). Mutations of D$^{3.49}$ preclude this ionic interaction and trigger receptor activation, i. e., the mutants show constitutive activity and higher agonist affinities. In contrast, mutations of R$^{3.50}$ led to highly instable and inactive receptors not interacting with G-proteins (Alewijnse et al., 2000; Schneider et al., 2010).
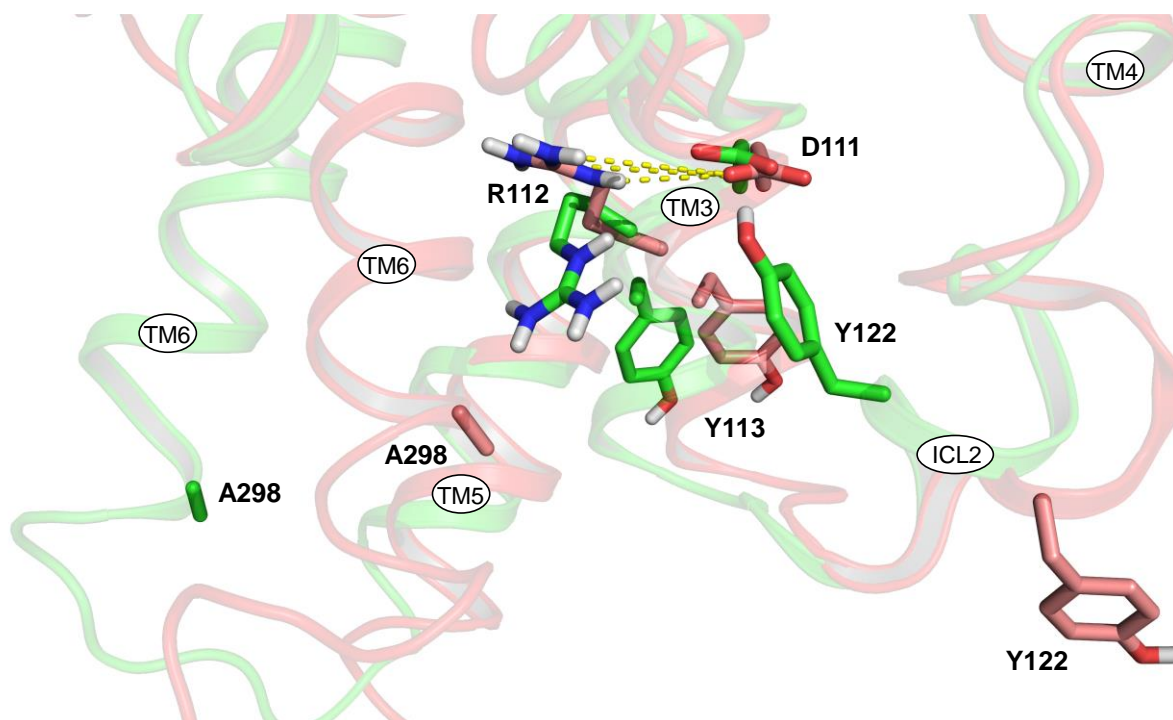
Figure 3.5: Relocation of the DRY motif during activation. Inactive hH$_4$R state: red, based on the hH$_1$R, PDB ID: 3RZE; active hH$_4$R state: green, based on the β$_2$AR, PDB ID: 3P0G. In the inactive state, D111$^{3.49}$ forms an ionic interaction with R112$^{3.50}$. Activation relocates R112$^{3.50}$ and the ionic interaction is precluded. Moreover, the ionic lock between R112$^{3.50}$ and position 6.30 is missing due to the presence of A298$^{6.30}$. Y122^{ICL2} possibly forms an H-bond with D111$^{3.49}$ upon activation.

The so-called rotamer toggle switch of W$^{3.48}$ (hH$_4$R: W316$^{6.48}$) was previously assumed to be part of the signal transmission (Shi et al., 2002). A rearrangement of the side chains of C/S/T$^{6.47}$, W$^{6.48}$ (part of the FxxCWxP motif) and F$^{6.52}$ were supposed to modulate the P$^{6.50}$ kink in TM6 (Kobilka and Deupi, 2007). Result is the outward movement of the cytoplasmic face of TM6. However, the active states of neither the A$_{2A}$R (Xu et al., 2011) nor the β$_2$AR (PDB ID: 3P0G; Rasmussen et al., 2011a) indicate rotamer transitions of W$^{6.48}$. Consequently, the rotamer toggle switch cannot be detected when comparing inactive and active state hH$_4$R homology models (Figure 3.6). However, a transmission switch relocates the amino acids in TM3, TM5 and TM6, namely I/L$^{3.40}$, P$^{5.50}$, L$^{5.51}$, F$^{6.44}$ and W$^{6.48}$ (hH$_4$R: V102$^{3.40}$, P186$^{5.50}$, V187$^{5.51}$, F312$^{6.44}$ and W316$^{6.48}$; Figure 3.6) (Deupi and Standfuss, 2011).
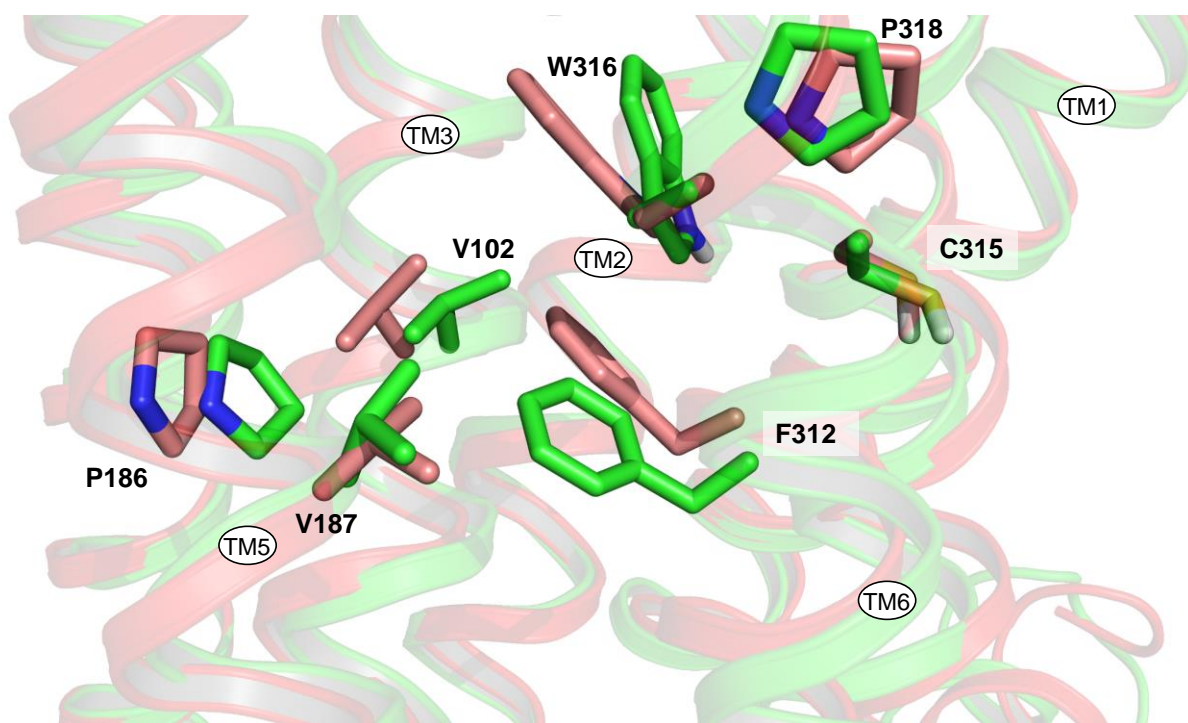
Figure 3.6: Amino acid movements from the inactive hH₄R state to the active hH₄R state. Inactive state: red, based on the hH₁R, PDB ID: 3RZE; active state: green, based on the β₂AR, PDB ID: 3P0G. Shown are the amino acids putatively modulated by the controversial rotamer toggle switch (C315$^{6.47}$, W316$^{6.48}$ and P318$^{6.50}$; FxxCWxP motif) and the transmission switch (V102$^{3.40}$, P186$^{5.50}$, V187$^{5.51}$, F312$^{6.44}$ and W316$^{6.48}$).

In the inactive state, the so-called "hydrophobic barrier" separates the water-mediated hydrogen bond network between the binding pocket and the NPxxY motif from the DRY motif (essential for G-protein activation; Figure 3.7A, B; Standfuss et al., 2011; Trzaskowski et al., 2012). Activation of the receptor includes a rotation of TM6 responsible for opening the hydrophobic barrier. Y358$^{7.53}$ is rearranged (tyrosine toggle switch; Figure 3.7C) and the hydrogen bond network is expanded towards the DRY motif (Figure 3.7B).

As recently discovered at rhodopsin, an ionic interaction between position 3.28 and 7.43 (3-7 lock switch) in inactive states is precluded on receptor activation (Trzaskowski et al., 2012). In case of the hH₁R (Shimamura et al., 2011) and the D₃R (Chien et al., 2010), interactions between D$^{3.32}$ and Y$^{7.43}$ (hH₄R: D94$^{3.32}$ and W348$^{7.43}$) may replace this mechanism. However, this ionic interaction was also observed in active crystal structures as the β₂AR (Rasmussen et al., 2011a; Rasmussen et al., 2011b). Thus, the 3-7 lock switch seems not to be a common feature of GPCR activation.
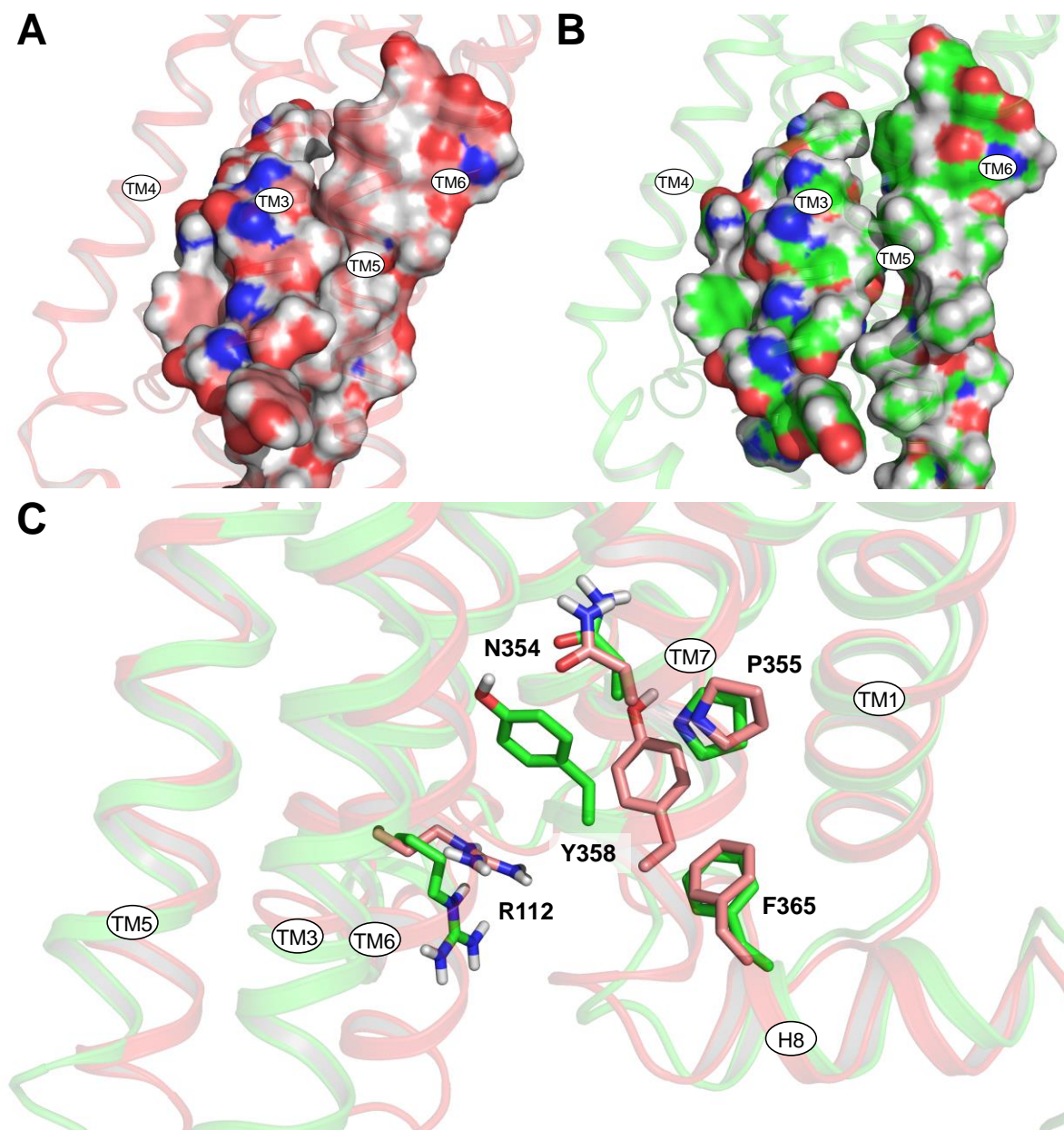
Figure 3.7: Hydrophobic barrier in (A) the inactive hH₄R (red) being dissolved in (B) the active state (green). Inactive state: based on the hH₁R, PDB ID: 3RZE; active state: based on the β₂AR, PDB ID: 3P0G. **(C)** Movements of TM6 lead to a rearrangement of Y358$^{7.53}$ in the NPxxY motif (N354$^{7.49}$, P355$^{7.50}$, Y358$^{7.53}$).

3.4.4 Analysis of the binding modes of the investigated H₄R ligands

3.4.4.1 Ligand-free basal hH₄R states

In contrast to the rodent orthologs, fractions of the hH₄R (and the hH₃R) are activated without ligands (Schneider et al., 2009; Schnell et al., 2011). Reason for this "preactivation" are intramolecular interactions stabilizing the receptor in the active state. These interactions are precluded in the case of rodent orthologs. A comparison of hH₄R, mH₄R and rH₄R may indicate amino acids being responsible for the high constitutive activity of the hH₄R. Experimentally, F168^{ECL2} and F169^{ECL2} on their own as well as F169^{ECL2} in concert with S179$^{5.43}$ were

determined as key amino acids in this respect (Chapters 4 and 5). The FF motif in ECL2, also present, e. g., in the hH$_3$R or the β$_2$AR, interacts with hydrophobic and aromatic amino acids such as Y95$^{3.33}$, P166^{ECL2}, L175$^{5.39}$, T178$^{5.42}$, Y319$^{6.51}$, T323$^{6.55}$, L326$^{6.58}$, T333^{ECL3} and Y340$^{7.35}$ (Figure 3.8A, D, F). Result is a hydrophobic cluster with the FF motif as essential component. This cluster contributes to the contraction of the binding pocket as illustrated in Figure 3.4A (Lebon et al., 2011; Lebon et al., 2012; Tse, 2011) and, by this, to the stabilization of an active state. However, mutation of F169 to V (Figure 3.8B, E) or F168 to A (Figure 3.8C, G) disrupts some of these hydrophobic and π-π interactions and therefore the contraction of the binding pocket is prevented in favour of the inactive state, i. e., constitutive activity decreases.
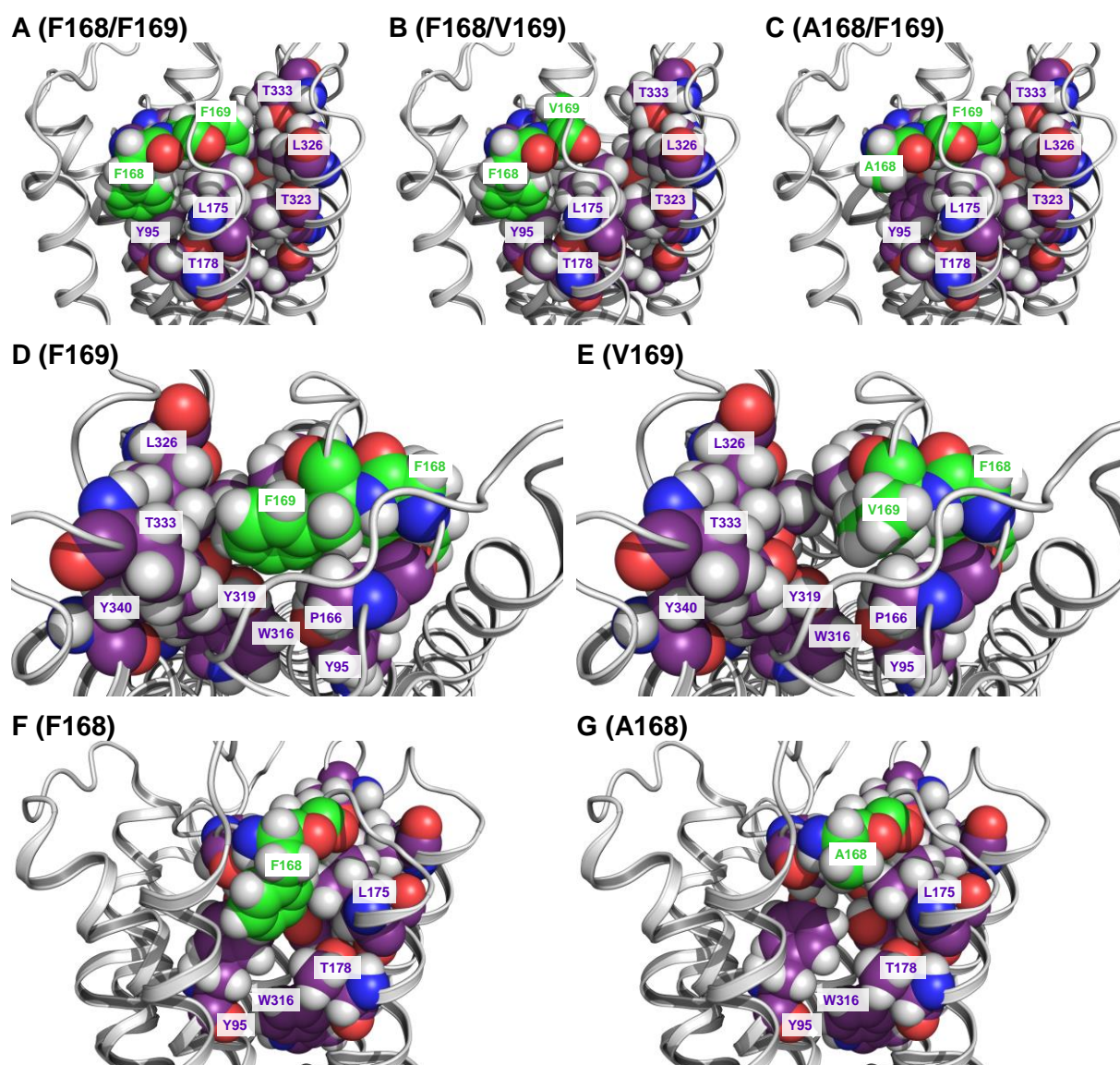
Figure 3.8: Interactions of the F168/F169 motif with hydrophobic and aromatic amino acids. (A, D, F) F168/F169 interacting with hydrophobic and aromatic amino acids. **(B, E)** Interactions of V169 with the hydrophobic cluster and **(C, G)** interactions of A168 with the hydrophobic cluster. Model based on the inactive state of the hH$_1$R (PDB ID: 3RZE).

Single mutations of S179$^{5.43}$ to M or A did not significantly change the level of constitutive activity, but the double mutation of F169^{ECL2} to V and S179$^{5.43}$ to M or A significantly dropped

constitutive activity, leading to an intrinsic activity of thioperamide comparable to that at mH_4R and rH_4R (Chapter 4). $S179^{5.43}$ forms an H-bond with $T323^{6.55}$ (Figure 3.9A) which is precluded in case of mutation into M or A (Figure 3.9B, C). With an intact FF motif (Figure 3.8A, D, F), this H-bond is not mandatory for the concomitant inward movements of TM5 and TM6 at the extracellular face, i. e., the contraction of the binding pocket. Therefore, $S179^{5.43}$ on its own does not contribute to the high constitutive activity of the hH_4R. But if both the FF motif is disrupted by mutation of $F169^{ECL2}$ into V and the H-bond between $S179^{5.43}$ and $T323^{6.55}$ is precluded, hydrophobic and π-π interactions with TM5 and TM6 are weakened (Figure 3.8B, E) and the aforementioned inward movements of TM5 and TM6 are impossible.
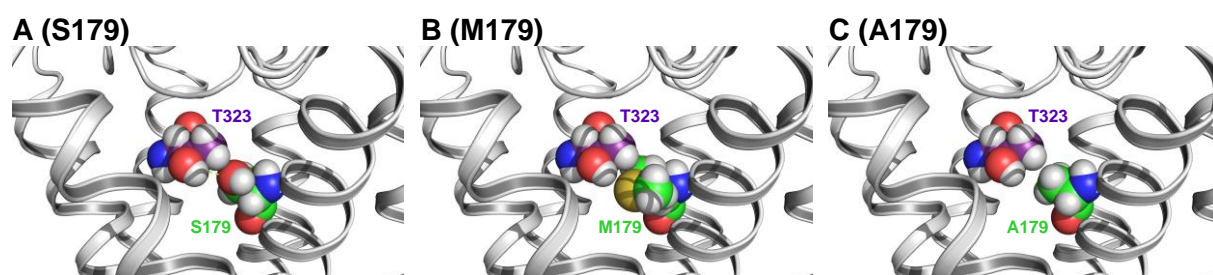
Figure 3.9: Effects of $S179^{5.43}$, S179M and S179A. (A) H-bond with $T323^{6.55}$; H-bond precluded in case of mutation to **(B)** M or **(C)** A. Model based on the inactive state of the hH_1R (PDB ID: 3RZE).

Furthermore, mutation of $R341^{7.36}$ to S or $S330^{ECL3}$ to R in the hH_4R caused a slight decrease in constitutive activity (Chapters 6 and 7). These mutations may destabilize the extracellular surface by changing the charges and polarities of the extracellular environment.

3.4.4.2 Histamine

The docking mode of histamine is described in Chapter 4.2

3.4.4.3 UR-PI294

Compared to histamine, the main interactions of UR-PI294 with the hH_4R, namely with $D94^{3.32}$, $E182^{5.46}$ and $Q347^{7.42}$ are maintained (Figure 3.10): The N^T hydrogen of the imidazole moiety forms an H-bond with $E182^{5.46}$ and the guanidinium hydrogens form H-bonds with $D94^{3.32}$ and $Q347^{7.42}$. The imidazolylpropyl moiety fits well in the hydrophobic surface composed of $Y95^{3.33}$, $P166^{ECL2}$, $F168^{ECL2}$, $F169^{ECL2}$, $L175^{5.39}$, $T178^{5.42}$, $W316^{6.48}$ and $Y319^{6.51}$.

Based on site-directed mutagenesis studies (Chapter 5), $F168^{ECL2}$ is assumed to interact with UR-PI294 as mutation to A decreased potency by approximately 1.5 orders of magnitude. Whereas S179, S330 and R341 were of minor influence, introduction of the critical F into the mH_4R (mH_4R-V171F mutant) increased potency by more than one order of magnitude supporting the key function of the FF motif in binding of UR-PI294 (Chapters 4, 6 and 7). However, intrinsic activities almost remained unaltered.
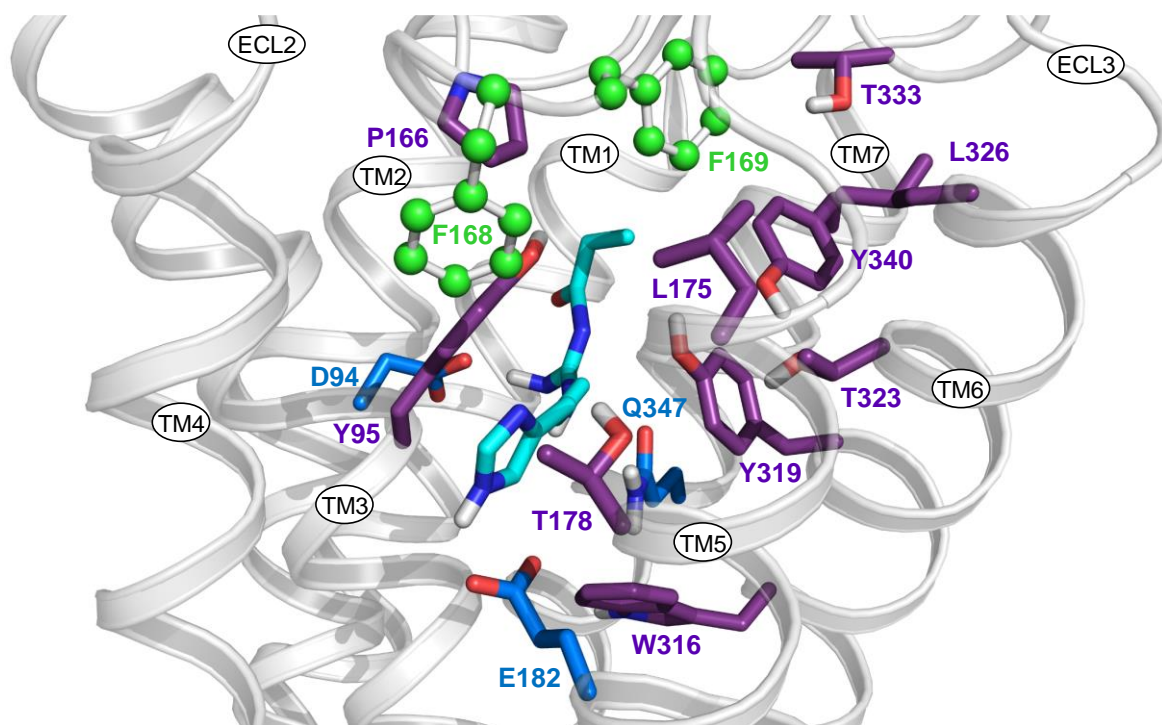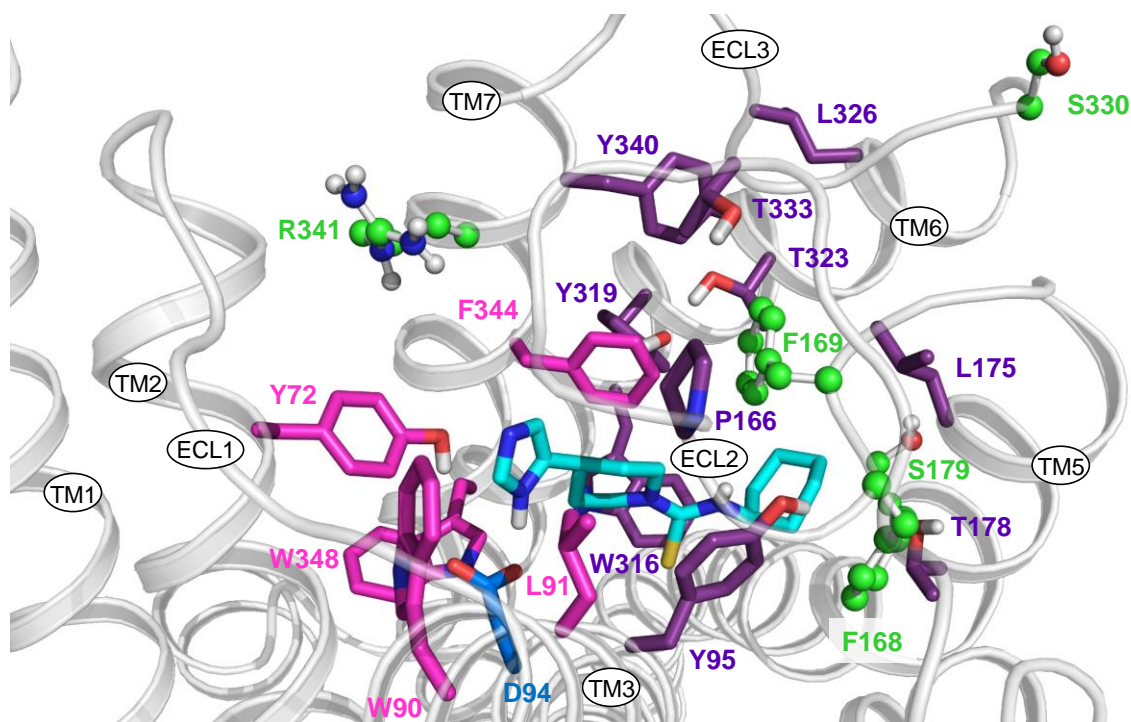
Figure 3.10: Docking pose of UR-PI294 in the hH$_4$R. Model based on the inactive state of the hH$_1$R (PDB ID: 3RZE). Colour code: oxygen – red, nitrogen – blue; carbon atoms are coloured individually: key interactions of UR-PI294 (D94$^{3.32}$, E182$^{5.46}$ and Q347$^{7.42}$) are illustrated in dark blue, the FF motif (F168^{ECL2} and F169^{ECL2}) is coloured in green and the amino acids of the hydrophobic cluster (Y95$^{3.33}$, P166^{ECL2}, L175$^{5.39}$, T178$^{5.42}$, W316$^{6.48}$, Y319$^{6.51}$, T323$^{6.55}$, L326$^{6.58}$, T333^{ECL3} and Y340$^{7.35}$) in magenta.

3.4.4.4 Thioperamide

The classical H$_3$R/H$_4$R inverse agonist thioperamide decreases activity below the level of constitutive activity, present at both histamine receptor subtypes. It was assumed that agonists especially bind at TM3, TM5, TM6 and TM7, but antagonists or inverse agonists partly also occupy a pocket between TM1 and TM2. Wittmann et al. (2014) proposed a binding mode of thioperamide at the hH$_3$R that can by analogy also be applied at the hH$_4$R: the cyclohexane moiety of thioperamide is embedded in a hydrophobic network of amino acids of the hydrophobic cluster and the FF motif, the thiourea moiety is positioned in the vicinity of F169 and the N$^\pi$-H of the imidazole ring contacts D94$^{3.32}$, whereas the key interactions of other ligands with E182$^{5.46}$ and Q347$^{7.42}$ are absent or only weak. The imidazole ring is rather embedded in a hydrophobic pocket consisting of amino acids such as Y72$^{2.61}$ and F344$^{7.39}$ (Figure 3.11). Probably this binding mode, in particular the missing interaction with E182$^{5.46}$ and Q347$^{7.42}$, prevents the contraction of the orthosteric binding pocket (inward movements of TMs 5, 6 and 7), characteristic of the conversion of the receptor to the active state (Rasmussen et al., 2011a). The hH$_3$R forms a similar pocket (Wittmann et al., 2014), but thioperamide acts as a weaker inverse agonist at the hH$_3$R due to its lower constitutive activity.

At the hH$_4$R-S330R, hH$_4$R-R341S, hH$_4$R-F169V, hH$_4$R-F169V+S179M/A or hH$_4$R-F168A mutants, thioperamide has a different ability to shift the more or less basally activated receptor

to an inactive state (Chapters 4, 5, 6 and 7). Therefore, the intrinsic activity of thioperamide decreased from full inverse agonism at the hH4R wild-type to partial inverse agonism or even neutral antagonism at the respective mutants. Potency and affinity changes at the generated receptor mutants were only marginal in most cases. The increase in pK$_b$ at the hH4R-F168A mutant by one order of magnitude compared to the wild-type receptor is compatible with higher affinity of thioperamide to inactive than to active state(s), represented by the mutant devoid of constitutive activity and the highly constitutively active wild-type hH4R.


Figure 3.11: Docking pose of thioperamide in the hH4R. MD simulation performed and model provided by Strasser (2014). Model based on the inactive state of the hH1R (PDB ID: 3RZE). Colour code: oxygen – red, nitrogen – blue, sulphur – yellow; carbon atoms are coloured individually: the key interaction of thioperamide (D94$^{3.32}$) is illustrated in dark blue, amino acids subjected to in-vitro mutagenesis (F168^{ECL2}, F169^{ECL2}, S179$^{5.43}$, S330^{ECL3} and R341$^{7.36}$) are coloured in green, the amino acids of the hydrophobic cluster (Y95$^{3.33}$, P166^{ECL2}, L175$^{5.39}$, T178$^{5.42}$, W316$^{6.48}$, Y319$^{6.51}$, T323$^{6.55}$, L326$^{6.58}$, T333^{ECL3} and Y340$^{7.35}$) in magenta and the amino acids close to the imidazole ring of thioperamide (Y72$^{2.61}$, W90$^{3.28}$, L91$^{3.29}$, F344$^{7.39}$ and W348$^{7.43}$) in pink.

3.4.4.5 JNJ7777120

We found a similar JNJ7777120 binding mode as Lim et al. (2010) and Schultes et al. (2013). The hydrogen of the positively charged piperazine nitrogen forms an H-bond with D94$^{3.32}$ and Q347$^{7.42}$, the carbonyl oxygen accepts an H-bond from C98$^{3.36}$ and the indole N-H is involved in an H-bond with the carboxylate group of E182$^{5.46}$ (Figure 3.12; Lim et al., 2010). The chlorinated indole ring is embedded between Y95$^{3.33}$ and Y319$^{6.51}$ occupying a pocket between TM3, TM5, TM6 and ECL2. It is furthermore enclosed in hydrophobic interactions with F168^{ECL2} and F169^{ECL2} and contacts L175$^{5.39}$ and S179$^{5.43}$. Structure activity relationships support this

binding mode, as the indole N-H and the carbonyl moiety are essential for ligand affinity (Jablonowski et al., 2003).
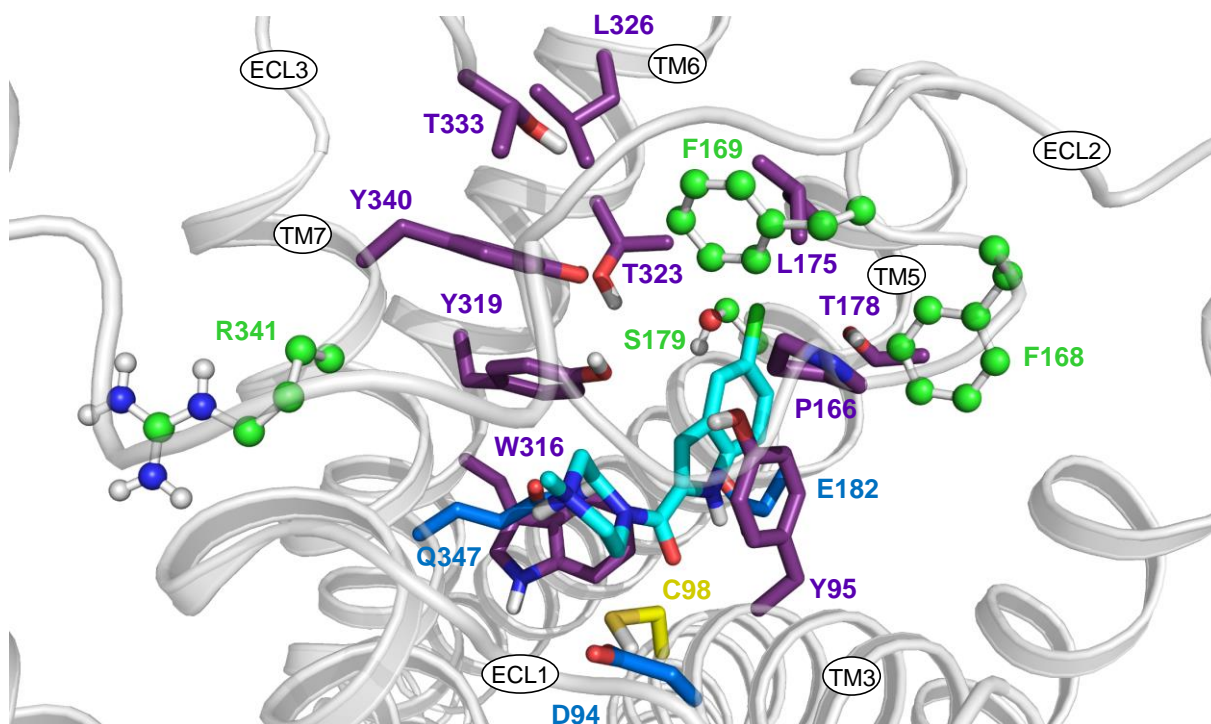

Figure 3.12: Docking pose of JNJ7777120 in the hH₄R. Model based on the inactive state of the hH₁R (PDB ID: 3RZE). Colour code: oxygen – red, nitrogen – blue, sulphur – yellow, chlorine – green; carbon atoms are coloured individually: key interactions of JNJ7777120 (D94$^{3.32}$, E182$^{5.46}$ and Q347$^{7.42}$) are illustrated in dark blue, interactions of JNJ7777120 with C98$^{3.36}$ in yellow, amino acids subjected to in-vitro mutagenesis (F168^{ECL2}, F169^{ECL2}, S179$^{5.43}$ and R341$^{7.36}$) are coloured in green and the amino acids of the hydrophobic cluster (Y95$^{3.33}$, P166^{ECL2}, L175$^{5.39}$, T178$^{5.42}$, W316$^{6.48}$, Y319$^{6.51}$, T323$^{6.55}$, L326$^{6.58}$, T333^{ECL3} and Y340$^{7.35}$) in magenta.

Compared to the hH₄R wild-type, a decrease in pK$_b$ (1.4 orders of magnitude) was experimentally detected at the hH₄R-F168A mutant, supporting direct interactions of F168 with JNJ7777120 (Figure 3.13B; Chapter 5). The hH₄R-F169V mutant revealed a significant decrease in potency (ΔpEC$_{50}$ = 0.9), albeit the decrease in affinity was smaller (ΔpK$_i$ = 0.3) (Chapter 4). These results suggest that also F169 interacts with the indole ring of JNJ7777120 (Figure 3.13A). Compared to the hH₄R wild-type, the hH₄R-S179M mutant did not change JNJ7777120 affinity. By contrast, the hH₄R-S179A mutant resulted in significantly increased potency and affinity (ΔpK$_i$ = 0.6), indicating repulsive interaction of S179 with the chlorinated indole ring (Figure 3.13A).

The differences in intrinsic activities of JNJ7777120 (partial inverse agonism at hH₄R and hH₄R-S179M/A, neutral antagonism at hH₄R-F169V+S179A and hH₄R-R341S, and partial agonism at hH₄R-F168A, hH₄R-F169V and hH₄R-F169V+S179M) are largely compatible with the different constitutive activities (Chapters 4, 5 and 7). The situation is similar to thioperamide, albeit JNJ7777120 acts as a protean agonist (Kenakin, 2001). JNJ7777120 may bind to both the inactive and the active hH₄R state, but with preference for the former one.

Depending on the basal activity of the receptor species (high, low or no constitutive activity), the affinity component for the active state leads to partial inverse agonism, neutral antagonism and partial agonism, respectively.
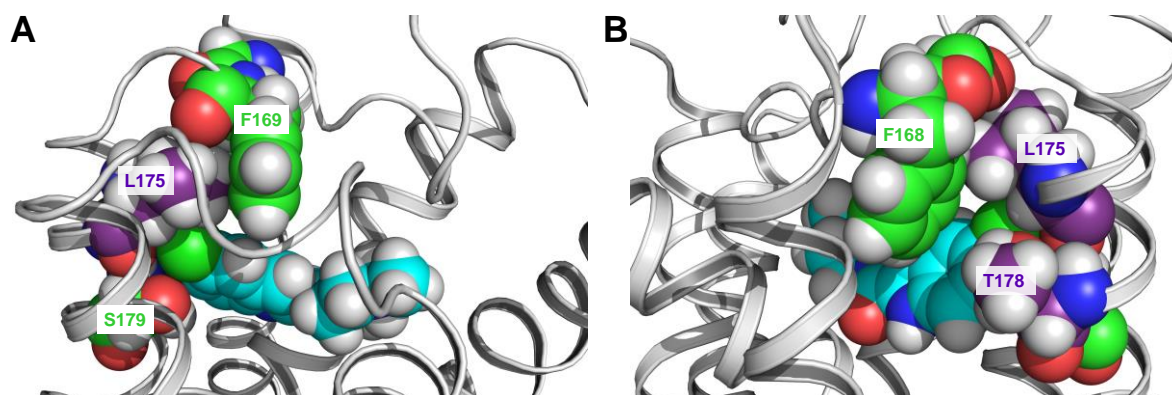
Figure 3.13: (A, B) Contacts of JNJ7777120 with the side chains of TM5 (L175$^{5.39}$, T178$^{5.42}$, S179$^{5.43}$) as well as interactions with (A) F169 and (B) F168. Model based on the inactive state of the hH$_1$R (PDB ID: 3RZE).

3.4.4.6 VUF8430

Jongejan et al. (2008) proposed a binding mode of VUF8430 interacting with D94$^{3.32}$, E182$^{5.46}$ and Q347$^{7.42}$ (Figure 3.14). The isothiourea moiety is embedded between TM5 and TM6, whereas the guanidinium group is involved in an H-bond network with TM3 and TM7.
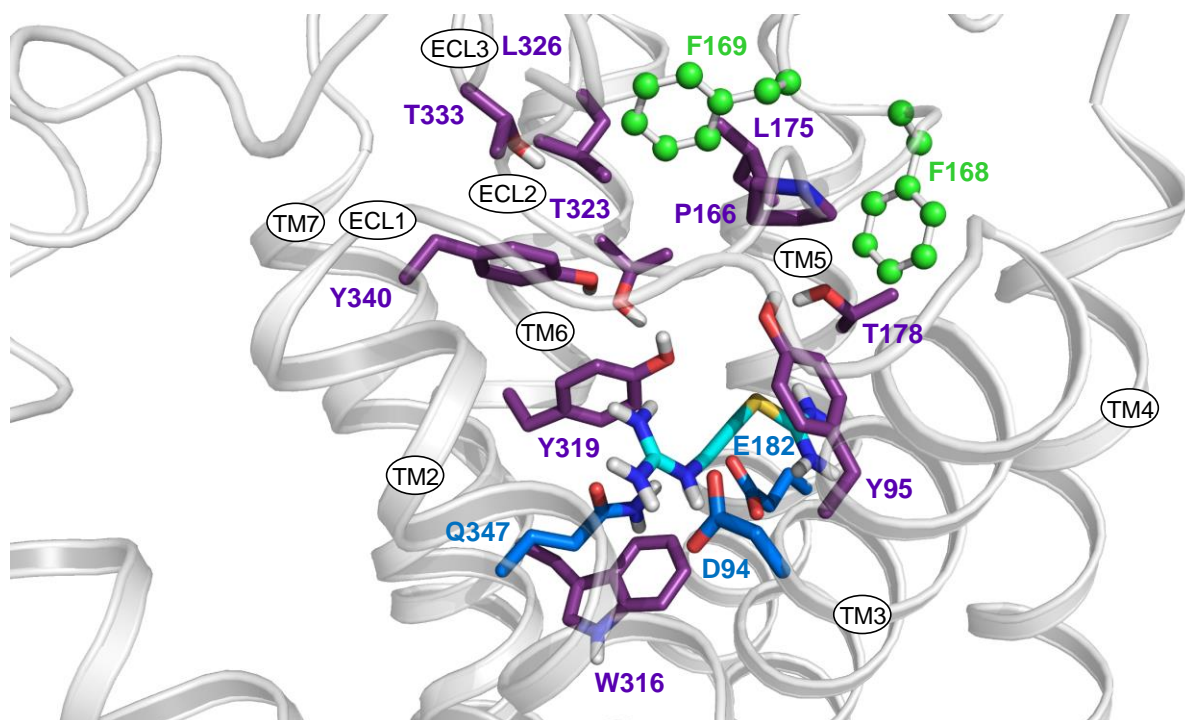
Figure 3.14: Docking pose of VUF8430 in the hH$_4$R. Model based on the inactive state of the hH$_1$R (PDB ID: 3RZE). Colour code: oxygen – red, nitrogen – blue, sulphur – yellow; carbon atoms are coloured individually: key interactions of VUF8430 (D94$^{3.32}$, E182$^{5.46}$ and Q347$^{7.42}$) are illustrated in dark blue, the FF motif (F168^{ECL2} and F169^{ECL2}) is coloured in green and the amino acids of the hydrophobic cluster (Y95$^{3.33}$, P166^{ECL2}, L175$^{5.39}$, T178$^{5.42}$, W316$^{6.48}$, Y319$^{6.51}$, T323$^{6.55}$, L326$^{6.58}$, T333^{ECL3} and Y340$^{7.35}$) in magenta.

Whereas the hH$_4$R-S330R and hH$_4$R-R341S/E mutants revealed a minor influence of these amino acids on binding and intrinsic activity, the potency of VUF8430 increased by about 0.7 orders of magnitude at the mH$_4$R-V171F mutant compared to the mH$_4$R wild-type (Chapters 4, 6 and 7). At the hH$_4$R-F168A mutant, a highly significant decrease of the potency of VUF8430 was observed (ΔpEC$_{50}$ = 1.7) with respect to the hH$_4$R wild-type (Chapter 5). Therefore, the thioethyl chain may interact with F168, possibly via amino acids of the hydrophobic cluster (Figure 3.14).

3.4.4.7 Immepip

The binding mode of immepip is highly similar to that of histamine and VUF8430 (Figure 3.15). However, immepip is more rigid in comparison to histamine and therefore the distance between the imidazole ring (carbon in 4-position) and the nitrogen interacting with D94$^{3.32}$ and Q347$^{7.42}$ is longer (5.09 Å vs. 3.84 Å).

Concerning the investigated mutants, hH$_4$R-S330R and hH$_4$R-R341S/E are without effect on affinity, potency and intrinsic activity (Chapters 6 and 7). However, introduction of F171 into the mH$_4$R (mH$_4$R-V171F) increased potency by about 0.8 orders of magnitude (Chapter 4). Compared to the hH$_4$R wild-type, the hH$_4$R-F168A mutant decreased potency by about 1.9 orders of magnitude (Chapter 5). As in case of VUF8430, interactions of F168 with immepip may be mediated by amino acids of the hydrophobic cluster.
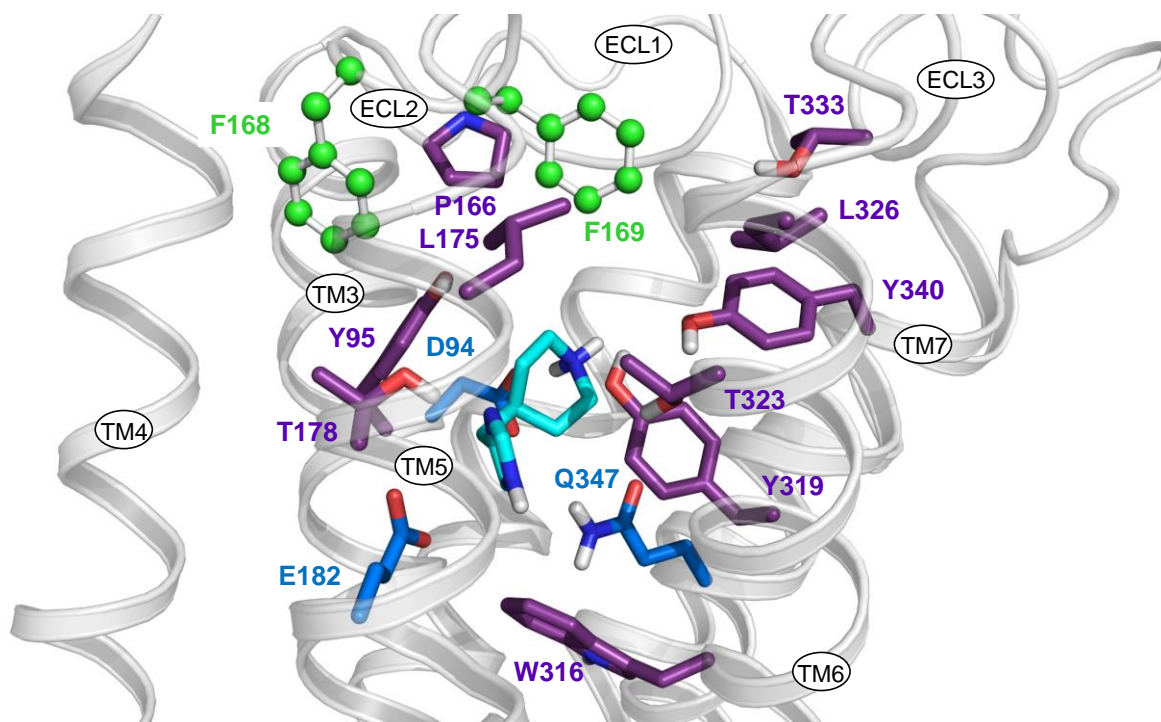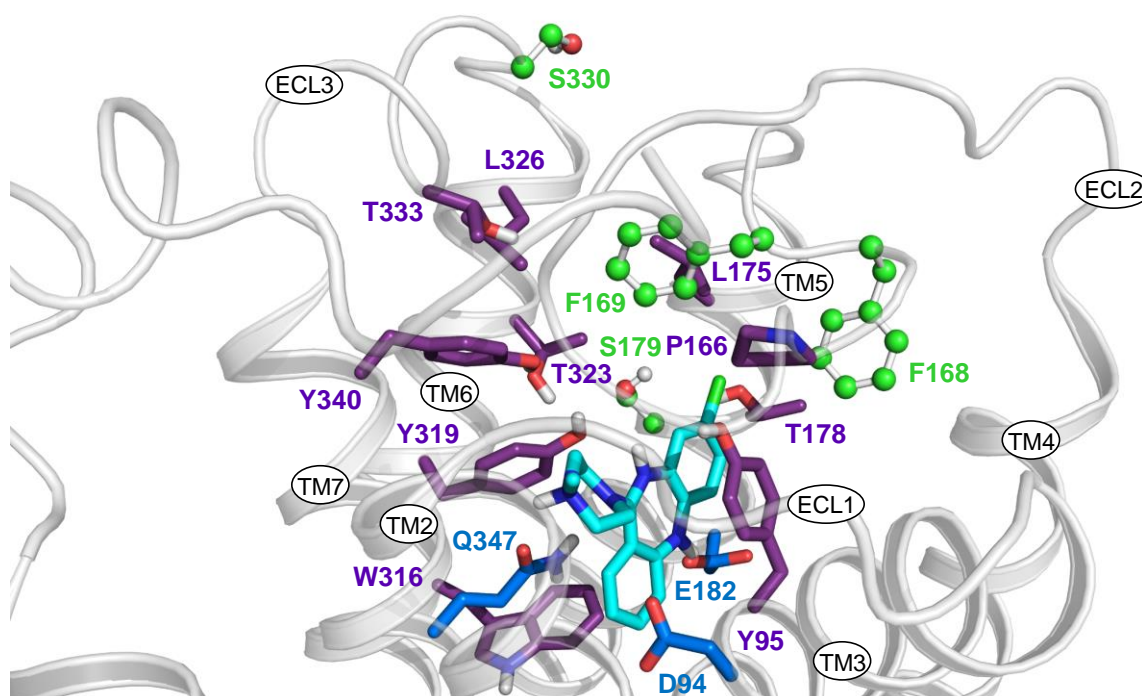

Figure 3.15: Docking pose of immepip in the hH$_4$R. Model based on the inactive state of the hH$_1$R (PDB ID: 3RZE). Colour code: oxygen – red, nitrogen – blue; carbon atoms are coloured individually: key interactions of immepip (D94$^{3.32}$, E182$^{5.46}$ and Q347$^{7.42}$) are illustrated in dark blue, the FF motif (F168^{ECL2} and F169^{ECL2}) is coloured in green and the amino acids of the hydrophobic cluster (Y95$^{3.33}$, P166^{ECL2}, L175$^{5.39}$, T178$^{5.42}$, W316$^{6.48}$, Y319$^{6.51}$, T323$^{6.55}$, L326$^{6.58}$, T333^{ECL3} and Y340$^{7.35}$) in magenta.
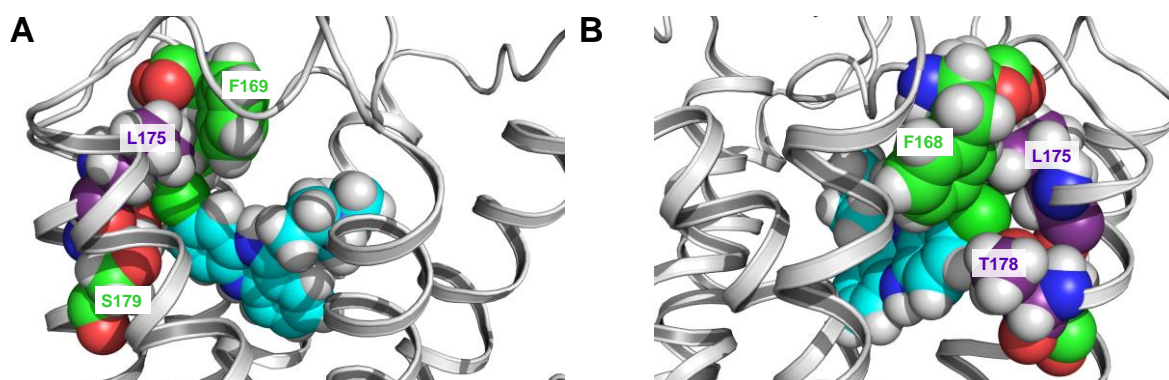
3.4.4.8 Clozapine

According to Jongejan et al. (2008), Lim et al. (2010) and Schultes et al. (2013), the hydrogen of the N-methylpiperazine ring of clozapine interacts with $D94^{3.32}$ and the N-H of the 7 membered ring system with the carboxylate group of $E182^{5.46}$ (Figure 3.16). The carbonyl moiety of $Q347^{7.42}$ forms an H-bond with the N-H function of the 7 membered ring as well as with the hydrogen of the N-methylpiperazine ring. However, in contrast to Jongejan et al. (2008) and Lim et al. (2010), the chlorine moiety of the tricyclic ring system was suggested to interact with TM5 as well as with the FF motif, i. e., the tricyclic ring is vertically oriented. This correlates with the binding mode shown for JNJ7777120, i. e., the chlorine of JNJ7777120 adopts a similar position as the chlorine of clozapine. Therefore, both JNJ7777120 and clozapine reveal a similar behaviour at the investigated mutants.

Figure 3.16: Docking pose of clozapine in the hH_4R. Model based on the inactive state of the hH_1R (PDB ID: 3RZE). Colour code: oxygen – red, nitrogen – blue, chlorine – green; carbon atoms are coloured individually: key interactions of clozapine ($D94^{3.32}$, $E182^{5.46}$ and $Q347^{7.42}$) are illustrated in dark blue, amino acids subjected to in-vitro mutagenesis ($F168^{ECL2}$, $F169^{ECL2}$, $S179^{5.43}$ and $S330^{ECL3}$) are coloured in green and the amino acids of the hydrophobic cluster ($Y95^{3.33}$, $P166^{ECL2}$, $L175^{5.39}$, $T178^{5.42}$, $W316^{6.48}$, $Y319^{6.51}$, $T323^{6.55}$, $L326^{6.58}$, $T333^{ECL3}$ and $Y340^{7.35}$) in magenta.

According to the key role of the FF motif in binding of clozapine, an exchange of F168 into A or F169 into V in the hH_4R significantly decreased the pEC_{50} values of clozapine from 6.24 at the hH_4R wild-type to 5.38 and 5.68, respectively (Chapter 5). By contrast, potency and intrinsic activity of clozapine significantly increased at the mH_4R-V171F and the mH_4R-V171F+M181S mutants compared to the mH_4R wild-type (Chapter 4). Neutral antagonism turned to partial agonism. These results support the suggested binding mode and the interaction of clozapine with the FF motif (Figure 3.17). Whereas compared to the hH_4R wild-type, the hH_4R-S179M

single mutant did not change potency and affinity, introduction of alanine significantly increased both potency and affinity of clozapine. Accordingly, pEC_{50} and pK_i values of clozapine at the hH_4R-F169V+S179A mutant were significantly higher than at the hH_4R-F169V+S179M mutant. This supports the hypothesis that the tricyclic ring interacts with TM5 more favourable in case of the smaller alanine (Figure 3.17). Due to a similar mechanism as proposed for JNJ7777120, less voluminous side chains of TM5 may improve the affinity of the ligand. The hH_4R-S330R mutant significantly decreased potency and affinity of clozapine compared to the hH_4R wild-type ($\Delta pEC_{50} = 0.7$; Chapter 6). Probably, altering the charge profile at the extracellular surface may impede the positively charged clozapine on entering the binding pocket. Moreover, steric repulsion may come into play.

Figure 3.17: (A, B) Contacts of clozapine with the side chains of TM5 (L175$^{5.39}$, T178$^{5.42}$, S179$^{5.43}$) as well as interactions with (A) F169 and (B) F168. Model based on the inactive state of the hH_1R (PDB ID: 3RZE).

3.4.4.9 Isoloxapine

The structures of clozapine and isoloxapine are highly similar apart from the exchange of the nitrogen by an oxygen. Thus, the binding mode of isoloxapine is comparable to that of clozapine (Figure 3.18). However, the oxygen probably interacts with the protonated carboxylic group of E182$^{5.46}$. Isoloxapine showed similar effects as clozapine at nearly all of the mutants, with the exception of a decrease in intrinsic activity at the hH_4R-R341S/E mutants compared to the hH_4R wild-type ($\Delta\alpha = 0.29$ and 0.30; Chapter 7).
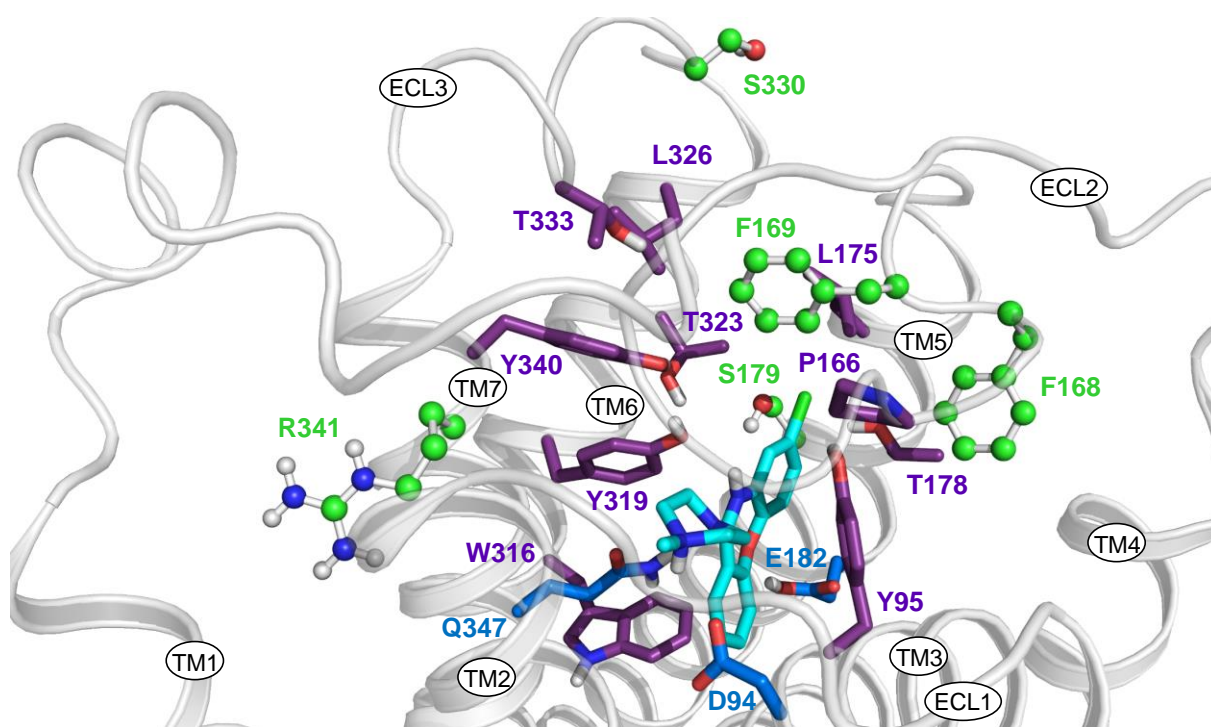
Figure 3.18: Docking pose of isoloxapine in the hH$_4$R. Model based on the inactive state of the hH$_1$R (PDB ID: 3RZE). Colour code: oxygen – red, nitrogen – blue, chlorine – green; carbon atoms are coloured individually: key interactions of isoloxapine (D94$^{3.32}$, E182$^{5.46}$ and Q347$^{7.42}$) are illustrated in dark blue, amino acids subjected to in-vitro mutagenesis (F168^{ECL2}, F169^{ECL2}, S179$^{5.43}$, S330^{ECL3} and R341$^{7.36}$) are coloured in green and the amino acids of the hydrophobic cluster (Y95$^{3.33}$, P166^{ECL2}, L175$^{5.39}$, T178$^{5.42}$, W316$^{6.48}$, Y319$^{6.51}$, T323$^{6.55}$, L326$^{6.58}$, T333^{ECL3} and Y340$^{7.35}$) in magenta.

3.4.4.10 UR-PI376

Igel et al. (2009a) proposed a binding mode where the phenylthioethyl moiety of UR-PI376 interacts with a pocket between TM2 and TM7. However, results from site-directed mutagenesis suggest an interaction of the FF motif with UR-PI376 (Chapter 5). A possible docking mode enabling interactions with both F168 and F169 as well as the surrounding amino acids of the hydrophobic cluster is shown in Figure 3.19. The carboxylic group of D94$^{3.32}$ and the carbonyl moiety of Q347$^{7.42}$ form H-bonds with the hydrogens of the cyanoguanidine moiety. Additionally, the N$^\pi$ nitrogen or the N$^\tau$ hydrogen of the imidazole moiety may be involved in an H-bond with the hydrogen of the protonated (Igel et al., 2009a) or with the deprotonated carboxylic group of E182$^{5.46}$, respectively (second variant shown in Figure 3.19). Moreover, the N$^\tau$ nitrogen may act as H-bond donor for the side chain oxygen of T178$^{5.42}$.

Compared to the hH$_4$R wild-type, both the hH$_4$R-F168A and hH$_4$R-F169V mutants revealed a significant decrease in UR-PI376 potency by 1.5 orders of magnitude (Chapter 5). Also intrinsic activities of UR-PI376 were reduced at both mutants by 0.6-0.7 units. These results support the binding mode illustrated in Figure 3.19. Only minor effects on UR-PI376 affinity were observed in case of the hH$_4$R-S179M/A mutants compared to the wild-type, but S179 mutation to M and A decreased intrinsic activity (Chapter 4). Accordingly, reduced intrinsic activity of UR-PI376 was also obvious at the double mutants hH$_4$R-F169V+S179M/A compared to the

hH$_4$R-F169V mutant and to the hH$_4$R. These changes in intrinsic activities may be due to the lower constitutive activity of these receptor mutants, i. e., the basal equilibrium between inactive and active states is shifted towards the inactive state, making the relative signal amplitude of the agonist smaller. The hH$_4$R-S330R mutant revealed both a decrease in potency (affinity) as well as a decrease in intrinsic activity compared to the hH$_4$R wild-type (Chapter 6). As discussed for clozapine, the entry of the bulky UR-PI376 into the binding pocket may be impeded by a more voluminous ECL3 or by electrostatic repulsion. UR-PI376 revealed a decrease in intrinsic activity at the hH$_4$R-R341S/E mutants compared to the hH$_4$R wild-type (Chapter 7). The pK$_i$ value of UR-PI376 was 0.6 orders of magnitude higher at the hH$_4$R-R341E mutant than at the wild-type, indicating H-bond formation between the carboxylic group of E341$^{7.36}$ and the cyanoguanidine moiety.
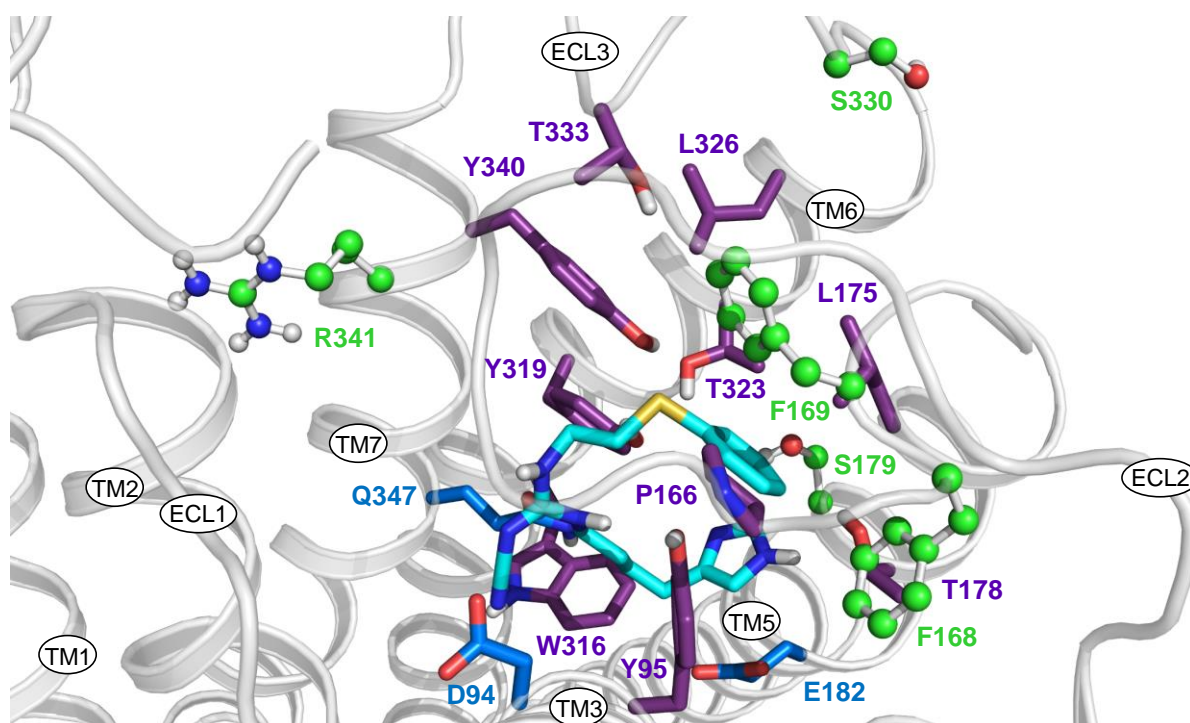
Figure 3.19: Docking pose of UR-PI376 in the hH$_4$R. Model based on the inactive state of the hH$_1$R (PDB ID: 3RZE). Colour code: oxygen – red, nitrogen – blue, sulphur – yellow; carbon atoms are coloured individually: key interactions of UR-PI376 (D94$^{3.32}$, E182$^{5.46}$ and Q347$^{7.42}$) are illustrated in dark blue, amino acids subjected to in-vitro mutagenesis (F168^{ECL2}, F169^{ECL2}, S179$^{5.43}$, S330^{ECL3} and R341$^{7.36}$) are coloured in green and the amino acids of the hydrophobic cluster (Y95$^{3.33}$, P166^{ECL2}, L175$^{5.39}$, T178$^{5.42}$, W316$^{6.48}$, Y319$^{6.51}$, T323$^{6.55}$, L326$^{6.58}$, T333^{ECL3} and Y340$^{7.35}$) in magenta.

3.4.4.11 Clobenpropit

Istyastono et al. (2011) and Feng et al. (2013) proposed two different binding modes of clobenpropit (Lim et al., 2009). However, our site-directed mutagenesis results support the binding mode where D94$^{3.32}$ and Q347$^{7.42}$ form H-bonds with the imidazole ring and E182$^{5.46}$ acts as H-bond acceptor for the hydrogens of the isothiourea moiety (Figure 3.20). The

p-chlorophenyl ring is involved in a network of aromatic amino acids, namely $Y95^{3.33}$, $Y319^{6.51}$, $F168^{ECL2}$ and $F169^{ECL2}$.

[^{3}H]histamine competition binding data indicated reduced affinity at the hH_4R-F169V and the hH_4R-S179M mutant compared to the wild-type (ΔpK_i = 0.5 and 0.6, respectively; Chapter 4). Substitution of S179 by A was without effect. The affinity of clobenpropit at the double mutants hH_4R-F169V+S179M/A was similar as at the hH_4R-F169V mutant. At the hH_4R-F168A mutant, the potency of clobenpropit was only slightly lower than at the hH_4R wild-type (Chapter 5). The intrinsic activity of clobenpropit significantly decreased from the hH_4R to the hH_4R-F169V, hH_4R-F168A, hH_4R-F169V+S179M/A and the hH_4R-S179M/A mutants. Again, this descending order is at least in part due to the different constitutive activities. The partial inverse agonistic effect of clobenpropit at the hH_4R-S179M mutant may be attributed to side chain clashes with TM5, preventing the contraction of the binding pocket, i. e., the inactive state is stabilized. At the hH_4R-S330R and hH_4R-R341S/E mutants, clobenpropit did not show significant changes of potency and intrinsic activity compared to the wild-type (Chapters 6 and 7).
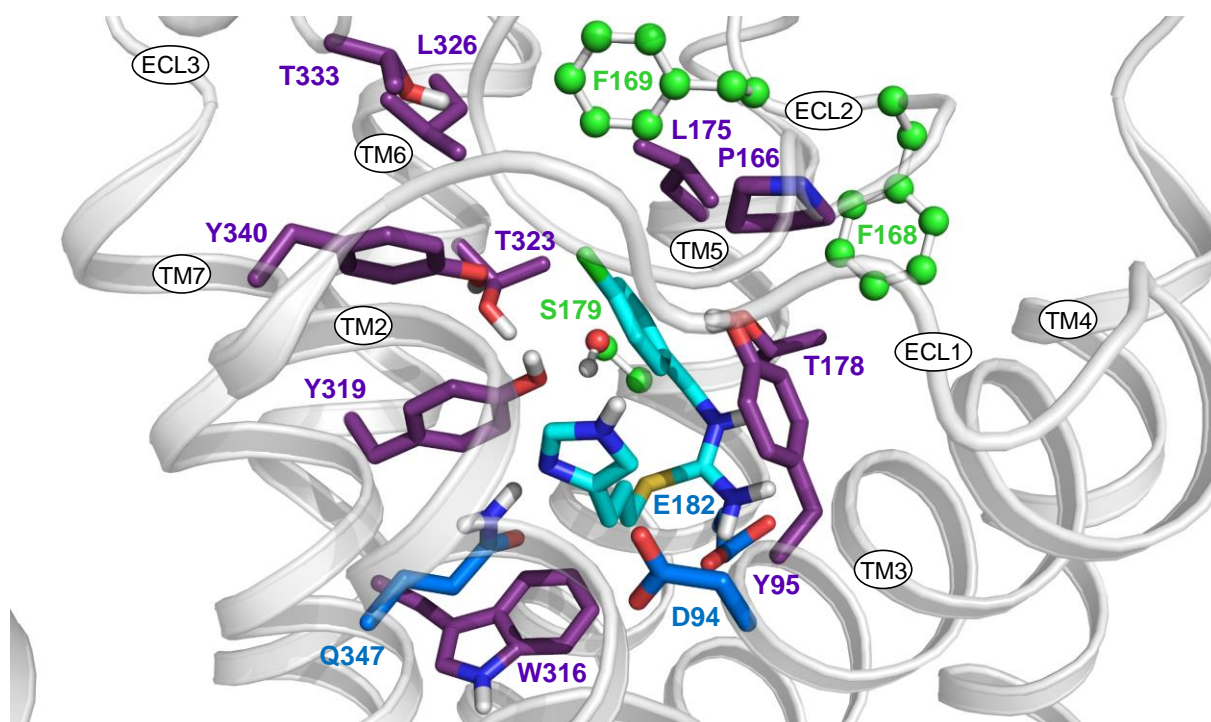

Figure 3.20: Docking pose of clobenpropit in the hH_4R. Model based on the inactive state of the hH_1R (PDB ID: 3RZE). Colour code: oxygen – red, nitrogen – blue, chlorine – green, sulphur – yellow; carbon atoms are coloured individually: key interactions of clobenpropit (D94$^{3.32}$, E182$^{5.46}$ and Q347$^{7.42}$) are illustrated in dark blue, amino acids subjected to in-vitro mutagenesis (F168^{ECL2}, F169^{ECL2} and S179$^{5.43}$) are coloured in green and the amino acids of the hydrophobic cluster (Y95$^{3.33}$, P166^{ECL2}, L175$^{5.39}$, T178$^{5.42}$, W316$^{6.48}$, Y319$^{6.51}$, T323$^{6.55}$, L326$^{6.58}$, T333^{ECL3} and Y340$^{7.35}$) in magenta.

3.5 Conclusions

Homology modelling and comparison of the models of H_4R species orthologs – hH_4R, mH_4R and rH_4R – enabled the suggestion of amino acids that may potentially be of relevance for

ligand binding and for the extraordinarily high constitutive activity of the hH$_4$R. In particular, F168^{ECL2}, F169^{ECL2}, S179$^{5.43}$, S330^{ECL3} and R341$^{7.36}$ were proposed as potential key amino acids with respect to constitutive activity. Moreover, a comparison of both inactive and active state models enabled a better understanding of the molecular basis of the phenomenon "constitutive activity". Based on our data from binding and functional assays on H$_4$R wild-types and mutants, docking studies with the investigated ligands have led to reasonable binding modes largely corresponding with experimental results.

3.6 References

Alewijnse, A. E.; Timmerman, H.; Jacobs, E. H.; Smit, M. J.; Roovers, E.; Cotecchia, S.; Leurs, R. (2000). The effect of mutations in the DRY motif on the constitutive activity and structural instability of the histamine H(2) receptor. *Mol. Pharmacol.* 57(5): 890-898.

Angelova, K.; Fanelli, F.; Puett, D. (2002). A model for constitutive lutropin receptor activation based on molecular simulation and engineered mutations in transmembrane helices 6 and 7. *J. Biol. Chem.* 277(35): 32202-32213.

Ballesteros, J.; Kitanovic, S.; Guarnieri, F.; Davies, P.; Fromme, B. J.; Konvicka, K.; Chi, L.; Millar, R. P.; Davidson, J. S.; Weinstein, H.; Sealfon, S. C. (1998). Functional microdomains in G-protein-coupled receptors. The conserved arginine-cage motif in the gonadotropin-releasing hormone receptor. *J. Biol. Chem.* 273(17): 10445-10453.

Ballesteros, J. A.; Jensen, A. D.; Liapakis, G.; Rasmussen, S. G.; Shi, L.; Gether, U.; Javitch, J. A. (2001). Activation of the beta 2-adrenergic receptor involves disruption of an ionic lock between the cytoplasmic ends of transmembrane segments 3 and 6. *J. Biol. Chem.* 276(31): 29171-29177.

Bernstein, F. C.; Koetzle, T. F.; Williams, G. J.; Meyer, E. F., Jr.; Brice, M. D.; Rodgers, J. R.; Kennard, O.; Shimanouchi, T.; Tasumi, M. (1977). The Protein Data Bank: a computer-based archival file for macromolecular structures. *J. Mol. Biol.* 112(3): 535-542.

Bokoch, M. P.; Zou, Y.; Rasmussen, S. G.; Liu, C. W.; Nygaard, R.; Rosenbaum, D. M.; Fung, J. J.; Choi, H. J.; Thian, F. S.; Kobilka, T. S.; Puglisi, J. D.; Weis, W. I.; Pardo, L.; Prosser, R. S.; Mueller, L.; Kobilka, B. K. (2010). Ligand-specific regulation of the extracellular surface of a G-protein-coupled receptor. *Nature* 463(7277): 108-112.

Brunskole, I.; Strasser, A.; Seifert, R.; Buschauer, A. (2011). Role of the second and third extracellular loops of the histamine H(4) receptor in receptor activation. *Naunyn Schmiedebergs Arch. Pharmacol.* 384(3): 301-317.

Cherezov, V.; Rosenbaum, D. M.; Hanson, M. A.; Rasmussen, S. G.; Thian, F. S.; Kobilka, T. S.; Choi, H. J.; Kuhn, P.; Weis, W. I.; Kobilka, B. K.; Stevens, R. C. (2007). High-resolution crystal structure of an engineered human beta2-adrenergic G protein-coupled receptor. *Science* 318(5854): 1258-1265.

Chien, E. Y.; Liu, W.; Zhao, Q.; Katritch, V.; Han, G. W.; Hanson, M. A.; Shi, L.; Newman, A. H.; Javitch, J. A.; Cherezov, V.; Stevens, R. C. (2010). Structure of the human dopamine D3 receptor in complex with a D2/D3 selective antagonist. *Science* 330(6007): 1091-1095.

Christopher, J. A.; Brown, J.; Dore, A. S.; Errey, J. C.; Koglin, M.; Marshall, F. H.; Myszka, D. G.; Rich, R. L.; Tate, C. G.; Tehan, B.; Warne, T.; Congreve, M. (2013). Biophysical

fragment screening of the beta1-adrenergic receptor: identification of high affinity arylpiperazine leads using structure-based drug design. *J. Med. Chem.* 56(9): 3446-3455.

Cornell, W. D.; Cieplak, P.; Bayly, C. I.; Gould, I. R.; Merz, K. M.; Ferguson, D. M.; Spellmeyer, D. C.; Fox, T.; Caldwell, J. W.; Kollman, P. A. (1995). A Second Generation Force Field for the Simulation of Proteins, Nucleic Acids, and Organic Molecules. *J. Am. Chem. Soc.* 117(19): 5179-5197.

Deupi, X.; Standfuss, J. (2011). Structural insights into agonist-induced activation of G-protein-coupled receptors. *Curr. Opin. Struct. Biol.* 21(4): 541-551.

Dore, A. S.; Robertson, N.; Errey, J. C.; Ng, I.; Hollenstein, K.; Tehan, B.; Hurrell, E.; Bennett, K.; Congreve, M.; Magnani, F.; Tate, C. G.; Weir, M.; Marshall, F. H. (2011). Structure of the adenosine A(2A) receptor in complex with ZM241385 and the xanthines XAC and caffeine. *Structure* 19(9): 1283-1293.

Feng, Z.; Hou, T.; Li, Y. (2013). Docking and MD study of histamine H4R based on the crystal structure of H1R. *J. Mol. Graph. Model.* 39: 1-12.

Gonnet, G. H.; Cohen, M. A.; Benner, S. A. (1992). Exhaustive matching of the entire protein sequence database. *Science* 256(5062): 1443-1445.

Granier, S.; Kobilka, B. (2012). A new era of GPCR structural and chemical biology. *Nat. Chem. Biol.* 8(8): 670-673.

Greasley, P. J.; Fanelli, F.; Rossier, O.; Abuin, L.; Cotecchia, S. (2002). Mutagenesis and modelling of the alpha(1b)-adrenergic receptor highlight the role of the helix 3/helix 6 interface in receptor activation. *Mol. Pharmacol.* 61(5): 1025-1032.

Haga, K.; Kruse, A. C.; Asada, H.; Yurugi-Kobayashi, T.; Shiroishi, M.; Zhang, C.; Weis, W. I.; Okada, T.; Kobilka, B. K.; Haga, T.; Kobayashi, T. (2012). Structure of the human M2 muscarinic acetylcholine receptor bound to an antagonist. *Nature* 482(7386): 547-551.

Hanson, M. A.; Cherezov, V.; Griffith, M. T.; Roth, C. B.; Jaakola, V. P.; Chien, E. Y.; Velasquez, J.; Kuhn, P.; Stevens, R. C. (2008). A specific cholesterol binding site is established by the 2.8 A structure of the human beta2-adrenergic receptor. *Structure* 16(6): 897-905.

Huang, J.; Chen, S.; Zhang, J. J.; Huang, X. Y. (2013). Crystal structure of oligomeric beta1-adrenergic G protein-coupled receptors in ligand-free basal state. *Nat. Struct. Mol. Biol.* 20(4): 419-425.

Hulme, E. C. (2013). GPCR activation: a mutagenic spotlight on crystal structures. *Trends Pharmacol. Sci.* 34(1): 67-84.

Igel, P.; Geyer, R.; Strasser, A.; Dove, S.; Seifert, R.; Buschauer, A. (2009a). Synthesis and structure-activity relationships of cyanoguanidine-type and structurally related histamine H4 receptor agonists. *J. Med. Chem.* 52(20): 6297-6313.

Istyastono, E. P.; Nijmeijer, S.; Lim, H. D.; van de Stolpe, A.; Roumen, L.; Kooistra, A. J.; Vischer, H. F.; de Esch, I. J.; Leurs, R.; de Graaf, C. (2011). Molecular determinants of ligand binding modes in the histamine H(4) receptor: linking ligand-based three-dimensional quantitative structure-activity relationship (3D-QSAR) models to in silico guided receptor mutagenesis studies. *J. Med. Chem.* 54(23): 8136-8147.

Jablonowski, J. A.; Grice, C. A.; Chai, W.; Dvorak, C. A.; Venable, J. D.; Kwok, A. K.; Ly, K. S.; Wei, J.; Baker, S. M.; Desai, P. J.; Jiang, W.; Wilson, S. J.; Thurmond, R. L.; Karlsson, L.; Edwards, J. P.; Lovenberg, T. W.; Carruthers, N. I. (2003). The first potent and selective non-imidazole human histamine H4 receptor antagonists. *J. Med. Chem.* 46(19): 3957-3960.

Jongejan, A.; Lim, H. D.; Smits, R. A.; de Esch, I. J.; Haaksma, E.; Leurs, R. (2008). Delineation of agonist binding to the human histamine H4 receptor using mutational analysis, homology modeling, and ab initio calculations. *J. Chem. Inf. Model.* 48(7): 1455-1463.

Kabsch, W.; Sander, C. (1983). Dictionary of protein secondary structure: pattern recognition of hydrogen-bonded and geometrical features. *Biopolymers* 22(12): 2577-2637.

Kenakin, T. (2001). Inverse, protean, and ligand-selective agonism: matters of receptor conformation. *FASEB J.* 15(3): 598-611.

Kobilka, B. K.; Deupi, X. (2007). Conformational complexity of G-protein-coupled receptors. *Trends Pharmacol. Sci.* 28(8): 397-406.

Kruse, A. C.; Hu, J.; Pan, A. C.; Arlow, D. H.; Rosenbaum, D. M.; Rosemond, E.; Green, H. F.; Liu, T.; Chae, P. S.; Dror, R. O.; Shaw, D. E.; Weis, W. I.; Wess, J.; Kobilka, B. K. (2012). Structure and dynamics of the M3 muscarinic acetylcholine receptor. *Nature* 482(7386): 552-556.

Kruse, A. C.; Kobilka, B. K.; Gautam, D.; Sexton, P. M.; Christopoulos, A.; Wess, J. (2014). Muscarinic acetylcholine receptors: novel opportunities for drug development. *Nat. Rev. Drug Discov.* 13(7): 549-560.

Kruse, A. C.; Ring, A. M.; Manglik, A.; Hu, J.; Hu, K.; Eitel, K.; Hubner, H.; Pardon, E.; Valant, C.; Sexton, P. M.; Christopoulos, A.; Felder, C. C.; Gmeiner, P.; Steyaert, J.; Weis, W. I.; Garcia, K. C.; Wess, J.; Kobilka, B. K. (2013). Activation and allosteric modulation of a muscarinic acetylcholine receptor. *Nature* 504(7478): 101-106.

Larkin, M. A.; Blackshields, G.; Brown, N. P.; Chenna, R.; McGettigan, P. A.; McWilliam, H.; Valentin, F.; Wallace, I. M.; Wilm, A.; Lopez, R.; Thompson, J. D.; Gibson, T. J.; Higgins, D. G. (2007). Clustal W and Clustal X version 2.0. *Bioinformatics* 23(21): 2947-2948.

Laskowski, R. A.; MacArthur, M. W.; Moss, D. S.; Thornton, J. M. (1993). PROCHECK - a program to check the stereochemical quality of protein structures. *J. App. Cryst.* 26: 283-291.

Lebon, G.; Warne, T.; Edwards, P. C.; Bennett, K.; Langmead, C. J.; Leslie, A. G.; Tate, C. G. (2011). Agonist-bound adenosine A2A receptor structures reveal common features of GPCR activation. *Nature* 474(7352): 521-525.

Lebon, G.; Warne, T.; Tate, C. G. (2012). Agonist-bound structures of G protein-coupled receptors. *Curr. Opin. Struct. Biol.* 22(4): 482-490.

Lim, H. D.; de Graaf, C.; Jiang, W.; Sadek, P.; McGovern, P. M.; Istyastono, E. P.; Bakker, R. A.; de Esch, I. J.; Thurmond, R. L.; Leurs, R. (2010). Molecular determinants of ligand binding to H4R species variants. *Mol. Pharmacol.* 77(5): 734-743.

Lim, H. D.; Istyastono, E. P.; van de Stolpe, A.; Romeo, G.; Gobbi, S.; Schepers, M.; Lahaye, R.; Menge, W. M.; Zuiderveld, O. P.; Jongejan, A.; Smits, R. A.; Bakker, R. A.; Haaksma, E. E.; Leurs, R.; de Esch, I. J. (2009). Clobenpropit analogs as dual activity ligands for the histamine H3 and H4 receptors: synthesis, pharmacological evaluation, and cross-target QSAR studies. *Bioorg. Med. Chem.* 17(11): 3987-3994.

Lin, H.; Sassano, M. F.; Roth, B. L.; Shoichet, B. K. (2013). A pharmacological organization of G protein-coupled receptors. *Nat. Methods* 10(2): 140-146.

Liu, W.; Wacker, D.; Gati, C.; Han, G. W.; James, D.; Wang, D.; Nelson, G.; Weierstall, U.; Katritch, V.; Barty, A.; Zatsepin, N. A.; Li, D.; Messerschmidt, M.; Boutet, S.; Williams, G. J.; Koglin, J. E.; Seibert, M. M.; Wang, C.; Shah, S. T.; Basu, S.; Fromme, R.; Kupitz, C.; Rendek, K. N.; Grotjohann, I.; Fromme, P.; Kirian, R. A.; Beyerlein, K. R.; White, T. A.; Chapman, H. N.; Caffrey, M.; Spence, J. C.; Stevens, R. C.; Cherezov, V. (2013). Serial femtosecond crystallography of G protein-coupled receptors. *Science* 342(6165): 1521-1524.

Lovell, S. C.; Word, J. M.; Richardson, J. S.; Richardson, D. C. (2000). The penultimate rotamer library. *Proteins* 40(3): 389-408.

Miller-Gallacher, J. L.; Nehme, R.; Warne, T.; Edwards, P. C.; Schertler, G. F.; Leslie, A. G.; Tate, C. G. (2014). The 2.1 A resolution structure of cyanopindolol-bound beta1-adrenoceptor identifies an intramembrane Na+ ion that stabilises the ligand-free receptor. *PLoS One* 9(3): e92727.

Mirzadegan, T.; Benko, G.; Filipek, S.; Palczewski, K. (2003). Sequence analyses of G-protein-coupled receptors: similarities to rhodopsin. *Biochemistry* 42(10): 2759-2767.

Morris, A. L.; MacArthur, M. W.; Hutchinson, E. G.; Thornton, J. M. (1992). Stereochemical quality of protein structure coordinates. *Proteins* 12(4): 345-364.

Moukhametzianov, R.; Warne, T.; Edwards, P. C.; Serrano-Vega, M. J.; Leslie, A. G.; Tate, C. G.; Schertler, G. F. (2011). Two distinct conformations of helix 6 observed in antagonist-bound structures of a beta1-adrenergic receptor. *Proc. Natl. Acad. Sci. U. S. A.* 108(20): 8228-8232.

Palczewski, K.; Kumasaka, T.; Hori, T.; Behnke, C. A.; Motoshima, H.; Fox, B. A.; Le Trong, I.; Teller, D. C.; Okada, T.; Stenkamp, R. E.; Yamamoto, M.; Miyano, M. (2000). Crystal structure of rhodopsin: A G protein-coupled receptor. *Science* 289(5480): 739-745.

Peeters, M. C.; van Westen, G. J.; Li, Q.; AP, I. J. (2011). Importance of the extracellular loops in G protein-coupled receptors for ligand recognition and receptor activation. *Trends Pharmacol. Sci.* 32(1): 35-42.

Powell, M. J. D. (1964). An efficient method for finding the minimum of a function of several variables without calculating derivatives. *Comput. J.* 7(2): 155-162.

Rasmussen, S. G.; Choi, H. J.; Fung, J. J.; Pardon, E.; Casarosa, P.; Chae, P. S.; Devree, B. T.; Rosenbaum, D. M.; Thian, F. S.; Kobilka, T. S.; Schnapp, A.; Konetzki, I.; Sunahara, R. K.; Gellman, S. H.; Pautsch, A.; Steyaert, J.; Weis, W. I.; Kobilka, B. K. (2011a). Structure of a nanobody-stabilized active state of the beta(2) adrenoceptor. *Nature* 469(7329): 175-180.

Rasmussen, S. G.; Choi, H. J.; Rosenbaum, D. M.; Kobilka, T. S.; Thian, F. S.; Edwards, P. C.; Burghammer, M.; Ratnala, V. R.; Sanishvili, R.; Fischetti, R. F.; Schertler, G. F.; Weis, W. I.; Kobilka, B. K. (2007). Crystal structure of the human beta2 adrenergic G-protein-coupled receptor. *Nature* 450(7168): 383-387.

Rasmussen, S. G.; DeVree, B. T.; Zou, Y.; Kruse, A. C.; Chung, K. Y.; Kobilka, T. S.; Thian, F. S.; Chae, P. S.; Pardon, E.; Calinski, D.; Mathiesen, J. M.; Shah, S. T.; Lyons, J. A.; Caffrey, M.; Gellman, S. H.; Steyaert, J.; Skiniotis, G.; Weis, W. I.; Sunahara, R. K.; Kobilka, B. K. (2011b). Crystal structure of the beta2 adrenergic receptor-Gs protein complex. *Nature* 477(7366): 549-555.

Ring, A. M.; Manglik, A.; Kruse, A. C.; Enos, M. D.; Weis, W. I.; Garcia, K. C.; Kobilka, B. K. (2013). Adrenaline-activated structure of beta2-adrenoceptor stabilized by an engineered nanobody. *Nature* 502(7472): 575-579.

Rosenbaum, D. M.; Zhang, C.; Lyons, J. A.; Holl, R.; Aragao, D.; Arlow, D. H.; Rasmussen, S. G.; Choi, H. J.; Devree, B. T.; Sunahara, R. K.; Chae, P. S.; Gellman, S. H.; Dror, R. O.; Shaw, D. E.; Weis, W. I.; Caffrey, M.; Gmeiner, P.; Kobilka, B. K. (2011). Structure and function of an irreversible agonist-beta(2) adrenoceptor complex. *Nature* 469(7329): 236-240.

Rossi, K. A.; Weigelt, C. A.; Nayeem, A.; Krystek, S. R., Jr. (2007). Loopholes and missing links in protein modeling. *Protein Sci.* 16(9): 1999-2012.

Scheer, A.; Fanelli, F.; Costa, T.; De Benedetti, P. G.; Cotecchia, S. (1996). Constitutively active mutants of the alpha 1B-adrenergic receptor: role of highly conserved polar amino acids in receptor activation. *EMBO J.* 15(14): 3566-3578.

Scheer, A.; Fanelli, F.; Costa, T.; De Benedetti, P. G.; Cotecchia, S. (1997). The activation process of the alpha1B-adrenergic receptor: potential role of protonation and hydrophobicity of a highly conserved aspartate. *Proc. Natl. Acad. Sci. U. S. A.* 94(3): 808-813.

Schneider, E. H.; Schnell, D.; Papa, D.; Seifert, R. (2009). High constitutive activity and a G-protein-independent high-affinity state of the human histamine H(4)-receptor. *Biochemistry* 48(6): 1424-1438.

Schneider, E. H.; Schnell, D.; Strasser, A.; Dove, S.; Seifert, R. (2010). Impact of the DRY motif and the missing "ionic lock" on constitutive activity and G-protein coupling of the human histamine H4 receptor. *J. Pharmacol. Exp. Ther.* 333(2): 382-392.

Schnell, D.; Brunskole, I.; Ladova, K.; Schneider, E. H.; Igel, P.; Dove, S.; Buschauer, A.; Seifert, R. (2011). Expression and functional properties of canine, rat, and murine histamine H(4) receptors in Sf9 insect cells. *Naunyn Schmiedebergs Arch. Pharmacol.* 383(5): 457-470.

Schultes, S.; Nijmeijer, S.; Engelhardt, H.; Kooistra, A. J.; Vischer, H. F.; de Esch, I. J. P.; Haaksma, E. E. J.; Leurs, R.; de Graaf, C. (2013). Mapping histamine H4 receptor-ligand binding modes. *MedChemComm* 4(1): 193-204.

Shapiro, D. A.; Kristiansen, K.; Weiner, D. M.; Kroeze, W. K.; Roth, B. L. (2002). Evidence for a model of agonist-induced activation of 5-hydroxytryptamine 2A serotonin receptors that involves the disruption of a strong ionic interaction between helices 3 and 6. *J. Biol. Chem.* 277(13): 11441-11449.

Shi, L.; Liapakis, G.; Xu, R.; Guarnieri, F.; Ballesteros, J. A.; Javitch, J. A. (2002). Beta2 adrenergic receptor activation. Modulation of the proline kink in transmembrane 6 by a rotamer toggle switch. *J. Biol. Chem.* 277(43): 40989-40996.

Shimamura, T.; Shiroishi, M.; Weyand, S.; Tsujimoto, H.; Winter, G.; Katritch, V.; Abagyan, R.; Cherezov, V.; Liu, W.; Han, G. W.; Kobayashi, T.; Stevens, R. C.; Iwata, S. (2011). Structure of the human histamine H1 receptor complex with doxepin. *Nature* 475(7354): 65-70.

Shin, N.; Coates, E.; Murgolo, N. J.; Morse, K. L.; Bayne, M.; Strader, C. D.; Monsma, F. J., Jr. (2002). Molecular modeling and site-specific mutagenesis of the histamine-binding site of the histamine H4 receptor. *Mol. Pharmacol.* 62(1): 38-47.

Standfuss, J.; Edwards, P. C.; D'Antona, A.; Fransen, M.; Xie, G.; Oprian, D. D.; Schertler, G. F. (2011). The structural basis of agonist-induced activation in constitutively active rhodopsin. *Nature* 471(7340): 656-660.

Strader, C. D.; Fong, T. M.; Tota, M. R.; Underwood, D.; Dixon, R. A. (1994). Structure and function of G protein-coupled receptors. *Annu. Rev. Biochem.* 63: 101-132.

Strasser, A. (2014). Personal Communication. University of Regensburg, Regensburg, Germany.

Strasser, A.; Wittmann, H. J. (2013). Molecular modeling studies give hint for the existence of a symmetric hbeta(2)R-Galphabetagamma-homodimer. *J. Mol. Model.* 19(10): 4443-4457.

Thorsen, T. S.; Matt, R.; Weis, W. I.; Kobilka, B. K. (2014). Modified T4 Lysozyme Fusion Proteins Facilitate G Protein-Coupled Receptor Crystallogenesis. *Structure* 22(11): 1657-1664.

Trzaskowski, B.; Latek, D.; Yuan, S.; Ghoshdastider, U.; Debinski, A.; Filipek, S. (2012). Action of molecular switches in GPCRs--theoretical and experimental studies. *Curr. Med. Chem.* 19(8): 1090-1109.

Tse, M. T. (2011). G protein-coupled receptors: Crystallizing how agonists bind. *Nat. Rev. Drug Discov.* 10(2): 97.

UniProt, C. (2013). Update on activities at the Universal Protein Resource (UniProt) in 2013. *Nucleic Acids Res.* 41(Database issue): D43-47.

Venkatakrishnan, A. J.; Deupi, X.; Lebon, G.; Tate, C. G.; Schertler, G. F.; Babu, M. M. (2013). Molecular signatures of G-protein-coupled receptors. *Nature* 494(7436): 185-194.

Wacker, D.; Fenalti, G.; Brown, M. A.; Katritch, V.; Abagyan, R.; Cherezov, V.; Stevens, R. C. (2010). Conserved binding mode of human beta2 adrenergic receptor inverse agonists and antagonist revealed by X-ray crystallography. *J. Am. Chem. Soc.* 132(33): 11443-11445.

Wacker, D.; Wang, C.; Katritch, V.; Han, G. W.; Huang, X. P.; Vardy, E.; McCorvy, J. D.; Jiang, Y.; Chu, M.; Siu, F. Y.; Liu, W.; Xu, H. E.; Cherezov, V.; Roth, B. L.; Stevens, R. C. (2013). Structural features for functional selectivity at serotonin receptors. *Science* 340(6132): 615-619.

Wang, C.; Jiang, Y.; Ma, J.; Wu, H.; Wacker, D.; Katritch, V.; Han, G. W.; Liu, W.; Huang, X. P.; Vardy, E.; McCorvy, J. D.; Gao, X.; Zhou, X. E.; Melcher, K.; Zhang, C.; Bai, F.; Yang, H.; Yang, L.; Jiang, H.; Roth, B. L.; Cherezov, V.; Stevens, R. C.; Xu, H. E. (2013). Structural basis for molecular recognition at serotonin receptors. *Science* 340(6132): 610-614.

Warne, T.; Edwards, P. C.; Leslie, A. G.; Tate, C. G. (2012). Crystal structures of a stabilized beta1-adrenoceptor bound to the biased agonists bucindolol and carvedilol. *Structure* 20(5): 841-849.

Warne, T.; Moukhametzianov, R.; Baker, J. G.; Nehme, R.; Edwards, P. C.; Leslie, A. G.; Schertler, G. F.; Tate, C. G. (2011). The structural basis for agonist and partial agonist action on a beta(1)-adrenergic receptor. *Nature* 469(7329): 241-244.

Warne, T.; Serrano-Vega, M. J.; Baker, J. G.; Moukhametzianov, R.; Edwards, P. C.; Henderson, R.; Leslie, A. G.; Tate, C. G.; Schertler, G. F. (2008). Structure of a beta1-adrenergic G-protein-coupled receptor. *Nature* 454(7203): 486-491.

Weichert, D.; Kruse, A. C.; Manglik, A.; Hiller, C.; Zhang, C.; Hubner, H.; Kobilka, B. K.; Gmeiner, P. (2014). Covalent agonists for studying G protein-coupled receptor activation. *Proc. Natl. Acad. Sci. U. S. A.* 111(29): 10744-10748.

Wheatley, M.; Wootten, D.; Conner, M. T.; Simms, J.; Kendrick, R.; Logan, R. T.; Poyner, D. R.; Barwell, J. (2012). Lifting the lid on GPCRs: the role of extracellular loops. *Br. J. Pharmacol.* 165(6): 1688-1703.

Wifling, D.; Bernhardt, G.; Dove, S.; Buschauer, A. (2015a). The Extracellular Loop 2 (ECL2) of the Human Histamine H4 Receptor Substantially Contributes to Ligand Binding and Constitutive Activity. *PLoS One* 10(1): e0117185.

Wifling, D.; Löffel, K.; Nordemann, U.; Strasser, A.; Bernhardt, G.; Dove, S.; Seifert, R.; Buschauer, A. (2015b). Molecular determinants for the high constitutive activity of the human histamine H4 receptor: functional studies on orthologues and mutants. *Br. J. Pharmacol.* 172(3): 785-798.

Wittmann, H. J.; Seifert, R.; Strasser, A. (2014). Mathematical analysis of the sodium sensitivity of the human histamine H3 receptor. *In Silico Pharmacol.* 2(1): 1-14.

Xu, F.; Wu, H.; Katritch, V.; Han, G. W.; Jacobson, K. A.; Gao, Z. G.; Cherezov, V.; Stevens, R. C. (2011). Structure of an agonist-bound human A2A adenosine receptor. *Science* 332(6027): 322-327.

Zou, Y.; Weis, W. I.; Kobilka, B. K. (2012). N-terminal T4 lysozyme fusion facilitates crystallization of a G protein coupled receptor. *PLoS One* 7(10): e46039.

Chapter 4

Molecular determinants for the high constitutive activity of the human histamine H$_4$ receptor: Functional studies on orthologs and mutants

Note: Major parts of this chapter were already published prior to submission of this thesis in *Br. J. Pharmacol.* (Wifling et al., 2015b). John Wiley & Sons granted me the permission to use the material incorporated in Wifling et al. (2015b) for this thesis. For detailed information on the contributions by co-authors, cf. "Danksagungen".

4.1 Summary

Background and purpose: Some histamine H$_4$ receptor (H$_4$R) ligands act as inverse agonists at the human H$_4$R (hH$_4$R), a receptor with exceptionally high constitutive activity, but as neutral antagonists or partial agonists at the constitutively inactive mouse H$_4$R (mH$_4$R) and rat H$_4$R (rH$_4$R). To study molecular determinants of constitutive activity, H$_4$R reciprocal mutants were constructed: single mutants: hH$_4$R-F169V, mH$_4$R-V171F, hH$_4$R-S179A, hH$_4$R-S179M; double mutants: hH$_4$R-F169V+S179A, hH$_4$R-F169V+S179M and mH$_4$R-V171F+M181S.

Experimental approach: Site-directed mutagenesis with pVL1392 plasmids containing hH$_4$R or mH$_4$R were performed. Wild-type or mutant receptors were co-expressed with Gα_{i2} and G$\beta_1\gamma_2$ in Sf9 cells. Membranes were studied in saturation and competition binding assays ([^{3}H]histamine) as well as in functional [^{35}S]GTPγS assays with inverse, partial and full agonists of the hH$_4$R.

Key results: Constitutive activity decreased from the hH$_4$R via the hH$_4$R-F169V mutant to the hH$_4$R-F169V+S179A and hH$_4$R-F169V+S179M double mutants. F169 alone or in concert with S179 plays a major role in stabilizing a ligand-free active state of the hH$_4$R. Partial inverse hH$_4$R agonists like JNJ7777120 behaved as neutral antagonists or partial agonists at species

orthologs with lower or no constitutive activity. Some partial and full hH$_4$R agonists showed decreased maximal effects and potencies at hH$_4$R-F169V and double mutants. However, the mutation of S179 in the hH$_4$R to M as in mH$_4$R or A as in rH$_4$R did not significantly reduce constitutive activity.

Conclusions and implications: F169 and S179 are key amino acids for the high constitutive activity of the hH$_4$R and may also be of relevance for other constitutively active GPCRs.

4.2 Introduction

The human histamine H$_4$ receptor (hH$_4$R) was independently discovered by several groups (Liu et al., 2001a; Morse et al., 2001; Nakamura et al., 2000; Nguyen et al., 2001; Oda and Matsumoto, 2001; Zhu et al., 2001). The H$_4$R is coupled to Gα_i-proteins, leading to inhibition of adenylyl cyclase and, *via* release of G$\beta\gamma$-complexes, to the activation of phospholipase C (for reviews, see, e. g. Leurs et al. (2009); Seifert et al. (2013); Thurmond et al. (2008)). H$_4$R-mediated Gα_i activation in membrane preparation is monitored by agonist-stimulated [^{35}S]GTPγS binding to Gα_i-proteins or Gα_i-mediated [γ-^{32}P]GTP hydrolysis (Schneider et al., 2009). The H$_4$R is primarily expressed in cells of the immune system and seems to play a pro-inflammatory role in bronchial asthma, atopic dermatitis and pruritus (de Esch et al., 2005; Dunford and Holgate, 2011; Dunford et al., 2006; Marson, 2011; Schnell et al., 2011; Zampeli and Tiligada, 2009). Human H$_4$R expression and function has been unequivocally demonstrated by several independent groups in eosinophils (Buckland et al., 2003; Ling et al., 2004; O'Reilly et al., 2002; Reher et al., 2012). However, eosinophils are very difficult to purify in sufficient amounts for pharmacological studies so that experiments with recombinant hH$_4$R are very important.

A G-protein-coupled receptor (GPCR) capable of producing its biological response in the absence of a bound ligand is termed constitutively active (Seifert and Wenzel-Seifert, 2002). Previous studies have shown that the hH$_4$R possesses an unusually high constitutive activity, resulting in high agonist-independent Gα_i-protein activation (Morse et al., 2001; Seifert et al., 2013; Strasser et al., 2013). A plausible cause could be the missing ionic lock between an arginine in the DRY motif (TM3) and an acidic amino acid in TM6 (replaced by an alanine in the hH$_4$R). However, this was not confirmed by reconstitution of this motif in the hH$_4$R (Schneider et al., 2010). The constitutive activity of canine, murine and rat H$_4$R species isoforms (cH$_4$R, mH$_4$R and rH$_4$R, respectively) is substantially lower (Schneider et al., 2010; Schnell et al., 2011; Strasser et al., 2013). Another striking difference was observed with the prototypical H$_4$R antagonist JNJ7777120 (1-[(5-chloro-1*H*-indol-2-yl)carbonyl]-4-methyl-piperazine, Figure 4.1), a partial agonist at the cH$_4$R, the rH$_4$R and the mH$_4$R, but a partial inverse agonist at the hH$_4$R. Also H$_4$R agonists (Igel et al., 2010) from the class of N^G-acylated

imidazolylpropylguanidines and cyanoguanidines differed with respect to affinity, potency and efficacy among H_4R species isoforms (Schnell et al., 2011).
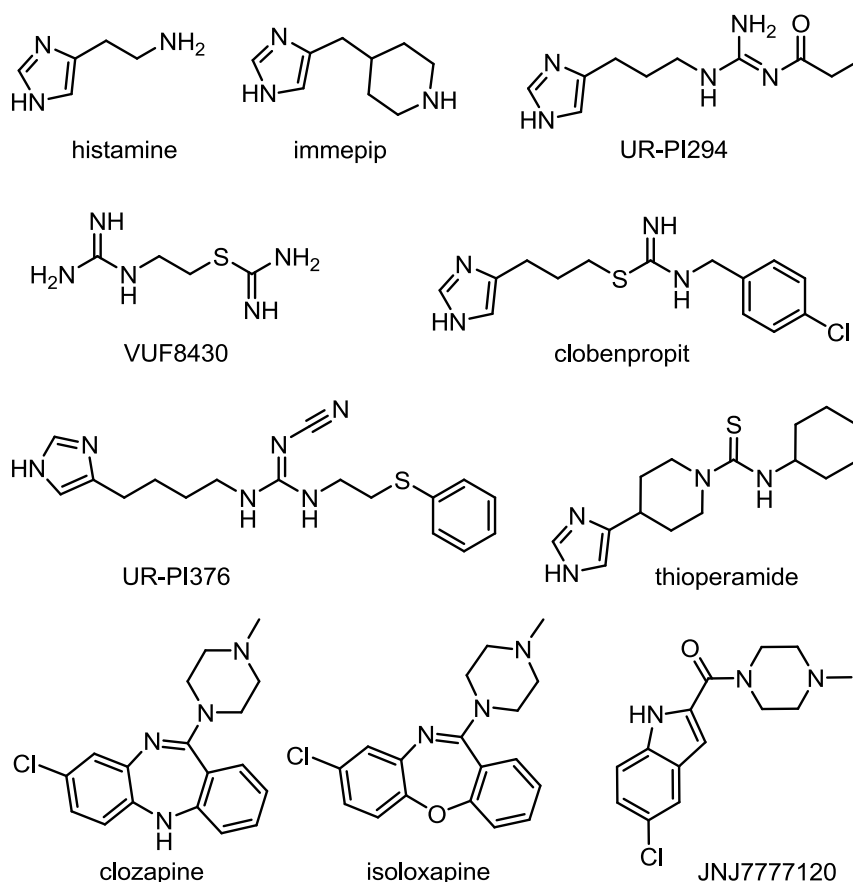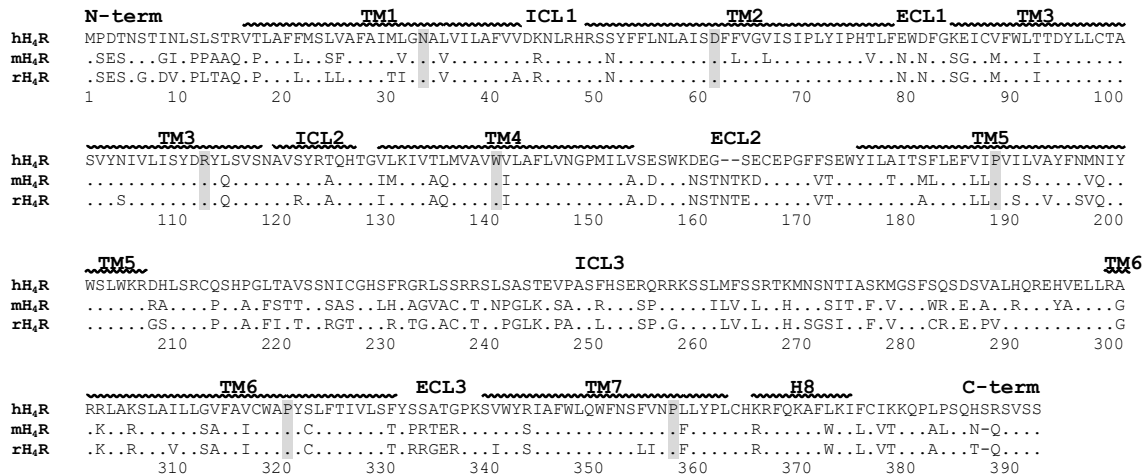

Figure 4.1: Structures of investigated H_4R ligands.

Mouse, rat and dog are important laboratory animal species for assessing the pathophysiological role of the H_4R (Dunford et al., 2006; Liu et al., 2001b; Rossbach et al., 2009b). It is, therefore, important to characterize the effects of ligands at those H_4R species orthologs in comparison to the hH_4R. Considering the rather low sequence identity of H_4R species isoforms (see alignment of hH_4R, mH_4R and rH_4R, Figure 4.2), the question arises which molecular determinants account for the species differences in constitutive activity, ligand binding and intrinsic activity.

A systematic investigation with chimeras localized the region between $V141^{4.51}$ and $E182^{5.46}$ (superscripts according to the Ballesteros and Weinstein numbering (Ballesteros and Weinstein, 1995)) involving the second extracellular loop (ECL2) to be responsible for differences in agonist affinity between the hH_4R and the mH_4R (Lim et al., 2008). Moreover, among single hH_4R-mH_4R amino acid exchanges in this region, the hH_4R-F169V mutant resulted in the largest shifts towards the K_d and pK_i values at the mH_4R, suggesting that this residue in ECL2 is "the key amino acid" for differential interactions of certain agonists with the hH_4R and the mH_4R (Lim et al., 2008). As in the case of the two corresponding consecutive phenylalanine residues in the β_2-adrenoceptor structure (Cherezov et al., 2007), it was

assumed that F169 is involved in a network of hydrophobic interactions, stabilizing ECL2 in a conformation, which positions F168 towards the binding pocket (Lim et al., 2008).

```
            N-term                    TM1         ICL1              TM2        ECL1      TM3
hH₄R  MPDTNSTINLSLSTRVTLAFFMSLVAFAIMLGNALVILAFVVDKNLRHRSSYFFLNLAISDFFVGVISIPLYIPHTLFEWDFGKEICVFWLTTDYLLCTA
mH₄R  .SES...GI.PPAAQ.P...L..SF.....V..V........R......N..........L..L.........V..N.N..SG..M...I.........
rH₄R  .SES.G.DV.PLTAQ.P...L..LL....TI..V.....A.R......N.....................N.N..SG..M..I.........
      1      10      20      30      40      50      60      70      80      90      100

              TM3        ICL2           TM4              ECL2                    TM5
hH₄R  SVYNIVLISYDRYLSVSNAVSYRTQHTGVLKIVTLMVAVWVLAFLVNGPMILVSESWKDEG--SECEPGFFSEWYILAITSFLEFVIPVILVAYFNMNIY
mH₄R  ...........Q......A....IM...AQ....I...........A.D...NSTNTKD.....VT.....T..ML..LL..S.....VQ..
rH₄R  ...S........Q......R..A....I....AQ....I...........A.D...NSTNTE......VT........A....LL..S..V..SVQ..
      110      120      130      140      150      160      170      180      190      200

        TM5                                       ICL3                                        TM6
hH₄R  WSLWKRDHLSRCQSHPGLTAVSSNICGHSFRGRLSSRRSLSASTEVPASFHSERQRRKSSLMFSSRTKMNSNTIASKMGSFSQSDSVALHQREHVELLRA
mH₄R  ......RA....P..A.FSTT..SAS..LH.AGVAC.T.NPGLK.SA..R...SP.....ILV.L..H...SIT.F.V...WR.E..A..R...YA....G
rH₄R  ......GS....P..A.FI.T..RGT...R.TG.AC.T..PGLK.PA..L...SP.G....LV.L..H.SGSI..F.V...CR.E.PV..........G
      210      220      230      240      250      260      270      280      290      300

                  TM6          ECL3         TM7           H8          C-term
hH₄R  RRLAKSLAILLGVFAVCWAPYSLFTIVLSFYSSATGPKSVWYRIAFWLQWFNSFVNPLLYPLCHKRFQKAFLKIFCIKKQPLPSQHSRSVSS
mH₄R  .K..R......SA..I....C.......T.PRTER......S.............F......R......W..L.VT...AL..N-Q....
rH₄R  .K..R...V..SA..I....C.......T.RRGER...I..S...........LI..F......R......W..L.VT...A...T-Q....
      310      320      330      340      350      360      370      380      390
```

Figure 4.2: Sequence alignment of hH₄R, rH₄R and mH₄R. TMs are indicated by wavy lines. N-term, N-terminus (extracellular); C-term, C-terminus (intracellular); ICL1, ICL2, and ICL3, first, second, and third intracellular loops; ECL1, ECL2, ECL3, first, second, and third extracellular loops. Dots in the sequences indicate identity with the hH₄R. The most conserved residues in each TM domain are highlighted by grey shading. TMs were defined according to the hH₄R homology model based on the crystal structure of the hH₁R.

To further investigate the role of F169, we generated the single mutants hH₄R-F169V and mH₄R-V171F. Up to now, no functional studies on G-protein coupling at these mutants exist to discriminate between agonist, antagonist and inverse agonist effects. We therefore tested H₄R ligands with different qualities of action in functional [^{35}S]GTPγS assays.

Figure 4.3 shows the putative histamine binding pocket of the hH₄R and various amino acids in the vicinity of this pocket which are specific for the hH₄R compared to the mH₄R and the rH₄R. According to results from in-vitro mutagenesis (Shin et al., 2002), the positively charged amino group of histamine forms a salt bridge with D94$^{3.32}$. The ethylamine side chain is embedded between Y95$^{3.33}$ and Y319$^{6.51}$, whereas the N^{π} nitrogen of the imidazolyl moiety is hydrogen bonded to the side chain of E182$^{5.46}$. F168 (ECL2) points into the binding pocket, albeit direct contacts with histamine are not obvious. Hydrogen bonds of the N^{τ} nitrogen with the hydroxyls of T178$^{5.42}$ and S179$^{5.43}$ are possible, but on the single mutants hH₄R-T178A, hH₄R-S179A (Shin et al., 2002) and hH₄R-S179M (Lim et al., 2008), histamine affinity and activity was only slightly reduced compared to the wild-type hH₄R (factor 2 to 4). However, S179$^{5.43}$ is mutated in the mH₄R (M) and the rH₄R (A) and therefore a promising candidate for more detailed investigations. In order to study the pharmacological profile including the constitutive activity of the single hH₄R-S179A and hH₄R-S179M mutants, we expressed these constructs in Sf9 cells.
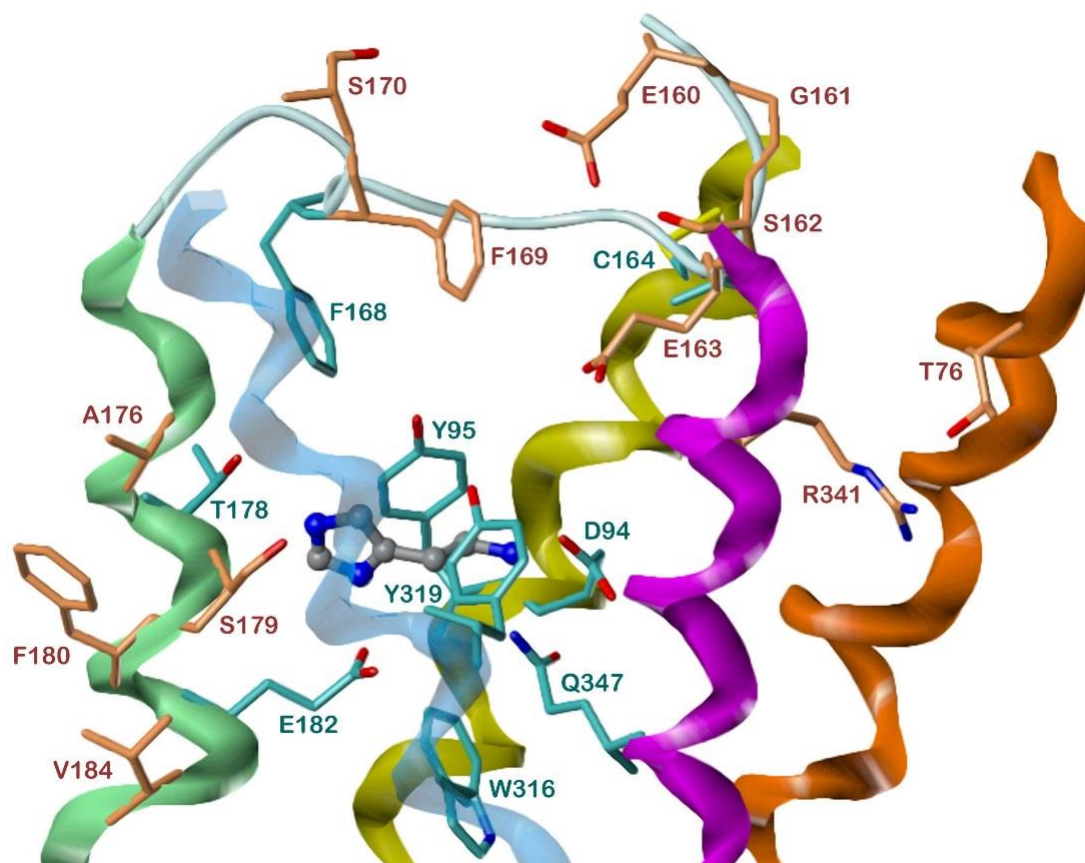
Figure 4.3: Ligand binding pocket of the hH₄R in complex with histamine. The model is based on the crystal structure of the hH₁R as template (Shimamura et al., 2011). Histamine (ball and stick model) was manually docked considering interactions with the hH₄R suggested from results of in-vitro mutagenesis. Colours of atoms if not otherwise indicated: C – grey, N – blue, O – red. S – yellow. Carbons and backbone nitrogens of amino acids, which are different in the rH₄R and mH₄R, are orange-coloured. Other important amino acids of or close to the ligand binding pocket are represented by cyan-coloured C and backbone N atoms. TMs are drawn as ribbons: TM2 – orange, TM3 – yellow, TM5 – green, TM6 – light blue, TM7 – magenta. The C-terminal part of ECL2 is shown as tube.

Although our hH₄R model does not indicate direct interactions of S179[5.43] and F169 (Figure 4.3), the question arose whether there is an additive effect of both amino acids with respect to the selectivity of ligands for the human H₄R ortholog. We therefore prepared the double mutants of the hH₄R, hH₄R-F169V+S179A and hH₄R-F169V+S179M, corresponding to the rat and mouse H₄R in positions 169 and 179, as well as the reciprocal double mutant of the mH₄R, mH₄R-V171F+M181S.

4.3 Methods

4.3.1 Materials

The pcDNA3.1 vector containing the hH₄R sequence was obtained from the UMR cDNA Resource Centre at the University of Missouri-Rolla (Rolla, MO USA). The cDNAs encoding the mouse and rat H₄Rs were a kind gift of Dr. R. Thurmond (Johnson & Johnson Pharmaceutical R&D, San Diego, CA USA). The construction of the human, mouse and rat

pVL1392-SF-H$_4$R-His$_6$ and of the pGEM-3Z-SF-mH$_4$R-His$_6$ plasmids, respectively, was described previously (Schneider et al., 2009; Schnell et al., 2011). Baculovirus encoding Gα$_{i2}$ was kindly provided by Dr. A. G. Gilman (Department of Pharmacology, University of Southwestern Medical Centre, Dallas, TX USA). Recombinant baculovirus encoding the unmodified version of the Gβ$_1$γ$_2$ subunits was a kind gift of Dr. P. Gierschik (Department of Pharmacology and Toxicology, University of Ulm, Ulm, Germany). *Pfu* Ultra II DNA polymerase was obtained from Agilent (Böblingen, Germany). The DNA primers for polymerase chain reaction (PCR) were synthesized by MWG-Biotech (Ebersberg, Germany). Restriction enzymes and T4-DNA ligase were from New England Biolabs (Ipswich, MA USA). Gradient gels (8-16 %, 12 well nUView gels), the "prestained" peqGOLD protein marker III, used for western blotting as well as the "unstained" peqGOLD protein marker I, used for Coomassie brilliant blue R staining, were from Peqlab (Erlangen, Germany). The antibody selective for Gαi$_{1/2}$ was from Calbiochem (Darmstadt, Germany). The anti-FLAG M1 antibody, the amino-terminal FLAG-BAP fusion protein and histamine were from Sigma-Aldrich (Taufkirchen, Germany). The binding of secondary antibodies coupled to peroxidase (HRP) was detected with the ECL Western Blotting Substrate (Thermo Scientific, Nidderau, Germany). UR-PI294 and UR-PI376 were synthesized as described (Igel et al., 2009a; Igel et al., 2009b). Thioperamide, JNJ7777120, and VUF8430 were synthesized according to Lange et al. (1995), Jablonowski et al. (2003), and Lim et al. (2006). Isoloxapine (Schmutz et al., 1967; Smits et al., 2006) was provided by S. Gobleder (Institute of Pharmacy, University of Regensburg, Regensburg, Germany). All other H$_4$R ligands were purchased from Tocris (Avonmouth, Bristol, UK). The chemical structures of the ligands are depicted in Figure 4.1. UR-PI376 (10 mM) was dissolved in 50 % (*v/v*) dimethyl sulfoxide (DMSO) and dilutions were prepared in 20 % (*v/v*) DMSO in order to attain a final DMSO concentration of 2 % (*v/v*) in each well. 10 mM stock solutions of clozapine and isoloxapine were prepared in Millipore water containing 3 and 2 mole equivalents of HCl, respectively. All other stock solutions were prepared with Millipore water. [^{35}S]GTPγS (≥ 1000 Ci/mmol, radiochemical purity > 95 %) and [^{3}H]histamine (14.2 Ci/mmol) were from Hartmann Analytic (Braunschweig, Germany). All other reagents were from standard suppliers and of the highest purity available.

4.3.2 Construction of the cDNA for hH$_4$R-F169V, hH$_4$R-S179A/M, hH$_4$R-F169V+S179A/M, mH$_4$R-V171F and mH$_4$R-V171F+M181S

In order to introduce the F169V mutation into the pVL1392-SF-hH$_4$R-His$_6$ expression vector a site directed mutagenesis PCR was performed using the complementary single mismatching primers 5'-GT GAA TGT GAA CCT GGA TTT **GTT** TCG GAA TGG TAC ATC C-3' and 5'-G GAT GTA CCA TTC CGA **AAC** AAA TCC AGG TTC ACA TTC AC-3' and the pVL1392-SF-hH$_4$R-His$_6$ plasmid as template. The mutation hH$_4$R-S179A was introduced with the mismatching primers

5'-C CTT GCC ATC ACA **GCA** TTC TTG GAA TTC GTG ATC CC-3' as well as 5'-GG GAT CAC GAA TTC CAA GAA **TGC** TGT GAT GGC AAG G-3', whereas the mutation hH$_4$R-S179M was generated with mismatching primers 5'-GG TAC ATC CTT GCC ATC ACA **ATG** TTC TTG GAA TTC GTG ATC CCA G-3' and 5'-C TGG GAT CAC GAA TTC CAA GAA **CAT** TGT GAT GGC AAG GAT GTA CC-3' using the pVL1392-SF-hH$_4$R-His$_6$ plasmid as template. The hH$_4$R double mutants were established with the generated pVL1392-SF-hH$_4$R-F169V-His$_6$ plasmid as template. The S179A mutation was introduced using the mismatching primers 5'-C CTT GCC ATC ACA **GCA** TTC TTG GAA TTC GTG ATC CC-3' and 5'-GG GAT CAC GAA TTC CAA GAA **TGC** TGT GAT GGC AAG G-3'. For the exchange S179M, two complementary mismatching primers were applied (5'-G GAA TGG TAC ATC CTT GCC ATC ACA **ATG** TTC TTG GAA TTC GTG ATC CC-3' and 5'-GG GAT CAC GAA TTC CAA GAA **CAT** TGT GAT GGC AAG GAT GTA CCA TTC C-3').

The V171F mutation was introduced into the pGEM-3Z-SF-mH$_4$R-His$_6$ cloning vector by using the primers 5'-C TGT GAG CCT GGC TTT **TTT** ACA GAG TGG TAC ATC C-3' and 5'-G GAT GTA CCA CTC TGT **AAA** AAA GCC AGG CTC ACA G-3'. The pGEM-3Z-SF-mH$_4$R-V171F-His$_6$ and pVL1392-SF-hH$_4$R-His$_6$ plasmids were digested with *Sac*I and *Xba*I and the mH$_4$R-V171F cDNA fragment was cloned into the pVL1392 vector backbone. For generation of the mH$_4$R-V171F+M181S mutation, pVL1392-SF-mH$_4$R-V171F-His$_6$ was used and a second mutation (M181S) was introduced with the primers 5'-GG TAC ATC CTC ACC ATT ACA **AGC** CTC TTG GAA TTC CTG C-3' as well as 5'-G CAG GAA TTC CAA GAG **GCT** TGT AAT GGT GAG GAT GTA CC-3'. The sequences of the mutated H$_4$R cDNAs and the pVL1392 backbone were verified by sequencing and agarose gel electrophoresis, respectively.

4.3.3 Cell culture, generation of recombinant baculoviruses, membrane preparation

Cell culture and generation of high-titre recombinant baculovirus stocks (Schneider et al., 2009) as well as the co-infection of Sf9 cells with high-titre baculovirus stocks encoding Gα$_{i2}$, Gβ$_1$γ$_2$ and the respective H$_4$R (Brunskole et al., 2011) were performed as described recently. Membrane preparations were performed according to Gether et al. (1995) in the presence of 0.2 mM phenylmethylsulfonyl fluoride, 1 mM ethylenediaminetetraacetic acid (EDTA), 10 µg/mL leupeptin and 10 µg/mL benzamidine as protease inhibitors. Prepared membranes were resuspended in binding buffer (75 mM Tris/HCl, 12.5 mM MgCl2, 1 mM EDTA, pH 7.4) and stored at -80 °C in 0.5 or 1.0 mL aliquots.

4.3.4 SDS-PAGE and Coomassie staining

Prior to incubation at 30 °C for 15 min, 15 µg of the respective membranes including a negative control (Sf9 cells transfected with pVL1392 devoid of an insert) were loaded onto the gel as

well as 5 µL of the "unstained" protein marker I. A 2x Laemmli sample buffer without urea was used for sample preparation. The gels were stained in an aqueous solution of 0.1 % Coomassie brilliant blue G250 in 50 % methanol and 10 % acetic acid and subsequently destained with an aqueous solution containing 13 % methanol and 7 % acetic acid.

4.3.5 Western blotting

For the detection of the FLAG-tagged receptor, a sample buffer containing urea was used and the samples were incubated for 15 min at room temperature to prevent aggregation (Ren et al., 2009). For loading control, 10 ng of the amino-terminal FLAG-BAP fusion protein, heated for 5 min at 95 °C in Laemmli sample buffer, was added to 10 µg of the membranes. For detection of the $G\alpha_{i2}$ protein, the samples were incubated for 15 min at 30 °C in sample buffer without urea prior to loading of 0.5 µg protein.

4.3.6 [³H]histamine saturation binding experiments

The experiments were performed in 96-well plates. Each well contained 43-150 µg of protein in a total volume of 100 µL. For saturation binding, membranes were incubated in binding buffer containing [³H]histamine (1-200 nM) and 0.2 % (*w/v*) BSA for 60 min at room temperature under shaking at 200 rpm. Non-specific binding, amounting to 6.4–16.0 % of total binding at 100 nM [³H]histamine, was determined in the presence of 10 µM unlabelled histamine. Filtration through glass microfibre filters (Whatman GF/C), pretreated with polyethylenimine 0.3 % (*w/v*), using a Brandel 96 sample harvester separated unbound from membrane-associated [³H]histamine. After three washing steps with binding buffer, for each well filter pieces were punched and transferred into 96-well sample plates 1450-401 (Perkin Elmer, Rodgau, Germany). Each well was supplemented with 200 µL of scintillation cocktail (Rotiscint Eco plus, Roth, Karlsruhe, Germany) and incubated in the dark under shaking at 200 rpm. Radioactivity was measured with a Micro Beta2 1450 scintillation counter.

4.3.7 [³H]histamine competition binding assay

Each well contained 13-50 µg of protein in a total volume of 100 µL. BSA concentration, incubation time as well as the use of scintillation cocktail, polyethylenimine and 96-well sample plates 1450-401 (Perkin Elmer, Rodgau, Germany) was the same as shown for the [³H]histamine saturation binding assay. But [³H]histamine was added at concentrations reflecting the K_d value of the respective receptor, determined in [³H]histamine saturation binding assays.

4.3.8 [³⁵S]GTPγS binding assay

Membranes were thawed, centrifuged for 10 min at 4 °C and 13,000 g and carefully resuspended in binding buffer. Experiments were performed in 96-well plates in a total volume

of 100 µL per well. Each well contained 6-15 µg of protein, 1 µM GDP, 100 mM NaCl, 0.05 % (*w/v*) bovine serum albumin (BSA), 20 nCi of [^{35}S]GTPγS (≥ 0.2 nM) and ligand at concentrations as indicated in the results section. Neutral antagonists were incubated in the presence of histamine at concentrations corresponding to the 10-fold of the EC_{50} value at the respective receptor. Nonspecific binding was determined in the presence of 10 µM unlabelled GTPγS. After incubation under shaking at 200 rpm at room temperature for 2 h, bound [^{35}S]GTPγS was separated from free [^{35}S]GTPγS by filtration through glass microfibre filters using a 96-well Brandel harvester (Brandel Inc., Unterföhring, Germany). The filters were washed three to four times with binding buffer (4 °C), dried over night and impregnated with meltable scintillation wax prior to counting with a Micro Beta2 1450 scintillation counter (Perkin Elmer, Rodgau, Germany).

Ligands were tested in triplicate and curves were fitted with variable slope. Means ± SEM of pEC_{50}, pK_b and α were calculated from the means of all individual curves. The maximal response to histamine at the respective wild-types and mutants was set to 100 % and all other ligands, including inverse agonists, were referenced to histamine.

4.3.9 Homology model of the hH_4R

Cf. Chapter 3.3.3.

4.3.10 Miscellaneous

Protein concentrations of all membrane preparations were determined with the Bio-Rad DC protein assay kit (München, Germany) in one experiment. Because UR-PI376 had to be dissolved in 20 % DMSO, the water control as well as the full agonist histamine (α = 1.0), to which all other ligands were referenced, were also dissolved in 20 % DMSO in case of this ligand. Data from the [^{3}H]histamine saturation binding, [^{3}H]histamine competition binding and the [^{35}S]GTPγS assays were analysed with the Prism 5.01 software (GraphPad, San Diego, CA USA). K_b- and K_i-values were calculated according to the Cheng-Prusoff equation (Cheng and Prusoff, 1973). All values are given as mean ± SEM of at least three (up to nine) independent experiments performed in triplicate. Significances were calculated using one-way analysis of variance (ANOVA), followed by Bonferroni's multiple comparison test.

The drug/molecular target nomenclature conforms to BJP's Guide to Receptors and Channels (Alexander et al., 2011).

4.4 Results

4.4.1 Expression of recombinant proteins

Histamine H$_4$ receptor wild-types (hH$_4$R, mH$_4$R and rH$_4$R) as well as mutants (hH$_4$R-F169V, mH$_4$R-V171F, hH$_4$R-S179A, hH$_4$R-S179M, hH$_4$R-F169V+S179A, hH$_4$R-F169V+S179M and mH$_4$R-V171F+M181S) were expressed in Sf9 insect cells together with G-protein subunits Gα$_{i2}$ and Gβ$_1$γ$_2$ (Schneider et al., 2010). High expression at comparable ratios of both, receptors (wild-types and mutants) and G-proteins, was confirmed by SDS-PAGE with Coomassie staining and densitometric analysis referred to the bands with apparent molecular weights of 78, 76, 33 and 30 kDa, respectively, present in all samples including the negative control (Figure 4.4).
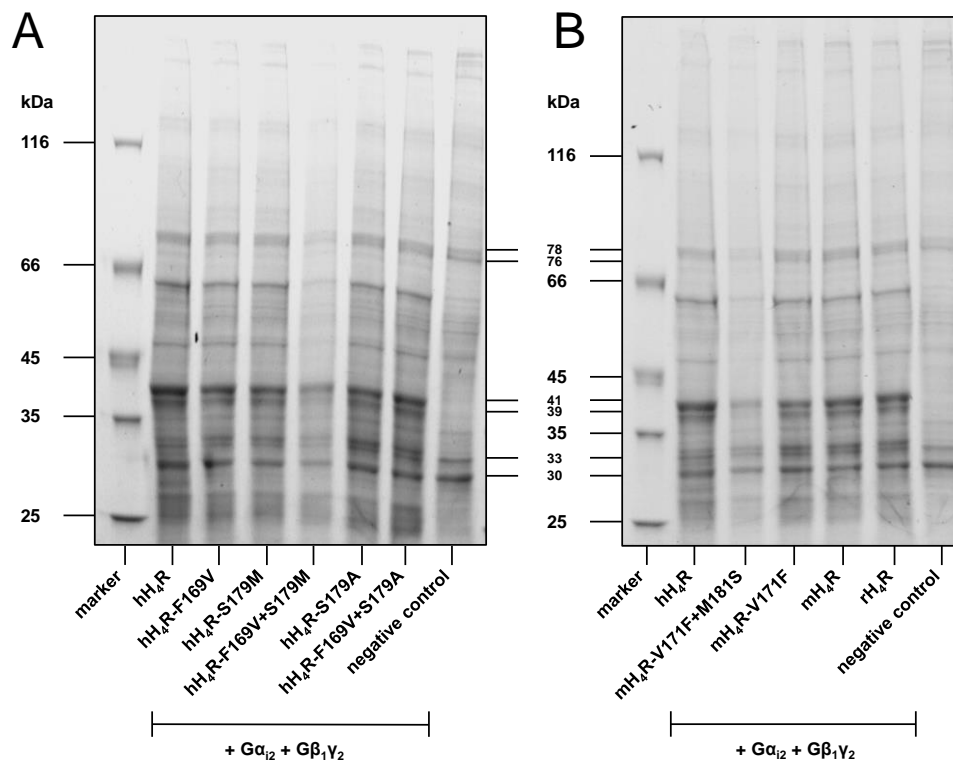
Figure 4.4: Coomassie stained gels of the respective receptors, co-expressed with Gα$_{i2}$ and Gβ$_1$γ$_2$. A negative control (transfection with pVL1392 devoid of an insert) is included.

Western blots using anti FLAG M1 and anti Gα$_{i1/2}$ antibodies identified bands at 39 and 71 kDa, probably, representing the unglycosylated and the glycosylated or the dimeric form of the receptor, as exemplarily shown for hH$_4$R-F169V in Figure 4.5. The Gα$_{i2}$-protein appeared at 41 kDa (Figure 4.5).
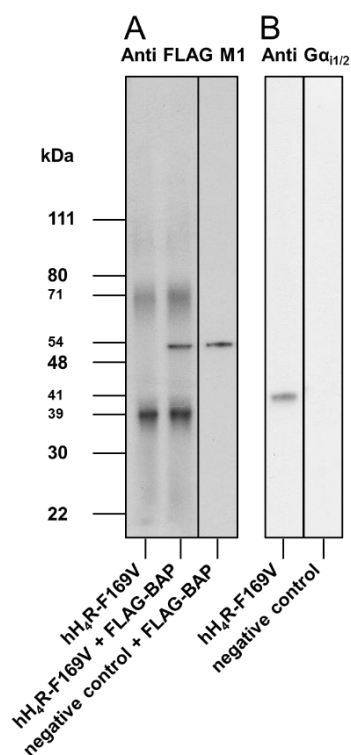
Figure 4.5: (A) Western blot (10 µg total protein per lane, spiked with 10 ng amino-terminal FLAG-BAP) with anti-FLAG M1 antibody. (B) Western blot with anti-Gα$_{i1/2}$ antibody (0.5 µg protein per lane). Figures indicate the "prestained" peqGOLD protein marker III proteins, referenced to the molecular mass of the "unstained" peqGOLD protein marker I.

Regardless of the high expression of the mH$_4$R, the rH$_4$R and the mH$_4$R mutants, in these cases almost no specific binding of [^{3}H]histamine was detectable, which is in agreement with reported data for the mH$_4$R and rH$_4$R (Schnell et al., 2011), most probably due to the low affinity of histamine to these receptor proteins. Therefore, competition binding experiments with [^{3}H]histamine were not feasible at mH$_4$R, mH$_4$R mutants and rH$_4$R.

By contrast, high specific binding of [^{3}H]histamine to the hH$_4$R, hH$_4$R-F169V, hH$_4$R-S179A, hH$_4$R-S179M mutant and to the hH$_4$R-F169V+S179A and hH$_4$R-F169V+S179M double mutants was detected. B$_{max}$ values ranged from 1.5 to 2.3 pmol [^{3}H]histamine per mg of soluble membrane protein and the K$_d$ values of [^{3}H]histamine from 11.2 to 36.6 nM (Table 4.1 and Figure 4.6).

Table 4.1: Saturation binding data for [^{3}H]histamine at H$_4$R wild-types and mutants.

Receptor	K$_d$ [nM]	B$_{max}$ [pmol/mg]
hH$_4$R	11.16 ± 1.92	1.93 ± 0.32
hH$_4$R-F169V	20.15 ± 4.47	1.92 ± 0.23
hH$_4$R-S179M	17.81 ± 3.26	2.08 ± 0.02
hH$_4$R-F169V+S179M	36.59 ± 4.24	1.52 ± 0.07
hH$_4$R-S179A	14.81 ± 3.84	2.25 ± 0.16
hH$_4$R-F169V+S179A	28.65 ± 3.57	1.46 ± 0.09

K$_d$ and B$_{max}$ values are given as mean ± SEM for three independent experiments, each performed in triplicate. Non-specific binding, amounting to 6.4–16.0 % of total binding at 100 nM [^{3}H]histamine, was determined in the presence of 10 µM unlabelled histamine.
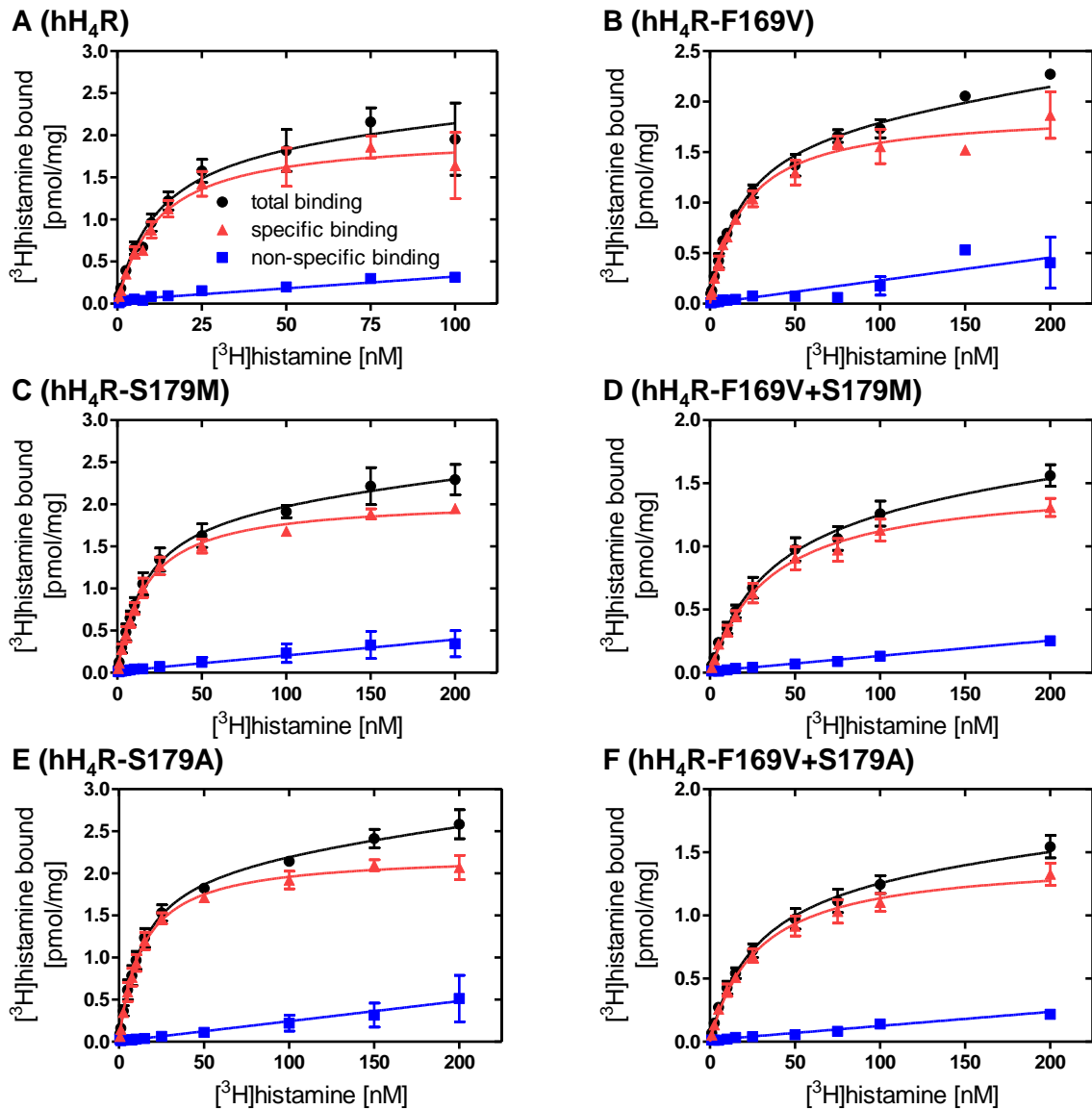
Figure 4.6: Saturation binding curves for [³H]histamine at H₄R wild-type and mutants shown as mean values ± SEM from three independent experiments performed in triplicate.

4.4.2 [³H]histamine competition binding experiments

The affinity at the hH₄R-F169V mutant was in the same range or lower compared to the data at the wild-type hH₄R (Table 4.2). The decrease in affinity was pronounced for UR-PI376 (pK_i 6.33 vs. 7.27), clozapine (pK_i 5.51 vs. 6.18), isoloxapine (pK_i 6.05 vs. 6.93) and clobenpropit (pK_i 7.21 vs. 7.73). Effects of a single S179A or S179M mutation on affinity were marginal for most compounds, but higher affinity at hH₄R-S179A compared to the wild-type was determined in case of thioperamide, JNJ7777120, clozapine, isoloxapine and UR-PI376. At the double mutants, clozapine, isoloxapine and UR-PI376 showed reduced affinity, whereas the affinity of thioperamide and JNJ7777120 for the hH₄R-F169V+S179A variant was even higher than for the hH₄R. In general, the pK_i values were higher at the hH₄R-S179A than at the hH₄R-S179M

single mutants and higher at the hH_4R-F169V+S179A than at the hH_4R-F169V+S179M double mutants (Table 4.2).

**Table 4.2: [^{3}H]histamine binding on hH_4R wild-type and mutants.**

Ligand	hH_4R	hH_4R-F169V	hH_4R-S179M	hH_4R-F169V +S179M	hH_4R-S179A	hH_4R-F169V +S179A
histamine	7.89 ± 0.04	7.59 ± 0.05 •	7.49 ± 0.03 ••	7.40 ± 0.06 •••	7.61 ± 0.07 •	7.45 ± 0.07 •••
UR-PI294	7.84 ± 0.03	7.83 ± 0.04	7.93 ± 0.16	7.81 ± 0.05	7.90 ± 0.09	7.72 ± 0.08
thioperamide	6.75 ± 0.07	6.98 ± 0.15	6.67 ± 0.04	6.58 ± 0.06	7.34 ± 0.14 •	7.29 ± 0.16
JNJ7777120	7.16 ± 0.05	6.83 ± 0.05 ••	7.23 ± 0.07	6.81 ± 0.02 ••	7.78 ± 0.02 •••	7.48 ± 0.04 •
VUF8430	7.84 ± 0.03	7.44 ± 0.02	7.55 ± 0.07	7.42 ± 0.15	7.81 ± 0.14	7.69 ± 0.15
immepip	7.73 ± 0.16	7.47 ± 0.00	7.49 ± 0.09	7.54 ± 0.13	7.44 ± 0.08	7.52 ± 0.08
clozapine	6.18 ± 0.03	5.51 ± 0.16 •	6.36 ± 0.12	5.23 ± 0.14 •••	6.59 ± 0.11	5.48 ± 0.04 •
isoloxapine	6.93 ± 0.02	6.05 ± 0.13 •••	7.02 ± 0.10	6.24 ± 0.08 ••	7.47 ± 0.08 •	6.68 ± 0.09
UR-PI376	7.27 ± 0.07	6.33 ± 0.11 •••	7.10 ± 0.12	6.18 ± 0.06 •••	7.60 ± 0.04	6.40 ± 0.07 •••
clobenpropit	7.73 ± 0.07	7.21 ± 0.03 ••	7.14 ± 0.09 •••	7.23 ± 0.04 ••	7.56 ± 0.06	7.22 ± 0.02 ••

pK_i-values ([^{3}H]histamine competition binding) are given as mean ± SEM of at least three independent experiments, performed in triplicate. Results of statistical tests (one-way ANOVA and Bonferroni post hoc tests): significant differences with respect to hH_4R - • $p < 0.05$, •• $p < 0.01$, ••• $p < 0.001$.

4.4.3 Functional analysis of wild-type and mutant H_4 receptors in the [^{35}S]GTPγS assay

We determined potencies (pEC_{50}) and maximal effects (α) as well as antagonist activities (pK_b) at wild-type and mutated receptors in the [^{35}S]GTPγS-assay, using agonists and antagonists, respectively (Figure 4.1, Table 4.3 and Table 4.4). Amounts of [^{35}S]GTPγS bound were similar except for mH_4R-V171F+M181S, mH_4R-V171F, mH_4R and rH_4R (Figure 4.7A). To facilitate comparison of the ratio of agonism to inverse agonism at the H_4R orthologs and mutants, the changes in [^{35}S]GTPγS binding were expressed as relative values in Figure 4.7B. In this representation, the span between maximal increase in [^{35}S]GTPγS binding elicited by the full agonist histamine and maximal decrease induced by the inverse agonist thioperamide was set to 100 %. [^{35}S]GTPγS binding in the absence of ligand (water control) was set to zero (Figure 4.7B). The inverse agonism of thioperamide reflects the extent of constitutive activity of the respective wild-type or mutated H_4R (Figure 4.7). The response to thioperamide decreased in the order: hH_4R > hH_4R-S179M > hH_4R-S179A > hH_4R-F169V > hH_4R-F169V+S179M > hH_4R-F169V+S179A > mH_4R-V171F+M181S > mH_4R-V171F = rH_4R = mH_4R. Thus, the single mutation F169V significantly decreased the exceptionally high constitutive activity of the hH_4R, and the mutation of hH_4R-F169 and S179 into the corresponding amino acids of the mH_4R and rH_4R caused a further decrease. The single hH_4R-S179A or S179M mutation did not reduce constitutive activity significantly. Accordingly, F169 alone and in concert with S179 contributed to the high constitutive activity of the hH_4R. The mH_4R and the rH_4R did not show constitutive activity under the same conditions; thioperamide behaved as a neutral antagonist in the [^{35}S]GTPγS assay. This was also the case

for the mH$_4$R-V171F mutant, and there was no significant increase in constitutive activity for the mH$_4$R-V171F+M181S mutant. The higher the constitutive activity, the lower is the relative "residual" receptor capacity for activation by agonists (Figure 4.7B). Thus, the relative maximal response to histamine increased in the order: hH$_4$R < hH$_4$R-S179M < hH$_4$R-S179A < hH$_4$R-F169V < hH$_4$R-F169V+S179M < hH$_4$R-F169V+S179A < mH$_4$R-V171F+M181S < mH$_4$R-V171F = rH$_4$R = mH$_4$R.
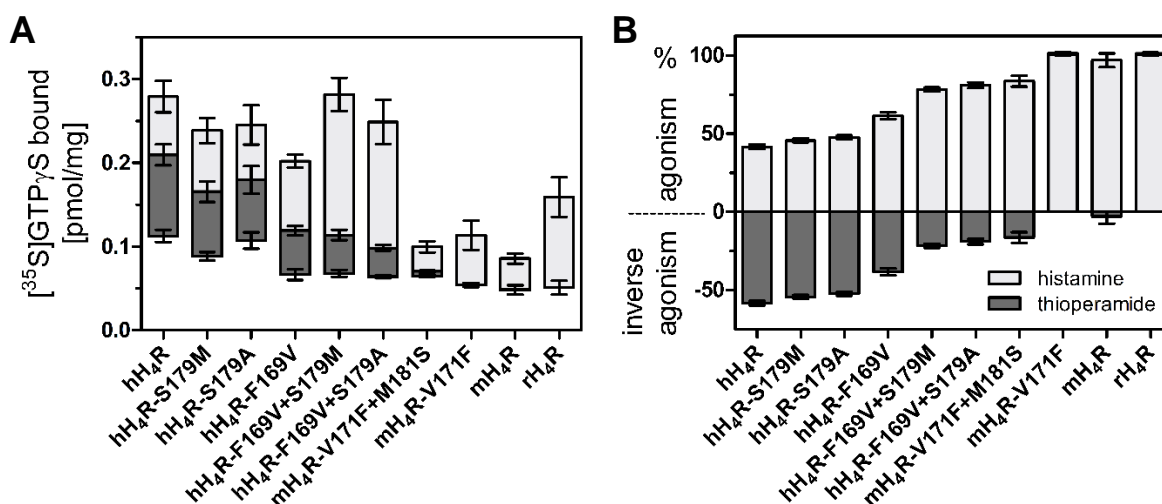
Figure 4.7: Maximal agonistic effects of histamine (light grey) and maximal inverse agonistic effects of thioperamide (dark grey) in [^{35}S]GTPγS assays. (A) Absolute values of bound [^{35}S]GTPγS [pmol/mg protein] in the presence of histamine and thioperamide. Values demarcating light and dark grey bars represent the basally (in the absence of ligand) bound [^{35}S]GTPγS. **(B)** For each H$_4$R species, the sum of the histamine and thioperamide effects was scaled to 100 %; the zero line represents the ligand-free control. Significant changes: hH$_4$R vs. hH$_4$R-F169V ($p < 0.001$), hH$_4$R vs. hH$_4$R-F169V+S179A ($p < 0.001$), hH$_4$R vs. hH$_4$R-F169V+S179M ($p < 0.001$), hH$_4$R-F169V vs. hH$_4$R-F169V+S179A ($p < 0.001$), hH$_4$R-F169V vs. hH$_4$R-F169V+S179M ($p < 0.001$) and mH$_4$R vs. mH$_4$R-V171F+M181S ($p < 0.05$).

Concentration-response curves of histamine normalized to a percentual scale (maximal effect 100 %) are shown in Figure 4.8A and Figure 4.9A. The potency of histamine decreased from the hH$_4$R via hH$_4$R-F169V, hH$_4$R-S179A and hH$_4$R-S179M mutants to the hH$_4$R double mutants by up to one order of magnitude (Table 4.3, Figure 4.8A and Figure 4.9A). The potencies of histamine at the mH$_4$R and the rH$_4$R were low (pEC$_{50}$ ~ 4-5, Table 4.4, Figure 4.8A and Figure 4.9A). Corresponding to the key role of F169 in the hH$_4$R, the potency was significantly higher at the mH$_4$R-V171F and mH$_4$R-V171F+M181S mutant than at the mH$_4$R wild-type.

UR-PI294 (Igel et al., 2009b) was a full agonist with potencies being five to ten times higher than those of histamine at all H$_4$R species variants (Table 4.3 and Table 4.4, Figure 4.8B and Figure 4.9B). The rank order at the hH$_4$R mutants corresponded to that of histamine. The pEC$_{50}$ value at mH$_4$R-V171F was in between the values at the hH$_4$R and mH$_4$R wild-types, i. e., the presence of F169, making the mH$_4$R more similar to the hH$_4$R, substantially increased the potency of UR-PI294, too.

The inverse agonistic response to thioperamide was highest at the hH$_4$R, slightly smaller at the hH$_4$R-S179A (Figure 4.9C) and hH$_4$R-S179M (Figure 4.8C) mutants, significantly reduced at the hH$_4$R-F169V mutant and, in particular, at the double mutants, hH$_4$R-F169V+S179A and hH$_4$R-F169V+S179M (Table 4.3, Figure 4.8C and Figure 4.9C). Whereas thioperamide acted as a weak partial inverse agonist at the mH$_4$R-V171F+M181S mutant, it behaved as a neutral antagonist at the mH$_4$R, the rH$_4$R and the mH$_4$R-V171F mutant with pK$_b$ values of 7.84, 7.12, 6.44 and 7.73, respectively.

JNJ7777120 was a partial inverse agonist at the highly constitutively active hH$_4$R and hH$_4$R-S179A/M (Table 4.3 and Table 4.4, Figure 4.8D and Figure 4.9D) but a partial agonist at the hH$_4$R-F169V mutant, the mH$_4$R, the rH$_4$R and the mH$_4$R-V171F mutant. At the double mutants as well as at the mH$_4$R-V171F+M181S mutant, the compound rather behaved as a neutral antagonist.

Clozapine and isoloxapine were weak partial agonists or neutral antagonists at the mH$_4$R and the rH$_4$R (Table 4.4, Figure 4.8E, F and Figure 4.9E, F). Introduction of phenylalanine into the mH$_4$R (mH$_4$R-V171F mutant) significantly increased partial agonism of both compounds. Also at the hH$_4$R and its mutants, clozapine and isoloxapine acted as partial agonists. At the hH$_4$R-F169V and the double mutants, the potencies were lower than at the wild-type receptor, with the maximal effects only decreasing in case of clozapine. In contrast, at the hH$_4$R-S179M and S179A mutants, potencies of both clozapine and isoloxapine were similar to those at the hH$_4$R; maximal effects were reduced only at the S179M mutant. Generally, the potencies and the maximal effects of isoloxapine were higher than those of clozapine.

Both clobenpropit, a partial, and UR-PI376 (Igel et al., 2009a), a full agonist at the hH$_4$R, showed a considerable decrease in the maximal effects from the hH$_4$R wild-type over the hH$_4$R-F169V mutant to the double mutants, where clobenpropit revealed neutral antagonism (Table 4.3, Figure 4.8G, H and Figure 4.9G, H). At the hH$_4$R-S179M mutant, clobenpropit was a partial inverse agonist. At the hH$_4$R the pEC$_{50}$-values of UR-PI376 and clobenpropit were similar, whereas at the double mutants the pK$_b$ values of UR-PI376 were much lower than those of clobenpropit. At the mH$_4$R, the rH$_4$R, the mH$_4$R-V171F and the mH$_4$R-V171F+M181S mutant, both compounds behaved as weak partial agonists or neutral antagonists with maximal effects increasing from mH$_4$R over the mH$_4$R-V171F to the mH$_4$R-V171F+M181S mutants (Table 4.4).

The potent hH$_4$R agonists VUF8430 (Table 4.3 and Table 4.4, Figure 4.8I and Figure 4.9I) and immepip (Table 4.3 and Table 4.4, Figure 4.8J and Figure 4.9J) showed only little changes in pEC$_{50}$ and α values at the five hH$_4$R mutants in comparison to the wild-type. However, at the mH$_4$R, the rH$_4$R and the mH$_4$R-V171F mutant, potencies and maximal effects were much lower.

**Table 4.3: [^{35}S]GTPγS binding on hH$_4$R wild-type and mutants.**

Ligand	Para-meter	hH$_4$R	hH$_4$R-F169V	hH$_4$R-S179M	hH$_4$R-F169V +S179M	hH$_4$R-S179A	hH$_4$R-F169V +S179A
histamine	α	1	1	1	1	1	1
	pEC$_{50}$	8.13 ± 0.06 ▪▪▪, ♦♦♦	7.72 ± 0.07 ••, ▪▪▪, ♦♦♦	7.48 ± 0.08 •••, ▪▪▪, ♦♦♦	7.24 ± 0.02 •••, ▪▪▪, ♦♦♦	7.50 ± 0.05 •••, ▪▪▪, ♦♦♦	7.36 ± 0.07 •••, ▪▪▪, ♦♦♦
UR-PI294	α	1.02 ± 0.03	1.00 ± 0.07	0.98 ± 0.00	0.94 ± 0.05	0.92 ± 0.03	0.86 ± 0.08
	pEC$_{50}$	8.35 ± 0.04 ▪▪▪, ♦♦♦	8.00 ± 0.11 ▪▪▪, ♦♦♦	7.98 ± 0.11 ▪▪▪, ♦♦♦	7.82 ± 0.02 ••, ▪▪▪, ♦♦♦	8.16 ± 0.04 ▪▪▪, ♦♦♦	7.84 ± 0.01 ••, ▪▪▪, ♦♦♦
thioperamide	α	-1.39 ± 0.08 ▪▪▪, ♦♦♦	-0.63 ± 0.06 •••, ▪▪▪, ♦♦♦	-1.19 ± 0.06 ▪▪▪, ♦♦♦	-0.28 ± 0.04 •••	-1.12 ± 0.06 •, ▪▪▪, ♦♦♦	-0.23 ± 0.03 •••
	pEC$_{50}$	6.58 ± 0.06 ▪▪▪	6.52 ± 0.05 ▪▪▪	6.51 ± 0.04 ▪▪▪	6.60 ± 0.05 ▪▪	6.78 ± 0.06	7.28 ± 0.11
	pK$_b$	6.83 ± 0.05			6.81 ± 0.07		7.60 ± 0.10 •••, ▪▪, ♦♦♦
JNJ7777120	α	-0.39 ± 0.03 ▪▪▪, ♦♦♦	0.43 ± 0.03 •••, ♦♦	-0.48 ± 0.03 ▪▪▪, ♦♦♦	0.18 ± 0.04 •••, ▪▪▪	-0.66 ± 0.06 •••, ▪▪▪, ♦♦♦	0 •••, ▪▪▪, ♦♦♦
	pEC$_{50}$	7.10 ± 0.08 ▪▪▪, ♦♦♦	6.21 ± 0.12 •••, ♦♦♦	7.12 ± 0.03 ▪▪▪, ♦♦♦	7.28 ± 0.11	7.99 ± 0.08 •••, ▪▪▪, ♦♦♦	n.a.
	pK$_b$	7.60 ± 0.05			6.85 ± 0.16 ▪▪, ♦♦♦		7.47 ± 0.09 ▪▪▪, ♦♦♦
VUF8430	α	0.84 ± 0.06 ♦♦♦	0.91 ± 0.06 ♦♦♦	0.85 ± 0.03 ♦♦♦	0.86 ± 0.01 ♦♦♦	0.85 ± 0.05 ♦♦♦	0.75 ± 0.06 ♦
	pEC$_{50}$	7.42 ± 0.12 ▪▪▪, ♦♦♦	7.61 ± 0.07 ▪▪▪, ♦♦♦	7.41 ± 0.08 ▪▪▪, ♦♦♦	7.06 ± 0.13 ▪▪▪, ♦♦♦	7.53 ± 0.09 ▪▪▪, ♦♦♦	7.36 ± 0.09 ▪▪▪, ♦♦♦
immepip	α	0.81 ± 0.03	0.85 ± 0.05	0.84 ± 0.09	0.84 ± 0.03	0.85 ± 0.06	0.65 ± 0.08
	pEC$_{50}$	7.67 ± 0.05 ▪▪▪, ♦♦♦	7.73 ± 0.19 ▪▪▪, ♦♦♦	7.45 ± 0.10 ▪▪▪, ♦♦♦	7.45 ± 0.10 ▪▪▪, ♦♦♦	7.67 ± 0.09 ▪▪▪, ♦♦♦	7.68 ± 0.11 ▪▪▪, ♦♦♦
clozapine	α	0.67 ± 0.04 ▪▪▪, ♦♦♦	0.56 ± 0.03 ▪▪▪, ♦♦♦	0.49 ± 0.08 ▪▪▪, ♦♦♦	0.49 ± 0.03 ▪▪▪, ♦♦♦	0.62 ± 0.09 ▪▪▪, ♦♦♦	0.36 ± 0.02 ••, ▪▪, ♦♦
	pEC$_{50}$	6.24 ± 0.10 ▪▪▪, ♦♦♦	5.68 ± 0.12 •, ♦ ▪▪▪, ♦♦♦	6.26 ± 0.12 ▪▪▪, ♦♦♦	5.25 ± 0.04 •••	6.59 ± 0.10 ▪▪▪, ♦♦♦	5.71 ± 0.07 •, ♦ ▪▪▪, ♦♦♦
isoloxapine	α	0.81 ± 0.03 ▪▪▪, ♦♦♦	0.85 ± 0.09 ▪▪▪, ♦♦♦	0.62 ± 0.03 ▪▪▪, ♦♦	0.90 ± 0.03 ▪▪▪, ♦♦♦	0.77 ± 0.06 ▪▪▪, ♦♦♦	0.83 ± 0.10 ▪▪▪, ♦♦♦
	pEC$_{50}$	7.08 ± 0.13 ▪▪▪, ♦♦♦	6.36 ± 0.10 •••, ▪▪▪, ♦♦♦	7.26 ± 0.08 ▪▪▪, ♦♦♦	6.24 ± 0.09 •••, ▪▪▪, ♦♦♦	7.36 ± 0.07 ▪▪▪, ♦♦♦	6.69 ± 0.03 ▪▪▪, ♦♦♦
UR-PI376	α	1.11 ± 0.08 ▪▪▪, ♦♦♦	0.49 ± 0.02 •••, ▪▪▪, ♦♦♦	0.80 ± 0.04 •••, ▪▪▪, ♦♦♦	0.12 ± 0.01 •••	1.02 ± 0.06 ▪▪▪, ♦♦♦	0.25 ± 0.01 •••, ▪▪, ♦
	pEC$_{50}$	7.79 ± 0.08 ▪▪▪, ♦♦♦	6.25 ± 0.11 •••, ♦♦	6.93 ± 0.06 •••, ▪▪, ♦♦♦	7.23 ± 0.12	7.28 ± 0.04 ▪▪▪, ♦♦♦	6.88 ± 0.18 •••, ▪▪, ♦♦♦
	pK$_b$				5.82 ± 0.14 •••		6.31 ± 0.22
clobenpropit	α	0.45 ± 0.04 ▪▪▪, ♦♦♦	0.27 ± 0.05 •, ♦ ♦♦♦	-0.44 ± 0.04 •••, ▪▪▪, ♦♦♦	0 •••, ▪	0 •••, ▪	0 •••, ▪
	pEC$_{50}$	7.65 ± 0.11 ▪▪, ♦♦♦	7.63 ± 0.15 ▪▪, ♦♦♦	6.10 ± 0.15 •••	n.a.	n.a.	n.a.
	pK$_b$				7.06 ± 0.07 ♦ ♦♦♦	7.42 ± 0.08 ♦♦♦	7.56 ± 0.16 ▪, ♦♦♦

pEC$_{50}$-values ([^{35}S]GTPγS agonist mode), pK$_b$-values ([^{35}S]GTPγS antagonist mode) and α (intrinsic activity, maximal effect relative to histamine = 1.0) are given as mean ± SEM of at least three (up to nine) independent experiments, performed in triplicate. Results of statistical tests (one-way ANOVA and Bonferroni post hoc tests): significant differences with respect to hH$_4$R - • $p < 0.05$, •• $p < 0.01$, ••• $p < 0.001$; significant differences with respect to mH$_4$R - ▪ $p < 0.05$, ▪▪ $p < 0.01$, ▪▪▪ $p < 0.001$; significant differences with respect to rH$_4$R - ♦ $p < 0.05$, ♦♦ $p < 0.01$, ♦♦♦ $p < 0.001$. In case of neutral antagonism (-0.25 ≤ α ≤ 0.25), pK$_b$-values were considered for statistical analysis instead of pEC$_{50}$-values. Maximal effect α = 0: neutral antagonism, n.d.: not determined, n.a.: pEC$_{50}$ or pK$_b$ not applicable from performed experiments. Functional data for hH$_4$R cf. Nordemann et al. (2013).

Table 4.4: [³⁵S]GTPγS binding on mH₄R and rH₄R wild-types and mH₄R mutants.

Ligand	Para-meter	hH₄R	mH₄R-V171F +M181S	mH₄R-V171F	mH₄R	rH₄R
histamine	α	1	1	1	1	1
	pEC₅₀	8.13 ± 0.06 ■■■, ♦♦♦	5.87 ± 0.05 •••, ■■■, ♦♦♦	5.95 ± 0.08 •••, ■■■, ♦♦♦	5.17 ± 0.14 •••, ♦♦♦	4.28 ± 0.06 •••, ■■■
UR-PI294	α	1.02 ± 0.03	0.94 ± 0.04	0.99 ± 0.09	0.95 ± 0.03	1.09 ± 0.03
	pEC₅₀	8.35 ± 0.04 ■■■, ♦♦♦	6.95 ± 0.11 •••, ■■■, ♦♦♦	7.25 ± 0.02 •••, ■■■, ♦♦♦	6.10 ± 0.11 •••, ♦♦	5.48 ± 0.08 •••, ■■
thioperamide	α	-1.39 ± 0.08 ■■■, ♦♦♦	-0.20 ± 0.03 •••	0 •••	0 •••	0 •••
	pEC₅₀	6.58 ± 0.06 ■■■	7.11 ± 0.08	n.a.	n.a.	n.a.
	pKᵦ	6.83 ± 0.05	7.84 ± 0.04 •••, ■■■, ♦♦♦	7.73 ± 0.09 •••, ■■■, ♦♦♦	7.12 ± 0.09 •••, ♦♦♦	6.44 ± 0.09 ■■■
JNJ7777120	α	-0.39 ± 0.03 ■■■, ♦♦♦	0 •••, ■■■, ♦♦♦	0.42 ± 0.03 •••, ♦♦	0.44 ± 0.02 •••, ♦♦	0.24 ± 0.01 •••, ■■
	pEC₅₀	7.10 ± 0.08 ■■■, ♦♦♦	n.a.	6.93 ± 0.12 ■■, ♦♦♦	6.10 ± 0.07 •••, ♦♦♦	6.13 ± 0.14
	pKᵦ	7.60 ± 0.05	5.90 ± 0.03 •••, ♦♦♦			4.93 ± 0.16 •••, ■■■
VUF8430	α	0.84 ± 0.06 ♦♦♦	0.73 ± 0.07 ♦	0.67 ± 0.05	0.68 ± 0.04	0.43 ± 0.05 •••
	pEC₅₀	7.42 ± 0.12 ■■■, ♦♦♦	5.83 ± 0.16 •••, ■, ♦♦♦	5.75 ± 0.18 •••, ■, ♦♦♦	5.06 ± 0.14 •••	4.47 ± 0.15 •••
immepip	α	0.81 ± 0.03	0.95 ± 0.03	0.66 ± 0.09	0.67 ± 0.08	0.68 ± 0.10
	pEC₅₀	7.67 ± 0.05 ■■■, ♦♦♦	5.73 ± 0.06 •••, ♦♦♦	6.10 ± 0.12 •••, ■■■, ♦♦♦	5.27 ± 0.06 •••	4.95 ± 0.07 •••
clozapine	α	0.67 ± 0.04 ■■■, ♦♦♦	0.41 ± 0.08 •, ■■■, ♦♦♦	0.45 ± 0.04 ■■■, ♦♦♦	0 •••	0 •••
	pEC₅₀	6.24 ± 0.10 ■■■, ♦♦♦	5.71 ± 0.16 •, ■■■, ♦♦♦	5.35 ± 0.03 •••	n.a.	n.a.
	pKᵦ				4.92 ± 0.04 •••	4.90 ± 0.09 •••
isoloxapine	α	0.81 ± 0.03 ■■■, ♦♦♦	0.68 ± 0.05 ■■■, ♦♦♦	0.44 ± 0.01 •, ■	0 •••	0.19 ± 0.03 •••
	pEC₅₀	7.08 ± 0.13 ■■■, ♦♦♦	6.01 ± 0.05 •••, ■■■, ♦♦♦	5.69 ± 0.16 •••, ♦♦	n.a.	5.82 ± 0.16
	pKᵦ				5.26 ± 0.03 •••	5.12 ± 0.02 •••
UR-PI376	α	1.11 ± 0.08 ■■■, ♦♦♦	0.33 ± 0.04 •••, ■■■, ♦♦	0 •••	0 •••	0 •••
	pEC₅₀	7.79 ± 0.08 ■■■, ♦♦♦	6.08 ± 0.03 •••	n.a.	n.a.	n.a.
	pKᵦ		6.08 ± 0.11	6.30 ± 0.10 •••, ♦♦	6.06 ± 0.17 •••	5.48 ± 0.03 •••
clobenpropit	α	0.45 ± 0.04 ■■■, ♦♦♦	0.35 ± 0.03 ♦♦♦	0.27 ± 0.04 •, ♦♦♦	0.20 ± 0.02 •••, ♦	0 •••, ■
	pEC₅₀	7.65 ± 0.11 ■■, ♦♦♦	6.72 ± 0.13 •••	7.00 ± 0.15 •, ♦	6.07 ± 0.09	n.a.
	pKᵦ				6.79 ± 0.00 ••	6.28 ± 0.04 •••

cf. Table 4.3; functional data for mH₄R and rH₄R cf. Nordemann et al. (2013).
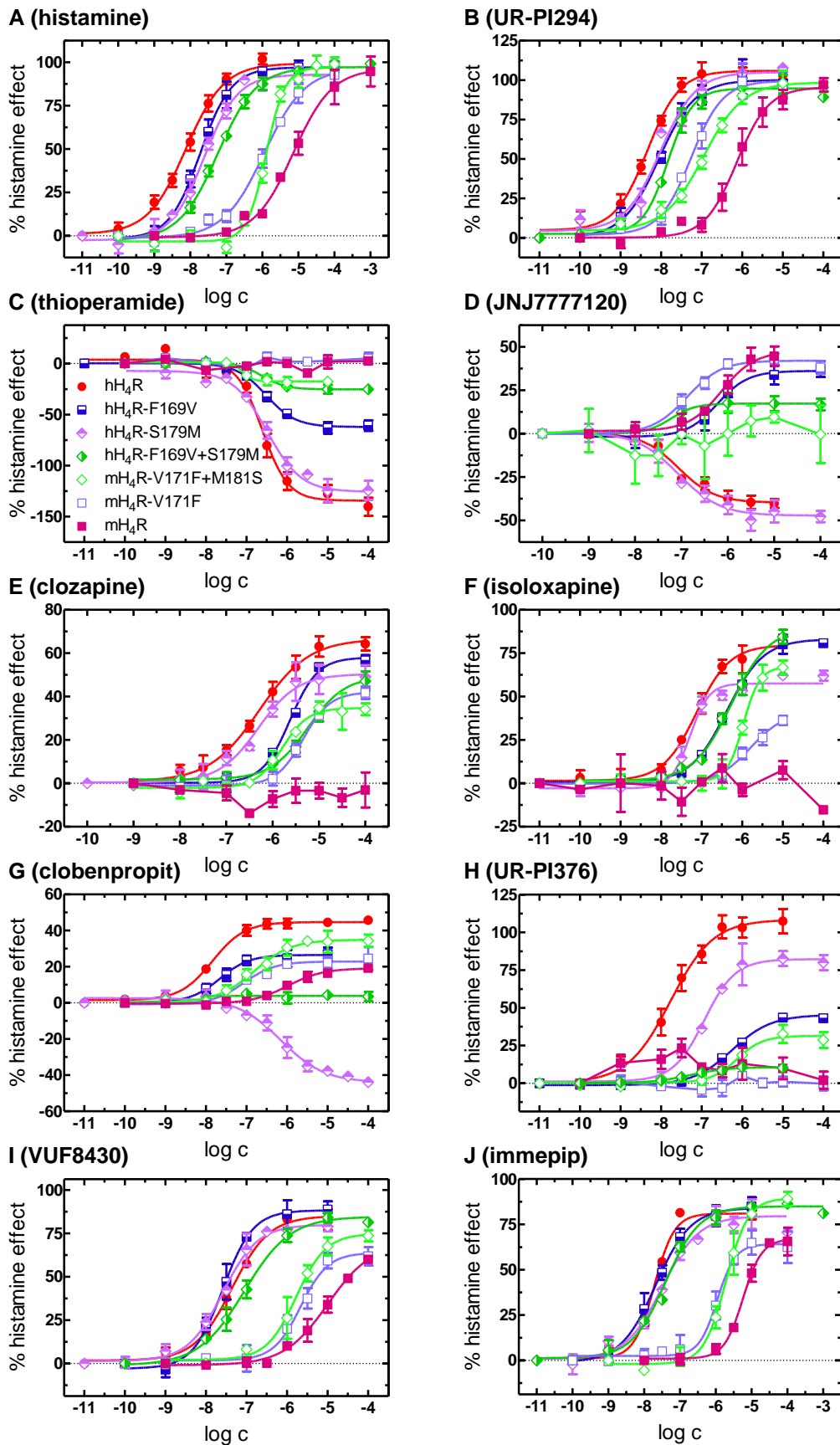
Figure 4.8: Concentration-response curves of ligands investigated in [³⁵S]GTPγS and [³H]histamine competition binding assays. All curves are scaled with respect to a maximal histamine effect of 100 %. Symbols and colours refer to the species variants and mutants, respectively. Filled symbols: wild-types; open symbols: mutants. **(A)** histamine; **(B)** UR-PI294; **(C)** thioperamide; **(D)** JNJ7777120; **(E)** clozapine; **(F)** isoloxapine; **(G)** clobenpropit; **(H)** UR-PI376; **(I)** VUF8430; **(J)** immepip.
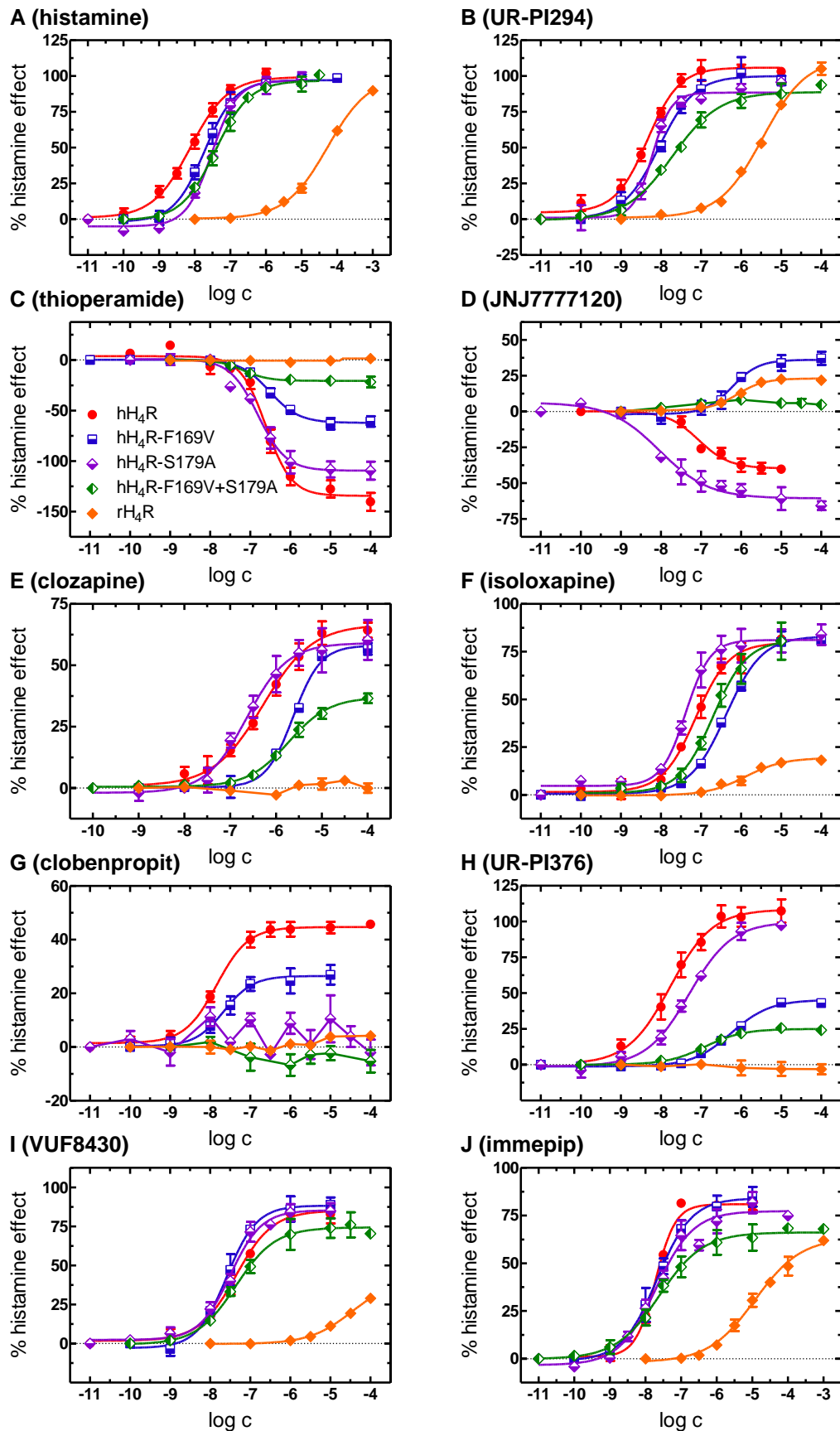
Figure 4.9: Concentration-response curves of ligands investigated in [^{35}S]GTPγS and [^{3}H]histamine competition binding assays. All curves are scaled with respect to a maximal histamine effect of 100 %. Symbols and colours refer to the species variants and mutants, respectively. Filled symbols: wild-types; open symbols: mutants. **(A)** histamine; **(B)** UR-PI294; **(C)** thioperamide; **(D)** JNJ7777120; **(E)** clozapine; **(F)** isoloxapine; **(G)** clobenpropit; **(H)** UR-PI376; **(I)** VUF8430; **(J)** immepip.

4.5 Discussion

4.5.1 Affinities and potencies of the investigated ligands at H$_4$R orthologs and mutants

Except for clobenpropit at hH$_4$R-S179M, binding data were in the same range as the respective EC$_{50}$ values from functional studies in the [^{35}S]GTPγS-assay (Table 4.2 and Table 4.3). Comparing mutant with wild-type receptors, changes in potency (Figure 4.10B and Figure 4.11B) were higher than changes in affinity (Figure 4.10C and Figure 4.11C), e. g. in case of histamine and UR-PI294, indicating that the higher potencies of ligands at the hH$_4$R were a result of the higher constitutive activity. For most agonists, potencies were lower at hH$_4$R-F169V and/or the double mutants than at the hH$_4$R and higher at the mH$_4$R-V171F and/or mH$_4$R-V171F+M181S mutant than at the mH$_4$R (Table 4.3 and Table 4.4). Remarkable exceptions were VUF8430 and immepip with only minor effects of the F169V and the double mutations. With respect to histamine, clozapine and VUF8430, our results correlate with previous data (Lim et al., 2008), showing markedly reduced affinity for the hH$_4$R-F169V compared to the wild-type in the case of histamine and clozapine, whereas the affinity of VUF8430 was only slightly lowered.
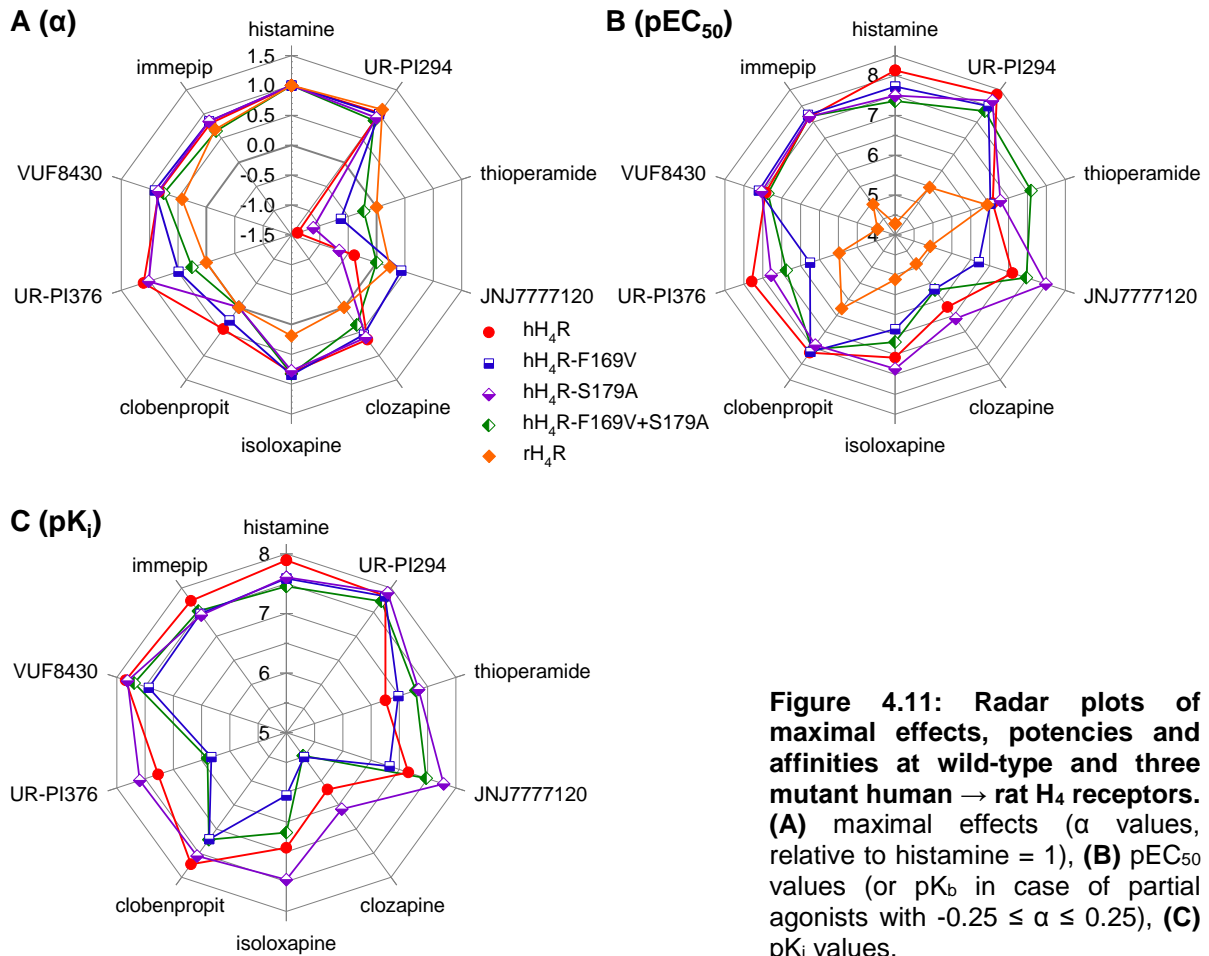
For clozapine and JNJ7777120, binding modes were proposed in which the phenyl and chlorophenyl moieties, respectively, occupy a pocket between TMs 3, 5, 6 and ECL2 (Kooistra et al., 2013; Lim et al., 2010). The phenyl rings of isoloxapine and UR-PI376 may adopt similar positions. For UR-PI294, clobenpropit, VUF8430 and immepip, the potencies at the hH$_4$R-F169V mutant indicate no influence of F169 on binding (Table 4.3). However, at the mH$_4$R-V171F mutant these compounds are more potent than at the mH$_4$R wild-type (Table 4.4). The structures of these ligands suggest a binding mode different to that of JNJ7777120, clozapine and isoloxapine (pK$_i$ values: cf. Table 4.2). The potencies of histamine, JNJ7777120, clozapine, clobenpropit and UR-PI376 are different on at least one of the double mutants compared to the hH$_4$R-F169V single mutant (Figure 4.10B and Figure 4.11B). The additional mutation may either lead to a decrease in potency (histamine) or an increase (JNJ7777120) at both double mutants. The docking poses of histamine (Figure 4.3), clozapine and JNJ7777120 (Kooistra et al., 2013; Lim et al., 2010) do not indicate direct interactions with F169, but its substitution by valine may alter or destabilize the topology of the ligand binding pocket, in particular the conformation of L175$^{5.39}$, L326$^{6.58}$ and Y340$^{7.35}$ (Figure 4.12) and, in turn, selectively affect ligand-receptor interactions. Alternatively or additionally, F169 at the entrance of the pocket may be part of the "optimal" ligand binding path.

In accordance with previous reports (Lim et al., 2008; Shin et al., 2002) the hH$_4$R-S179A and S179M mutants suggest a minor role of S179$^{5.43}$ on histamine binding. An increase in both potency and affinity (cf. thioperamide, JNJ7777120, clozapine, isoloxapine) due to S179A

exchange may be interpreted as a hint that hydrophobic interactions come into play. For most ligands pEC_{50} and pK_i values are lower at hH_4R-S179M than at hH_4R-S179A (Table 4.2 and Table 4.3), possibly due to steric hindrance of ligand binding by the methionine side chain.
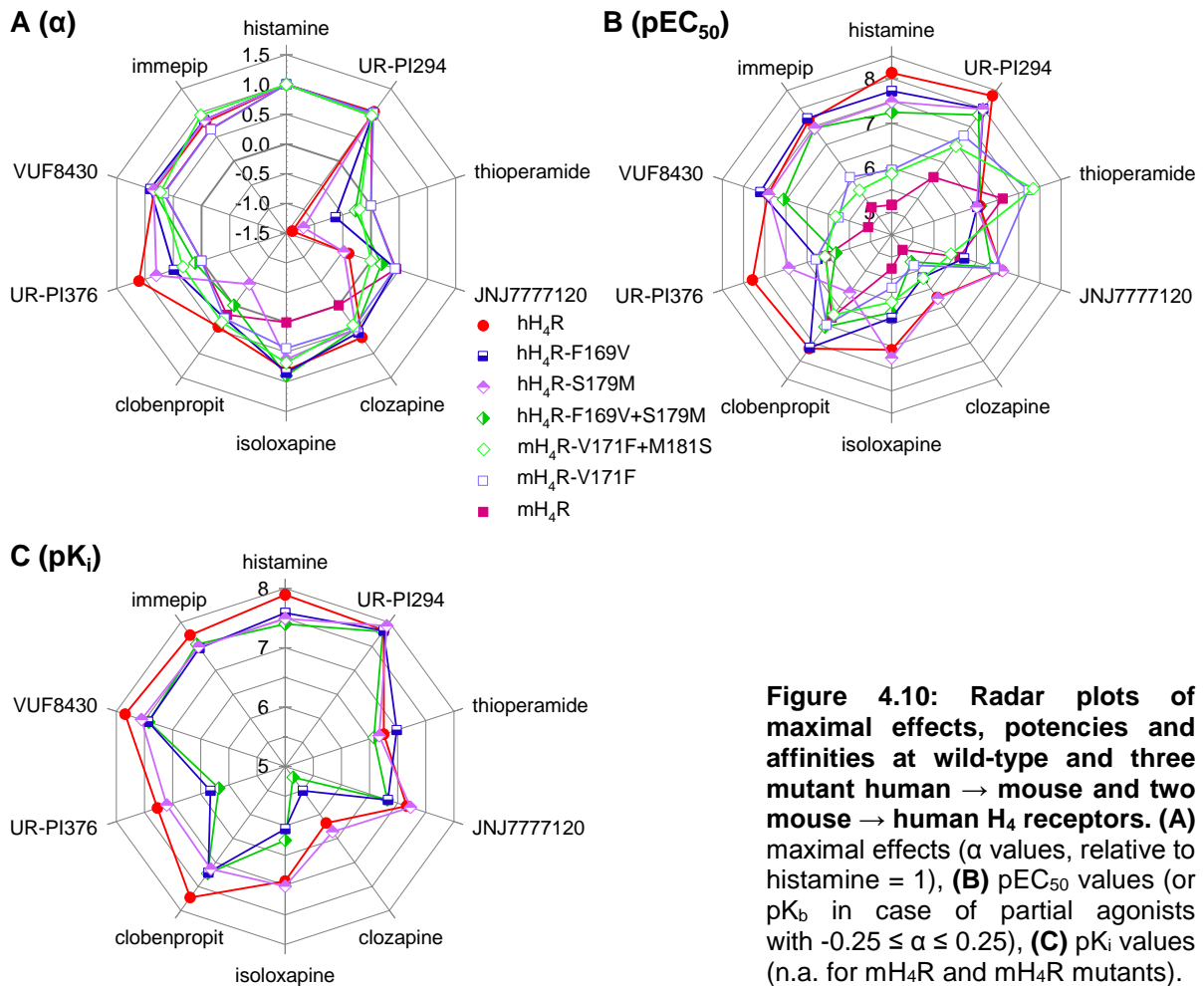
Figure 4.10: Radar plots of maximal effects, potencies and affinities at wild-type and three mutant human → mouse and two mouse → human H_4 receptors. (A) maximal effects (α values, relative to histamine = 1), **(B)** pEC_{50} values (or pK_b in case of partial agonists with -0.25 ≤ α ≤ 0.25), **(C)** pK_i values (n.a. for mH_4R and mH_4R mutants).

A (α)

B (pEC$_{50}$)

C (pK$_i$)

Legend:
- ● hH$_4$R
- □ hH$_4$R-F169V
- ◇ hH$_4$R-S179A
- ◆ hH$_4$R-F169V+S179A
- ◆ rH$_4$R

Figure 4.11: Radar plots of maximal effects, potencies and affinities at wild-type and three mutant human → rat H$_4$ receptors. (A) maximal effects (α values, relative to histamine = 1), **(B)** pEC$_{50}$ values (or pK$_b$ in case of partial agonists with -0.25 ≤ α ≤ 0.25), **(C)** pK$_i$ values.
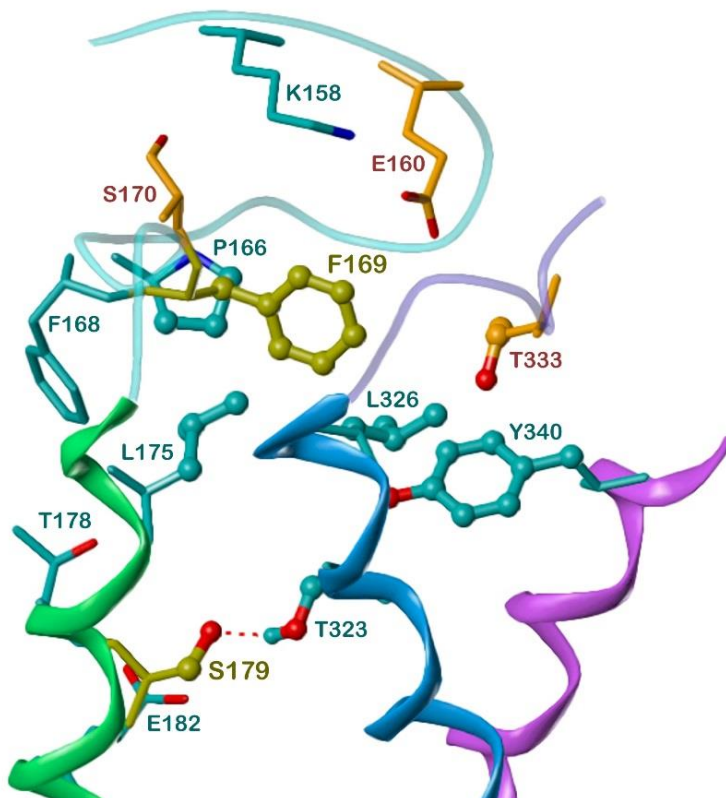
Figure 4.12: Intramolecular interactions specific for the hH$_4$R suggested from site-directed mutagenesis – F169V (mH$_4$R, rH$_4$R), S179M (mH$_4$R) and S179A (rH$_4$R) – and from an hH$_4$R model based on the crystal structure of the hH$_1$R. Colours of side chain atoms: N – blue, O – red. Interacting amino acids are represented as ball and stick model. Colours of carbons and backbone nitrogens: F169 and S179 – ochery, other amino acids different in the rH$_4$R and mH$_4$R – orange, further residues essential for interactions – cyan. A red dashed line indicates a hydrogen bond between S179[5.43] and T323[6.55]. TMs are drawn as ribbons: TM5 – green, TM6 – light blue, TM7 – magenta. The C-terminal part of ECL2 and the N-terminal part of ECL3 are shown by tubes (cyan- and violet-coloured, respectively).

4.5.2 Different quality of action of JNJ7777120

The different degrees of constitutive activity of H_4R species orthologs become obvious from different qualities of action, inverse agonism, neutral antagonism or agonism, of one and the same ligand. JNJ7777120 is a partial inverse agonist at the wild-type hH_4R, the hH_4R-S179M and hH_4R-S179A single mutants, becomes a neutral antagonist at the double mutants hH_4R-F169V+S179M and hH_4R-F169V+S179A as well as at the mH_4R-V171F+M181S mutant and a partial agonist at the mH_4R, the rH_4R and the mH_4R-V171F mutant. Thus, JNJ7777120 fulfils the criteria of a protean agonist: inverse agonism at highly constitutively active receptors and partial agonism at lower or not constitutively active receptors (Kenakin, 2001). A striking exception is the hH_4R-F169V mutant at which JNJ7777120 actually had to be expected to act as a weak partial inverse agonist, but showed partial agonism with similar potency as at the mH_4R and the rH_4R. Possibly, a ligand-specific stabilization of an active state due to the F169V exchange accounts for this apparent discrepancy. The chloro substituent in JNJ7777120 is suggested to interact with the side chain of hH_4R-L175[5.39] (Kooistra et al., 2013; Lim et al., 2010), which is close to F/V169 (Figure 4.12). These interactions within the JNJ7777120-occupied binding pocket may result in different qualities of action by stabilizing distinct conformations in wild-type and mutant receptors.

4.5.3 Maximal effects of agonists at H_4R orthologs and mutants

Among the investigated hH_4R agonists, histamine, UR-PI294, isoloxapine, VUF8430 and immepip do not show significantly reduced maximal effects at the hH_4R mutants compared to the wild-type receptor (Figure 4.10A and Figure 4.11A). By contrast, in case of clozapine, clobenpropit and especially UR-PI376, decreasing maximal responses became obvious from the hH_4R over the F169V mutant to the double mutants. Except for UR-PI294 and immepip, which produced responses comparable to that of histamine at all tested H_4R species variants, the maximal agonistic effects (α values) were lowest at the mH_4R and the rH_4R (Figure 4.10A and Figure 4.11A). A significant influence of the mH_4R-V171F mutation was only observed with clozapine and isoloxapine. UR-PI376 was a partial agonist only at the mH_4R-V171F+M181S mutant. Taking the different constitutive activities of the H_4R species variants into consideration, the situation becomes more complex in case of the agonists, too. Equal maximal effects at H_4R orthologs and mutants with high and low constitutive activity, respectively, result from different contributions to the stabilization of the active receptor state by one and the same agonist. Therefore, comparing maximal effects does not allow for drawing conclusions on selective impacts of F169 and/or S179 on receptor activation by different ligands. Furthermore, stabilization of an active state by agonists may be based on interactions different from those in the ligand-free, constitutively active receptor, i. e., multiple active states must be taken into consideration. Therefore, beyond the G-protein activation used as readout in the present study,

ligand-specific receptor conformations may trigger different signalling pathways according to the concept of functional selectivity (biased signalling; cf. conventional G-protein activation versus β-arrestin recruitment (Nijmeijer et al., 2012; Rosethorne and Charlton, 2011)).

4.5.4 Constitutive activity

More than 40 % of the GPCRs studied in vitro have been found to exhibit constitutive activity (Seifert and Wenzel-Seifert, 2002). Active GPCR states may be stabilized by intramolecular interactions in the ligand binding region, also in the absence of agonists. The key result of this study is the fact that the exceptionally high constitutive activity of the hH₄R is significantly reduced by the single F169V and the double F169V+S179M and F169V+S179A mutations, whereas the single S179M and S179A mutations do not significantly reduce constitutive activity. The effect of both amino acids, F169 (ECL2) and S179$^{5.43}$, on the constitutive activity is cumulative. The mH₄R, the rH₄R and the mH₄R-V171F mutant are not constitutively active. The constitutive activity is slightly increasing at the mH₄R-V171F+M181S mutant. By contrast, high constitutive activity of the hH₄R is reflected by maximal inverse agonism of thioperamide, described as a full (Lim et al., 2005) or partial (Schneider et al., 2009) inverse agonist. In this context, the question arises whether thioperamide is a weaker partial inverse agonist at the hH₄R mutants than at the wild-type or whether the maximal inverse agonistic effects only depend on different levels of constitutive activity. The assumption of comparable inverse agonism is supported by the fact that, at the hH₄R-F169V and at the double mutants, but not at the hH₄R-S179A and hH₄R-S179M mutants, the minimum of [^{35}S]GTPγS binding in the presence of thioperamide approximately corresponds to that at the mH₄R and the rH₄R (Figure 4.7A). Moreover, in the case of the hH₄R and the double mutants, the pEC$_{50}$, pK$_b$ and pK$_i$ values are similar (Table 4.2 and Table 4.3, Figure 4.8 and Figure 4.9). All criteria of constitutive activity (Seifert et al., 1998), high basal activity, high intrinsic activity and potency of partial agonists and a high inverse agonistic effect of inverse agonists, are fulfilled.

A possible explanation for the dependence of the high constitutive activity on the presence of F169 and S179 can be derived from a homology model of the hH₄R based on the crystal structure of the hH₁R (Shimamura et al., 2011). Our model indicates that F169 may adopt different conformations. Its phenyl ring may be directed towards the upper part of ECL2 like the corresponding tyrosine in the hH₁R or point to the ligand binding pocket. The first variant is rather unlikely due to an unfavourable polar environment and putative clashes with P166 (ECL2). In the second case shown in Figure 4.12, F169 is part of a hydrophobic cluster consisting of P166 (ECL2), L175$^{5.39}$, L326$^{6.58}$ and Y340$^{7.35}$. Additionally, F169 contacts T333 (ECL3). A valine side chain as in the mH₄R, rH₄R and the hH₄R-F169V mutants may interact only with P166 and/or L175. Furthermore, S179$^{5.43}$ forms a hydrogen bond with T323$^{6.55}$, which is impossible when S179 is exchanged by alanine or methionine as in the rH₄R and the mH₄R,

respectively. The cumulative effect on constitutive activity by mutation of both, F169 and S179, indicates that the agonist-free active state of the hH_4R is stabilized by hydrophobic interactions between ECL2 and the extracellular parts of TMs 5, 6 and 7 as well as the hydrogen bond between $S179^{5.43}$ and $T323^{6.55}$. In concert, these contacts favour a specific arrangement in particular of TMs 5 and 6, comparable to the stabilization of an active conformation by an agonist. An inward bulge of TM5 around position 5.46 and smaller inward movements of TMs 6 and 7 are characteristic of the activated β_2-adrenoceptor (β_2AR) compared to the inactive state (Rasmussen et al., 2011a; Rosenbaum et al., 2011). At the cytoplasmic face of the receptor, an outward move of TM6 and rearrangements of TMs 5 and 7 are necessary for G-protein binding and contribute to the stabilization of active GPCR states. The TMs are suggested to behave as "oscillating arms". When they move inwards at the extracellular side, they move outwards at the intracellular side and vice versa. Thus, the inward movement of TM5 and TM6 close to the agonist binding pocket results in an outward movement of these TMs at the "bottom" of the receptor. In case of the hH_4R, a proximal arrangement of TMs 5 and 6 at the extracellular side becomes possible in the absence of bound agonist due to a network of interactions involving F169 and S179. However, also other amino acids contribute to the agonist-free stabilization of the active state of the hH_4R, since the double mutants still show a moderate degree of constitutive activity.

In case of the β_2AR, an S204A+S207A double mutant showed about 50 to 60 % lower constitutive activity than the β_2AR wild-type (Ambrosio et al., 2000). $S204^{5.43}$ forms a hydrogen bond with $N293^{6.55}$ (Rasmussen et al., 2011a), corresponding to the suggested interaction of $S179^{5.43}$ with $T323^{6.55}$ in the hH_4R. A contribution of phenylalanine in ECL2 to constitutive activity by a network of hydrophobic interactions with amino acids in TMs 5, 6 and 7 has not been shown for other GPCRs, but may also play a role in other constitutively active receptors such as the hH_3R and the β_2AR, which both contain the same FF motif as the hH_4R.

4.6 Conclusions

Up to now, most studies on the constitutive activity of GPCRs have focused on the intracellular face, the DRY motif and the N-terminal part of TM6. The present study provides further evidence that intramolecular interactions in the agonist binding region contribute to the stabilization of ligand-free active GPCR states. Key result is the decrease in constitutive activity from the hH_4R over the hH_4R-F169V mutant to the hH_4R-F169V+S179A and hH_4R-F169V+S179M double mutants. Thus, F169 in ECL2 and S179 in TM5 play a major role in stabilizing a ligand-free active state of the hH_4R. Similar results on the β_2AR suggest a common principle that may be of relevance for other GPCRs as well.

4.7 References

Alexander, S. P.; Mathie, A.; Peters, J. A. (2011). Guide to Receptors and Channels (GRAC), 5th edition. *Br. J. Pharmacol.* 164 Suppl 1: S1-324.

Ambrosio, C.; Molinari, P.; Cotecchia, S.; Costa, T. (2000). Catechol-binding serines of beta(2)-adrenergic receptors control the equilibrium between active and inactive receptor states. *Mol. Pharmacol.* 57(1): 198-210.

Ballesteros, J. A.; Weinstein, H. (1995). Integrated methods for the construction of three dimensional models and computational probing of structure function relations in G protein-coupled receptors. *Methods Neurosci.* 25: 366-428.

Brunskole, I.; Strasser, A.; Seifert, R.; Buschauer, A. (2011). Role of the second and third extracellular loops of the histamine H(4) receptor in receptor activation. *Naunyn Schmiedebergs Arch. Pharmacol.* 384(3): 301-317.

Buckland, K. F.; Williams, T. J.; Conroy, D. M. (2003). Histamine induces cytoskeletal changes in human eosinophils via the H(4) receptor. *Br. J. Pharmacol.* 140(6): 1117-1127.

Cheng, Y.; Prusoff, W. H. (1973). Relationship between the inhibition constant (K1) and the concentration of inhibitor which causes 50 per cent inhibition (I50) of an enzymatic reaction. *Biochem. Pharmacol.* 22(23): 3099-3108.

Cherezov, V.; Rosenbaum, D. M.; Hanson, M. A.; Rasmussen, S. G.; Thian, F. S.; Kobilka, T. S.; Choi, H. J.; Kuhn, P.; Weis, W. I.; Kobilka, B. K.; Stevens, R. C. (2007). High-resolution crystal structure of an engineered human beta2-adrenergic G protein-coupled receptor. *Science* 318(5854): 1258-1265.

de Esch, I. J.; Thurmond, R. L.; Jongejan, A.; Leurs, R. (2005). The histamine H4 receptor as a new therapeutic target for inflammation. *Trends Pharmacol. Sci.* 26(9): 462-469.

Dunford, P. J.; Holgate, S. T. (2011). The role of histamine in asthma. *Adv. Exp. Med. Biol.* 709: 53-66.

Dunford, P. J.; O'Donnell, N.; Riley, J. P.; Williams, K. N.; Karlsson, L.; Thurmond, R. L. (2006). The histamine H4 receptor mediates allergic airway inflammation by regulating the activation of CD4+ T cells. *J. Immunol.* 176(11): 7062-7070.

Gether, U.; Lin, S.; Kobilka, B. K. (1995). Fluorescent labeling of purified beta 2 adrenergic receptor. Evidence for ligand-specific conformational changes. *J. Biol. Chem.* 270(47): 28268-28275.

Igel, P.; Dove, S.; Buschauer, A. (2010). Histamine H4 receptor agonists. *Bioorg. Med. Chem. Lett.* 20(24): 7191-7199.

Igel, P.; Geyer, R.; Strasser, A.; Dove, S.; Seifert, R.; Buschauer, A. (2009a). Synthesis and structure-activity relationships of cyanoguanidine-type and structurally related histamine H4 receptor agonists. *J. Med. Chem.* 52(20): 6297-6313.

Igel, P.; Schneider, E.; Schnell, D.; Elz, S.; Seifert, R.; Buschauer, A. (2009b). N(G)-acylated imidazolylpropylguanidines as potent histamine H4 receptor agonists: selectivity by variation of the N(G)-substituent. *J. Med. Chem.* 52(8): 2623-2627.

Jablonowski, J. A.; Grice, C. A.; Chai, W.; Dvorak, C. A.; Venable, J. D.; Kwok, A. K.; Ly, K. S.; Wei, J.; Baker, S. M.; Desai, P. J.; Jiang, W.; Wilson, S. J.; Thurmond, R. L.; Karlsson,

L.; Edwards, J. P.; Lovenberg, T. W.; Carruthers, N. I. (2003). The first potent and selective non-imidazole human histamine H4 receptor antagonists. *J. Med. Chem.* 46(19): 3957-3960.

Kenakin, T. (2001). Inverse, protean, and ligand-selective agonism: matters of receptor conformation. *FASEB J.* 15(3): 598-611.

Kooistra, A. J.; Kuhne, S.; de Esch, I. J.; Leurs, R.; de Graaf, C. (2013). A structural chemogenomics analysis of aminergic GPCRs: lessons for histamine receptor ligand design. *Br. J. Pharmacol.* 170(1): 101-126.

Lange, J. H. M.; Wals, H. C.; Vandenhoogenband, A.; Vandekuilen, A.; Denhartog, J. A. J. (1995). 2 Novel Syntheses of the Histamine H-3 Antagonist Thioperamide. *Tetrahedron* 51(48): 13447-13454.

Leurs, R.; Chazot, P. L.; Shenton, F. C.; Lim, H. D.; de Esch, I. J. (2009). Molecular and biochemical pharmacology of the histamine H4 receptor. *Br. J. Pharmacol.* 157(1): 14-23.

Lim, H. D.; de Graaf, C.; Jiang, W.; Sadek, P.; McGovern, P. M.; Istyastono, E. P.; Bakker, R. A.; de Esch, I. J.; Thurmond, R. L.; Leurs, R. (2010). Molecular determinants of ligand binding to H4R species variants. *Mol. Pharmacol.* 77(5): 734-743.

Lim, H. D.; Jongejan, A.; Bakker, R. A.; Haaksma, E.; de Esch, I. J.; Leurs, R. (2008). Phenylalanine 169 in the second extracellular loop of the human histamine H4 receptor is responsible for the difference in agonist binding between human and mouse H4 receptors. *J. Pharmacol. Exp. Ther.* 327(1): 88-96.

Lim, H. D.; Smits, R. A.; Bakker, R. A.; van Dam, C. M.; de Esch, I. J.; Leurs, R. (2006). Discovery of S-(2-guanidylethyl)-isothiourea (VUF 8430) as a potent nonimidazole histamine H4 receptor agonist. *J. Med. Chem.* 49(23): 6650-6651.

Lim, H. D.; van Rijn, R. M.; Ling, P.; Bakker, R. A.; Thurmond, R. L.; Leurs, R. (2005). Evaluation of histamine H1-, H2-, and H3-receptor ligands at the human histamine H4 receptor: identification of 4-methylhistamine as the first potent and selective H4 receptor agonist. *J. Pharmacol. Exp. Ther.* 314(3): 1310-1321.

Ling, P.; Ngo, K.; Nguyen, S.; Thurmond, R. L.; Edwards, J. P.; Karlsson, L.; Fung-Leung, W. P. (2004). Histamine H4 receptor mediates eosinophil chemotaxis with cell shape change and adhesion molecule upregulation. *Br. J. Pharmacol.* 142(1): 161-171.

Liu, C.; Ma, X.; Jiang, X.; Wilson, S. J.; Hofstra, C. L.; Blevitt, J.; Pyati, J.; Li, X.; Chai, W.; Carruthers, N.; Lovenberg, T. W. (2001a). Cloning and pharmacological characterization of a fourth histamine receptor (H(4)) expressed in bone marrow. *Mol. Pharmacol.* 59(3): 420-426.

Liu, C.; Wilson, S. J.; Kuei, C.; Lovenberg, T. W. (2001b). Comparison of human, mouse, rat, and guinea pig histamine H4 receptors reveals substantial pharmacological species variation. *J. Pharmacol. Exp. Ther.* 299(1): 121-130.

Marson, C. M. (2011). Targeting the histamine H4 receptor. *Chem. Rev.* 111(11): 7121-7156.

Morse, K. L.; Behan, J.; Laz, T. M.; West, R. E., Jr.; Greenfeder, S. A.; Anthes, J. C.; Umland, S.; Wan, Y.; Hipkin, R. W.; Gonsiorek, W.; Shin, N.; Gustafson, E. L.; Qiao, X.; Wang, S.; Hedrick, J. A.; Greene, J.; Bayne, M.; Monsma, F. J., Jr. (2001). Cloning and Characterization of a Novel Human Histamine Receptor. *J. Pharmacol. Exp. Ther.* 296(3): 1058-1066.

Nakamura, T.; Itadani, H.; Hidaka, Y.; Ohta, M.; Tanaka, K. (2000). Molecular cloning and characterization of a new human histamine receptor, HH4R. *Biochem. Biophys. Res. Commun.* 279(2): 615-620.

Nguyen, T.; Shapiro, D. A.; George, S. R.; Setola, V.; Lee, D. K.; Cheng, R.; Rauser, L.; Lee, S. P.; Lynch, K. R.; Roth, B. L.; O'Dowd, B. F. (2001). Discovery of a novel member of the histamine receptor family. *Mol. Pharmacol.* 59(3): 427-433.

Nijmeijer, S.; Vischer, H. F.; Rosethorne, E. M.; Charlton, S. J.; Leurs, R. (2012). Analysis of multiple histamine H(4) receptor compound classes uncovers Galphai protein- and beta-arrestin2-biased ligands. *Mol. Pharmacol.* 82(6): 1174-1182.

Nordemann, U.; Wifling, D.; Schnell, D.; Bernhardt, G.; Stark, H.; Seifert, R.; Buschauer, A. (2013). Luciferase reporter gene assay on human, murine and rat histamine H4 receptor orthologs: correlations and discrepancies between distal and proximal readouts. *PLoS One* 8(9): e73961.

O'Reilly, M.; Alpert, R.; Jenkinson, S.; Gladue, R. P.; Foo, S.; Trim, S.; Peter, B.; Trevethick, M.; Fidock, M. (2002). Identification of a histamine H4 receptor on human eosinophils--role in eosinophil chemotaxis. *J. Recept. Signal Transduct. Res.* 22(1-4): 431-448.

Oda, T.; Matsumoto, S. (2001). [Identification and characterization of histamine H4 receptor]. *Nippon Yakurigaku Zasshi* 118(1): 36-42.

Rasmussen, S. G.; Choi, H. J.; Fung, J. J.; Pardon, E.; Casarosa, P.; Chae, P. S.; Devree, B. T.; Rosenbaum, D. M.; Thian, F. S.; Kobilka, T. S.; Schnapp, A.; Konetzki, I.; Sunahara, R. K.; Gellman, S. H.; Pautsch, A.; Steyaert, J.; Weis, W. I.; Kobilka, B. K. (2011a). Structure of a nanobody-stabilized active state of the beta(2) adrenoceptor. *Nature* 469(7329): 175-180.

Reher, T. M.; Neumann, D.; Buschauer, A.; Seifert, R. (2012). Incomplete activation of human eosinophils via the histamine H4-receptor: evidence for ligand-specific receptor conformations. *Biochem. Pharmacol.* 84(2): 192-203.

Ren, H.; Yu, D.; Ge, B.; Cook, B.; Xu, Z.; Zhang, S. (2009). High-level production, solubilization and purification of synthetic human GPCR chemokine receptors CCR5, CCR3, CXCR4 and CX3CR1. *PLoS One* 4(2): e4509.

Rosenbaum, D. M.; Zhang, C.; Lyons, J. A.; Holl, R.; Aragao, D.; Arlow, D. H.; Rasmussen, S. G.; Choi, H. J.; Devree, B. T.; Sunahara, R. K.; Chae, P. S.; Gellman, S. H.; Dror, R. O.; Shaw, D. E.; Weis, W. I.; Caffrey, M.; Gmeiner, P.; Kobilka, B. K. (2011). Structure and function of an irreversible agonist-beta(2) adrenoceptor complex. *Nature* 469(7329): 236-240.

Rosethorne, E. M.; Charlton, S. J. (2011). Agonist-biased signaling at the histamine H4 receptor: JNJ7777120 recruits beta-arrestin without activating G proteins. *Mol. Pharmacol.* 79(4): 749-757.

Rossbach, K.; Wendorff, S.; Sander, K.; Stark, H.; Gutzmer, R.; Werfel, T.; Kietzmann, M.; Baumer, W. (2009b). Histamine H4 receptor antagonism reduces hapten-induced scratching behaviour but not inflammation. *Exp. Dermatol.* 18(1): 57-63.

Schmutz, J.; Kuenzle, G.; Hunziker, F.; Gauch, R. (1967). Heterocycles with 7-membered rings. IX. 11- Amino substituted dibenzo[b,f]-1,4-thiazepines and -oxazepines. *Helv. Chim. Acta* 50(1): 245-254.

Schneider, E. H.; Schnell, D.; Papa, D.; Seifert, R. (2009). High constitutive activity and a G-protein-independent high-affinity state of the human histamine H(4)-receptor. *Biochemistry* 48(6): 1424-1438.

Schneider, E. H.; Schnell, D.; Strasser, A.; Dove, S.; Seifert, R. (2010). Impact of the DRY motif and the missing "ionic lock" on constitutive activity and G-protein coupling of the human histamine H4 receptor. *J. Pharmacol. Exp. Ther.* 333(2): 382-392.

Schnell, D.; Brunskole, I.; Ladova, K.; Schneider, E. H.; Igel, P.; Dove, S.; Buschauer, A.; Seifert, R. (2011). Expression and functional properties of canine, rat, and murine histamine H(4) receptors in Sf9 insect cells. *Naunyn Schmiedebergs Arch. Pharmacol.* 383(5): 457-470.

Seifert, R.; Strasser, A.; Schneider, E. H.; Neumann, D.; Dove, S.; Buschauer, A. (2013). Molecular and cellular analysis of human histamine receptor subtypes. *Trends Pharmacol. Sci.* 34(1): 33-58.

Seifert, R.; Wenzel-Seifert, K. (2002). Constitutive activity of G-protein-coupled receptors: cause of disease and common property of wild-type receptors. *Naunyn Schmiedebergs Arch. Pharmacol.* 366(5): 381-416.

Seifert, R.; Wenzel-Seifert, K.; Lee, T. W.; Gether, U.; Sanders-Bush, E.; Kobilka, B. K. (1998). Different effects of Gsalpha splice variants on beta2-adrenoreceptor-mediated signaling. The Beta2-adrenoreceptor coupled to the long splice variant of Gsalpha has properties of a constitutively active receptor. *J. Biol. Chem.* 273(18): 5109-5116.

Shimamura, T.; Shiroishi, M.; Weyand, S.; Tsujimoto, H.; Winter, G.; Katritch, V.; Abagyan, R.; Cherezov, V.; Liu, W.; Han, G. W.; Kobayashi, T.; Stevens, R. C.; Iwata, S. (2011). Structure of the human histamine H1 receptor complex with doxepin. *Nature* 475(7354): 65-70.

Shin, N.; Coates, E.; Murgolo, N. J.; Morse, K. L.; Bayne, M.; Strader, C. D.; Monsma, F. J., Jr. (2002). Molecular modeling and site-specific mutagenesis of the histamine-binding site of the histamine H4 receptor. *Mol. Pharmacol.* 62(1): 38-47.

Smits, R. A.; Lim, H. D.; Stegink, B.; Bakker, R. A.; de Esch, I. J.; Leurs, R. (2006). Characterization of the histamine H4 receptor binding site. Part 1. Synthesis and pharmacological evaluation of dibenzodiazepine derivatives. *J. Med. Chem.* 49(15): 4512-4516.

Strasser, A.; Wittmann, H. J.; Buschauer, A.; Schneider, E. H.; Seifert, R. (2013). Species-dependent activities of G-protein-coupled receptor ligands: lessons from histamine receptor orthologs. *Trends Pharmacol. Sci.* 34(1): 13-32.

Thurmond, R. L.; Gelfand, E. W.; Dunford, P. J. (2008). The role of histamine H1 and H4 receptors in allergic inflammation: the search for new antihistamines. *Nat. Rev. Drug Discov.* 7(1): 41-53.

Wifling, D.; Löffel, K.; Nordemann, U.; Strasser, A.; Bernhardt, G.; Dove, S.; Seifert, R.; Buschauer, A. (2015b). Molecular determinants for the high constitutive activity of the human histamine H4 receptor: functional studies on orthologues and mutants. *Br. J. Pharmacol.* 172(3): 785-798.

Zampeli, E.; Tiligada, E. (2009). The role of histamine H4 receptor in immune and inflammatory disorders. *Br. J. Pharmacol.* 157(1): 24-33.

Zhu, Y.; Michalovich, D.; Wu, H.; Tan, K. B.; Dytko, G. M.; Mannan, I. J.; Boyce, R.; Alston, J.; Tierney, L. A.; Li, X.; Herrity, N. C.; Vawter, L.; Sarau, H. M.; Ames, R. S.; Davenport, C. M.; Hieble, J. P.; Wilson, S.; Bergsma, D. J.; Fitzgerald, L. R. (2001). Cloning, expression, and pharmacological characterization of a novel human histamine receptor. *Mol. Pharmacol.* 59(3): 434-441.

Chapter 5

The extracellular loop 2 (ECL2) of the human histamine H_4 receptor substantially contributes to ligand binding and constitutive activity

Note: Major parts of this chapter were already published prior to submission of this thesis in *PLoS One* (Wifling et al., 2015a). For detailed information on the contributions by co-authors, cf. "Danksagungen".

5.1 Summary

In contrast to the corresponding mouse and rat orthologs, the human histamine H_4 receptor (hH_4R) shows extraordinarily high constitutive activity. In the extracellular loop (ECL), replacement of F169 by V as in the mouse H_4R significantly reduced constitutive activity. Stabilization of the inactive state was even more pronounced for a double mutant, in which, in addition to F169V, S179 in the ligand binding site was replaced by M. To study the role of the FF motif in ECL2, we generated the hH_4R-F168A mutant. The receptor was co-expressed in Sf9 insect cells with the G-protein subunits $G\alpha_{i2}$ and $G\beta_1\gamma_2$, and the membranes were studied in [^{3}H]histamine binding and functional [^{35}S]GTPγS assays. The potency of various ligands at the hH_4R-F168A mutant decreased compared to the wild-type hH_4R, for example by 30- and more than 100-fold in case of the H_4R agonist UR-PI376 and histamine, respectively. The high constitutive activity of the hH_4R was completely lost in the hH_4R-F168A mutant, as reflected by neutral antagonism of thioperamide, a full inverse agonist at the wild-type hH_4R. By analogy, JNJ7777120 was a partial inverse agonist at the hH_4R, but a partial agonist at the hH_4R-F168A mutant, again demonstrating the decrease in constitutive activity due to F168A mutation. Thus, F168 was proven to play a key role not only in ligand binding and potency, but also in the high constitutive activity of the hH_4R.

5.2 Introduction

Among the extracellular loops (ECLs) of class A GPCRs, the ECL2 is the largest and the most diverse one (Peeters et al., 2011). ECL2 contributes to ligand recognition, binding, selectivity, allosteric modulation and activation of GPCRs (Peeters et al., 2011; Wheatley et al., 2012). In the absence of ligand, ECL2 is a putative "gatekeeper" (Peeters et al., 2011), assumed to adopt an open conformation giving access to the binding pocket. Ligand binding can induce a partially closed conformation. Massotte and Kieffer (2005) and Klco et al. (2005) suggested that ECL2 is involved in interactions stabilizing the inactive state of the receptor. However, specific amino acid sequences in the ECL2 of some GPCRs may stabilize active receptor states and play a role in constitutive activity (Nanevicz et al., 1996; Sum et al., 2009). For instance, ECL2 was reported to be involved in the activation of the human muscarinic M_3 (hM_3R; Scarselli et al., 2007) and the human histamine H_4 receptor (hH_4R; Brunskole et al., 2011; Wifling et al., 2015b). Additionally, the disulphide bond between cysteines in both ECL2 and transmembrane domain 3 (TM3) (Figure 5.1) is of relevance for GPCR function, as shown, for example, for rhodopsin (Davidson et al., 1994), the M_1R (Shi and Javitch, 2002), the β_2-adrenergic (β_2AR; Noda et al., 1994) and the gonadotropin releasing hormone receptor (GnRH-R; Cook and Eidne, 1997). Furthermore, ECL2 contributes to the high affinity state of the β_2AR (Noda et al., 1994). Apart from modifying ligand-free states, ECL2 was shown to have an impact on ligand binding and selectivity (Avlani et al., 2007; Shi and Javitch, 2002; 2004).

Constitutive activity describes the ability of a GPCR to produce a biological response in the absence of a bound ligand (Lefkowitz et al., 1993; Milligan, 2003). The degree of constitutive activity reflects the shift of the basal equilibrium from the inactive to the active state of a GPCR. Inverse agonists stabilize the inactive receptor conformation and are therefore capable of reducing or blocking constitutive activity. Consequently, constitutive activity of a GPCR is a prerequisite to determine inverse agonism and vice versa (Seifert et al., 1998).

In contrast to the rodent orthologs mH_4R and rH_4R, high constitutive activity is characteristic of the hH_4R (Brunskole et al., 2011; Schnell et al., 2011; Seifert et al., 2013; Wifling et al., 2015b). H_4R species orthologs are well suited for exploring the molecular basis of this phenomenon, because there are not too many differences between the sequences in ECL2. Site-directed mutagenesis within the ECL2 of the hH_4R compared to the mH_4R revealed that the hH_4R-F169V mutant is similar to the mH_4R in terms of ligand affinities and potencies, suggesting that F169 is a key amino acid for differential interactions of certain agonists with the human and mouse H_4R orthologs (Lim et al., 2008). The assumption that F169 also contributes to constitutive activity was confirmed by investigations on the mutants hH_4R-F169V and F169V+S179M (Wifling et al., 2015b). F169 alone or in concert with S179 (TM5, ligand

binding site) plays a major role in stabilizing a ligand-free active state of the hH$_4$R. The constitutive activity of the hH$_4$R-F169V mutant was significantly reduced compared to the wild-type hH$_4$R. In particular, the inverse agonistic effect of thioperamide decreased.

F169 is part of the FF motif, which is located on top of the ligand binding pocket (Figure 5.1) and conserved in a number of class A GPCRs, e. g., the hβ$_2$AR, hH$_3$R, monkey H$_4$R, canine H$_4$R and the hM$_2$R. Instead of the FF motif, other GPCRs, such as the hβ$_1$AR, hM$_1$R, hM$_3$R, hM$_4$R, and the hM$_5$R, as well as several H$_4$R species orthologs, e. g., pig H$_4$R, guinea pig H$_4$R, mouse H$_4$R and rat H$_4$R, contain only one phenylalanine, which is located in a position corresponding to that of F168 in the hH$_4$R. In these cases, in the adjacent position a non-aromatic hydrophobic amino acid such as valine or leucine is present instead of phenylalanine.
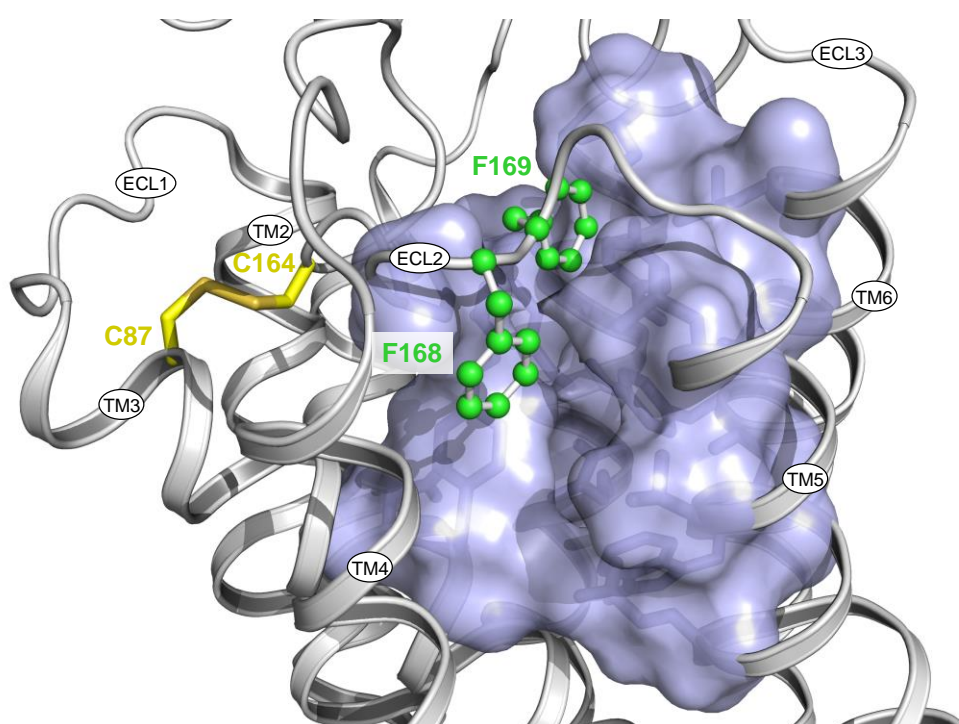
Figure 5.1: View from the extracellular side into the binding pocket of the human H$_4$R. Homology model (Wifling et al., 2015b) based on the crystal structure of the hH$_1$R inactive state (Shimamura et al., 2011). The FF motif (F168 and F169), pointing to the ligand binding pocket, is illustrated as green balls and sticks, the disulphide bond connecting TM3 with ECL2 as yellow sticks and the binding pocket as a semitransparent surface coloured in magenta. Generated with PyMOL Molecular Graphics System, Version 1.6 (Schrödinger LLC, Portland, OR USA).

Crystal structures provide information on the position and the conformation of the FF motif. The side chain of the first phenylalanine (in case of the hM$_2$R also of the second one (Haga et al., 2012)) points into the ligand binding pocket. In the hβ$_2$AR and in the hH$_1$R, the second phenylalanine (and a tyrosine in case of hH$_1$R) is oriented in the opposite direction (Rasmussen et al., 2011a; Shimamura et al., 2011). Our recent results on the contribution of F169 to the constitutive activity of the hH$_4$R suggested that F168 plays a significant role as well. In order to investigate the influence of F168 on both receptor activation and ligand binding (Wifling et al., 2015b), we generated and characterized the hH$_4$R-F168A mutant in comparison

to the wild-type and the recently described hH_4R-F169V mutant. The mutant receptors were expressed in Sf9 insect cells, and membrane preparations were used for saturation binding with [^{3}H]histamine and functional studies were performed with inverse agonists, neutral antagonists and agonists in the [^{35}S]GTPγS assay (Figure 5.2).
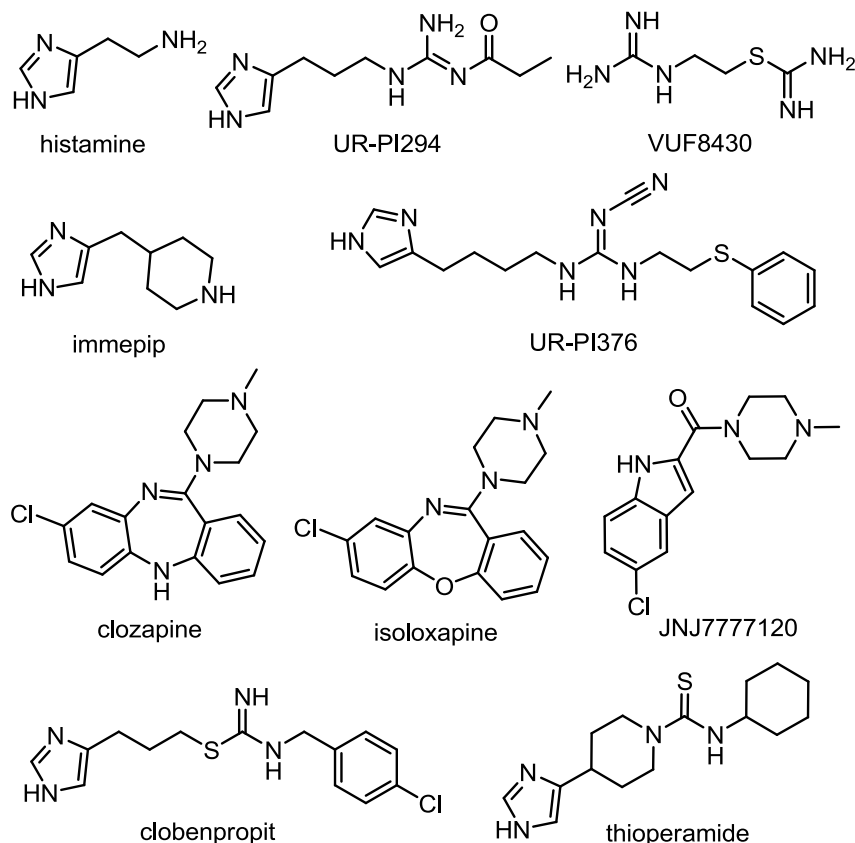
Figure 5.2: Structures of the investigated H_4R ligands.

5.3 Materials and Methods

5.3.1 Materials

The pcDNA3.1 vector containing the hH_4R sequence was from the cDNA Resource Centre at the University of Missouri-Rolla (Rolla, MO USA). The pVL1392-SF-H_4R-His$_6$ plasmid was constructed as described previously (Schneider et al., 2009; Schnell et al., 2011). Baculovirus encoding $Gα_{i2}$ was kindly provided by Dr. A. G. Gilman (Department of Pharmacology, University of Southwestern Medical Centre, Dallas, TX USA). Recombinant baculovirus encoding the $Gβ_1γ_2$ subunits was a kind gift of Dr. P. Gierschik (Department of Pharmacology and Toxicology, University of Ulm, Ulm, Germany). *Pfu* Ultra II DNA polymerase was from Agilent (Böblingen, Germany). The DNA primers for polymerase chain reaction (PCR) were from MWG-Biotech (Ebersberg, Germany). Restriction enzymes were from New England Biolabs (Ipswich, MA USA). Gradient gels (8-16 %, 12 well nUView gels) as well as the peqGOLD protein marker I, used for Coomassie brilliant blue R staining, were from Peqlab

(Erlangen, Germany). UR-PI294 and UR-PI376 were synthesized as described (Igel et al., 2009a; Igel et al., 2009b). Thioperamide, JNJ7777120 and VUF8430 were synthesized according to Lange et al. (1995), Jablonowski et al. (2003), and Lim et al. (2006). Isoloxapine (Schmutz et al., 1967; Smits et al., 2006) was synthesized and provided by Dr. S. Gobleder (Institute of Pharmacy, University of Regensburg, Regensburg, Germany). All other H_4R ligands were from Tocris (Avonmouth, Bristol, UK). For chemical structures of the investigated compounds cf. Figure 5.2. UR-PI376 (10 mM) was dissolved in 50 % (*v/v*) dimethyl sulfoxide (DMSO) and dilutions were prepared in 20 % (*v/v*) DMSO in order to attain a final DMSO concentration of 2 % (*v/v*) in each well. Stock solutions (10 mM) of clozapine or isoloxapine were prepared in Millipore water containing 3 and 2 mol equivalents of HCl, respectively. All other stock solutions were prepared with Millipore water. [^{35}S]GTPγS (1000 Ci/mmol) and [^{3}H]histamine (25 Ci/mmol) were from Hartmann Analytic (Braunschweig, Germany). All other reagents were from standard suppliers and of the highest purity available.

5.3.2 Methods

5.3.2.1 Site-directed mutagenesis of the hH_4R

The preparation of the hH_4R-F168A cDNA was essentially performed as described for the hH_4R-F169V mutant (Wifling et al., 2015b). To introduce the F168A mutation into the pVL1392-SF-hH_4R-His$_6$ expression vector a site-directed mutagenesis PCR was performed using the following primers 5'-GGT AGT GAA TGT GAA CCT GGA **GCC** TTT TCG AAT GGG TAC ATC C-3' and 5'-G GAT GTA CCA TTC GGA AAA **GGC** TCC AGG TTC ACA TTC ACT ACC-3'.

5.3.2.2 Cell culture, generation of recombinant baculoviruses and membrane preparation

Cell culture and generation of high-titre recombinant baculovirus stocks (Schneider et al., 2009) as well as the co-infection of Sf9 cells with high-titre baculovirus stocks encoding $Gα_{i2}$, $Gβ_1γ_2$ and the respective H_4R (Brunskole et al., 2011) were performed as described recently (Wifling et al., 2015b). Membrane preparations were performed according to Gether et al. (1995) in the presence of 0.2 mM phenylmethylsulfonyl fluoride, 1 mM ethylenediaminetetraacetic acid (EDTA), 10 µg/mL leupeptin and 10 µg/mL benzamidine as protease inhibitors. Prepared membranes were resuspended in binding buffer (75 mM Tris/HCl, 12.5 mM $MgCl_2$, 1 mM EDTA, pH 7.4) and stored at -80 °C in 0.5 or 1.0 mL aliquots.

5.3.2.3 SDS-PAGE and Coomassie staining

Prior to incubation at 30 °C for 15 min, the respective membrane preparation (15 µg protein) as well as a negative control (Sf9 cells transfected with pVL1392 devoid of an insert) were loaded onto the gel as well as 5 µL of the protein marker I (Wifling et al., 2015b). A 2x sample

buffer without urea was used for sample preparation. The gels were stained in a solution of 0.1 % Coomassie brilliant blue G250 in 50 % methanol and 10 % acetic acid and subsequently destained with a solution containing 13 % methanol and 7 % acetic acid.

5.3.2.4 [³H]histamine saturation binding experiments

The experiments were performed in 96-well plates (Wifling et al., 2015b). Each well contained 43-133 µg of protein in a total volume of 100 µL. For saturation binding, membranes were incubated in binding buffer containing [³H]histamine (1-200 nM) and 0.2 % (*w/v*) BSA at room temperature under shaking at 200 rpm for 60 min. Non-specific binding was determined in the presence of 10 µM unlabelled histamine. Filtration through glass microfibre filters (Whatman GF/C), pretreated with polyethylenimine 0.3 % (*w/v*), using a Brandel 96 sample harvester (Brandel, Unterföhring, Germany), was performed to separate unbound from membrane-associated [³H]histamine. After three washing steps with binding buffer, filter pieces were punched out, transferred into 96-well sample plates 1450-401 (Perkin Elmer, Rodgau, Germany), and 200 µL of scintillation cocktail (Rotiscint Eco plus, Roth, Karlsruhe, Germany) per well were added before incubation in the dark under shaking at 200 rpm. Radioactivity was measured with a Micro Beta2 1450 scintillation counter (Perkin Elmer, Rodgau, Germany).

5.3.2.5 [³⁵S]GTPγS binding assay

Membranes were thawed, centrifuged for 10 min at 4 °C and 13,000 g and carefully resuspended in binding buffer (Wifling et al., 2015b). Experiments were performed in 96-well plates in a total volume of 100 µL per well. Each well contained 7-19 µg of protein (7-10 µg for hH$_4$R, 10-14 µg for hH$_4$R-F169V and 10-19 µg for hH$_4$R-F168A), 1 µM GDP, 100 mM NaCl, 0.05 % (*w/v*) bovine serum albumin (BSA), 20 nCi of [³⁵S]GTPγS (0.2 nM) and ligand at concentrations as indicated in the results section. Antagonism was determined in the presence of histamine (10-fold EC$_{50}$ at the respective receptor). Nonspecific binding was determined in the presence of 10 µM unlabelled GTPγS. After incubation under shaking at 200 rpm at room temperature for 2 h, bound [³⁵S]GTPγS was separated from free [³⁵S]GTPγS by filtration through glass microfibre filters using a 96-well Brandel harvester. The filters were washed three to four times with binding buffer (4 °C), dried over night and impregnated with meltable scintillation wax prior to counting with a Micro Beta2 1450 scintillation counter.

5.3.2.6 Miscellaneous

Protein concentrations of all membrane preparations were determined with the Bio-Rad DC protein assay kit (München, Germany) in one experiment. Because UR-PI376 had to be dissolved in 20 % DMSO, the water control as well as the full agonist histamine (α = 1.0), to which all other ligands were referenced, were also dissolved in 20 % DMSO in case of this ligand. Concentration-response curves were constructed by fitting the data according to the

four parameter logistic fit (variable slope), and analysed with the Prism 5.01 software (GraphPad, San Diego, CA USA). K_b values were calculated according to the Cheng-Prusoff equation (Cheng and Prusoff, 1973). All values are given as mean ± SEM of at least three independent experiments performed in triplicate. Significances were calculated using one-way analysis of variance (ANOVA), followed by Bonferroni's multiple comparison test.

5.4 Results

5.4.1 Receptor expression

Human histamine H_4 receptor wild-type as well as mutants (hH$_4$R-F169V and hH$_4$R-F168A) were expressed in Sf9 insect cells together with G-protein subunits $G\alpha_{i2}$ and $G\beta_1\gamma_2$ (Schneider et al., 2010; Wifling et al., 2015b). As previously shown by SDS PAGE and western blots (Wifling et al., 2015b), the wild-type or mutated H_4 receptors migrated with an apparent molecular weight of 39 kDa and the $G\alpha_{i2}$ protein with an apparent molecular weight of 41 kDa. The hH$_4$R wild-type and both mutant receptors, hH$_4$R-F169V and hH$_4$R-F168A, respectively as well as the $G\alpha_{i2}$ protein were expressed at comparably high levels as becomes obvious from Coomassie stained SDS gels (Figure 5.3). However, specific binding of [^{3}H]histamine to the hH$_4$R-F168A mutant was too low to determine the K_d value (highest concentration of radioligand used: 200 nM). By contrast, the wild-type hH$_4$R as well as the hH$_4$R-F169V mutant revealed high specific binding as described previously (cf. Wifling et al. (2015b), saturation binding curves are depicted in Figure 4.6A and B).
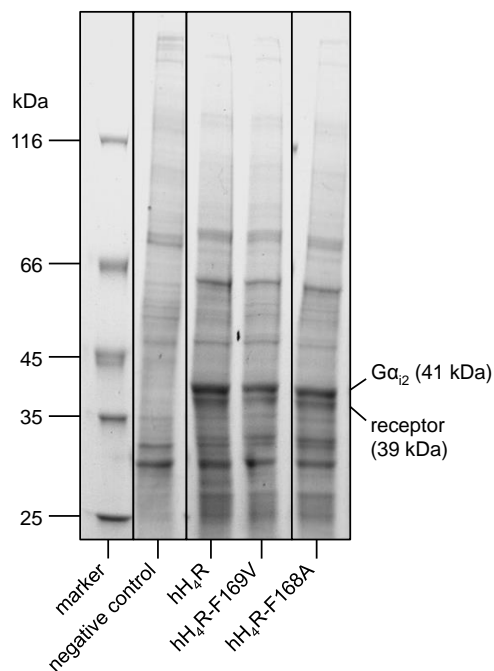
Figure 5.3: Coomassie stained SDS gels. Membrane proteins of Sf9 insect cells, co-expressing the respective receptor as indicated and $G\alpha_{i2}$ as well as $G\beta_1\gamma_2$ were separated on 8-16 % polyacrylamide gradient gels. All samples were analysed on the same gel. In the interest of clarity, the membranes prepared from Sf9 cells transfected with pVL1392 devoid of an insert (negative control) were placed next to the molecular weight standard.

5.4.2 Functional analysis of wild-type and mutant H₄ receptors

Functional data – intrinsic activities (α), potencies (pEC_{50}) and antagonist activities (pK_b) – were determined in the [^{35}S]GTPγS assay using standard agonists as well as inverse agonists and neutral antagonists (Figure 5.2 and Table 5.1). For comparison, data from the hH₄R-F169V mutant (Wifling et al., 2015b) are included in Table 5.1. Upon maximal stimulation with histamine, the amounts of bound [^{35}S]GTPγS were significantly different, decreasing in the order hH₄R wild-type > hH₄R-F169V > hH₄R-F168A (Figure 5.4). The effect of the inverse agonist thioperamide reflects constitutive activity of wild-type and mutant receptors. The response to thioperamide decreased in the order hH₄R > hH₄R-F169V > hH₄R-F168A (Figure 5.4), i. e., constitutive activity was highest at the hH₄R wild-type, significantly smaller at the hH₄R-F169V mutant (Wifling et al., 2015b) and absent at the hH₄R-F168A mutant, where thioperamide acted as a neutral antagonist.
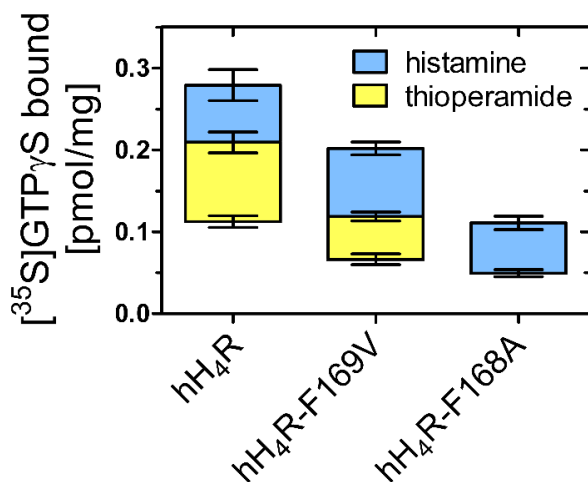
Figure 5.4: Maximal agonistic effects of histamine (light blue) and maximal inverse agonistic effects of thioperamide (yellow) in the [^{35}S]GTPγS-assay. Data represent [^{35}S]GTPγS [pmol/mg protein] specifically bound to wild-type and mutated H₄Rs. The line separating light blue and yellow bar represents [^{35}S]GTPγS binding in the absence of ligand.

The normalized concentration-response curves of histamine (maximal effect of histamine at the respective receptors, set to 100 %) are depicted in Figure 5.5A. The potency of histamine decreased from the hH₄R via the hH₄R-F169V to the hH₄R-F168A mutant by more than two orders of magnitude (Figure 5.5A and Table 5.1). The same holds for the full agonist UR-PI294 (Igel et al., 2009b) with a decrease in potency by about 1.5 orders of magnitude from the hH₄R to the hH₄R-F168A mutant without significant changes of intrinsic activity (Figure 5.5B).

The potency of clozapine and the structurally related isoloxapine decreased from the hH₄R via the hH₄R-F169V to the hH₄R-F168A mutant with maximal shift of the curve by one order of magnitude (Figure 5.5C, D). The intrinsic activity of clobenpropit, a partial agonist, and UR-PI376 (Igel et al., 2009a), a full agonist at the hH₄R significantly decreased at the two mutants (Figure 5.5E, F). For clobenpropit, despite reduced maximal responses, no significant changes of the potency were observed. By contrast, the potency of UR-PI376 was by more than one order of magnitude lower at the mutants than at the wild-type.

Compared to the wild-type hH_4R, the potencies and intrinsic activities of the partial agonists immepip and VUF8430 were not significantly affected by the hH_4R-F169V mutation (Wifling et al., 2015b). By contrast, at the hH_4R-F168A mutant, the potencies decreased by about two orders of magnitude (Figure 5.5G, H).

Inverse agonism of thioperamide was highest at the hH_4R, significantly lower at the hH_4R-F169V (Wifling et al., 2015b) and not detectable at the hH_4R-F168A mutant (Figure 5.5I). Instead, thioperamide behaved as a neutral antagonist with a pK_b value of 7.97. JNJ7777120 was a partial inverse agonist at the hH_4R but, surprisingly, acted as a partial agonist at the hH_4R-F169V and hH_4R-F168A mutants (Figure 5.5J).

Table 5.1: [^{35}S]GTPγS binding on hH_4R wild-type, hH_4R-F169V and hH_4R-F168A mutant.

Ligand	Parameter	hH_4R	hH_4R-F169V	hH_4R-F168A
histamine	α	1	1	1
	pEC_{50}	8.13 ± 0.06	7.72 ± 0.07 ••	5.98 ± 0.06 •••
UR-PI294	α	1.02 ± 0.03	1.00 ± 0.07	0.91 ± 0.06
	pEC_{50}	8.35 ± 0.04	8.00 ± 0.11	6.78 ± 0.11 •••
thioperamide	α	-1.39 ± 0.08	-0.63 ± 0.06 •••	0 •••
	pEC_{50}	6.58 ± 0.06	6.52 ± 0.05	n.a.
	pK_b	6.83 ± 0.05		7.97 ± 0.07 •••
JNJ7777120	α	-0.39 ± 0.03	0.43 ± 0.03 •••	0.20 ± 0.01 •••
	pEC_{50}	7.10 ± 0.08	6.21 ± 0.12 ••	6.40 ± 0.17
	pK_b	7.60 ± 0.05		6.17 ± 0.19 ••
VUF8430	α	0.84 ± 0.06	0.91 ± 0.06	0.69 ± 0.06
	pEC_{50}	7.42 ± 0.12	7.61 ± 0.07	5.74 ± 0.03 •••
immepip	α	0.81 ± 0.03	0.85 ± 0.05	0.81 ± 0.02
	pEC_{50}	7.67 ± 0.05	7.73 ± 0.19	5.82 ± 0.11 •••
clozapine	α	0.67 ± 0.04	0.56 ± 0.03	0.40 ± 0.01 ••
	pEC_{50}	6.24 ± 0.10	5.68 ± 0.12 •	5.38 ± 0.10 ••
isoloxapine	α	0.81 ± 0.03	0.85 ± 0.09	0.83 ± 0.07
	pEC_{50}	7.08 ± 0.13	6.36 ± 0.10 ••	6.10 ± 0.05 •••
UR-PI376	α	1.11 ± 0.08	0.49 ± 0.02 •••	0.39 ± 0.05 •••
	pEC_{50}	7.79 ± 0.08	6.25 ± 0.11 •••	6.30 ± 0.15 •••
clobenpropit	α	0.45 ± 0.04	0.27 ± 0.05 •	0.14 ± 0.02 ••
	pEC_{50}	7.65 ± 0.11	7.63 ± 0.15	7.40 ± 0.13
	pK_b			7.24 ± 0.06

pEC_{50}-values ([^{35}S]GTPγS agonist mode), pK_b-values ([^{35}S]GTPγS antagonist mode) and α (intrinsic activity, maximal effect relative to histamine = 1.0) are given as mean ± SEM of at least three independent experiments, performed in triplicate. Results of statistical tests (one-way ANOVA and Bonferroni post hoc tests): significant differences with respect to hH_4R - • $p < 0.05$, •• $p < 0.01$, ••• $p < 0.001$. In case of neutral antagonism ($-0.25 ≤ α ≤ 0.25$), pK_b-values were considered for statistical analysis instead of pEC_{50}-values. Maximal effect α = 0: neutral antagonism. Data for hH_4R and hH_4R-F169V cf. Wifling et al. (2015b).
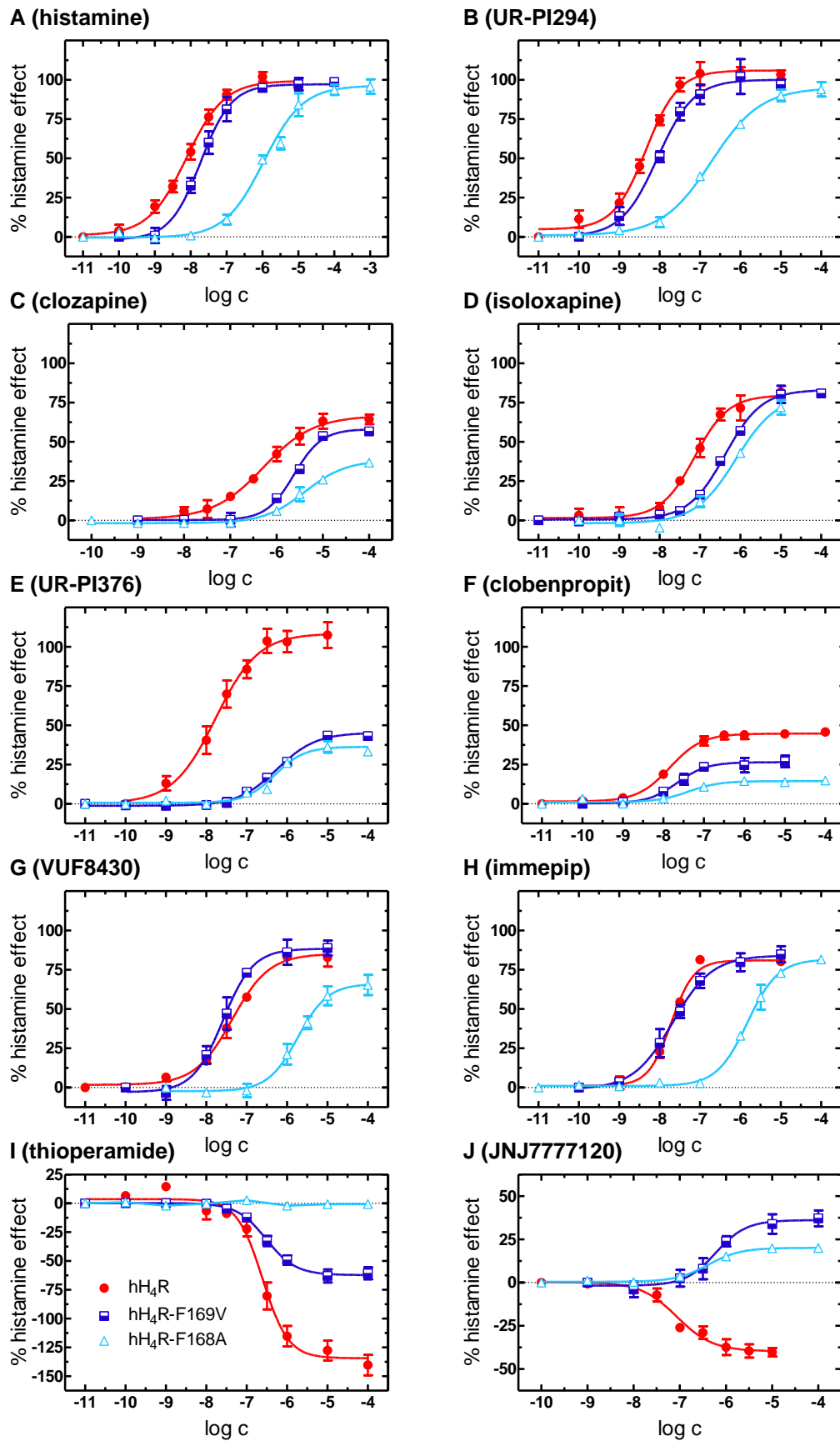
Figure 5.5: Concentration-response curves of ligands investigated in the [^{35}S]GTPγS assay. All curves are normalized with respect to the maximal effect of histamine (100 %) at the respective receptor.

5.5 Discussion

5.5.1 Potencies of ligands at mutated H$_4$ receptors

With respect to potency at mutant H$_4$ receptors, except thioperamide, the investigated ligands are divided in two groups. The first group, comprising JNJ7777120, clozapine, isoloxapine, UR-PI376 and clobenpropit, has similar potency at both the hH$_4$R-F169V and the hH$_4$R-F168A mutant. These ligands contain bulky aromatic groups. The phenyl and chlorophenyl moieties of clozapine and JNJ7777120, respectively, were suggested to occupy a hydrophobic pocket between TMs 3, 5, 6 and ECL2 (Kooistra et al., 2013; Lim et al., 2010). Most notably, MD simulations with JNJ7777120 indicated that the chloro substituent is surrounded by a relatively tight pocket formed by E163[ECL2], F168[ECL2], F169[ECL2], L175[5.39] and T323[6.55] (Schultes et al., 2013). Mutations of these amino acids, especially, affect binding modes directed towards ECL2. Affinity of ligands may be reduced due to loss of direct contacts and/or by distortion of the pocket. The binding mode of clobenpropit is probably different, because of similar potency at the wild-type and both mutants.

The second group, histamine, UR-PI294, VUF8430 and immepip, comprises rather small ligands devoid of hydrophobic substituents. Characteristic of this group is a significant decrease in potency by about two orders of magnitude at the hH$_4$R-F168A mutant compared to the wild-type hH$_4$R (Figure 5.6A). By contrast, there were only minor effects on potency at the hH$_4$R-F169V mutant. Thus, F168 is probably involved in direct interactions with the ligands of this group.
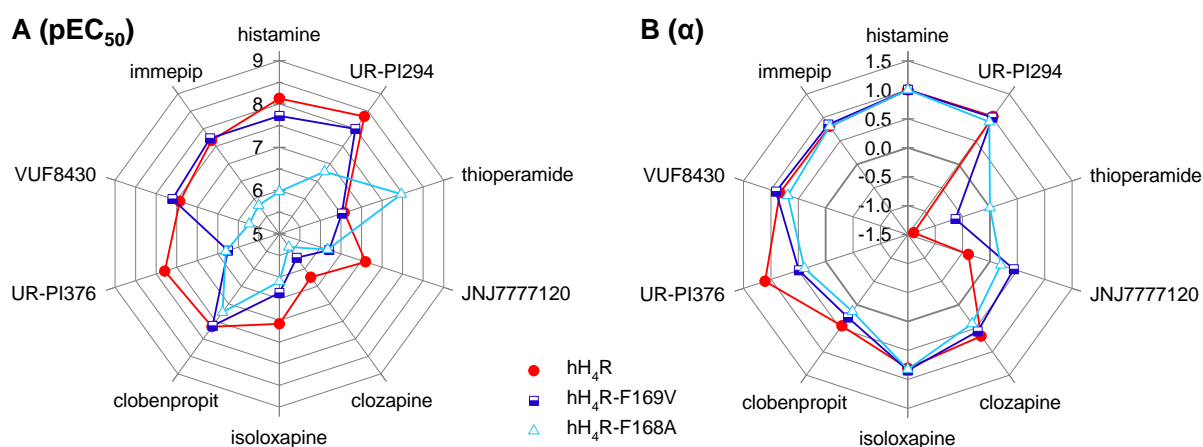
Figure 5.6: Radar plots of potencies and maximal effects at wild-type human H$_4$R, hH$_4$R-F169V and hH$_4$R-F168A mutants. (A) pEC$_{50}$ values (or pK$_b$ in case of partial agonists/inverse agonists with -0.25 ≤ α ≤ 0.25). **(B)** maximal effects (α values, relative to histamine = 1).

The ligands of both groups are full or partial agonists, apart from JNJ7777120 at the wild-type hH$_4$R. According to docking on hH$_4$R homology models, agonists as well as several antagonists and inverse agonists probably bind between TMs 3, 5, 6 and 7 via key interactions with D94[3.32], E182[5.46] and Q347[7.42] (Kooistra et al., 2013; Lim et al., 2010; Schultes et al., 2013).

Thioperamide is an exception as it binds only to inactive hH_4R state(s). By analogy, thioperamide is known to stabilize the inactive conformation of the closely related hH_3R. Molecular dynamics simulations of an hH_3R-thioperamide complex revealed a binding mode characterized by an extended conformation of the ligand, which is oriented parallel to the membrane plane, an interaction of the imidazolyl moiety with tyrosine in position 2.61, and the thiourea group positioned in the vicinity of F193, which corresponds to F169 in the hH_4R (Wittmann et al., 2014). It may be speculated that thioperamide binds to the hH_4R in the same way, selectively contacting $Y72^{2.61}$ and $F344^{7.39}$, whereas interactions with $E182^{5.46}$ and $Q347^{7.42}$, proven essential in case of other H_4R ligands, are precluded or only weak. Such a binding mode would prevent the constriction of the orthosteric binding site (inward movements of TMs 5, 6 and 7), characteristic of the conversion of the receptor to the active state (Rasmussen et al., 2011a). Direct interactions of thioperamide with F168 or F169 cannot be deduced from the data in Table 5.1. The increase in pK_b at the hH_4R-F168A mutant by one order of magnitude compared to the wild-type receptor is compatible with higher affinity of thioperamide to inactive than to active state(s), represented by the mutant devoid of constitutive activity and the highly constitutively active wild-type H_4R.

5.5.2 Intrinsic activities of ligands and constitutive activity of receptors

The hH_4R agonists histamine, UR-PI294, isoloxapine, VUF8430 and immepip did not show significantly reduced intrinsic activities at both hH_4R mutants compared to the wild-type, whereas the maximal effects of clozapine, clobenpropit and UR-PI376 were diminished (Figure 5.6B). In case of inverse agonists, the reduced constitutive activity of the mutants is reflected by lower maximal (inverse) responses. The partial inverse hH_4R agonist JNJ7777120 was a partial agonist at the mutant receptors. Thioperamide was a partial inverse agonist at hH_4R-F169V, the mutant with reduced constitutive activity, and a neutral antagonist at the hH_4R-F168A mutant, which is devoid of constitutive activity. The results support the hypothesis that both F168 and F169 play a role in stabilizing an active state of the wild-type hH_4R.

Constitutive activity (Lefkowitz et al., 1993) reflects a ligand-independent interconversion between inactive and active receptor conformations. Interactions at the intracellular face involving the DRY motif have been proven crucial for basal and agonist-induced receptor activation and signalling (Alewijnse et al., 2000; Schneider et al., 2010). In case of the hH_4R, which is devoid of the ionic lock, we demonstrated that interactions close to the ligand binding pocket and ECL2 account for the high constitutive activity (Wifling et al., 2015b). The mutation of F169 alone and, even more pronounced, the mutation of both F169 (ECL2) and $S179^{5.43}$ (numbering according to the Ballesteros nomenclature (Ballesteros and Weinstein, 1995)) into the corresponding amino acids of the mouse and rat H_4R orthologs (F169V, S179M, S179A) resulted in a highly significant reduction of the constitutive activity (Wifling et al., 2014).

The hH$_4$R model in Figure 5.7 suggests mutual effects of both phenylalanines, F168 and F169 (the FF motif), on the conformation of ECL2 (Lim et al., 2008). Our present results with the hH$_4$R-F168A mutant support this idea. Compared to hH$_4$R-F169V, which has still a low constitutive activity, hH$_4$R-F168A is completely devoid of constitutive activity. Accordingly, the single mutation of either F169 into V and, especially, F168 into A weakens interactions within ECL2 and the surrounding hydrophobic pocket consisting of amino acids as Y95[3.33], P166[ECL2], L175[5.39], T178[5.42], T323[6.55], L326[6.58], T333[ECL3], and Y340[7.35] (Figure 5.7). Therefore, replacement of F168 or F169 probably causes major conformational changes, which destabilize active and stabilize inactive receptor states.
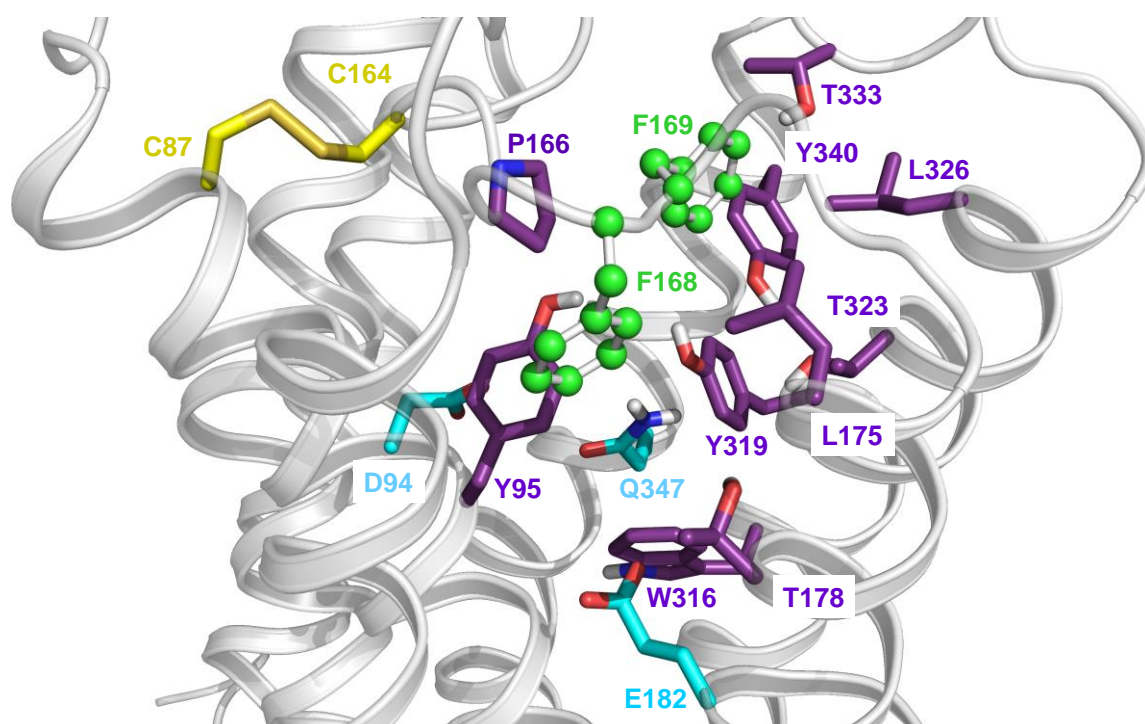
Figure 5.7: Binding pocket of the hH$_4$R, homology model (Wifling et al., 2015b) based on the inactive state crystal structure of the hH$_1$R (Shimamura et al., 2011). Nitrogens are coloured in blue, oxygens in red and sulphurs in yellow. The carbons are differently coloured: the two cysteines forming the disulphide bond in yellow, the amino acids representing the hydrophobic cluster in magenta, important amino acids for ligand binding in cyan and the two adjacent phenylalanines forming the FF motif in green.

5.6 Conclusions

The present study demonstrates a highly significant influence of the hH$_4$R-F168A mutant on ligand binding as well as on constitutive activity, even surpassing the consequences of hH$_4$R-F169V mutation, revealing a key role of the FF motif for both, ligand-receptor interaction and interconversion between inactive and active conformation of the wild-type hH$_4$R. The results may also be of relevance for other class A GPCRs comprising the FF motif, such as the β$_2$AR, the H$_3$R and the M$_2$R.

5.7 References

Alewijnse, A. E.; Timmerman, H.; Jacobs, E. H.; Smit, M. J.; Roovers, E.; Cotecchia, S.; Leurs, R. (2000). The effect of mutations in the DRY motif on the constitutive activity and structural instability of the histamine H(2) receptor. *Mol. Pharmacol.* 57(5): 890-898.

Avlani, V. A.; Gregory, K. J.; Morton, C. J.; Parker, M. W.; Sexton, P. M.; Christopoulos, A. (2007). Critical role for the second extracellular loop in the binding of both orthosteric and allosteric G protein-coupled receptor ligands. *J. Biol. Chem.* 282(35): 25677-25686.

Ballesteros, J. A.; Weinstein, H. (1995). Integrated methods for the construction of three dimensional models and computational probing of structure function relations in G protein-coupled receptors. *Methods Neurosci.* 25: 366-428.

Brunskole, I.; Strasser, A.; Seifert, R.; Buschauer, A. (2011). Role of the second and third extracellular loops of the histamine H(4) receptor in receptor activation. *Naunyn Schmiedebergs Arch. Pharmacol.* 384(3): 301-317.

Cheng, Y.; Prusoff, W. H. (1973). Relationship between the inhibition constant (K1) and the concentration of inhibitor which causes 50 per cent inhibition (I50) of an enzymatic reaction. *Biochem. Pharmacol.* 22(23): 3099-3108.

Cook, J. V.; Eidne, K. A. (1997). An intramolecular disulfide bond between conserved extracellular cysteines in the gonadotropin-releasing hormone receptor is essential for binding and activation. *Endocrinology* 138(7): 2800-2806.

Davidson, F. F.; Loewen, P. C.; Khorana, H. G. (1994). Structure and function in rhodopsin: replacement by alanine of cysteine residues 110 and 187, components of a conserved disulfide bond in rhodopsin, affects the light-activated metarhodopsin II state. *Proc. Natl. Acad. Sci. U. S. A.* 91(9): 4029-4033.

Gether, U.; Lin, S.; Kobilka, B. K. (1995). Fluorescent labeling of purified beta 2 adrenergic receptor. Evidence for ligand-specific conformational changes. *J. Biol. Chem.* 270(47): 28268-28275.

Haga, K.; Kruse, A. C.; Asada, H.; Yurugi-Kobayashi, T.; Shiroishi, M.; Zhang, C.; Weis, W. I.; Okada, T.; Kobilka, B. K.; Haga, T.; Kobayashi, T. (2012). Structure of the human M2 muscarinic acetylcholine receptor bound to an antagonist. *Nature* 482(7386): 547-551.

Igel, P.; Geyer, R.; Strasser, A.; Dove, S.; Seifert, R.; Buschauer, A. (2009a). Synthesis and structure-activity relationships of cyanoguanidine-type and structurally related histamine H4 receptor agonists. *J. Med. Chem.* 52(20): 6297-6313.

Igel, P.; Schneider, E.; Schnell, D.; Elz, S.; Seifert, R.; Buschauer, A. (2009b). N(G)-acylated imidazolylpropylguanidines as potent histamine H4 receptor agonists: selectivity by variation of the N(G)-substituent. *J. Med. Chem.* 52(8): 2623-2627.

Jablonowski, J. A.; Grice, C. A.; Chai, W.; Dvorak, C. A.; Venable, J. D.; Kwok, A. K.; Ly, K. S.; Wei, J.; Baker, S. M.; Desai, P. J.; Jiang, W.; Wilson, S. J.; Thurmond, R. L.; Karlsson, L.; Edwards, J. P.; Lovenberg, T. W.; Carruthers, N. I. (2003). The first potent and selective non-imidazole human histamine H4 receptor antagonists. *J. Med. Chem.* 46(19): 3957-3960.

Klco, J. M.; Wiegand, C. B.; Narzinski, K.; Baranski, T. J. (2005). Essential role for the second extracellular loop in C5a receptor activation. *Nat. Struct. Mol. Biol.* 12(4): 320-326.

Kooistra, A. J.; Kuhne, S.; de Esch, I. J.; Leurs, R.; de Graaf, C. (2013). A structural chemogenomics analysis of aminergic GPCRs: lessons for histamine receptor ligand design. *Br. J. Pharmacol.* 170(1): 101-126.

Lange, J. H. M.; Wals, H. C.; Vandenhoogenband, A.; Vandekuilen, A.; Denhartog, J. A. J. (1995). 2 Novel Syntheses of the Histamine H-3 Antagonist Thioperamide. *Tetrahedron* 51(48): 13447-13454.

Lefkowitz, R. J.; Cotecchia, S.; Samama, P.; Costa, T. (1993). Constitutive activity of receptors coupled to guanine nucleotide regulatory proteins. *Trends Pharmacol. Sci.* 14(8): 303-307.

Lim, H. D.; de Graaf, C.; Jiang, W.; Sadek, P.; McGovern, P. M.; Istyastono, E. P.; Bakker, R. A.; de Esch, I. J.; Thurmond, R. L.; Leurs, R. (2010). Molecular determinants of ligand binding to H4R species variants. *Mol. Pharmacol.* 77(5): 734-743.

Lim, H. D.; Jongejan, A.; Bakker, R. A.; Haaksma, E.; de Esch, I. J.; Leurs, R. (2008). Phenylalanine 169 in the second extracellular loop of the human histamine H4 receptor is responsible for the difference in agonist binding between human and mouse H4 receptors. *J. Pharmacol. Exp. Ther.* 327(1): 88-96.

Lim, H. D.; Smits, R. A.; Bakker, R. A.; van Dam, C. M.; de Esch, I. J.; Leurs, R. (2006). Discovery of S-(2-guanidylethyl)-isothiourea (VUF 8430) as a potent nonimidazole histamine H4 receptor agonist. *J. Med. Chem.* 49(23): 6650-6651.

Massotte, D.; Kieffer, B. L. (2005). The second extracellular loop: a damper for G protein-coupled receptors? *Nat. Struct. Mol. Biol.* 12(4): 287-288.

Milligan, G. (2003). Constitutive activity and inverse agonists of G protein-coupled receptors: a current perspective. *Mol. Pharmacol.* 64(6): 1271-1276.

Nanevicz, T.; Wang, L.; Chen, M.; Ishii, M.; Coughlin, S. R. (1996). Thrombin receptor activating mutations. Alteration of an extracellular agonist recognition domain causes constitutive signaling. *J. Biol. Chem.* 271(2): 702-706.

Noda, K.; Saad, Y.; Graham, R. M.; Karnik, S. S. (1994). The high affinity state of the beta 2-adrenergic receptor requires unique interaction between conserved and non-conserved extracellular loop cysteines. *J. Biol. Chem.* 269(9): 6743-6752.

Peeters, M. C.; van Westen, G. J.; Li, Q.; AP, I. J. (2011). Importance of the extracellular loops in G protein-coupled receptors for ligand recognition and receptor activation. *Trends Pharmacol. Sci.* 32(1): 35-42.

Rasmussen, S. G.; Choi, H. J.; Fung, J. J.; Pardon, E.; Casarosa, P.; Chae, P. S.; Devree, B. T.; Rosenbaum, D. M.; Thian, F. S.; Kobilka, T. S.; Schnapp, A.; Konetzki, I.; Sunahara, R. K.; Gellman, S. H.; Pautsch, A.; Steyaert, J.; Weis, W. I.; Kobilka, B. K. (2011a). Structure of a nanobody-stabilized active state of the beta(2) adrenoceptor. *Nature* 469(7329): 175-180.

Scarselli, M.; Li, B.; Kim, S. K.; Wess, J. (2007). Multiple residues in the second extracellular loop are critical for M3 muscarinic acetylcholine receptor activation. *J. Biol. Chem.* 282(10): 7385-7396.

Schmutz, J.; Kuenzle, G.; Hunziker, F.; Gauch, R. (1967). Heterocycles with 7-membered rings. IX. 11- Amino substituted dibenzo[b,f]-1,4-thiazepines and -oxazepines. *Helv. Chim. Acta* 50(1): 245-254.

Schneider, E. H.; Schnell, D.; Papa, D.; Seifert, R. (2009). High constitutive activity and a G-protein-independent high-affinity state of the human histamine H(4)-receptor. *Biochemistry* 48(6): 1424-1438.

Schneider, E. H.; Schnell, D.; Strasser, A.; Dove, S.; Seifert, R. (2010). Impact of the DRY motif and the missing "ionic lock" on constitutive activity and G-protein coupling of the human histamine H4 receptor. *J. Pharmacol. Exp. Ther.* 333(2): 382-392.

Schnell, D.; Brunskole, I.; Ladova, K.; Schneider, E. H.; Igel, P.; Dove, S.; Buschauer, A.; Seifert, R. (2011). Expression and functional properties of canine, rat, and murine histamine H(4) receptors in Sf9 insect cells. *Naunyn Schmiedebergs Arch. Pharmacol.* 383(5): 457-470.

Schultes, S.; Nijmeijer, S.; Engelhardt, H.; Kooistra, A. J.; Vischer, H. F.; de Esch, I. J. P.; Haaksma, E. E. J.; Leurs, R.; de Graaf, C. (2013). Mapping histamine H4 receptor-ligand binding modes. *MedChemComm* 4(1): 193-204.

Seifert, R.; Strasser, A.; Schneider, E. H.; Neumann, D.; Dove, S.; Buschauer, A. (2013). Molecular and cellular analysis of human histamine receptor subtypes. *Trends Pharmacol. Sci.* 34(1): 33-58.

Seifert, R.; Wenzel-Seifert, K.; Lee, T. W.; Gether, U.; Sanders-Bush, E.; Kobilka, B. K. (1998). Different effects of Gsalpha splice variants on beta2-adrenoreceptor-mediated signaling. The Beta2-adrenoreceptor coupled to the long splice variant of Gsalpha has properties of a constitutively active receptor. *J. Biol. Chem.* 273(18): 5109-5116.

Shi, L.; Javitch, J. A. (2002). The binding site of aminergic G protein-coupled receptors: the transmembrane segments and second extracellular loop. *Annu. Rev. Pharmacol. Toxicol.* 42: 437-467.

Shi, L.; Javitch, J. A. (2004). The second extracellular loop of the dopamine D2 receptor lines the binding-site crevice. *Proc. Natl. Acad. Sci. U. S. A.* 101(2): 440-445.

Shimamura, T.; Shiroishi, M.; Weyand, S.; Tsujimoto, H.; Winter, G.; Katritch, V.; Abagyan, R.; Cherezov, V.; Liu, W.; Han, G. W.; Kobayashi, T.; Stevens, R. C.; Iwata, S. (2011). Structure of the human histamine H1 receptor complex with doxepin. *Nature* 475(7354): 65-70.

Smits, R. A.; Lim, H. D.; Stegink, B.; Bakker, R. A.; de Esch, I. J.; Leurs, R. (2006). Characterization of the histamine H4 receptor binding site. Part 1. Synthesis and pharmacological evaluation of dibenzodiazepine derivatives. *J. Med. Chem.* 49(15): 4512-4516.

Sum, C. S.; Tikhonova, I. G.; Costanzi, S.; Gershengorn, M. C. (2009). Two arginine-glutamate ionic locks near the extracellular surface of FFAR1 gate receptor activation. *J. Biol. Chem.* 284(6): 3529-3536.

Wheatley, M.; Wootten, D.; Conner, M. T.; Simms, J.; Kendrick, R.; Logan, R. T.; Poyner, D. R.; Barwell, J. (2012). Lifting the lid on GPCRs: the role of extracellular loops. *Br. J. Pharmacol.* 165(6): 1688-1703.

Wifling, D.; Bernhardt, G.; Dove, S.; Buschauer, A. (2015a). The Extracellular Loop 2 (ECL2) of the Human Histamine H4 Receptor Substantially Contributes to Ligand Binding and Constitutive Activity. *PLoS One* 10(1): e0117185.

Wifling, D.; Löffel, K.; Nordemann, U.; Strasser, A.; Bernhardt, G.; Dove, S.; Seifert, R.; Buschauer, A. (2015b). Molecular determinants for the high constitutive activity of the

human histamine H4 receptor: functional studies on orthologues and mutants. *Br. J. Pharmacol.* 172(3): 785-798.

Wittmann, H. J.; Seifert, R.; Strasser, A. (2014). Mathematical analysis of the sodium sensitivity of the human histamine H3 receptor. *In Silico Pharmacol.* 2(1): 1-14.

Chapter 6

Effect of S330R mutation in ECL3 on ligand binding and function of the human H$_4$R
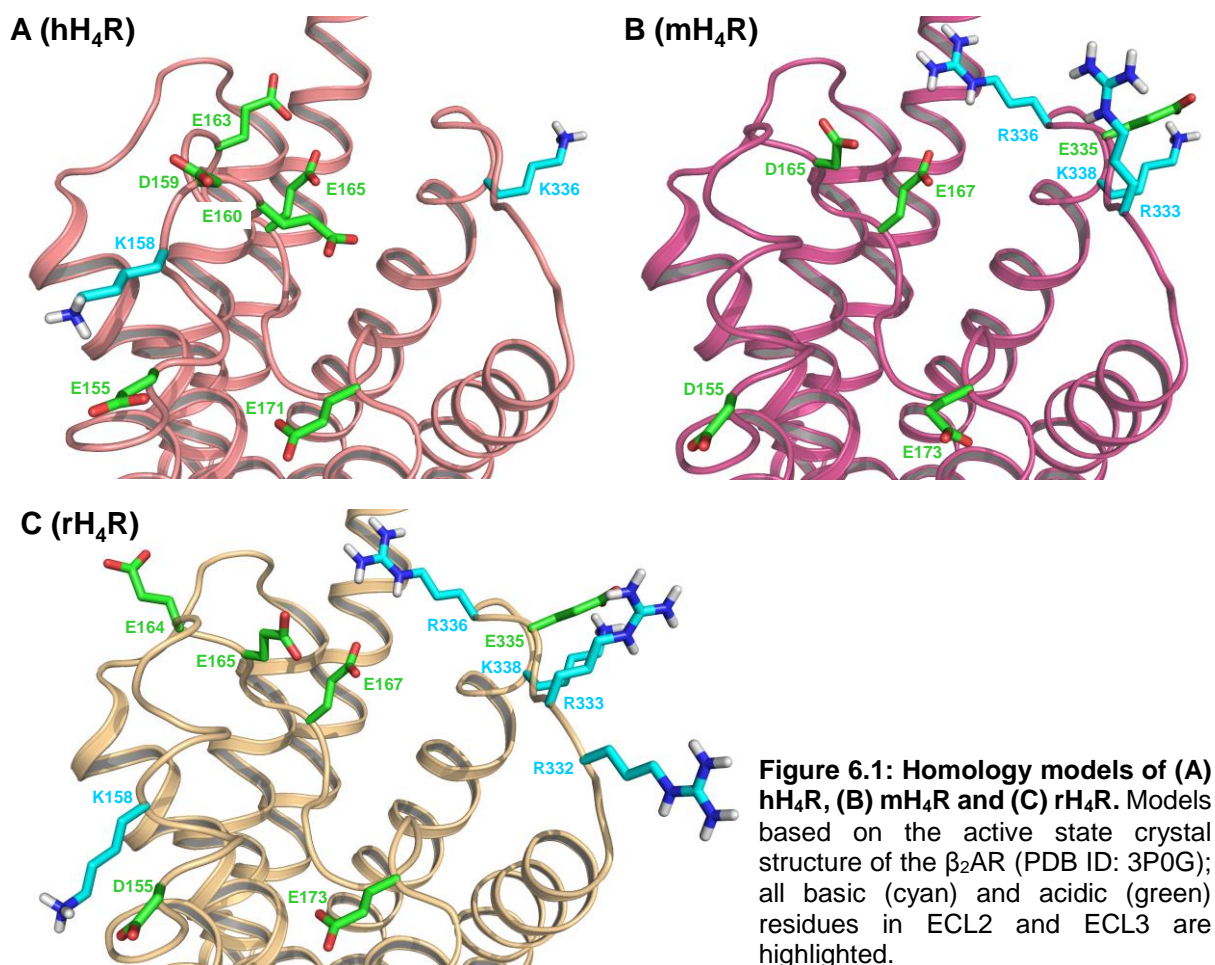
6.1 Summary

Different numbers of basic residues in ECL3 (one in case of the hH$_4$R, three in case of the mH$_4$R and four in case of the rH$_4$R) of H$_4$R species orthologs led to the hypothesis that these residues play a role in ligand binding and constitutive activity. In order to test this hypothesis, the hH$_4$R-S330R mutant was generated to introduce one additional basic residue in the ECL3 of the hH$_4$R. The receptor was co-expressed in Sf9 insect cells with the G-protein subunits Gα$_{i2}$ and Gβ$_1$γ$_2$, and the membranes were studied in [^{3}H]histamine saturation and competition binding as well as in functional [^{35}S]GTPγS assays. The constitutive activity of the hH$_4$R-S330R mutant was clearly reduced compared to the hH$_4$R wild-type, whereas changes in ligand binding affinities were negligible. The results are compatible with the hypothesis that basic amino acids in ECL3 of the H$_4$R contribute to the stabilization of the rodent orthologs in the inactive state. Apart from hH$_4$R-S330R, additional charged amino acids in extracellular loops should be taken into consideration to study this phenomenon in more detail.

6.2 Introduction

Hoffmann et al. (1999) explored the influence of both, ECL2 and ECL3, on ligand binding of the human P2Y$_1$ receptor. The amino acids D204^{ECL2} and E209^{ECL2} as well as R287^{ECL3} of the P2Y$_1$R were identified as key residues in receptor function. Mutations of D204^{ECL2} to A, N or E revealed a decrease in potency of the investigated ligands, whereas mutations of E209^{ECL2} to A or R287^{ECL3} to A or E resulted in a complete loss of receptor function. Thus, changing the charge of the amino acid in the respective positions, i. e., replacing an acidic residue by a non-polar or basic residue and vice versa, can influence the binding of ligands. In search for molecular determinants of the high constitutive activity of the human H$_4$R, the number of acidic

and basic residues in the extracellular loops of the respective H_4R species orthologs, hH_4R, mH_4R and rH_4R, were compared (Figure 6.1). Remarkably, one basic amino acid (K336) is present in ECL3 in case of the hH_4R, three basic residues are present in case of the mH_4R (R333, R336 and K338) and even four in case of the rH_4R (R332, R333, R336 and K338) (Figure 6.1). By contrast, acidic residues are present in a similar number in ECL2 among all three H_4R species orthologs (Figure 6.1). In order to examine, whether an additional basic residue in ECL3 of the hH_4R contributes to ligand binding and influences constitutive activity, hH_4R-S330R was generated and the mutant receptor was co-expressed with $G\alpha_{i2}$ and $G\beta_1\gamma_2$ in Sf9 insect cells. [3H]histamine saturation and competition binding as well as functional [35S]GTPγS assays were performed with ten H_4R agonists and inverse agonists, respectively (for structures of the investigated ligands cf. Figure 4.1 and Figure 5.2). Instead of S330[ECL3] in the hH_4R, P is present in the mH_4R and R in the rH_4R. Therefore, the hH_4R-S330R mutant reflects differences between the hH_4R, mH_4R (no basic residue in equivalent position) and rH_4R (R332[ECL3] in equivalent position) and should be suitable to uncover changes in the pharmacology of the hH_4R caused by one additional basic residue in ECL3.

Figure 6.1: Homology models of (A) hH_4R, (B) mH_4R and (C) rH_4R. Models based on the active state crystal structure of the β_2AR (PDB ID: 3P0G); all basic (cyan) and acidic (green) residues in ECL2 and ECL3 are highlighted.

6.3 Materials and Methods

6.3.1 Materials

Cf. Chapters 4.3.1 and 5.3.1.

6.3.2 Site-directed mutagenesis of the hH$_4$R

The construction of the hH$_4$R-S330R mutant was essentially performed as described (Wifling et al., 2015b). To introduce the S330R mutation into the pVL1392-SF-hH$_4$R-His$_6$ expression vector a site-directed mutagenesis PCR was performed, using the two complementary primers 5'-C CTT TCA TTT TAT **CGC** TCA GCA ACA GGT CCT AAA TCA GTT TGG-3' and 5'-CCA AAC TGA TTT AGG ACC TGT TGC TGA **GCG** ATA AAA TGA AAG G-3'

6.3.3 Cell culture, generation of recombinant baculoviruses and membrane preparation

Cf. Chapters 4.3.3 and 5.3.2.2.

6.3.4 SDS-PAGE and Coomassie staining

Cf. Chapters 4.3.4 and 5.3.2.3.

6.3.5 [^{3}H]histamine saturation binding experiments

Performed according to the procedure described in Chapters 4.3.6 and 5.3.2.4 with the exception that each well contained 35-47 µg protein in case of the hH$_4$R-S330R mutant.

6.3.6 [^{3}H]histamine competition binding assay

Performed according to the procedure described in Chapter 4.3.7 with the exception that each well contained 15-18 µg protein in case of the hH$_4$R-S330R mutant.

6.3.7 [^{35}S]GTPγS binding assay

Performed according to the procedure described in Chapters 4.3.8 and 5.3.2.5 with the exception that each well contained 8-12 µg protein in case of the hH$_4$R-S330R mutant.

6.3.8 Miscellaneous

Cf. Chapters 4.3.10 and 5.3.2.6

6.4 Results

6.4.1 Expression of recombinant proteins

The respective wild-type H$_4$R ortholog (hH$_4$R, mH$_4$R or rH$_4$R) or the hH$_4$R-S330R mutant and the G-protein subunits Gα$_{i2}$ and Gβ$_1$γ$_2$ were co-expressed in Sf9 cells (Wifling et al., 2015a;

Wifling et al., 2015b). As shown for the hH$_4$R-F169V mutant by western blots, the wild-type and mutated receptors migrated with an apparent molecular weight of 39 kDa and the Gα$_{i2}$ protein with an apparent molecular weight of 41 kDa (cf. Chapter 4.4.1; Wifling et al., 2015b). These two bands were absent in the negative control (Sf9 cells transfected with pVL1392 devoid of an insert; Figure 6.2). As becomes obvious from Coomassie stained SDS gels (Figure 6.2), both, wild-type H$_4$Rs (hH$_4$R, mH$_4$R and rH$_4$R) and the hH$_4$R-S330R mutant, were expressed at comparable levels.
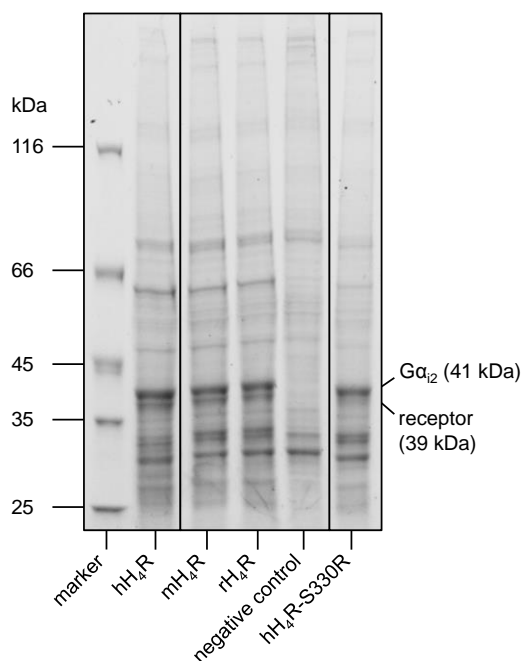
Figure 6.2: Coomassie stained SDS gels. Membrane proteins of Sf9 insect cells, co-expressing the respective receptor as indicated and Gα$_{i2}$ as well as Gβ$_1$γ$_2$, were separated on 8-16 % polyacrylamide gradient gels. All samples were analysed on the same gel.

The K$_d$ value of [^{3}H]histamine at the hH$_4$R-S330R mutant (15.32 nM) was comparable with the K$_d$ value at the hH$_4$R (11.16 nM) (Table 6.1 and Figure 6.3).

Table 6.1: Saturation binding data for [^{3}H]histamine at hH$_4$R and the hH$_4$R-S330R mutant.

Receptor	K$_d$ [nM]	B$_{max}$ [pmol/mg]
hH$_4$R	11.16 ± 1.92	1.93 ± 0.32
hH$_4$R-S330R	15.32 ± 1.82	2.60 ± 0.05

K$_d$ and B$_{max}$ values are given as mean ± SEM for at least two independent experiments, each performed in triplicate. Non-specific binding, amounting to 7.1-16.0 % of total binding at 100 nM of [^{3}H]histamine, was determined in the presence of 10 µM of unlabelled histamine.
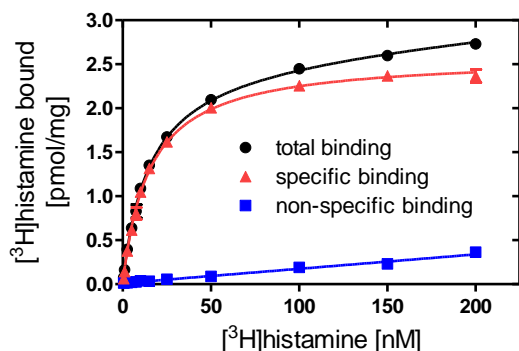
Figure 6.3: Saturation binding curve for [^{3}H]histamine at the hH$_4$R-S330R mutant. Data represent mean values ± SEM from two independent experiments performed in triplicate.

6.4.2 Competition binding data of H$_4$R ligands at the hH$_4$R-S330R mutant

Competition binding studies using [^{3}H]histamine as the radioligand revealed only minor differences between the pK$_i$ values determined at the hH$_4$R wild-type and the hH$_4$R-S330R mutant (Table 6.2).

Table 6.2: [^{3}H]histamine competition binding on hH$_4$R wild-type and hH$_4$R-S330R mutant.

Ligand	hH$_4$R	hH$_4$R-S330R
histamine	7.89 ± 0.04	7.54 ± 0.03 ••
UR-PI294	7.84 ± 0.03	7.81 ± 0.08
thioperamide	6.75 ± 0.07	6.70 ± 0.10
JNJ7777120	7.16 ± 0.05	7.41 ± 0.06
VUF8430	7.84 ± 0.03	7.77 ± 0.05
immepip	7.73 ± 0.16	7.43 ± 0.01
clozapine	6.18 ± 0.03	5.92 ± 0.06 •
isoloxapine	6.93 ± 0.02	6.65 ± 0.07 •
UR-PI376	7.27 ± 0.07	7.03 ± 0.00
clobenpropit	7.73 ± 0.07	7.51 ± 0.06

pK$_i$ values are given as mean ± SEM of at least two independent experiments, performed in triplicate. Results of statistical tests (unpaired t test): significant differences with respect to hH$_4$R - • $p < 0.05$, •• $p < 0.01$, ••• $p < 0.001$.

6.4.3 Functional analysis of the hH$_4$R-S330R mutant compared to wild-type H$_4$Rs in the [^{35}S]GTPγS assay

The amounts of bound [^{35}S]GTPγS [pmol/mg] were lower at the hH$_4$R-S330R mutant than at the hH$_4$R wild-type (Figure 6.4A). Generally, [^{35}S]GTPγS binding at the rodent orthologs was significantly lower than at the human receptor. The signal amplitude was lowest at the mH$_4$R. Transforming the amounts of bound [^{35}S]GTPγS into relative scales, revealed highest constitutive activity (reflected by the maximal inverse agonistic effect of thioperamide) for the hH$_4$R wild-type, followed by the hH$_4$R-S330R mutant at a significantly lower level. By contrast, the rodent orthologs were devoid of constitutive activity (Figure 6.4B).
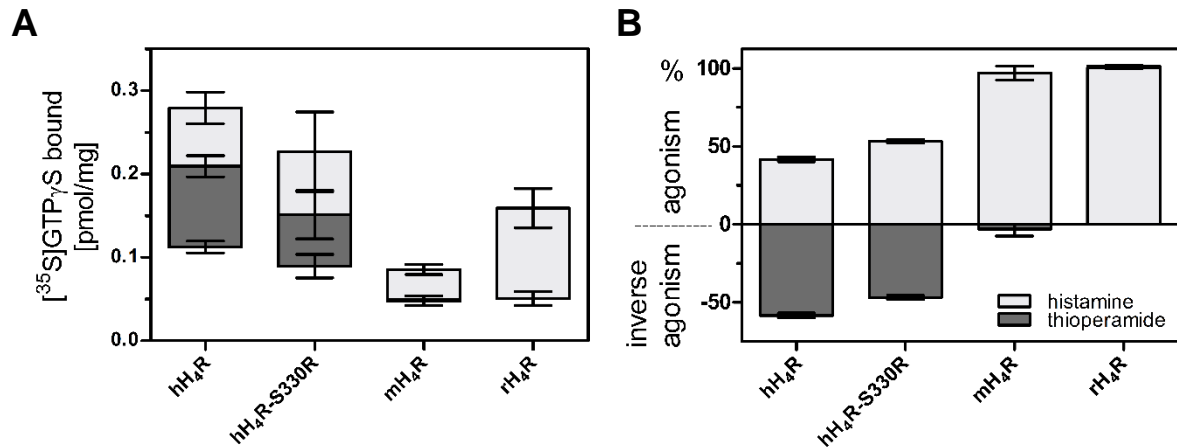
Figure 6.4: Maximal agonistic effects of histamine and maximal inverse agonistic effects of thioperamide in the [^{35}S]GTPγS assay. (A) Data represent [^{35}S]GTPγS [pmol/mg protein] specifically bound to wild-type and mutated H$_4$Rs in the presence of histamine (light grey) and thioperamide (dark grey). Values demarcating light and dark grey bars represent the basal amount (in the absence of ligand) of bound [^{35}S]GTPγS. **(B)** Relative effects of histamine and thioperamide. The sum of histamine and thioperamide of each construct was scaled to 100 %, and the zero line represents the ligand-free control.

Consequently, the intrinsic activity of thioperamide was significantly higher at the hH$_4$R-S330R mutant than at the hH$_4$R wild-type due to the lower constitutive activity of the hH$_4$R-S330R mutant (Table 6.3 and Figure 6.5C).

Regarding pEC$_{50}$ values there was a decrease in potency, comparing the hH$_4$R wild-type with the hH$_4$R-S330R mutant (Table 6.3 and Figure 6.5A, G, H, I), by 0.4, 0.7, 0.6 and 0.5 logarithmic units in case of histamine, clozapine, isoloxapine and UR-PI376.

Table 6.3: [^{35}S]GTPγS binding on hH$_4$R wild-type and hH$_4$R-S330R mutant.

Receptor	hH$_4$R		hH$_4$R-S330R	
Ligand	α	pEC$_{50}$	α	pEC$_{50}$
histamine	1	8.13 ± 0.06 ■■■, ♦♦♦	1	7.69 ± 0.14 •, ■■■, ♦♦♦
UR-PI294	1.02 ± 0.03	8.35 ± 0.04 ■■■, ♦♦♦	0.99 ± 0.06	8.10 ± 0.01 ■■■, ♦♦♦
thioperamide	-1.39 ± 0.08 ■■■, ♦♦♦	6.58 ± 0.06 ■■	-0.88 ± 0.04 •••, ■■■, ♦♦♦	6.47 ± 0.05 ■■■
JNJ7777120	-0.39 ± 0.03 ■■■, ♦♦♦	7.10 ± 0.08 ■■■, ♦♦♦	-0.30 ± 0.04 ■■■, ♦♦♦	6.96 ± 0.07 ■■, ♦♦♦
VUF8430	0.84 ± 0.06 ♦♦	7.42 ± 0.12 ■■■, ♦♦♦	0.93 ± 0.04 ■, ♦♦♦	7.22 ± 0.14 ■■■, ♦♦♦
immepip	0.81 ± 0.03	7.67 ± 0.05 ■■■, ♦♦♦	0.73 ± 0.03	7.54 ± 0.10 ■■■, ♦♦♦
clozapine	0.67 ± 0.04 ■■■, ♦♦♦	6.24 ± 0.10 ■■■, ♦♦♦	0.59 ± 0.04 ■■■, ♦♦♦	5.50 ± 0.13 ••, ■■, ♦
isoloxapine	0.81 ± 0.03 ■■■, ♦♦♦	7.08 ± 0.13 ■■■, ♦♦♦	0.87 ± 0.01 ■■■, ♦♦♦	6.48 ± 0.12 ••, ■■■, ♦♦♦
UR-PI376	1.11 ± 0.08 ■■■, ♦♦♦	7.79 ± 0.08 ■■■, ♦♦♦	0.84 ± 0.06 ■■■, ♦♦♦	7.26 ± 0.08 •, ■■■, ♦♦♦
clobenpropit	0.45 ± 0.04 ■■, ♦♦♦	7.65 ± 0.11 ■■■, ♦♦♦	0.45 ± 0.05 ■■, ♦♦♦	7.85 ± 0.13 ■■■, ♦♦♦

pEC$_{50}$ values ([^{35}S]GTPγS agonist mode) and α (intrinsic activity, maximal effect relative to histamine = 1.0) are given as mean ± SEM of at least three independent experiments, performed in triplicate. Results of statistical tests (one-way ANOVA and Bonferroni post hoc tests; mH$_4$R and rH$_4$R were considered): significant differences with respect to hH$_4$R - • $p < 0.05$, •• $p < 0.01$, ••• $p < 0.001$; significant differences with respect to mH$_4$R - ■ $p < 0.05$, ■■ $p < 0.01$, ■■■ $p < 0.001$; significant differences with respect to rH$_4$R - ♦ $p < 0.05$, ♦♦ $p < 0.01$, ♦♦♦ $p < 0.001$. Functional data for hH$_4$R cf. Wifling et al. (2015b).
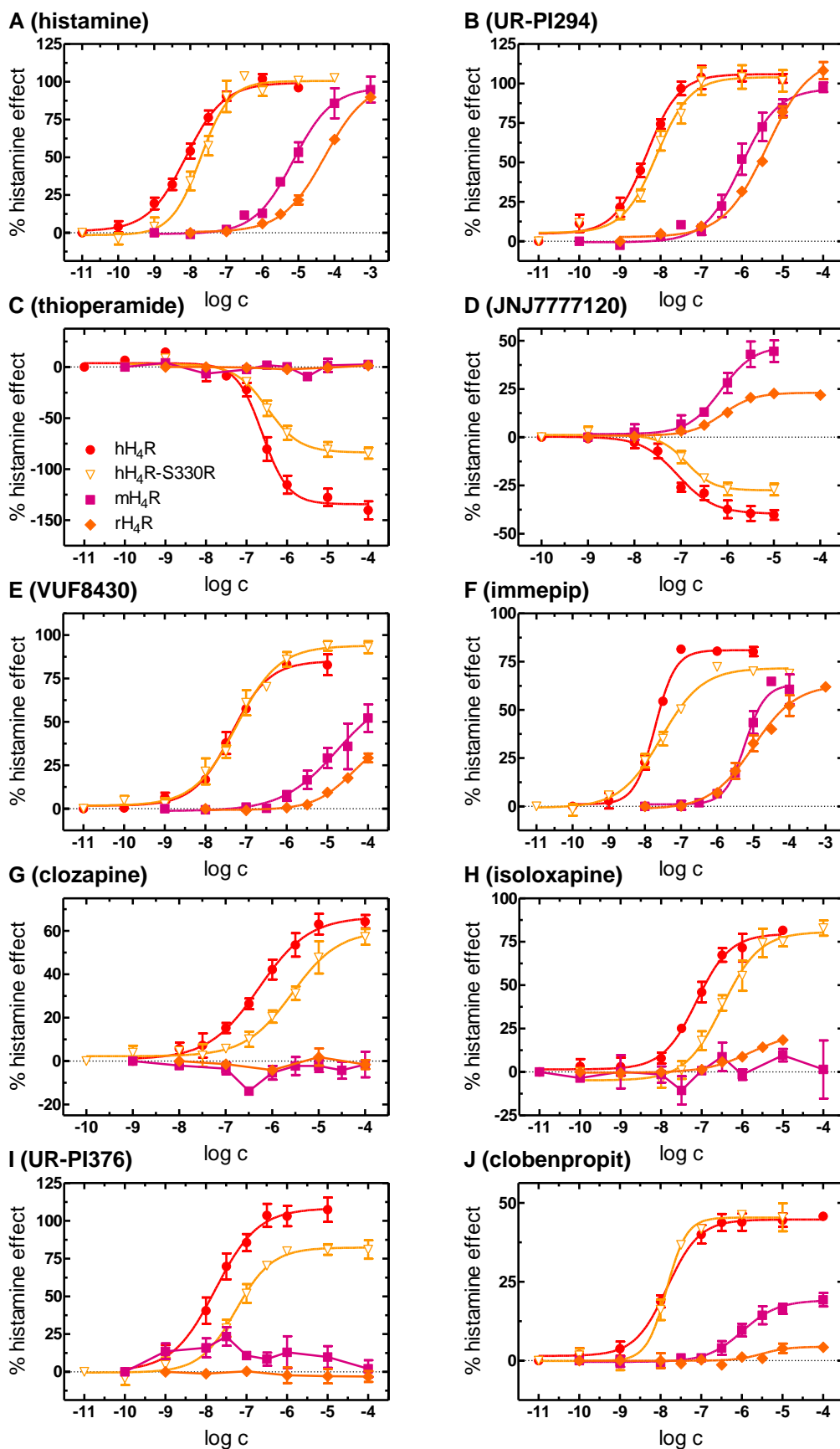
Figure 6.5: Concentration-response curves of H$_4$R ligands investigated in [^{35}S]GTPγS and [^{3}H]histamine competition binding assays. All curves are scaled with respect to a maximal histamine effect of 100 %. Symbols and colours refer to the species variants and mutants, respectively. Filled symbols: wild-types; open symbols: hH$_4$R-S330R. **(A)** histamine; **(B)** UR-PI294; **(C)** thioperamide; **(D)** JNJ7777120; **(E)** VUF8430; **(F)** immepip; **(G)** clozapine; **(H)** isoloxapine; **(I)** UR-PI376; **(J)** clobenpropit.

6.5 Discussion

6.5.1 Affinities and potencies of the investigated ligands at H$_4$R wild-types and the hH$_4$R-S330R mutant

The B$_{max}$ value of the hH$_4$R-S330R mutant was only slightly higher than that of the hH$_4$R wild-type (factor 1.35), so that a comparably high receptor expression level was assumed (Table 6.1 and Figure 6.3). Saturation and binding experiments using [^{3}H]histamine as the radioligand gave comparable K$_d$ and pK$_i$ values at the wild-type hH$_4$R and the S330R mutant (Table 6.1 and Table 6.2). [^{35}S]GTPγS assays (Table 6.3 and Figure 6.6B) revealed moderate changes of functional data of H$_4$R ligands, in particular, in case of histamine, clozapine, isoloxapine and UR-PI376.
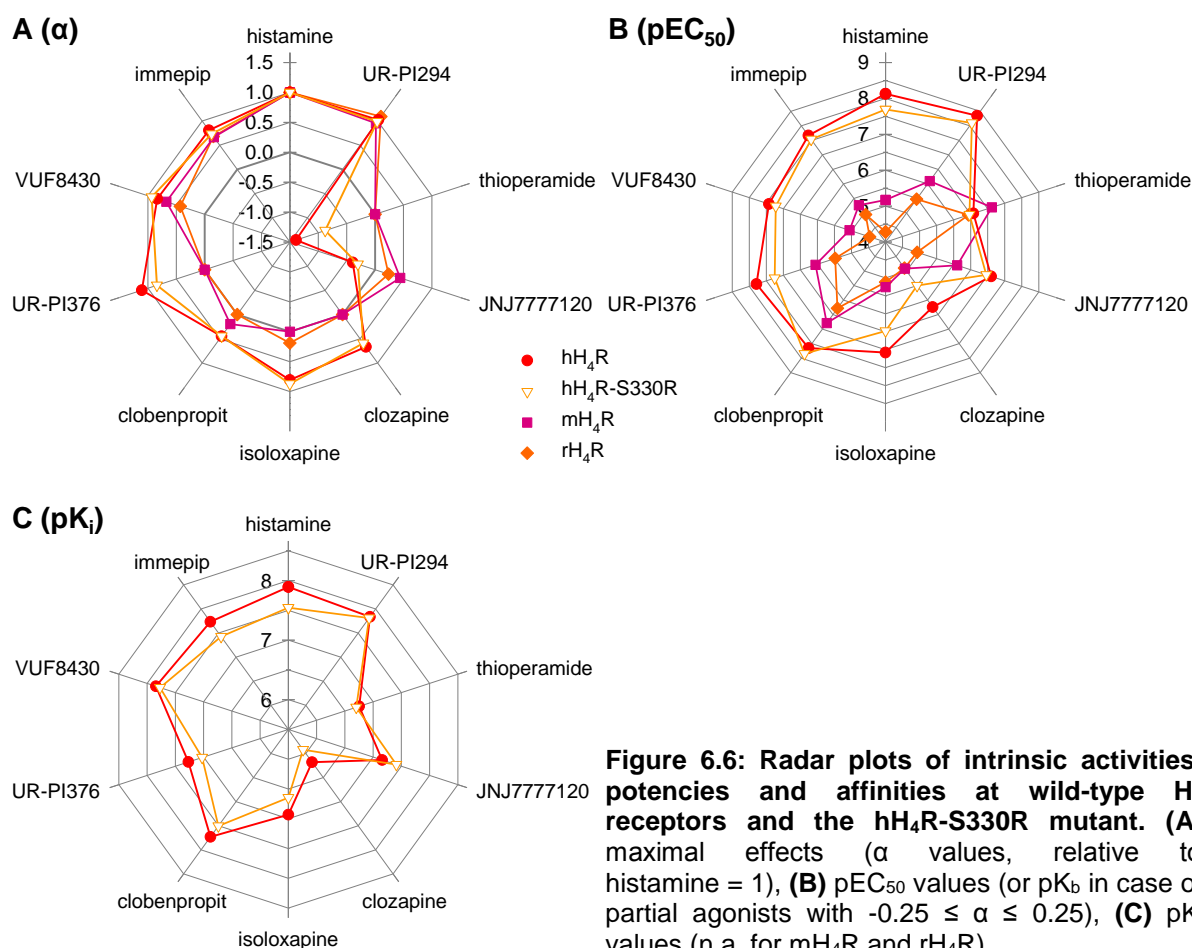
Figure 6.6: Radar plots of intrinsic activities, potencies and affinities at wild-type H$_4$ receptors and the hH$_4$R-S330R mutant. (A) maximal effects (α values, relative to histamine = 1), **(B)** pEC$_{50}$ values (or pK$_b$ in case of partial agonists with -0.25 ≤ α ≤ 0.25), **(C)** pK$_i$ values (n.a. for mH$_4$R and rH$_4$R).

6.5.2 Maximal agonist effects and constitutive activities determined at H$_4$R orthologs and hH$_4$R-S330R mutant

With respect to the intrinsic activity of the investigated H$_4$R ligands, thioperamide was an exception: replacement of S330 by R led to a decrease in the maximal inverse agonistic effect of thioperamide at the hH$_4$R-S330R mutant (-0.88) compared to the hH$_4$R wild-type (-1.39)

(Figure 6.6A). The decreased inverse agonistic response elicited by thioperamide reflects a reduced constitutive activity of the hH$_4$R-S330R mutant (Figure 6.4). This is in agreement with the observation that the inverse agonism at the hH$_4$R-S330R mutant was in between the responses elicited by thioperamide at the hH$_4$R and the rodent orthologs (Figure 6.4).

Exploring the potential role of charged amino acids in ECL3 in the thyroid stimulating hormone receptor (TSHR) by site-directed mutagenesis studies, Claus et al. (2005) suggested hydrogen bonds between ECL2 and ECL3 to be involved in ligand binding and function. By analogy with these results, interactions of acidic residues in ECL2 with basic residues in ECL3 such as R330 are conceivable in case of the hH$_4$R. This assumption is supported by the fact that constitutive activity decreased at the hH$_4$R-S330R mutant compared to the hH$_4$R wild-type, i. e., interactions between basic residues in ECL3 as R330 with acidic residues in ECL2 may contribute to the stabilization of the inactive hH$_4$R state.

6.6 Conclusions

The influence of an exchange of a neutral by a basic residue (hH$_4$R-S330R) in the extracellular loop 3 of the hH$_4$R was demonstrated for the first time. The results are compatible with the hypothesis that basic amino acids in ECL3 of the H$_4$R contribute to the stabilization of the rodent orthologs in the inactive state. Apart from hH$_4$R-S330R, additional charged amino acids in extracellular loops should be taken into consideration to study this phenomenon in more detail.

6.7 References

Claus, M.; Jaeschke, H.; Kleinau, G.; Neumann, S.; Krause, G.; Paschke, R. (2005). A hydrophobic cluster in the center of the third extracellular loop is important for thyrotropin receptor signaling. *Endocrinology* 146(12): 5197-5203.

Hoffmann, C.; Moro, S.; Nicholas, R. A.; Harden, T. K.; Jacobson, K. A. (1999). The role of amino acids in extracellular loops of the human P2Y1 receptor in surface expression and activation processes. *J. Biol. Chem.* 274(21): 14639-14647.

Wifling, D.; Bernhardt, G.; Dove, S.; Buschauer, A. (2015a). The Extracellular Loop 2 (ECL2) of the Human Histamine H4 Receptor Substantially Contributes to Ligand Binding and Constitutive Activity. *PLoS One* 10(1): e0117185.

Wifling, D.; Löffel, K.; Nordemann, U.; Strasser, A.; Bernhardt, G.; Dove, S.; Seifert, R.; Buschauer, A. (2015b). Molecular determinants for the high constitutive activity of the human histamine H4 receptor: functional studies on orthologues and mutants. *Br. J. Pharmacol.* 172(3): 785-798.

Chapter 7

Investigations on the contribution of R341$^{7.36}$ to ligand binding and function of the hH$_4$R

7.1 Summary

Instead of R341$^{7.36}$ in the hH$_4$R, amino acids of different chemical nature are present in the respective position of H$_4$R species orthologs: the positively charged R in the human receptor is replaced by S in the rodent orthologs, mH$_4$R and rH$_4$R, respectively, and by the acidic amino acid E in the cH$_4$R. Therefore, R341$^{7.36}$ was taken into consideration as a potential key residue for species-dependent differences regarding ligand binding and constitutive activity. To test this hypothesis, binding and functional investigations on hH$_4$R-R341S and hH$_4$R-R341E mutants were performed. The receptors were co-expressed with the G-protein subunits Gα$_{i2}$ and Gβ$_1$γ$_2$ in Sf9 insect cells, and the membranes were studied in [^{3}H]histamine saturation and competition binding as well as in [^{35}S]GTPγS assays. The results revealed a slightly decreased constitutive activity of the hH$_4$R-R341S mutant, whereas the constitutive activity of the hH$_4$R-R341E mutant remained unchanged compared to the hH$_4$R wild-type. Thus, a major contribution of R341$^{7.36}$ in the hH$_4$R to ligand binding and function was not confirmed.

7.2 Introduction

R341$^{7.36}$ is positioned at the top of TM7 enabling interactions with both, the binding pocket region as well as the extracellular surface (R341-1 and R341-2; Figure 7.1). Compared to the human receptor, in both the mH$_4$R and rH$_4$R, R is replaced by S, whereas E is present in case of the cH$_4$R. Previous investigation of three ligands (histamine, thioperamide and UR-PI376) on both mutants, hH$_4$R-R341S and hH$_4$R-R341E, respectively, in the [γ-^{33}P]GTP hydrolysis (GTPase) assay revealed only minor differences (Schnell et al., 2011). In the present study, a broader variety of hH$_4$R ligands, i. e., ten compounds including inverse agonists and agonists (for structures of the investigated ligands cf. Figure 4.1 and Figure 5.2), was investigated in

the [^{35}S]GTPγS assay. The latter was selected to preclude signal amplification, which can take place in the GTPase assay. In principle, signal amplification can reduce or abolish differences in intrinsic activities, e. g., by apparently elevating the intrinsic activity of partial agonists up to (almost) full agonism. At the same time, the level of constitutive activity is reduced and agonist potencies are most commonly increased (Kenakin, 2009).

To answer the question, whether R341$^{7.36}$ contributes to the differences in ligand binding and constitutive activity, comparing hH$_4$R, mH$_4$R, rH$_4$R (Table 4.4) and cH$_4$R (Brunskole et al., 2011), the positively charged arginine was replaced by serine, a neutral amino acid, or glutamate, a negatively charged amino acid. These mutations might change interactions with acidic and basic residues in the extracellular region, for instance, R15, E160, E163 and K336 (Figure 7.1).
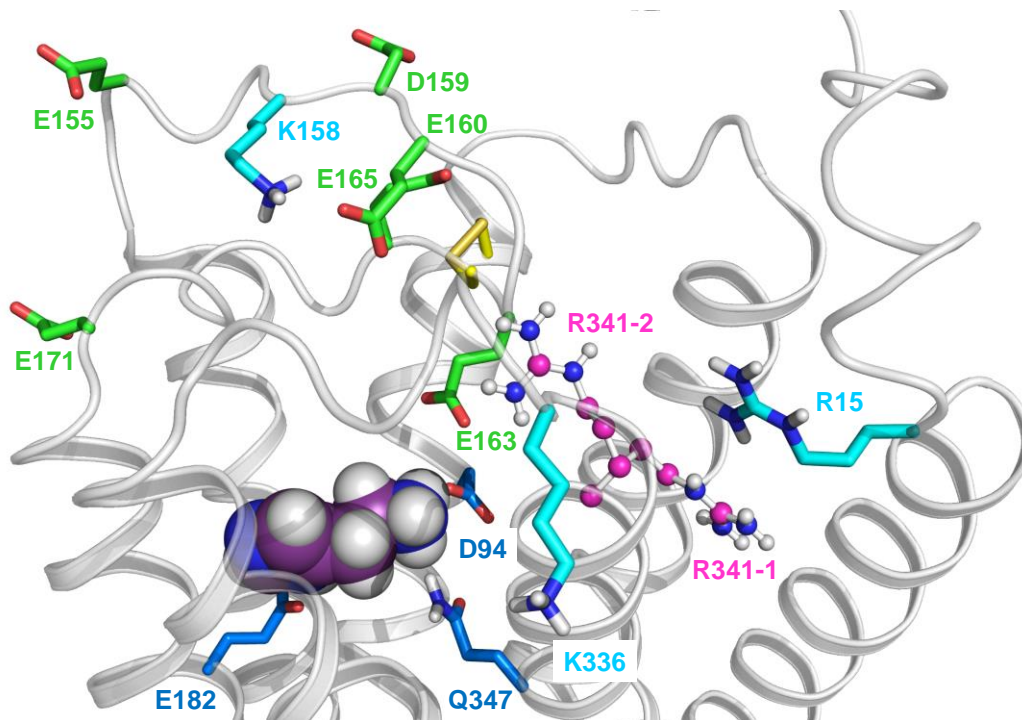
Figure 7.1: Homology model of the hH$_4$R based on the crystal structure of the hH$_1$R inactive state. Two different conformations of R341 (pink, R341-1 and R341-2) and the surrounding acidic (green) and basic (cyan) residues are shown. The docked histamine is illustrated in spherical calottes (magenta) and the key residues in ligand binding in dark blue.

7.3 Materials and Methods

7.3.1 Materials

Cf. Chapters 4.3.1 and 5.3.1.

7.3.2 Site-directed mutagenesis of the hH$_4$R

The two pVL1392-SF-hH$_4$R-R341S/E-His$_6$ plasmids were constructed by Katerina Ladova and Irena Brunskole (Pharmaceutical/Medicinal Chemistry II, University of Regensburg, Germany).

7.3.3 Cell culture, generation of recombinant baculoviruses and membrane preparation

Recombinant baculoviruses encoding the hH$_4$R-R341S/E mutants were kindly provided by Katerina Ladova and Irena Brunskole. Cell cultures and membrane preparations were performed according to the procedures described in Chapters 4.3.3 and 5.3.2.2.

7.3.4 SDS-PAGE and Coomassie staining

Cf. Chapters 4.3.4 and 5.3.2.3.

7.3.5 [^{3}H]histamine saturation binding experiments

Experiments were performed according to the procedures described in Chapters 4.3.6 and 5.3.2.4 with the exception that each well contained 53-85 µg protein in case of the hH$_4$R-R341S/E mutants.

7.3.6 [^{3}H]histamine competition binding assay

Experiments were performed according to the procedure described in Chapter 4.3.7 with the exception that each well contained 20-24 µg protein in case of the hH$_4$R-R341S/E mutants.

7.3.7 [^{35}S]GTPγS binding assay

Experiments were performed according to the procedures described in Chapters 4.3.8 and 5.3.2.5 with the exception that each well contained 9-14 µg protein in case of the hH$_4$R-R341S/E mutants.

7.3.8 Miscellaneous

Cf. Chapters 4.3.10 and 5.3.2.6

7.4 Results

7.4.1 Expression of the recombinant proteins hH$_4$R-R341S and hH$_4$R-R341E

As also shown for other mutants (cf. Chapter 4.4.1, 5.4.1 and 6.4.1; Wifling et al., 2015a; Wifling et al., 2015b), both, wild-type (hH$_4$R, mH$_4$R, rH$_4$R) and mutated (hH$_4$R-R341S and hH$_4$R-R341E) H$_4$ receptors, migrating with an apparent molecular weight of 39 kDa (cf. Western blots on the example of the hH$_4$R-F169V mutant, Chapter 4.4.1; Wifling et al., 2015b),

as well as the $G\alpha_{i2}$ protein subunit, migrating with an apparent molecular weight of 41 kDa, were expressed at comparable levels (Figure 7.2).
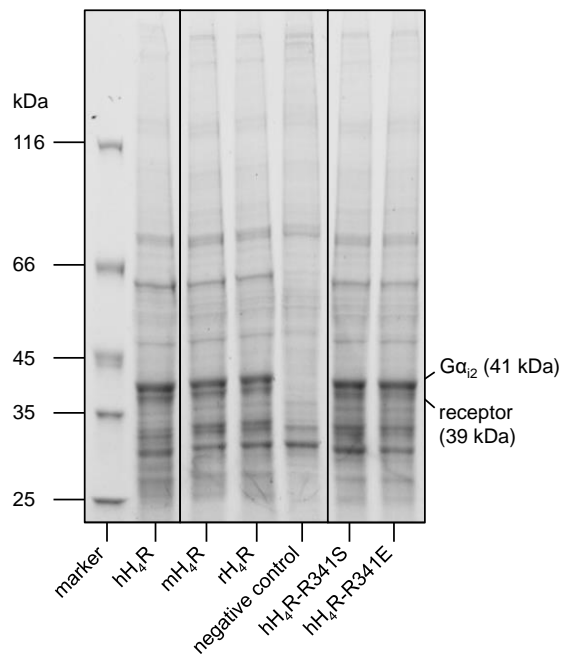

Figure 7.2: Coomassie stained SDS gels. Membrane proteins of Sf9 insect cells, co-expressing the respective receptor as indicated and $G\alpha_{i2}$ as well as $G\beta_1\gamma_2$ were separated on 8-16 % polyacrylamide gradient gels. All samples were analysed on the same gel.

Both the K_d and B_{max} values of the hH_4R wild-type as well as of the hH_4R-R341S and hH_4R-R341E mutants were in a comparable range (Table 7.1 and Figure 7.3).

Table 7.1: K_d and B_{max} values determined with [³H]histamine on hH_4R, hH_4R-R341S and hH_4R-R341E.

Receptor	K_d [nM]	B_{max} [pmol/mg]
hH_4R	11.16 ± 1.92	1.93 ± 0.32
hH_4R-R341S	11.52 ± 1.64	2.19 ± 0.03
hH_4R-R341E	8.62 ± 0.93	1.72 ± 0.04

Data are given as mean values ± SEM for at least two independent experiments, each performed in triplicate. Non-specific binding, amounting to 5.3-16.0 % of total binding at 100 nM [³H]histamine, was determined in the presence of 10 µM unlabelled histamine.
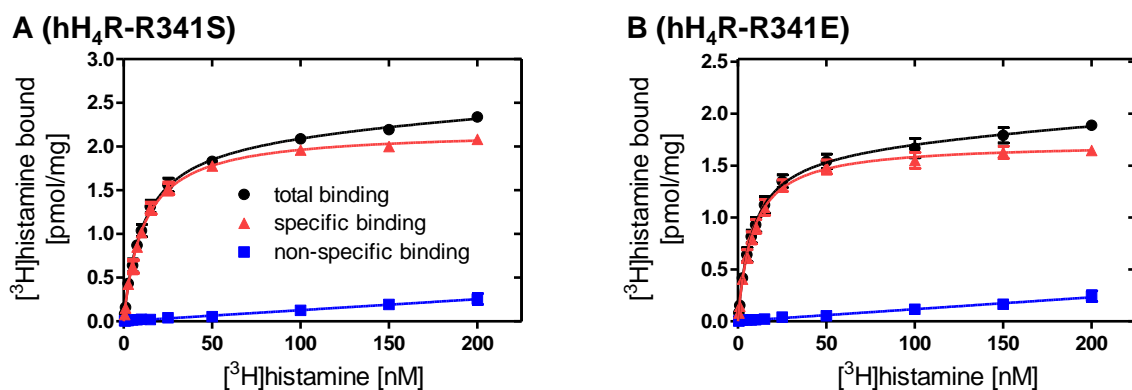
Figure 7.3: Saturation binding curves of [³H]histamine at (A) hH_4R-R341S and (B) hH_4R-R341E mutants. Data represent mean values ± SEM from two independent experiments performed in triplicate.

7.4.2 [^{3}H]histamine competition binding on hH$_4$R-R341S and hH$_4$R-R341E

For most of the compounds investigated in [^{3}H]histamine competition binding, the differences between pK$_i$ values at wild-type and mutant receptors were not significant. However, in case of thioperamide a decrease in affinity became obvious comparing the hH$_4$R wild-type and the hH$_4$R-R341S mutant, whereas the affinity at the hH$_4$R-R341E mutant increased by 0.3 and 0.6 logarithmic units in case of UR-PI294 and UR-PI376, respectively (Table 7.2).

Table 7.2: Binding data of H$_4$R ligands hH$_4$R, hH$_4$R-R341S and hH$_4$R-R341E.

Ligand	hH$_4$R	hH$_4$R-R341S	hH$_4$R-R341E
histamine	7.89 ± 0.04	7.68 ± 0.03	7.73 ± 0.08
UR-PI294	7.84 ± 0.03	7.80 ± 0.04	8.13 ± 0.04 •
thioperamide	6.75 ± 0.07	6.41 ± 0.04 •	6.66 ± 0.05
JNJ7777120	7.16 ± 0.05	7.22 ± 0.02	7.25 ± 0.07
VUF8430	7.84 ± 0.03	7.92 ± 0.10	8.10 ± 0.09
immepip	7.73 ± 0.16	7.62 ± 0.02	7.74 ± 0.03
clozapine	6.18 ± 0.03	5.99 ± 0.09	6.24 ± 0.07
isoloxapine	6.93 ± 0.02	6.83 ± 0.01	7.05 ± 0.12
UR-PI376	7.27 ± 0.07	7.45 ± 0.11	7.85 ± 0.01 •
clobenpropit	7.73 ± 0.07	7.67 ± 0.00	7.93 ± 0.07

pK$_i$ values ([^{3}H]histamine competition binding) are given as mean ± SEM of at least two independent experiments, performed in triplicate (n.a. for mH$_4$R and rH$_4$R). Results of statistical tests (one-way ANOVA and Bonferroni post hoc tests): significant differences with respect to hH$_4$R - • $p < 0.05$, •• $p < 0.01$, ••• $p < 0.001$.

7.4.3 Functional investigation of wild-type, hH$_4$R-R341S and hH$_4$R-R341E mutant H$_4$ receptors in the [^{35}S]GTPγS assay

The amounts of bound [^{35}S]GTPγS [pmol/mg] were comparable at the hH$_4$R wild-type and the hH$_4$R-R341E mutant, whereas the mutation of R341 to S resulted in a decrease in [^{35}S]GTPγS binding (Figure 7.4A). Normalization of the amounts of bound [^{35}S]GTPγS to percentual values facilitates the comparison of constitutive activities (Figure 7.4B): The constitutive activity of the hH$_4$R-R341E mutant remained essentially unchanged compared to the hH$_4$R wild-type. By contrast, the constitutive activity decreased, when R341 was replaced by S, making the hH$_4$R more similar to the rodent orthologs (mH$_4$R or rH$_4$R).
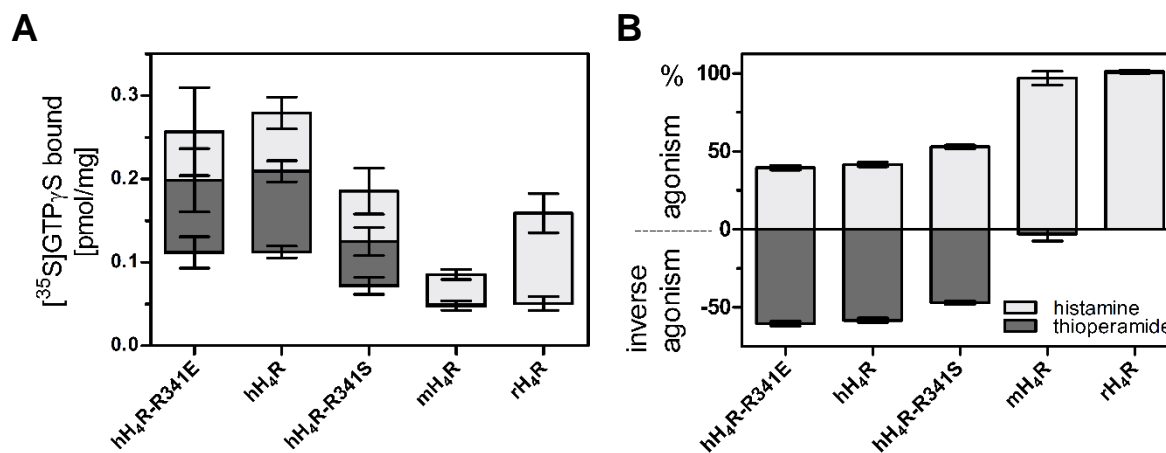
Figure 7.4: Maximal agonistic effects of histamine and maximal inverse agonistic effects of thioperamide in [^{35}S]GTPγS assays. (A) Amounts of [^{35}S]GTPγS [pmol/mg] bound to wild-type and mutated H$_4$Rs in the presence of histamine (light grey) and thioperamide (dark grey). Values demarcating light and dark grey bars represent the basally (in the absence of ligand) bound [^{35}S]GTPγS. **(B)** Relative effects of histamine and thioperamide. The sum of responses to histamine and thioperamide was scaled to 100 % and the zero line represents the ligand-free control.

The concentration-response curves of the respective ligands at the investigated human, mouse and rat H$_4$R wild-types and the hH$_4$R-R341S and hH$_4$R-R341E mutants are illustrated in Figure 7.5. The potency of histamine decreased on both of the hH$_4$R-R341S/E mutants (by up to half an order of magnitude in case of hH$_4$R-R341S) compared to the hH$_4$R wild-type (Table 7.3 and Figure 7.5A).

Whereas a slightly reduced intrinsic activity was detected in case of the hH$_4$R-R341S mutant, the potency of UR-PI294 decreased significantly by up to half an order of magnitude from the hH$_4$R wild-type over the hH$_4$R-R341S to the hH$_4$R-R341E mutant (Table 7.3 and Figure 7.5B). The intrinsic activity of thioperamide was comparable at the hH$_4$R-R341E mutant and the hH$_4$R wild-type, but was significantly increased at the hH$_4$R-R341S mutant (Table 7.3 and Figure 7.5C). JNJ7777120, a partial inverse agonist at the hH$_4$R, showed even more pronounced inverse agonism at the hH$_4$R-R341E mutant, but was a neutral antagonist at the hH$_4$R-R341S mutant (Table 7.3 and Figure 7.5D).

No significant differences between functional data on the three receptors were detected for immepip, VUF8430 and clobenpropit; UR-PI376 revealed a moderate decrease in intrinsic activity at the hH$_4$R-R341S mutant compared to the hH$_4$R (Table 7.3 and Figure 7.5E, F, I, J). Whereas clozapine showed no significant changes in agonist activity at the two mutant receptors, the structural analogue isoloxapine revealed a slight increase in potency at the hH$_4$R-R341E mutant as well as a significant decrease in intrinsic activity at both mutants, hH$_4$R-R341S and hH$_4$R-R341E, respectively (Table 7.3 and Figure 7.5G, H).

Table 7.3: $[^{35}S]GTP\gamma S$ binding on hH_4R wild-type and mutants.

Ligand	Parameter	hH_4R	hH_4R-R341S	hH_4R-R341E
histamine	α	1	1	1
	pEC_{50}	8.13 ± 0.06 ■■■, ♦♦♦	7.59 ± 0.15 ••, ■■■, ♦♦♦	7.71 ± 0.07 ■■■, ♦♦♦
UR-PI294	α	1.02 ± 0.03	0.78 ± 0.02 •••, ■■, ♦♦♦	0.93 ± 0.02 ♦♦
	pEC_{50}	8.35 ± 0.04 ■■■, ♦♦♦	8.13 ± 0.00 ■■■, ♦♦♦	7.89 ± 0.02 ••, ■■■, ♦♦♦
thioperamide	α	-1.39 ± 0.08 ■■■, ♦♦♦	-0.89 ± 0.04 ••, ■■■, ♦♦♦	-1.51 ± 0.10 ■■■, ♦♦♦
	pEC_{50}	6.58 ± 0.06 ■■	6.54 ± 0.03 ■■	6.62 ± 0.06 ■■
	pK_b	6.83 ± 0.05		
JNJ7777120	α	-0.39 ± 0.03 ■■■, ♦♦♦	0 •••, ■■■, ♦♦♦	-0.60 ± 0.03 •••, ■■■, ♦♦♦
	pEC_{50}	7.10 ± 0.08 ■■■, ♦♦♦	n.a.	7.39 ± 0.08 ■■■, ♦♦♦
	pK_b	7.60 ± 0.05	6.79 ± 0.14 ■, ♦♦♦	
VUF8430	α	0.84 ± 0.06 ♦♦	0.91 ± 0.08 ♦♦	0.82 ± 0.08 ♦
	pEC_{50}	7.42 ± 0.12 ■■■, ♦♦♦	7.54 ± 0.07 ■■■, ♦♦♦	7.67 ± 0.08 ■■■, ♦♦♦
immepip	α	0.81 ± 0.03	0.88 ± 0.09	0.74 ± 0.04
	pEC_{50}	7.67 ± 0.05 ■■■, ♦♦♦	7.67 ± 0.15 ■■■, ♦♦♦	7.83 ± 0.15 ■■■, ♦♦♦
clozapine	α	0.67 ± 0.04 ■■■, ♦♦♦	0.64 ± 0.02 ■■■, ♦♦♦	0.61 ± 0.03 ■■■, ♦♦♦
	pEC_{50}	6.24 ± 0.10 ■■■, ♦♦♦	6.04 ± 0.14 ■■■, ♦♦	6.48 ± 0.13 ■■■, ♦♦♦
isoloxapine	α	0.81 ± 0.03 ■■■, ♦♦♦	0.56 ± 0.01 ••, ■■■, ♦♦♦	0.55 ± 0.06 ••, ■■■, ♦♦♦
	pEC_{50}	7.08 ± 0.13 ■■■, ♦♦♦	7.11 ± 0.08 ■■■, ♦♦♦	7.52 ± 0.06 •, ■■■, ♦♦♦
UR-PI376	α	1.11 ± 0.08 ■■■, ♦♦♦	0.85 ± 0.05 •, ■■■, ♦♦♦	0.92 ± 0.07 ■■■, ♦♦♦
	pEC_{50}	7.79 ± 0.08 ■■■, ♦♦♦	7.63 ± 0.06 ■■■, ♦♦♦	7.85 ± 0.13 ■■■, ♦♦♦
clobenpropit	α	0.45 ± 0.04 ■■■, ♦♦♦	0.52 ± 0.01 ■■■, ♦♦♦	0.49 ± 0.02 ■■■, ♦♦♦
	pEC_{50}	7.65 ± 0.11 ■■, ♦♦♦	7.50 ± 0.08 ■, ♦♦♦	7.36 ± 0.19 ♦♦♦

pEC_{50} values ($[^{35}S]GTP\gamma S$ agonist mode), pK_b values ($[^{35}S]GTP\gamma S$ antagonist mode) and α (intrinsic activity, maximal effect relative to histamine = 1.0) are given as mean ± SEM of at least three independent experiments, performed in triplicate. Results of statistical tests (one-way ANOVA and Bonferroni post hoc tests; mH_4R and rH_4R were considered): significant differences with respect to hH_4R - • $p < 0.05$, •• $p < 0.01$, ••• $p < 0.001$; significant differences with respect to mH_4R - ■ $p < 0.05$, ■■ $p < 0.01$, ■■■ $p < 0.001$; significant differences with respect to rH_4R - ♦ $p < 0.05$, ♦♦ $p < 0.01$, ♦♦♦ $p < 0.001$. In case of neutral antagonism (-0.25 ≤ α ≤ 0.25), pK_b values were considered for statistical analysis instead of pEC_{50} values. Maximal effect α = 0: neutral antagonism. Functional data for hH_4R cf. Wifling et al. (2015b).
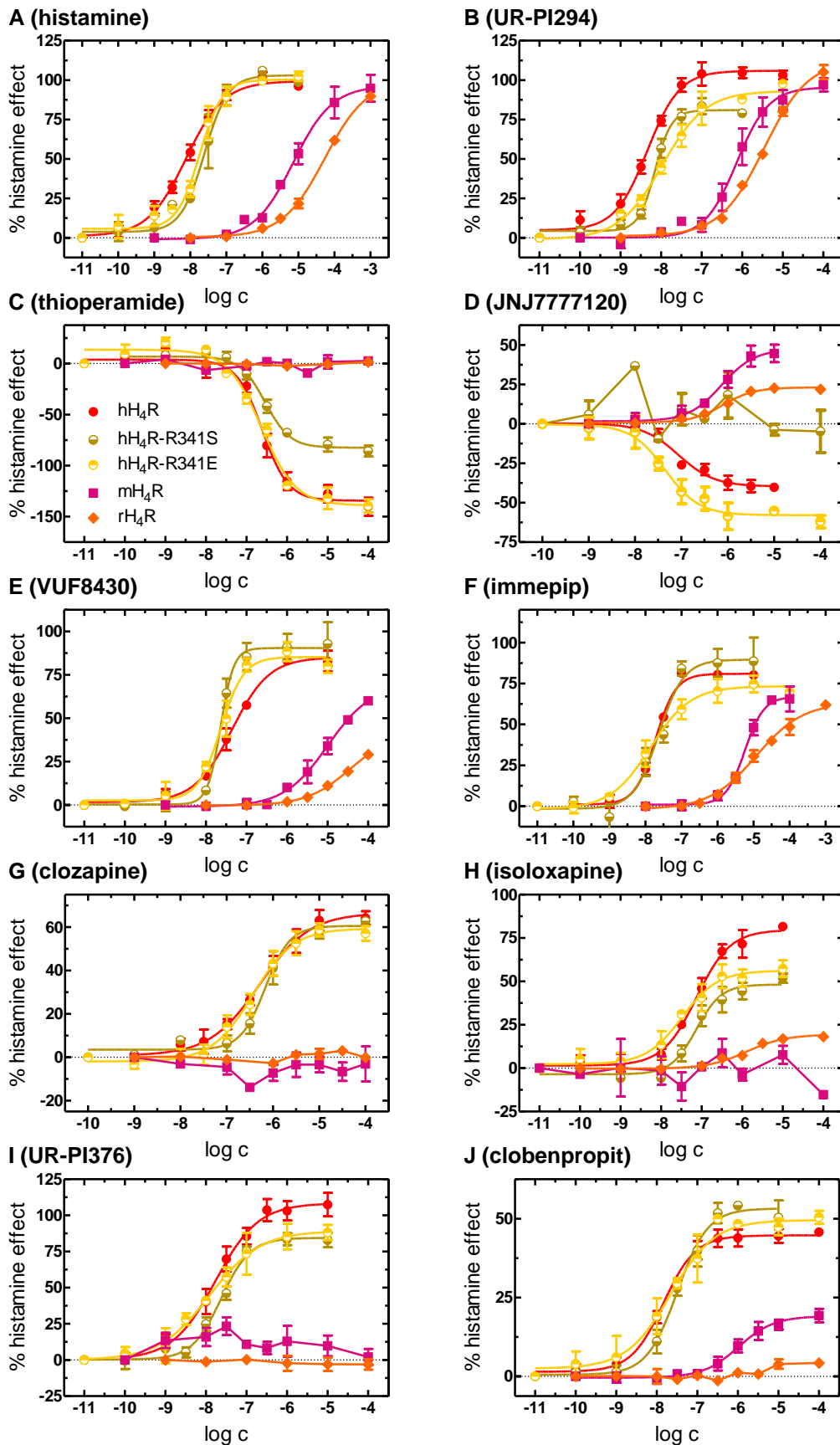
Figure 7.5: Concentration-response curves of H₄R ligands investigated in [³⁵S]GTPγS and [³H]histamine competition binding assays. All curves are scaled with respect to a maximal histamine effect of 100 %. Symbols and colours refer to the species variants and mutants, respectively. Filled symbols: wild-types; open symbols: mutants. **(A)** histamine; **(B)** UR-PI294; **(C)** thioperamide; **(D)** JNJ7777120; **(E)** VUF8430; **(F)** immepip; **(G)** clozapine; **(H)** isoloxapine; **(I)** UR-PI376; **(J)** clobenpropit.

7.5 Discussion

7.5.1 Affinities and potencies of ligands at H$_4$R wild-types and hH$_4$R-R341S/E mutants

A contribution of R341 in the human H$_4$R to [^{3}H]histamine binding was not detectable by investigations on hH$_4$R-R341S and hH$_4$R-R341E mutants (Table 7.1 and Figure 7.3).

The pEC$_{50}$ value of histamine was slightly decreased at the hH$_4$R-R341S mutant, presumably as a consequence of reduced constitutive activity of this mutant (Table 7.3 and Figure 7.6B). UR-PI294 revealed a minor increase in pK$_i$ values (Table 7.2 and Figure 7.6C), but a moderate decrease in pEC$_{50}$ values comparing the hH$_4$R and the hH$_4$R-R341E mutant (Table 7.3 and Figure 7.6B). The affinity of UR-PI376 unequivocally increased at the hH$_4$R-R341E mutant compared to the hH$_4$R wild-type (Table 7.2 and Figure 7.6C). This is in agreement with results by Schnell et al. (2011), who determined a ΔpEC$_{50}$ of 0.4.
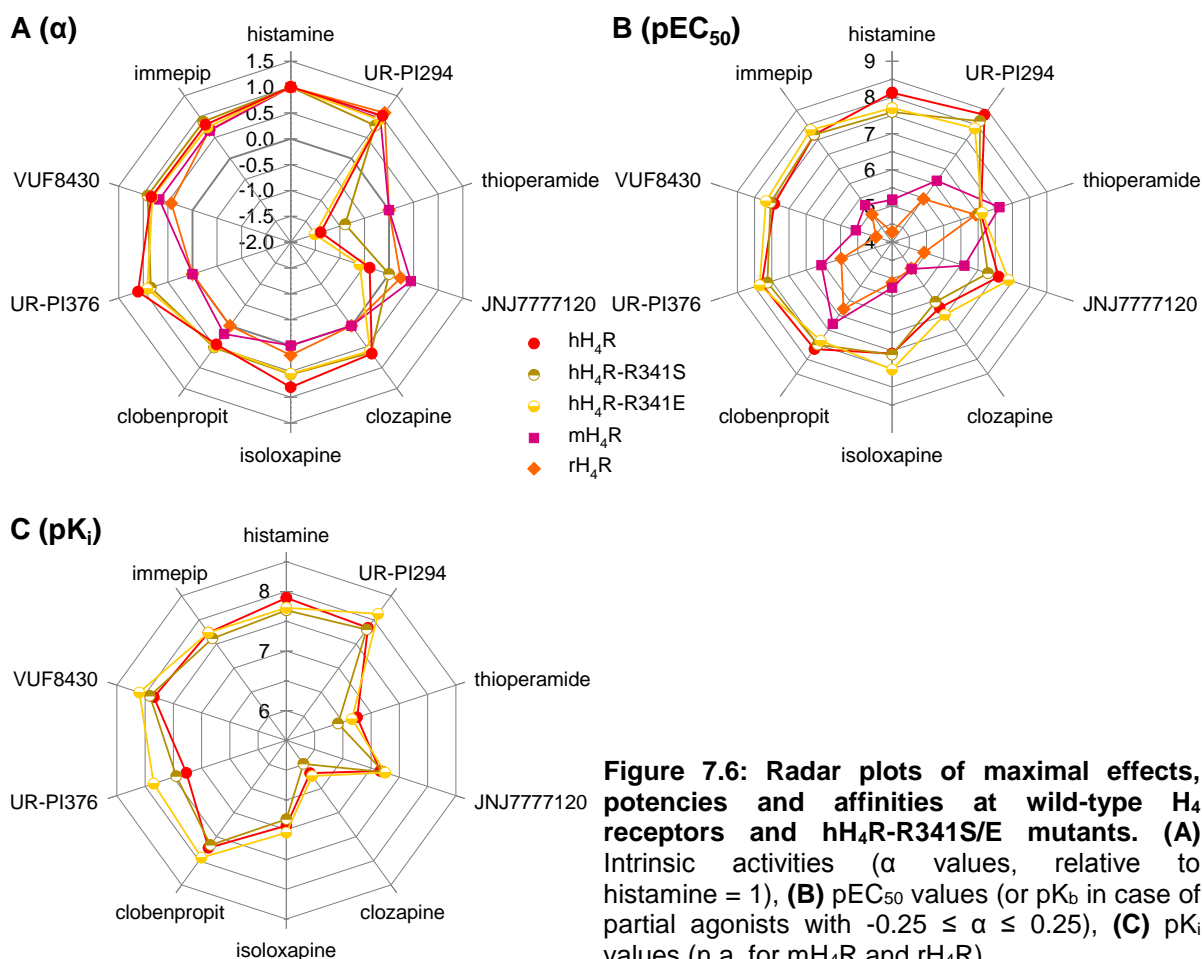
Figure 7.6: Radar plots of maximal effects, potencies and affinities at wild-type H$_4$ receptors and hH$_4$R-R341S/E mutants. (A) Intrinsic activities (α values, relative to histamine = 1), **(B)** pEC$_{50}$ values (or pK$_b$ in case of partial agonists with -0.25 ≤ α ≤ 0.25), **(C)** pK$_i$ values (n.a. for mH$_4$R and rH$_4$R).

7.5.2 Maximal agonist effects and constitutive activities determined at H$_4$R orthologs and hH$_4$R-R341S/E mutants

The hH$_4$R-R341S/E mutations caused mainly an impact on the constitutive activity (Figure 7.4). Whereas an extraordinarily high constitutive activity was characteristic of the hH$_4$R and the hH$_4$R-R341E mutant, constitutive activity significantly decreased upon introduction of serine in position 341$^{7.36}$ (cf. intrinsic activities of thioperamide: -1.39, -1.51 and -0.89; Table 7.3 and Figure 7.6A).

Concomitantly with the decreasing constitutive activity (increasing intrinsic activity of thioperamide at the hH$_4$R-R341S mutant), the intrinsic activities of UR-PI294 and UR-PI376 decreased at the hH$_4$R-R341S mutant compared to the hH$_4$R (Table 7.3 and Figure 7.6A). Moreover, the inverse agonist JNJ7777120 turned to neutral antagonism at the hH$_4$R-R341S mutant (Table 7.3 and Figure 7.6A). The intrinsic activity of isoloxapine dropped at both mutants, hH$_4$R-R341S and hH$_4$R-R341E, respectively. (Table 7.3 and Figure 7.6A).

Based on site-directed mutagenesis studies of the α$_{1B}$AR, Porter et al. (1996) suggested that K331$^{7.36}$, located on equivalent position than R341$^{7.36}$, interacts with the negatively charged D125$^{3.32}$, stabilizing the active conformation of the receptor in the absence of an agonist. Upon epinephrine binding, the positively charged ligand competes with the protonated amino group of K331$^{7.36}$. This assumption is supported by the fact that affinity and potency of epinephrine increased up to 6-fold at the α$_{1B}$AR mutants α$_{1B}$AR-K331A and α$_{1B}$AR-K331E. In case of the 5-HT$_{1B}$R, a decrease in affinity of serotonin by about 6-fold was shown for the 5-HT$_{1B}$R-D352A mutant, suggesting a substantial contribution of D352$^{7.36}$ to serotonin binding (Granas and Larhammar, 1999). Compared with the α$_{1B}$AR and 5-HT$_{1B}$R, a salt bridge between R341$^{7.36}$ and D94$^{3.32}$ is less likely. Instead, ionic interactions of R341$^{7.36}$ with acidic residues in ECL2 like E160 or E163 (Figure 7.1) are conceivable. This is in agreement with the fact that constitutive activity decreased at the hH$_4$R-R341S mutant. Nevertheless, the constitutive activity was comparable at the hH$_4$R wild-type and the hH$_4$R-R341E mutant. This may be interpreted as a hint that interactions of a charged amino acid in position 7.36 with acidic or basic residues in the extracellular loops promote the conversion of the inactive to the active receptor state.

7.6 Conclusions

It turned out that the constitutive activity of the hH$_4$R-R341S mutant was very similar to that of the hH$_4$R-S330R mutant, albeit JNJ7777120 was a neutral antagonist at the hH$_4$R-R341S mutant, but a partial inverse agonist at the hH$_4$R-S330R mutant. However, compared to the hH$_4$R-F168A mutant and the double mutants hH$_4$R-F169V+S179M/A, the changes in constitutive activity were rather small. The inverse agonistic effect of thioperamide varies

considerably depending on the assay used, even when comparing the [^{35}S]GTPγS and the [γ-^{33}P]GTPase assay: the more distal the readout the higher the extent of signal amplification. Consequently, with respect to the identification of molecular determinants of functional properties of GPCRs, the quantification of proximal signals, as close as possible to changes of receptor conformation, should be preferred.

7.7 References

Brunskole, I.; Strasser, A.; Seifert, R.; Buschauer, A. (2011). Role of the second and third extracellular loops of the histamine H(4) receptor in receptor activation. *Naunyn Schmiedebergs Arch. Pharmacol.* 384(3): 301-317.

Granas, C.; Larhammar, D. (1999). Identification of an amino acid residue important for binding of methiothepin and sumatriptan to the human 5-HT(1B) receptor. *Eur. J. Pharmacol.* 380(2-3): 171-181.

Kenakin, T. (2009). *A pharmacology primer: theory, applications, and methods.* 3 ed.; Academic Press/Elsevier: Amsterdam; Boston, p 416.

Porter, J. E.; Hwa, J.; Perez, D. M. (1996). Activation of the alpha1b-adrenergic receptor is initiated by disruption of an interhelical salt bridge constraint. *J. Biol. Chem.* 271(45): 28318-28323.

Schnell, D.; Brunskole, I.; Ladova, K.; Schneider, E. H.; Igel, P.; Dove, S.; Buschauer, A.; Seifert, R. (2011). Expression and functional properties of canine, rat, and murine histamine H(4) receptors in Sf9 insect cells. *Naunyn Schmiedebergs Arch. Pharmacol.* 383(5): 457-470.

Wifling, D.; Bernhardt, G.; Dove, S.; Buschauer, A. (2015a). The Extracellular Loop 2 (ECL2) of the Human Histamine H4 Receptor Substantially Contributes to Ligand Binding and Constitutive Activity. *PLoS One* 10(1): e0117185.

Wifling, D.; Löffel, K.; Nordemann, U.; Strasser, A.; Bernhardt, G.; Dove, S.; Seifert, R.; Buschauer, A. (2015b). Molecular determinants for the high constitutive activity of the human histamine H4 receptor: functional studies on orthologues and mutants. *Br. J. Pharmacol.* 172(3): 785-798.

Chapter 8

Summary

The histamine H_4R belongs to class A of G-protein coupled receptors (GPCRs) and is considered as a promising drug target for the treatment of inflammatory diseases such as allergic asthma. The validation of the H_4R in translational animal models is compromised by species-dependent differences regarding intrinsic activities, potencies and affinities of ligands, in particular, comparing the hH_4R (human) and the rodent orthologs, i. e., the mH_4R (mouse) and rH_4R (rat). In contrast to the mH_4R and rH_4R, the hH_4R shows a high degree of constitutive activity. Therefore, H_4R species orthologs represent ideal candidates to study the phenomenon of "constitutive activity". These species differences are supposed to be determined by one or several distinct amino acids in the ligand binding pocket of human, mouse and rat H_4R.

Aiming at more detailed insights into the molecular determinants of ortholog-dependent ligand-receptor interactions, a series of H_4R mutants were generated and expressed (Sf9 cells) to determine radioligand binding and functional data ($[^{35}S]$GTPγS assay). Apart from F169, which was identified by Lim et al. as a key amino acid for distinct ligand binding affinities at H_4R orthologs, S179, S330 and R341 were mutated, based on molecular modelling studies, to the corresponding amino acids of the rodent H_4Rs, resulting in hH_4R-F169V, hH_4R-S179M/A, hH_4R-F169V+S179M/A, hH_4R-S330R and hH_4R-R341S. The reciprocal mH_4R mutants, mH_4R-V171F and mH_4R-V171F+M181S, respectively, served as control. Moreover, to study the role of the F168/F169 motif, which is also found in, e. g., the β$_2$AR, H_3R and the M_2R, the hH_4R-F168A mutant was expressed in Sf9 cells. Additionally, R341 was mutated to the residue of the cH_4R (canine), resulting in hH_4R-R341E.

Coomassie staining together with western blotting revealed comparable ratios of receptor to G-protein expression in Sf9 cell membranes. Similar B_{max} values determined in $[^3H]$histamine saturation binding assays confirmed comparably high receptor expression levels throughout all preparations.

Compared to the hH_4R wild-type, especially UR-PI376, clozapine and isoloxapine revealed a significant decrease in potency and affinity at the hH_4R-F169V single and the hH_4R-F169V+A179M/A double mutants, respectively. With respect to several ligands, the

reverse mH_4R mutants, mH_4R-V171F and mH_4R-V171F+M181S, respectively, became more hH_4R-like. Moreover, the potency and/or affinity of most ligands was higher at the S179A than at the respective S179M mutants. As key result, the constitutive activity of the hH_4R-F169V and the double mutants was significantly reduced compared to the wild-type hH_4R. By contrast, an exchange of S179 by M or A alone did not significantly affect constitutive activity. Strikingly, the double mutants were comparable to the mH_4R and to the rH_4R, which are devoid of constitutive activity. The inverse agonism of thioperamide decreased from the hH_4R via the hH_4R-F169V mutant to the hH_4R-F169V+S179M/A double mutants, respectively.

The data for the hH_4R-F168A mutant revealed a major contribution of F168 to ligand binding with a concomitant, up to over 100-fold decrease in ligand potencies and a complete loss of constitutive activity, compared to the wild-type hH_4R. Thioperamide acted as a neutral antagonist and JNJ7777120 turned to partial agonism.

Potencies and affinities of the ligands clozapine, isoloxapine and UR-PI376 slightly decreased at the hH_4R-S330R mutant compared to the hH_4R wild-type. Constitutive activities slightly decreased at the hH_4R-S330R mutant.

Compared to the hH_4R, the affinity of UR-PI376 increased at the hH_4R-R341E mutant. By contrast, the constitutive activity of the hH_4R-R341S mutant decreased slightly.

Molecular modelling studies suggested that F168^{ECL2} and F169^{ECL2} interact with the surrounding hydrophobic and aromatic amino acids, which are supposed to be involved in the contraction of the binding pocket and, thus, in constitutive activity. S179$^{5.43}$ was proposed to form an H-bond with T323$^{6.55}$, which is precluded in case of mutation to M or A. S179$^{5.43}$ alone was not the cause for the high constitutive activity of the hH_4R. However, this amino acid in concert with F169^{ECL2} significantly contributed to the concomitant distal outward movement of TM5 and TM6.

In conclusion, especially F168 and F169 alone or F169 in concert with S179 favour the conversion of the inactive to the active state of the human H_4R. Similar motifs in other GPCRs such as the β_2AR or the H_3R suggest a common mechanism of receptor activation.

Chapter 9

Appendix

9.1 Plasmid map of pVL1392-SF-hH$_4$R-His$_6$
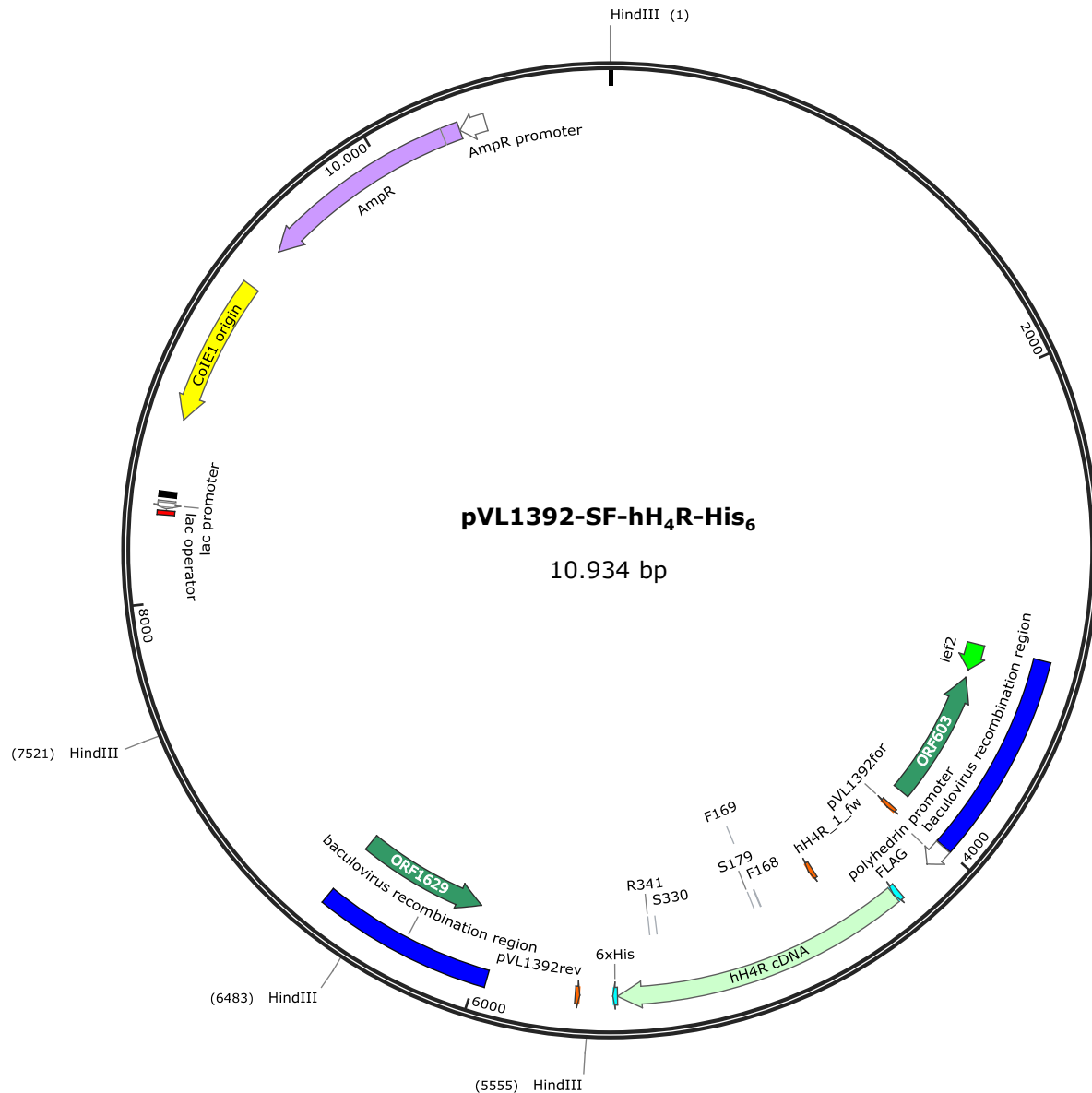
Figure 9.1: Map of the pVL1392-SF-hH$_4$R-His$_6$ plasmid. Baculovirus recombination regions (3170…3997 and 5956…6661) are coloured in blue, lef2 (baculovirus late expression factor 2, 3170…3294) in light green. ColE1 origin (8717…9305) is indicated in yellow and allows replication in TOP 10 cells. AmpR (9476…10336, purple) beginning with AmpR promoter (10337…10441, white) is responsible for expression of β-lactamase and therefore allows negative selection of TOP10 cells. ORF603 (baculovirus ORF603 protein, green, 3332…3937); ORF1629 (baculovirus capsid-associated protein, green, 6073…6661); lac promoter (white, 8363…8393) and operator (red, 8339…8355); CAP binding site (black, 8408…8429) activates transcription in presence of cAMP. *Hind*III cleavage sites are marked in black (1, 5555, 6483 and 7521). Important primers and mutated residues are also indicated: pVL1392for (orange, 4016…4034); pVL1392rev (orange, 5587…5604); hH$_4$R cDNA (light green, 4270…5439); polyhedrin promoter (white, 4001…4092); FLAG (light blue, 4246…4269); hH$_4$R_1_fw (orange, 4485…4505); hH$_4$R-F168 (black, 4771…4773); hH$_4$R-F169 (black, 4774…4776); hH$_4$R-S179 (black, 4804…4806); hH$_4$R-S330 (black, 5227…5229); hH$_4$R-R341 (black, 5290…5292); His$_6$ (light blue, 5440…5457). Sequence map was generated with SnapGene 1.5.1 trial version (GSL Biotech LLC, Chicago, IL USA).

## 9.2 Summary of potencies, intrinsic activities and affinities

9.2.1 Summary of potencies
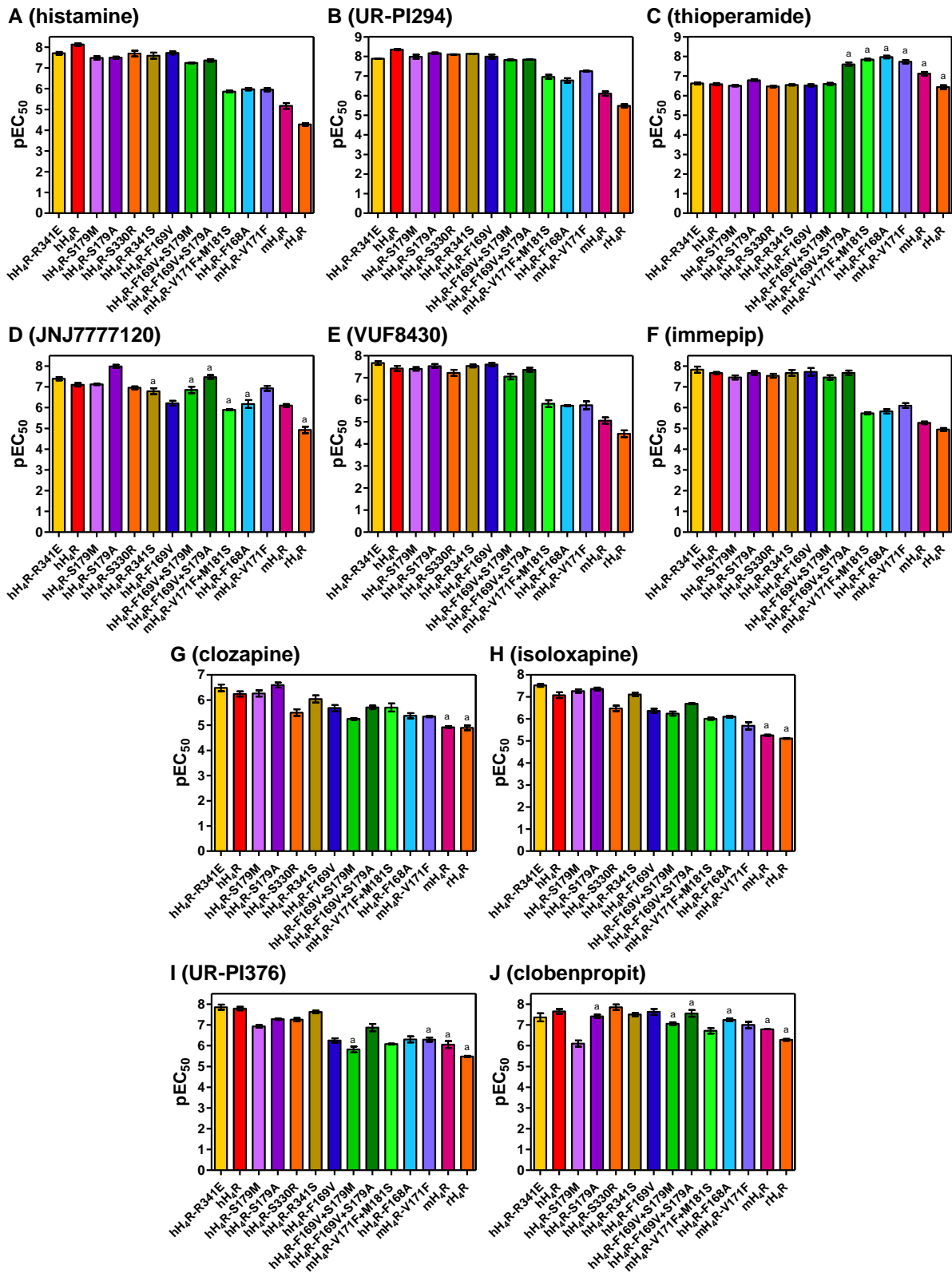
Figure 9.2: pEC$_{50}$ values (or ^{a}pK$_b$ in case of partial agonists with -0.25 ≤ α ≤ 0.25) of H$_4$R ligands at wild-type and mutant H$_4$ receptors. pEC$_{50}$ values were determined in [^{35}S]GTPγS assays. Data shown are mean values ± SEM of at least three independent experiments, performed in triplicate.

9.2.2 Summary of intrinsic activities
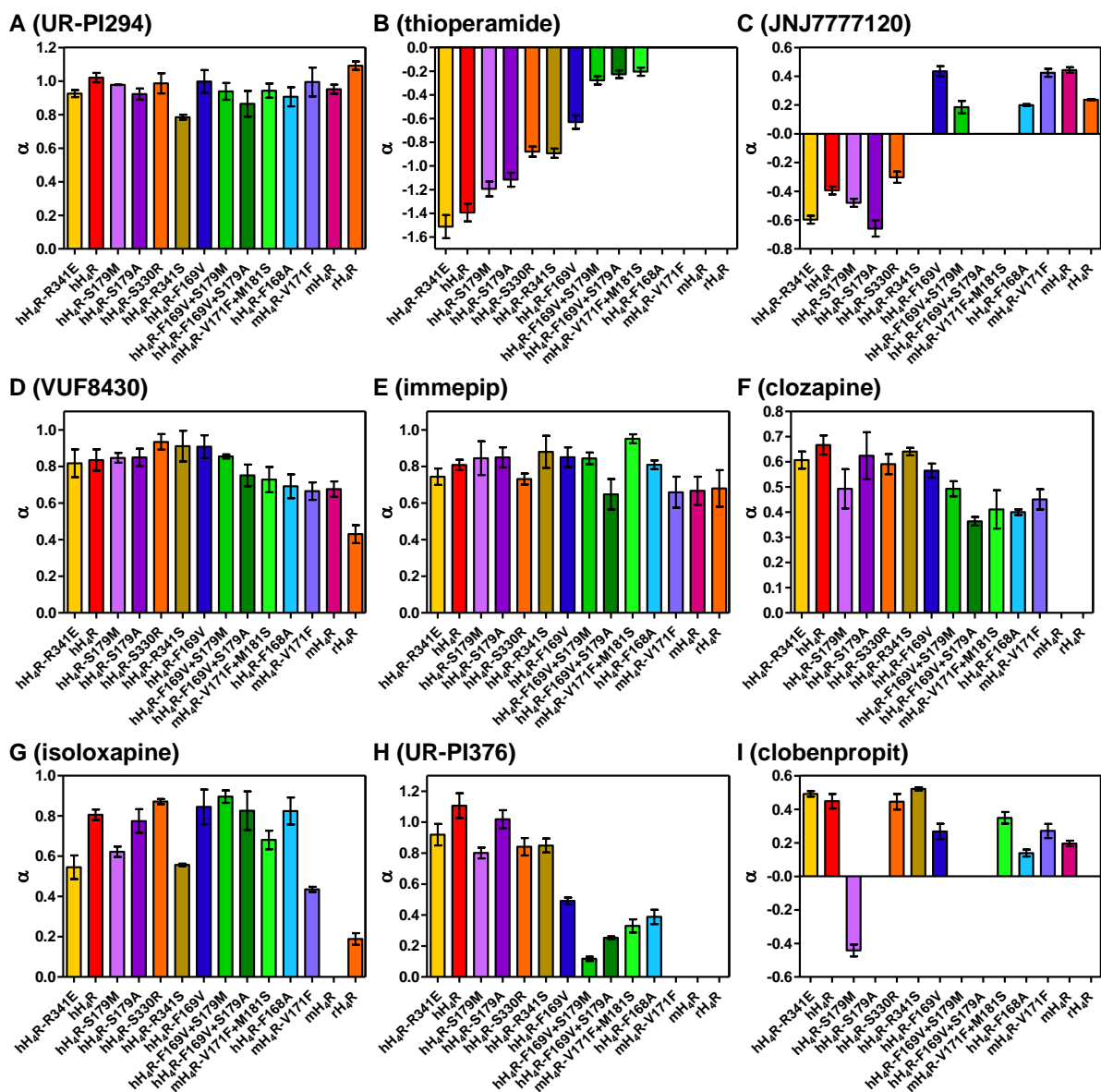
Figure 9.3: α values (intrinsic activities) of H$_4$R ligands at wild-type and mutant H$_4$ receptors. α values were determined in [^{35}S]GTPγ assays. The intrinsic activity of histamine was set to 1.0, and all other ligands, including inverse agonists, were referenced to histamine. Data shown are mean values ± SEM of at least three independent experiments, performed in triplicate. α = 0: neutral antagonism.

9.2.3 Summary of affinities
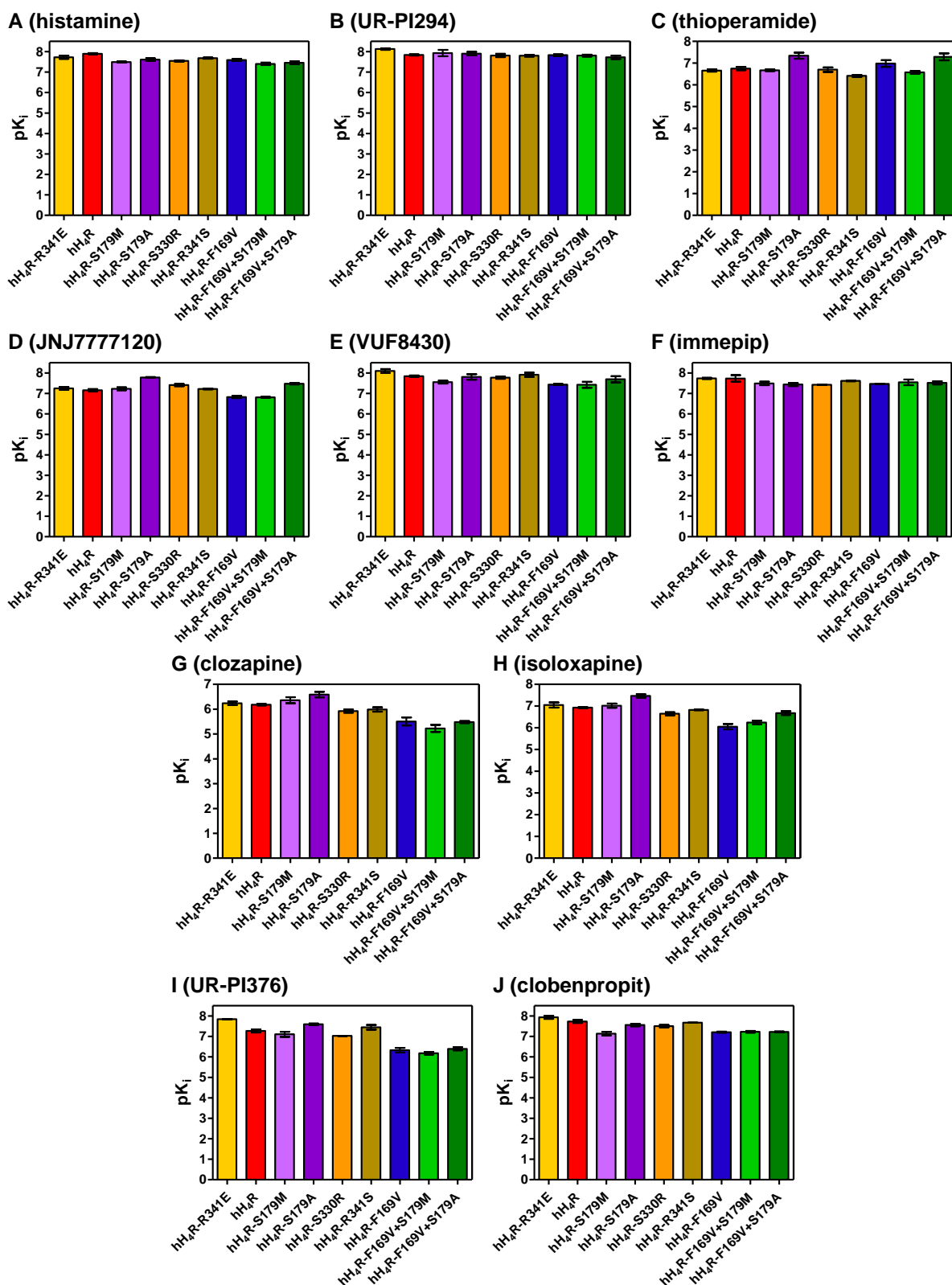
Figure 9.4: pK$_i$ values of H$_4$R ligands at wild-type and mutant H$_4$ receptors. pK$_i$ values were determined in [^{3}H]histamine competition binding assays. Data shown are mean values ± SEM of at least two independent experiments, performed in triplicate.
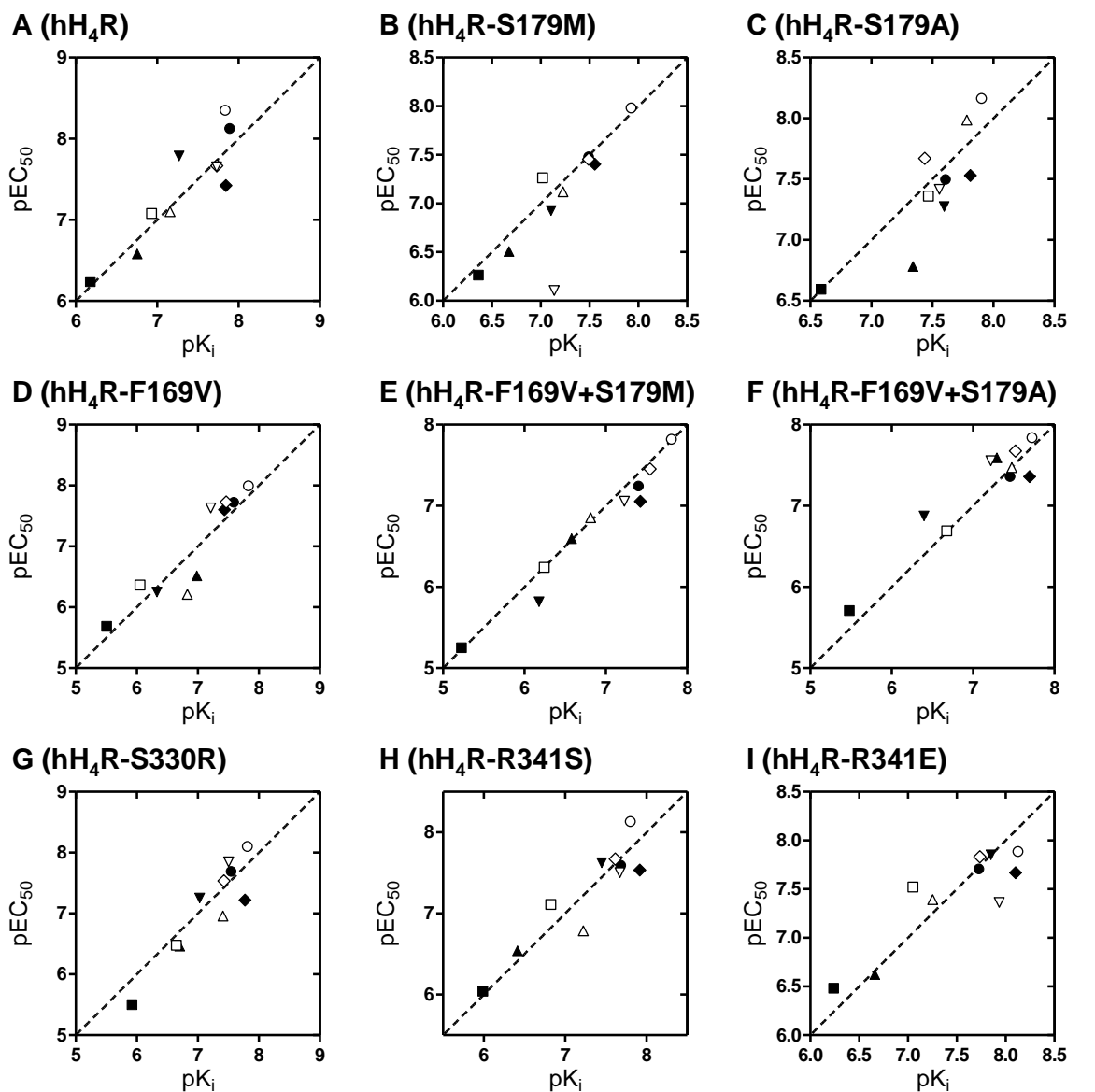
9.3   Comparison of affinities and potencies of H$_4$R ligands

Figure 9.5: Comparison of pK$_i$ values, determined in [^{3}H]histamine competition binding assays, and pEC$_{50}$ values, determined in [^{35}S]GTPγS assays. The dashed line represents the line of identity.

- ● histamine
- ○ UR-PI294
- ▲ thioperamide
- △ JNJ7777120
- ◆ VUF8430
- ◇ immepip
- ■ clozapine
- □ isoloxapine
- ▼ UR-PI376
- ▽ clobenpropit

9.4 Statistical analysis of wild-type and mutant H$_4$ receptors

9.4.1 Statistical analysis of H$_4$R ligand potencies

Table 9.1: Statistical analysis (one-way ANOVA and Bonferroni post hoc tests) of the pEC$_{50}$ values determined at wild-type and mutated H$_4$ receptors.

Receptor	histamine	UR-PI294	thioperamide	JNJ7777120	VUF8430	immepip	clozapine	isoloxapine	UR-PI376	clobenpropit
hH$_4$R	ααα, V, mmm, MMM, aaa, AAA, SS, E, R, sss, fff, μμμ, rrr	ααα, MM, AA, EE, sss, fff, μμμ, rrr	ααα, AAA, sss, fff, μμμ	ααα, VVV, aaa, sss, μμμ, rrr	ααα, sss, fff, μμμ, rrr	ααα, sss, fff, μμμ, rrr	αα, MMM, R, fff, μμμ, rrr	ααα, VVV, MMM, RRR, sss, fff, μμμ, rrr	ααα, VVV, mmm, MMM, AAA, sss, fff, μμμ, rrr	mmm, sss, f, μμ, rrr
hH$_4$R-F168A	hhh, VVV, MMM, AAA, SSS, EEE, μμμ, rrr, mmm, aaa, RRR	hhh, VVV, MMM, AAA, SSS, EEE, f, μμμ, rrr, mmm, aaa, RRR	hhh, VVV, MMM, A, SSS, EEE, μμμ, rrr, mmm, aaa, RRR	hhh, M, AAA, EEE, ff, rrr, mmm, aaa, RR	hhh, VVV, MMM, AAA, SSS, EEE, μ, rrr, mmm, aaa, RRR	hhh, VVV, MMM, AAA, SSS, EEE, rrr, mmm, aaa, RRR	hh, EEE, mm, aaa	hhh, AA, SSS, EEE, μμμ, rrr, mmm, aaa	hhh, SSS, EEE, rr, m, aaa, RRR	rr, mmm
hH4R-F169V	h, ααα, M, sss, fff, μμμ, rrr	ααα, sss, fff, μμμ, rrr	ααα, AAA, sss, fff, μμμ	hhh, mmm, M, aaa, AAA, EEE, RR, ff, rrr	ααα, sss, fff, μμμ, rrr	ααα, sss, fff, μμμ, rrr	aa, EEE, μ, r	hhh, mmm, aaa, SSS, EEE, fff, μμμ, rrr	hhh, mm, aaa, A, SSS, EEE, RRR, rrr	mmm, sss, μμ, rrr
hH$_4$R-S179M	hhh, ααα, fff, μμμ, rrr, sss	ααα, fff, μμμ, rrr, sss	ααα, AAA, fff, μμμ, sss	ααα, VVV, μμμ, rrr, aa, sss	ααα, fff, μμμ, rrr, sss	ααα, fff, μμμ, rrr, sss	αα, MMM, fff, μμμ, rrr, R	ααα, VVV, MMM, AA, fff, μμμ, rrr, RRR, sss	hhh, α, VV, MMM, SS, EEE, f, μμμ, rrr, sss	hhh, ααα, VVV, MMM, AAA, SSS, EEE, fff, aaa, RRR
hH$_4$R-F169V+S179M	hhh, V, ααα, sss, fff, μμμ, rrr	hh, ααα, sss, ff, μμμ, rrr	AAA, ααα, sss, fff, μμμ	V, A, α, aaa, sss, μμ, rrr	ααα, sss, fff, μμμ, rrr	ααα, sss, fff, μμμ, rrr	hhh, mmm, aaa, S, EEE	hhh, mmm, aaa, SSS, EEE, f, μμμ, rrr	hhh, AAA, mmm, aaa, SSS, EEE, RRR	mmm, R, r
hH$_4$R-S179A	hhh, ααα, fff, μμμ, rrr, sss	ααα, fff, μμμ, rrr, sss	ααα, AAA, fff, sss	hhh, ααα, VVV, mm, MMM, SSS, fff, μμμ, rrr, sss	ααα, fff, μμμ, rrr, sss	ααα, fff, μμμ, rrr, sss	ααα, VV, MMM, AA, fff, μμμ, rrr, RRR, ss	ααα, VVV, MMM, AAA, fff, μμμ, rrr, RRR, sss	ααα, VVV, MMM, fff, μμμ, rrr, sss	mmm, rrr
hH$_4$R-F169V+S179A	hhh, ααα, sss, fff, μμμ, rrr	hh, ααα, sss, fff, μμμ, rrr	hhh, VVV, α, mmm, MMM, aaa, SSS, EEE, RRR, μμ, rrr	VVV, ααα, M, S, sss, μμμ, rrr	ααα, sss, fff, μμμ, rrr	ααα, sss, fff, μμμ, rrr	aa, EEE, μμ, rr	αα, mm, aaa, EEE, sss, fff, μμμ, rrr	hhh, V, MMM, SSS, EEE, ss, μμ, rrr	mmm, ss, μ, rrr
hH$_4$R-R341S	hh, fff, μμμ, rrr, ααα, sss	fff, μμμ, rrr, ααα, sss	AAA, fff, μμμ, ααα, sss	A, μ, rrr, aaa, ss	fff, μμμ, rrr, ααα, sss	fff, μμμ, rrr, ααα, sss	M, f, μμμ, rrr	VVV, MMM, fff, μμμ, rrr, ααα, RR, sss	VVV, MMM, AAA, fff, μμμ, rrr, ααα, mm, sss	rrr, mmm, s
hH$_4$R-R341E	h, fff, μμμ, rrr, ααα, sss	hh, fff, μμμ, rrr, ααα, sss	AAA, fff, μμ, ααα, sss	VVV, μμμ, rrr, ααα, sss	fff, μμμ, rrr, ααα, sss	fff, μμμ, rrr, ααα, sss	VVV, MMM, AAA, fff, μμμ, rrr, ααα, RRR, sss	VVV, MMM, AAA, fff, μμμ, rrr, ααα, RRR, sss	VVV, MMM, AAA, fff, μμμ, rrr, ααα, mmm, sss	rrr, mmm
hH$_4$R-S330R	h, ααα, sss, fff, μμμ, rrr	ααα, sss, fff, μμμ, rrr	ααα, AAA, sss, fff, μμμ	αα, VV, aaa, sss, μμ, rrr	ααα, sss, fff, μμμ, rrr	ααα, sss, fff, μμμ, rrr	h, m, aaa, EEE	hhh, mmm, aaa, SS, EEE, fff, μμμ, rrr	ααα, VVV, MMM, sss, ff, μμμ, rrr	mmm, M, sss, ff, μμμ, rrr
mH$_4$R-V171F+M181S	hhh, VVV, mmm, MMM, aaa, AAA, SSS, EEE, μμμ, rrr, RRR	hhh, VVV, mmm, MMM, aaa, AAA, SSS, EEE, μμμ, rrr, RRR	hhh, VVV, mmm, MMM, aaa, SSS, EEE, fff, rrr, RRR	hhh, mmm, MMM, aaa, AAA, SS, EEE, fff, rrr, RRR	hhh, VVV, mmm, MMM, aaa, AAA, SSS, EEE, μμ, rrr, RRR	hhh, VVV, mmm, MMM, aaa, AAA, SSS, EEE, rrr, RRR	aa, EEE, μμ, rr	hhh, mmm, aaa, AAA, SSS, EEE, μμμ, rrr	hhh, mmm, aaa, AA, SSS, EEE, RRR	hhh, VVV, AA, S, RRR
mH$_4$R-V171F	hhh, VVV, MMM, AAA, μμμ, rrr, mmm, aaa, SSS, EEE, RRR	hhh, VVV, MM, AAA, μμμ, rrr, α, mmm, aaa, SSS, EEE, RRR	hhh, VVV, MMM, μμμ, rrr, mmm, aaa, SSS, EEE, RRR	VV, μμ, rrr, αα, aaa, sss	hhh, VVV, MMM, AAA, μ, rrr, mmm, aaa, SSS, EEE, RRR	hhh, VVV, MMM, AAA, μμμ, rrr, mmm, aaa, SSS, EEE, RRR	hhh, mmm, aaa, S, EEE	hhh, VVV, M, AAA, rr, mmm, aaa, SSS, EEE, RRR	hhh, rr, m, aaa, SSS, EEE, RRR	h, r, mmm, RR
mH$_4$R	hhh, VVV, MMM, AAA, ααα, mmm, aaa, SSS, EEE, RRR, sss, fff, rrr	hhh, VVV, MMM, AAA, ααα, mmm, aaa, SSS, EEE, RRR, sss, fff, rrr	hhh, VVV, MMM, AA, ααα, mmm, SSS, EE, RRR, sss, fff, rrr	hhh, MM, AAA, mmm, aaa, S, EEE, RR, ff, rrr	hhh, VVV, MMM, AAA, α, mmm, aaa, SSS, EEE, RRR, ss, f	hhh, VVV, MMM, AAA, mmm, aaa, SSS, EEE, RRR, fff	hhh, V, AA, mmm, aaa, SSS, EEE, ss	hhh, VVV, MMM, AAA, ααα, mmm, aaa, SSS, EEE, RRR, sss	hhh, AA, mmm, aaa, SSS, EEE, RRR	hh, VV, A, RRR
rH$_4$R	hhh, VVV, MMM, AAA, μμμ, ααα, mmm, aaa, SSS, EEE, RRR, sss, fff	hhh, VVV, MMM, AAA, μμμ, ααα, mmm, aaa, SSS, EEE, RRR, sss, fff	AAA, μμμ, ααα, sss, fff	hhh, VVV, MMM, AAA, μμμ, ααα, mmm, aaa, SSS, EEE, RRR, sss, fff	hhh, VVV, MMM, AAA, ααα, mmm, aaa, SSS, EEE, RRR, sss, fff	hhh, VVV, MMM, AAA, ααα, mmm, aaa, SSS, EEE, RRR, sss, fff	hhh, V, AA, mmm, aaa, SSS, EEE, ss	hhh, VVV, MMM, AAA, ααα, mmm, aaa, SSS, EEE, RRR, sss, ff	hhh, VVV, AAA, αα, mmm, aaa, SSS, EEE, RRR, ff	hhh, VVV, M, AAA, αα, aaa, SSS, EEE, RRR, f

Significances of the respective ligands (columns) at the respective receptors (rows) compared to other receptor constructs are depicted in the cell. Significant differences with respect to: hH$_4$R – h, hH$_4$R-F168A – α, hH$_4$R-F169V – V, hH$_4$R-S179M – m, hH$_4$R-F169V+S179M – M, hH$_4$R-S179A – a, hH$_4$R-F169V+S179A – A, hH$_4$R-R341S – S, hH$_4$R-R341E – E, hH$_4$R-S330R – R, mH$_4$R-V171F+M181S – s, mH$_4$R-V171F – f, mH$_4$R – μ, rH$_4$R – r (one letter: p < 0.05, two letters: p < 0.01, three letters: p < 0.001). In case of neutral antagonism (-0.25 ≤ α ≤ 0.25), pK$_b$ values were considered for statistical analysis instead of pEC$_{50}$ values.

9.4.2 Statistical analysis of intrinsic activities of H$_4$R ligands

Table 9.2: Statistical analysis (one-way ANOVA and Bonferroni post hoc tests) of α values (intrinsic activity) determined at wild-type and mutated H$_4$ receptors.

Receptor	histamine	UR-PI294	thioperamide	JNJ7777120	VUF8430	immepip	clozapine	isoloxapine	UR-PI376	clobenpropit
hH$_4$R			ααα, VVV, MMM, a, AAA, SSS, RRR, sss, fff, μμμ, rrr	ααα, VVV, MMM, aaa, AAA, SSS, EEE, sss, fff, μμμ, rrr	rr		α, AA, s, μμμ, rrr	ff, μμμ, rrr	ααα, VVV, mm, MMM, AAA, SS, R, sss, fff, μμμ, rrr	ααα, VV, mmm, MMM, aaa, AAA, f, μμμ, rrr
hH$_4$R-F168A			hhh, VVV, SSS, EEE, mmm, aaa, RRR	hhh, VVV, AAA, SS, EEE, fff, μμμ, mmm, aaa, RRR, ss			h, μμμ, rrr	ff, μμμ, rrr	hhh, MM, SSS, EEE, fff, μμμ, rrr, mmm, aaa, RRR	hhh, SSS, EEE, mmm, RRR, ss
hH$_4$R-F169V			hhh, ααα, mmm, MM, aaa, AAA, EEE, R, sss, fff, μμμ, rrr	hhh, ααα, mmm, MMM, aaa, AAA, SSS, EEE, RRR, sss, rr	rrr		μμμ, rrr	E, fff, μμμ, rrr	hhh, mmm, MMM, aaa, A, SSS, EEE, RRR, fff, μμμ, rrr	hh, mmm, MMM, aaa, AAA, SSS, EE, rrr
hH$_4$R-S179M			ααα, VVV, MMM, AAA, E, fff, μμμ, rrr, R, sss	ααα, VVV, MMM, AAA, SSS, fff, μμμ, rrr, a, R, sss	rr		μμμ, rrr	μμμ, rrr	hh, ααα, VVV, MMM, AAA, fff, μμμ, rrr, sss	hhh, ααα, VVV, MMM, AAA, SSS, EEE, fff, μμμ, rrr, aaa, RRR, sss
hH$_4$R-F169V+S179M			hhh, VV, mmm, aaa, SSS, EEE, RRR	hhh, VVV, AA, mmm, aaa, SS, EEE, RRR, ss, fff, μμμ	rr		μμμ, rrr	S, E, fff, μμμ, rrr	hhh, VVV, αα, mmm, aaa, SSS, EEE, RRR	hhh, VVV, mmm, SSS, EEE, RRR, sss, fff, μ
hH$_4$R-S179A			h, ααα, VVV, MMM, AAA, EEE, fff, μμμ, rrr, sss	hhh, ααα, VVV, m, MMM, AAA, SSS, fff, μμμ, rrr, RRR, sss	rr		A, μμμ, rrr	f, μμμ, rrr	ααα, VVV, MMM, AAA, fff, μμμ, rrr, sss	hhh, VVV, mmm, SSS, EEE, fff, μ, RRR, sss
hH$_4$R-F169V+S179A			hhh, VVV, mmm, aaa, SSS, EEE, RRR	hhh, VVV, ααα, mmm, MM, aaa, EEE, RRR, fff, μμμ, rrr	r		hh, a, S, EE, μμμ, rrr	ff, μμμ, rrr	hhh, V, mmm, aaa, SSS, EEE, RRR, f, μ	hhh, VVV, mmm, SSS, EEE, RRR, sss, fff, μ
hH$_4$R-R341S	r		hhh, MMM, AAA, fff, μμμ, rrr, ααα, EEE, sss	hhh, VVV, MM, fff, μμμ, rrr, αα, mmm, aaa, EEE, RRR	rrr		A, μμμ, rrr	M, μμμ, rr, R	hh, VVV, MMM, AAA, fff, μμμ, rrr, ααα, sss	VVV, MMM, AAA, fff, μμμ, rrr, ααα, mmm, aaa
hH$_4$R-R341E			VVV, MMM, AAA, SSS, fff, μμμ, rrr, ααα, m, aaa, RRR, sss	hhh, VVV, MMM, AAA, SSS, fff, μμμ, rrr, ααα, RRR, sss	rr		AA, μμμ, rrr	V, M, μμμ, rr, R	VVV, MMM, AAA, fff, μμμ, rrr, ααα, sss	VV, MMM, AAA, ff, μμμ, rrr, ααα, mmm, aaa
hH$_4$R-S330R			hhh, ααα, V, m, MMM, AAA, EEE, sss, fff, μμμ, rrr	ααα, VVV, m, MMM, aaa, AAA, SSS, EEE, sss, fff, μμμ, rrr	rrr		μμμ, rrr	S, E, fff, μμμ, rrr	h, ααα, VVV, MMM, AAA, sss, fff, μμμ, rrr	ααα, mmm, MMM, aaa, AAA, μμ, rrr
mH$_4$R-V171F+M181S			hhh, VVV, mmm, aaa, SSS, EEE, RRR	hhh, αα, VVV, mmm, MM, aaa, EEE, fff, μμμ, rrr, RRR			h, μμμ, rrr	μμμ, rrr	hhh, mmm, aaa, SSS, EEE, fff, μμ, rr, RRR	αα, mmm, MMM, aaa, AAA, rrr
mH$_4$R-V171F			hhh, VVV, mmm, aaa, SSS, EEE, RRR	hhh, MMM, AAA, rr, ααα, mmm, aaa, SSS, EEE, RRR, sss			μμμ, rrr	hh, VVV, MMM, AA, μμ, αα, a, RRR	hhh, VVV, A, ααα, mmm, aaa, SSS, EEE, RRR, sss	h, MMM, AAA, rrr, mmm, aaa, SSS, EE
mH$_4$R			hhh, VVV, mmm, aaa, SSS, EEE, RRR	hhh, MMM, AAA, ααα, mmm, aaa, SSS, EEE, RRR, sss, rr			hhh, VVV, MMM, AAA, ααα, mmm, aaa, SSS, EEE, RRR, sss, fff	hhh, VVV, MMM, AAA, ααα, mmm, aaa, SSS, EEE, RRR, sss, ff	hhh, VVV, A, ααα, mmm, aaa, SSS, EEE, RRR, ss	hhh, M, A, mmm, a, SSS, EEE, RR, r
rH$_4$R		S	hhh, VVV, mmm, aaa, SSS, EEE, RRR	hhh, VV, AAA, μμ, mmm, aaa, SSS, EEE, RRR, sss, ff	hh, VVV, MM, A, mm, aa, SSS, EE, RRR		hhh, VVV, MMM, AAA, ααα, mmm, aaa, SSS, EEE, RRR, sss, fff	hhh, VVV, MMM, AAA, ααα, mmm, aaa, SS, EE, RRR, sss	hhh, VVV, ααα, mmm, aaa, SSS, EEE, RRR, ss	hhh, VVV, μ, mmm, SSS, EEE, RRR, sss, fff

Significances of the respective ligands (columns) at the respective receptors (rows) compared to other receptor constructs are depicted in the cell. Significant differences with respect to: hH$_4$R – h, hH$_4$R-F168A – α, hH$_4$R-F169V – V, hH$_4$R-S179M – m, hH$_4$R-F169V+S179M – M, hH$_4$R-S179A – a, hH$_4$R-F169V+S179A – A, hH$_4$R-R341S – S, hH$_4$R-R341E – E, hH$_4$R-S330R – R, mH$_4$R-V171F+M181S – s, mH$_4$R-V171F – f, mH$_4$R – μ, rH$_4$R – r (one letter: $p < 0.05$, two letters: $p < 0.01$, three letters: $p < 0.001$). Blank cells indicate non-significant changes.

9.4.3 Statistical analysis of H₄ receptor affinities

Table 9.3: Statistical analysis (one-way ANOVA and Bonferroni post hoc tests) of pK$_i$ values determined at nine wild-type and mutated H₄ receptors.

Receptor	histamine	UR-PI294	thioperamide	JNJ7777120	VUF8430	immepip	clozapine	isoloxapine	UR-PI376	clobenpropit
hH₄R	V, mmm, MMM, a, AAA, R		a	V, MM, aaa, A			V, MMM, AA	VVV, MM, a	VVV, MMM, AAA, E	VVV, mmm, MM, AAA
hH₄R-F169V	h			h, mmm, aaa, AAA, SS, EEE, RRR	E		h, mmm, aaa, EE	hhh, mmm, aaa, AA, SS, EEE, R	hhh, mmm, aaa, SSS, EEE, RR	hhh, a, SS, EEE
hH₄R-S179M	hhh		aa	VVV, MMM, aaa			VVV, MMM, AAA	VVV, MMM	VVV, MMM, AAA, EE, a	hhh, SS, EEE, aa, R
hH₄R-F169V+S179M	hhh, E		AA, aaa	hh, AAA, mmm, aaa, SS, EEE, RRR	E		hhh, mmm, aaa, SS, EEE, R	hh, mmm, aaa, S, EEE	hhh, mmm, aaa, SSS, EEE, RRR	hh, S, EEE
hH₄R-S179A	h		h, mm, MMM, SSS, E, R	hhh, VVV, mmm, MMM, A, SSS, EEE, R			VVV, MMM, AAA, S, R	h, VVV, MMM, AAA, SS, RRR	VVV, m, MMM, AAA, R	V, mm, A, E
hH₄R-F169V+S179A	hhh		MM, SS	h, VVV, MMM, a			hh, mmm, aaa, EE	VV, aaa	hhh, mmm, aaa, SSS, EEE, RR	hhh, a, SS, EEE
hH₄R-R341S			AA, aaa	VV, MM, aaa			MM, a	VV, M, aa	VVV, MMM, AAA	VV, M, AA, mm
hH₄R-R341E	M		a	VVV, MMM, aaa	V, M		VV, MMM, AA	VVV, MMM	h, VVV, MMM, AAA, mm, RRR	VVV, MMM, AAA, mmm, a, R
hH₄R-S330R	h		a	VVV, MMM, a			M, a	V, aaa	VV, MMM, a, AA, EEE	m, E

Significances of the respective ligands (columns) at the respective receptors (rows) compared to other receptor constructs are depicted in the cell. Significant differences with respect to: hH₄R – h, hH₄R-F169V – V, hH₄R-S179M – m, hH₄R-F169V+S179M – M, hH₄R-S179A – a, hH₄R-F169V+S179A – A, hH₄R-R341S – S, hH₄R-R341E – E, hH₄R-S330R – R (one letter: $p < 0.05$, two letters: $p < 0.01$, three letters: $p < 0.001$). Blank cells indicate non-significant changes. Note: not applicable to mH₄R, rH₄R, mH₄R mutants and hH₄R-F168A.

9.5 Publications, short lectures, posters and awards

9.5.1 Publications

Wifling, D.; Bernhardt, G.; Dove, S.; Buschauer, A. (2015). The extracellular loop 2 (ECL2) of the human histamine H_4 receptor substantially contributes to ligand binding and constitutive activity. *PloS One* 10(1): e0117185.

Wifling, D.; Löffel, K.; Nordemann, U.; Strasser, A.; Bernhardt, G.; Dove, S.; Seifert, R.; Buschauer, A. (2015). Molecular determinants for the high constitutive activity of the human histamine H_4 receptor: functional studies on orthologues and mutants. *Br. J. Pharmacol.* 172(3): 785-798.

Nordemann, U.; **Wifling, D.**; Schnell, D.; Bernhardt, G.; Stark, H.; Seifert, R.; Buschauer, A. (2013). Luciferase reporter gene assay on human, murine and rat histamine H_4 receptor orthologs: correlations and discrepancies between distal and proximal readouts. *PLoS One* 8(9): e73961.

9.5.2 Short lectures

Wifling, D.; Löffel, K.; Nordemann, U.; Bernhardt, G.; Dove, S.; Seifert, R.; Buschauer, A. (7-10 May 2014). In search for key amino acids determining the high constitutive activity of the human histamine H_4 receptor. 43th annual meeting of the European Histamine Research Society (EHRS), Lyon, France. Abstract published in *Inflamm. Res.* (2014). 63: S20-S20.

Wifling, D.; Löffel, K.; Nordemann, U.; Bernhardt, G.; Dove, S.; Seifert, R.; Buschauer, A. (10-12 March 2014). Key residues determining the switch from the inactive to the active state of the human histamine H_4 receptor. International PhD Students Meeting 2014 of the DPhG, Wuppertal, Germany.

Wifling, D.; Löffel, K.; Bernhardt, G.; Dove, S.; Seifert, R.; Buschauer, A. (26-28 September 2012). Functional studies on mutated human, mouse and rat histamine H_4 receptor (H_4R) orthologs. 6th Summer School Medicinal Chemistry, Regensburg, Germany.

9.5.3 Poster presentations

Wifling, D.; Löffel, K.; Nordemann, U.; Bernhardt, G.; Dove, S.; Seifert, R.; Buschauer, A. (24-26 September 2014). Molecular insights into the high constitutive activity of the human histamine H_4 receptor. Jahrestagung der Deutschen Pharmazeutischen Gesellschaft e.V. (DPhG), Frankfurt, Germany.

Wifling, D.; Löffel, K.; Nordemann, U.; Bernhardt, G.; Dove, S.; Seifert, R.; Buschauer, A. (17-19 September 2014). Ligand binding and constitutive activity of the human histamine H_4

receptor: Molecular-pharmacological investigations. 7th Summer School Medicinal Chemistry, Regensburg, Germany.

Wifling, D.; Löffel, K.; Bernhardt, G.; Dove, S.; Seifert, R.; Buschauer, A. (17-20 March 2013). Molecular determinants of the high constitutive activity of the human histamine H_4 receptor. Frontiers in Medicinal Chemistry, Munich, Germany.

Wifling, D.; Löffel, K.; Bernhardt, G.; Dove, S.; Seifert, R.; Buschauer, A. (7-9 October 2012). Functional studies on mutated human, mouse and rat histamine H_4 receptor (H_4R) orthologs. 5th GPCR Symposium, Würzburg, Germany.

Wifling, D.; Löffel, K.; Bernhardt, G.; Dove, S.; Seifert, R.; Buschauer, A. (26-28 September 2012). Functional studies on mutated human, mouse and rat histamine H_4 receptor (H_4R) orthologs. 6th Summer School Medicinal Chemistry, Regensburg, Germany.

9.5.4 Poster Award

Wifling, D.; Löffel, K.; Bernhardt, G.; Dove, S.; Seifert, R.; Buschauer, A. (26-28 September 2012). Functional studies on mutated human, mouse and rat histamine H_4 receptor (H_4R) orthologs. 6th Summer School Medicinal Chemistry, Regensburg, Germany.

9.6 Eidesstattliche Erklärung

Ich erkläre hiermit an Eides statt, dass ich die vorliegende Arbeit ohne unzulässige Hilfe Dritter und ohne Benutzung anderer als der angegebenen Hilfsmittel angefertigt habe; die aus anderen Quellen direkt übernommenen Daten und Konzepte sind unter Angabe des Literaturzitats gekennzeichnet.

Weitere Personen waren an der inhaltlich-materiellen Herstellung der vorliegenden Arbeit nicht beteiligt. Insbesondere habe ich hierfür nicht die entgeltliche Hilfe eines Promotionsberaters oder anderer Personen in Anspruch genommen. Niemand hat von mir, weder unmittelbar noch mittelbar, geldwerte Leistungen für Arbeiten erhalten, die im Zusammenhang mit dem Inhalt der vorgelegten Dissertation stehen.

Die Arbeit wurde bisher weder im In- noch im Ausland in gleicher oder ähnlicher Form einer anderen Prüfungsbehörde vorgelegt.

Regensburg, den _____ _____

David Wifling